UNIVERSITY OF CALIFORNIA,
IRVINE

I. Controlled Aqueous C1 Synthesis of Telechelic Macromonomers for the Synthesis of Long-Chain Aliphatic Polyesters

II. Evaluation of 9-Borafluorene Derivatives as the Catalysts for the Polyhomologation Reaction

DISSERTATION

submitted in partial satisfaction of the requirements
for the degree of

DOCTOR OF PHILOSOPHY

in Chemistry

by

Ruobing Zhao

Dissertation Committee:
Professor Kenneth J. Shea, Chair
Professor Larry E. Overman
Professor Christopher D. Vanderwal

2017

DEDICATION

To

my family:

my parents: Zejian Zhao and Qinfen Sun;

my wife: Xilun Weng

For

always supporting and encouraging me

and my friends:

Chunhua Geng, Xiaoliang Chen, Zheng Wang, Cui Cheng and Qian Xie

For

your friendship, all the fun activities and brainstorms

TABLE OF CONTENTS

LIST OF FIGURES

LIST OF SCHEMES

LIST OF TABLES

ACKNOWLEDGMENTS

First and foremost, I would like to express my deepest gratitude to my research advisor, Professor Ken Shea, for his continuous support of my Ph.D. study. He is an excellent mentor who inspired me for a career in polymer chemistry. His passion, patience, encouragement and immense knowledge guided me through the rough road to complete this thesis.

I would like to thank my thesis committee members, Professor Larry Overman and Professor Christopher Vanderwal, as well as Professor Zhibin Guan, Professor Aaron Esser-Kahn and Professor Filipp Furche for helpful suggestions and discussions on my research.

Secondly, I would like to acknowledge the past and present members of the Shea research group. Special thanks go to Dr. Jun Luo for her trainings on many useful techniques when I joined the lab. Thanks to Dr. Fangfang Lu who shared experiences on research projects. Many thanks go to Dr. José E. Báez who has been a wonderful coworker to teach me meticulous and persistent attitudes on research as well as kindness and optimistic attitudes towards life. To Dr. Yan Zhang, thank you for helping me on the polyester project. To my dedicated undergraduate Gerald Chen, thanks for your effort on the project of air-stable catalyst. To David Lao, Dr. Xuefei Leng, Dr. Guang Shi and Dr. Haojie Yu, you have been great labmates to work together on the polyhomologation project. To Dr. Leah Cleary and Dr. Jennifer Pitzen, thanks for your helpful suggestions on organic synthesis and on my second-year/oral reports. To Dr. Shih-Hui Lee, Dr. Guoqing Pan, Dr. Keiichi Yoshimatsu, Dr. Hiroyuki Koide, Dr. Shunsuke Onogi, Dr. Zhiyang Zeng, Dr. Adam Weisman, Dr. Beverly Chou, Jaclynn Unangst, Jeff O'Brien, Krista Fruehauf, I thank you for your scientific suggestions and friendship in the lab.

In addition, I would like to acknowledge members from other research groups. To Dr. Mikko Muuronen from the Furche group, thank you for teaching me all the advanced computational calculations with fun coding. With your help, my work efficiency increased by one order of magnitude. To Dr. Jaeyoon Chung, Dr. Tobias Friedberger, Dr. Justin Crumrine, Dr. Olivia Cromwell and Dr. Yi-Xuan Lu from the Guan group, thank you for all the helps on instrumentations including tensile analysis, GPC, TGA and DSC.

I would like to thank Dr. Philip R. Dennison for NMR experiments, Dr. Beniam Berhane for mass spectral experiments, Dr. Dmitry Fishman for IR analysis and Dr. Nathan R. Crawford for trainings on the computational softwares. I also want to thank Marie Palmquist and Jaime M. Albano at the department office for their help during my graduate study.

Lastly, I would like to acknowledge American Chemical Society for permission to include copyrighted figures and contents as part of my thesis. Chapter 2 is reprinted with permission from *ACS Macro Lett*. **2016**, *5*, 854–857 ©2015 American Chemical Society. Chapter 3 is reprinted with permission from *ACS Macro Lett*. **2015**, *4*, 584–587 ©2016 American Chemical Society. Financial supports were provided by the University of California, Irvine, NSF Grant CHE-0848855 and CHE-1153118 for synthesis and polymerization study as well as NSF Grant CHE-0840513 for computational study.

Curriculum Vitae

Ruobing Zhao

Education

Ph.D. Chemistry, University of California, Irvine, **February 2017**
B.S. Chemistry, Peking University, **July 2010**

Academic Experiences

Graduate Research Assistant **Dec. 2011 – Feb. 2017**
Department of Chemistry, University of California, Irvine
Advisor: Prof. Kenneth J. Shea

Design, synthesis and evaluation of 9-borafluorene derivatives as single-site organoborane catalysts for synthesis of novel polymer structures.

- Computational study on the thermal and kinetic properties of complexation–migration reactions between various 9-borafluorene derivatives and sulfoxonium ylides.
- Synthesis of 9-borafluorene derivatives.

Controlled Aqueous C1 synthesis of for synthesis of long-chain aliphatic polyesters.

- Aqueous C1 synthesis of long-chain bolaamphiphiles.
- Synthesis of polyesters via condensation polymerizations.
- Analysis on thermal and mechanical properties of the polyester products.

Synthesis and characterization of gradient ersatz ethylene–propylene copolymers.

- Developed an efficient and economical method to synthesize new secondary ylide monomers.
- Synthesis and characterization of PE-based polymers with increased content of methyl branch along the polymer chain.

The role of oxygenated impurities in C1 polymerization and their influence on polymer PDI.

- Computational study on the competing reactions of oxygenated impurities in the C1 polymerization.
- Developed air-stable organoborane initiators for C1 polymerization.

Research Assistant **Jul. 2010 – Jan. 2011**
College of Chemistry and Molecular Engineering, Peking University
Advisor: Prof. Xuefeng Guo

A single-molecule detector embedded on single-wall carbon-nanotubes.

- Synthesis of triazine-based T-shaped molecules with pyridyl/alkynyl terminal groups.

Undergraduate Research Assistant **Feb. 2008 – Jul. 2010**
College of Chemistry and Molecular Engineering, Peking University
Advisor: Prof. Xuefeng Guo

Design, synthesis and fabrication of mesogen-jacketed liquid crystalline polymer semiconductor and tetracene-based liquid crystalline organic thin-film transistors.

- Synthesis of 2,8-bis(3,4,5-tris(dodecyloxy)phenyl)-tetracene and 2,3-dihexyloxy-8-vinyl-tetracene.
- Fabrication and characterization of the polymer and organic thin-film transistors.

UM/PKU REU Exchange Program **Jul. 2008 – Aug. 2008**
Department of Chemistry, University of Michigan, Ann Arbor
Advisor: Prof. Raoul Kopelman

Preparation of uniformed 30 nm nanoparticles by micro-emulsion polymerization of polyacrylamide.

Graduate Teaching Assistant **Sep. 2011 – Jun. 2016**
Department of Chemistry, University of California, Irvine
Organic Chemistry Lecture, Advanced Organic Chemistry Laboratory, Organic Chemistry Laboratory and General Chemistry Laboratory.

Instrument Assistant Manager
Materials Facility Center, University of California, Irvine **Sep. 2012 – Sep. 2015**
Operate and maintenance of GPC/DSC/TGA instruments; Instrument training on new users.

Honors & Awards

09/2016	University of California, Irvine	Dissertation Fellowship
10/2008	Peking University	President's Grant for Undergraduate Research
06/2008	Peking University	New York Yucai Scholarship
11/2006	Peking University	Freshman Scholarship

Professional Affiliations

Member of American Chemical Society

Publications

Peer Reviewed Journals:

• Zhao, R.; Zhang, Y.; Chung, J.; Shea, K. J. Convenient controlled aqueous C1 synthesis of long-chain aliphatic AB, AA, and BB macromonomers for the synthesis of polyesters with tunable hydrocarbon chain segments. *ACS Macro Lett*. **2016**, *5*, 854–857.

• Zhao, R.; Shea, K. J. Gradient methylidene–ethylidene copolymer via C1 polymerization: an Ersatz gradient ethylene–propylene copolymer. *ACS Macro Lett*. **2015**, *4*, 584–587.

• Luo, J.; Zhao, R.; Shea, K. J. Synthesis of high MW polymethylene via C1 polymerization. The role of oxygenated impurities and their influence on PDI. *Macromolecules* **2014**, *47*, 5484–5491.

• Pan, G.; Sun, S.; Zhang, W.; Zhao, R.; Cui, W.; He, F.; Huang, L.; Lee, S.; Shea, K. J.; Yang, H.; Shi, Q. Biomimetic design of mussel-derived bioactive peptides for dual-functionalization of Titanium-based biomaterials. *J. Am. Chem. Soc.* **2016**, *138*, 15078–15086.

• Báez, J.; Zhao, R.; Shea, K. J. Poly(methylene-*b*-ε-caprolactone) and poly(ε-caprolactone) with linear alkyl end groups. Synthesis, phase behavior and compatibilizing efficacy. Manuscript under review.

• Zhao, R.; Muuronen, M.; Furche, F.; Shea, K. J. Novel polyethylene-based polymer structures from a single-site organoborane initiator via C1 polymerization. Manuscript in preparation.

Presentations:

• Shea, K. J.; Zhao, R. "Controlled synthesis of simple hydrocarbon oligomers and polymers with precisely designed microstructures". 252nd ACS National Meeting, Philadelphia, Pennsylvania, PA August 2016.

• Zhao, R.; Shea, K. J. "Synthesis of poly(methylidene-co-ethylidene) with a new secondary ylide monomer via C1 polymerization". Presented at the 248th ACS National Meeting, San Francisco, CA August 2014.

ABSTRACT OF THE DISSERTATION

I. Controlled Aqueous C1 Synthesis of Telechelic Macromonomers for the Synthesis of Long-Chain Aliphatic Polyesters

II. Evaluation of 9-Borafluorene Derivatives as the Catalysts for the Polyhomologation Reaction

By

Ruobing Zhao

Doctor of Philosophy in Chemistry

University of California, Irvine, 2017

Professor Kenneth J. Shea, Chair

My dissertation includes five research projects on the polyhomologation reaction for synthesis of carbon backbone polymers. In chapter 1, an overview is provided on the polyhomologation reaction. The reaction builds linear sp^3 carbon chains one carbon at a time using an organoborane catalyst. The traditional method is a living polymerization using sulfoxonium ylides under anhydrous conditions. The newly developed aqueous method is a polymerization of sulfoxonium salts in an aqueous base.

Chapter 2 develops the synthesis of telechelic polymers including ω-hydroxyacid esters, α,ω-diols and α,ω-diacids using the aqueous polyhomologation reaction with control of chain length and PDI. These polymers were used as macromonomers to produce long-chain aliphatic polyesters. The obtained polyesters have thermal and mechanical properties indistinguishable compared to related materials derived from biomass.

Chapter 3 reports the synthesis of a gradient ersatz ethylene–propylene copolymer using the traditional polyhomologation reaction. A new and convenient source of the

ethylide monomer was developed for the introduction of methyl branch on the polymer backbone. The gradient copolymer contains a gradual change of methyl branch content along the polymer chain.

Chapter 4 focuses on the precise monomer insertion on a carbon chain using a sulfonium benzylide. The polymerization and validation protocols were established to demonstrate the precise insertion. A thermally more stable benzylide needs to be developed to complete this study.

In chapter 5, three 9-borafluorene derivatives are designed and evaluated in search of a single-site catalyst for the polyhomologation reaction. The catalyst is being developed for the synthesis of the yet unknown polyethylidene. Computational studies indicated a preferred 1,2-migration of the sp^3 over sp^2 carbon when an electron-withdrawing group is installed on the aromatic rings at the ortho position to boron. Experimental studies revealed the presence of competing sp^2 carbon migration due to the required high reaction temperature from the high activation energy of 1,2-migration. A side reaction produced ethylidene–methylidene copolymers rather than polyethylidene due to the competing decomposition of ethylide.

In chapter 6, an air-stable borane initiator was provided for convenient use in the polyhomologation reaction. Polymer molecular weight and polydispersity are well controlled using the amine–borane complex.

Chapter 1. Polyhomologation: A Living and Versatile C1 Polymerization

1.1. C1 Polymerization

Carbon backbone polymers, including simple hydrocarbon polymers such as polyethylene (PE), are ubiquitous in modern civilization. These inexpensive materials which include plastics, paraffin, waxes and oils have found applications that range from commodity packaging, lubricants to precision mechanical materials (artificial joint replacements).[1] Currently these simple carbon backbone polymers including polyethylene, polypropylene (PP), polystyrene (PS) and poly(methyl methacrylate) (PMMA) are synthesized by olefin polymerizations in large-scale industrial plants. The polymerization of C=C bonds is referred to as C2 polymerizations in which two carbon atoms are delivered at each chain-propagation step (Scheme 1.1a).

There are two major drawbacks with the C2 polymerization. First is the monomer source. The olefin monomers are mostly from petroleum, a finite supply that only serves as a temporary source of hydrocarbon polymers. A sustainable polymer industry must consider replacement of petroleum-derived PE/PP with alternative carbon sources such as more abundant coal and natural gas. Second is the synthetic challenge. Many highly substituted olefins and polar functionalized C=C substrates do not polymerize, and their polymers are still unknown. The functionalized olefin C2 monomers are polymerized *via* radical polymerization which does not have control of the polymer stereo-properties. Many highly functionalized and stereoregular polymers cannot be prepared *via* C2 polymerizations due to the incompatibility between the polar functional groups and most transition metal catalysts.

One approach to resolve these issues is to build carbon backbone polymers from monomers delivering only one carbon (C1 monomers) at each propagation step. This implies the use of carbenoid monomers (Scheme 1.1b). C1 monomers such as α,α-dihalogenated carbons[2-4], diazo compounds[5,6], sulfoxonium ylides[6,7] and arsonium ylides[8] have been used in C1 polymerizations. Some C1 carbon sources have used methyl halides which are obtained from methanol[9], a C1 molecule that is derived from a variety of non-petroleum sources.[10]

Scheme 1.1. Strategies between a) C2 vs b) C1 polymerizations.

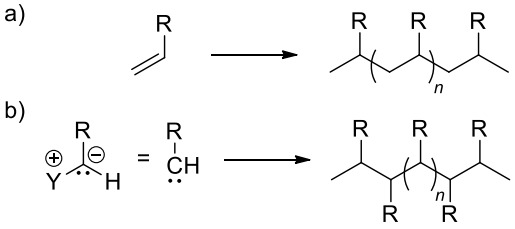

Several different C1 polymerization strategies were reported in the past half a century including magnesium mediated polymerization of α,α-dihalogenated carbons[3,4], the Lewis acid or transition metal mediated polymerization of diazo compounds[6], boron catalyzed polymerization of ylides[7,8] and anionic polymerization of C1 monomers[11]. Oligomers and polymers with unique structures such as oligo(phenylpropylidene)[11] and syndiotactic poly(ethyl 2-ylidene-acetate)[12] were first synthesized *via* C1 polymerizations (Figure 1.1).

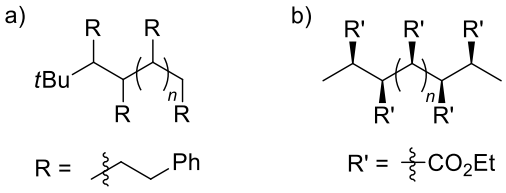

Figure 1.1. Novel polymer/oligomer structures synthesized *via* C1 polymerizations including a) oligo(phenylpropylidene) and b) syndiotactic poly(ethyl 2-ylidene-acetate).

Of all the various C1 polymerizations, very few methods are able to achieve high reaction yields, control of molecular weight (MW) and low polydispersity (PDI) of the polymer. One of

the few well-developed examples is the organoborane catalyzed polymerization of ylides, namely the polyhomologation reaction.

1.2. Polyhomologation: A Living C1 Polymerization of Ylides

In 1966, a procedure was developed by Tufariello and coworkers for the homologation of alkylboranes using dimethylsulfoxonium methylide **1** (Scheme 1.2).[13] Using equal molar amounts of methylide **1**, tri-*n*-hexylborane gave three products after the oxidation cleavage of the B–C bond. The products include the unhomologated product 1-hexanol (68%), mono-homologation product 1-heptanol (26%) and bis-homologation product 1-octanol (6%). The homologation reaction proceeds by methylene insertion between the boron atom and the alkyl group. The presence of small amounts of doubly homologated product suggested that the homologation could be repeated multiple times if excess of methylide **1** was used.

Scheme 1.2. Homologation of tri-*n*-hexylborane with methylide **1**.

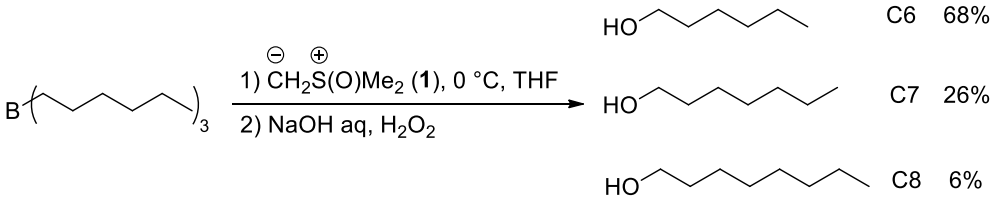

Inspired by Tufariello's work, the Shea group evaluated the repetitive homologation for the synthesis of polymethylene.[14] When tris(*p*-methoxyphenylethyl)borane **2** was treated with an excess of methylide **1** at elevated temperatures, ylide **1** was consumed within 10 minutes as determined by titration of an aliquot of the reaction mixture (Scheme 1.3). After oxidation, the resulting hydrocarbon material was obtained in high yield and characterized by NMR analysis as α-hydroxy-ω-(4-methoxyphenyl)polymethylene **3**. The polymer MW was well controlled as evidenced by Gel Permeation Chromatography (GPC) analysis. The experimental degree of polymerization (DP_{exp}) is consistent with the theoretical value DP_{th} (DP_{th} = 1/3 × [ylide

1]/[organoborane **2**]), as a result of the polymer chain growth on all three arms of the boron atom (Figure 1.2). Both the controlled MW and the observed unimodal MW distribution (PDI = 1.01) indicated the comparable rates of chain growth among different propagating chain ends and absence of chain termination reaction. These results suggested that the polyhomologation reaction is a living polymerization.

Scheme 1.3. Polyhomologation reaction catalyzed by functionalized organoborane **2**.

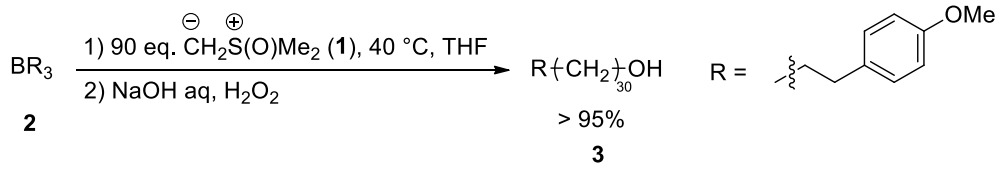

2 > 95% **3**

Analysis of the polymer **3** *via* Field Desorption Mass Spectrometry (FDMS) showed a narrow and unimodal distribution of peaks with a spacing of 14 a.u. (Figure 1.2).[15] It confirms that the polymer was built by methylene units one at a time. The experimental distribution of MWs is almost identical to the simulated curve plotted based on the equation of Poisson distribution for an ideal living polymerization.[16]

By use of the polyhomologation reaction, high MW polymethylenes (M_n = 354 kDa) have been successfully synthesized.[15] And the corresponding organoborane intermediate tris(polymethylene)borane has a MW of over 1.0×10^6 Da with the reaction time of less than 10 minutes. Thus the minimum turnover frequency can be estimated to be 6.4×10^3 kilogram of polymethylene (mol boron)$^{-1}$ h^{-1} at 120 ℃ which is comparable to many highly efficient transition metal-catalyzed homogeneous ethylene polymerizations.[17]

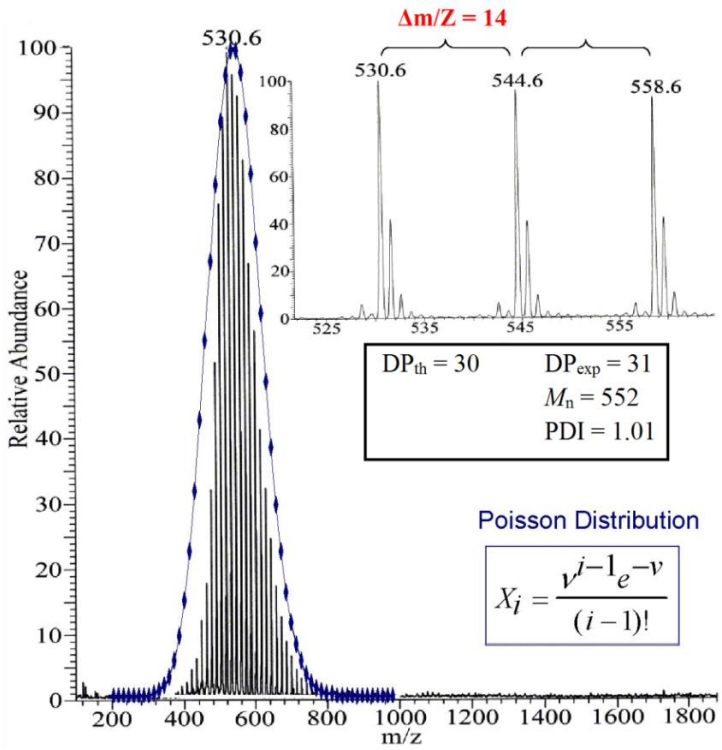

Figure 1.2. FDMS spectrum of α-hydroxy-ω-(4-methoxyphenyl)polymethylene **3**. Inset shows an expanded scale showing isotope patterns with adjacent major peaks separated by 14 m/Z. The blue curve is a plot of the simulated Poisson distribution of a polymer with the same MW from an ideal living polymerization. Symbol *i* represents the number average chain length. X_i is the mole fraction of *i*-mer among all polymers. And υ is the molar ratio of monomer/initiator. Reprinted with permission from *Acc. Chem. Res.* **2010**, *43*, 1420–1433. Copyright 2010 American Chemical Society

1.3. Mechanism of the Polyhomologation Reaction

In the polyhomologation reaction, each monomer addition is composed of two steps; complexation and 1,2-migration (Scheme 1.4). When the Lewis acidic organoborane catalyst **4** is treated with the nucleophilic sulfoxonium ylide **1**, a zwitterionic borate complex **5** is formed first. Then one of the initial three substituents on boron undergoes 1,2-migration to the carbon atom from the ylide **1**. As a result, a new carbon–carbon bond is formed in addition to a sulfoxide byproduct. The catalytic trivalent boron center is regenerated as in the homologated organoborane **6**. Repetition of this process affords organoborane **7** with three linear hydrocarbon

polymer chains. As the final polymer has a controlled MW with low PDI, all three growing polymer chains propagate with a similar rate. This results in a very similar chain length of the three arms on organoborane **7**, even though the monomer addition occurs randomly on all three chains among different catalytic sites. The polyhomologation reaction is not terminated before a complete consumption of the ylide monomer. A final oxidation and hydrolysis step will cleave the B–C bond to give the polymer ω-hydroxypolymethylene **8**.

Scheme 1.4. The mechanism of chain propagations in the polyhomologation reaction.

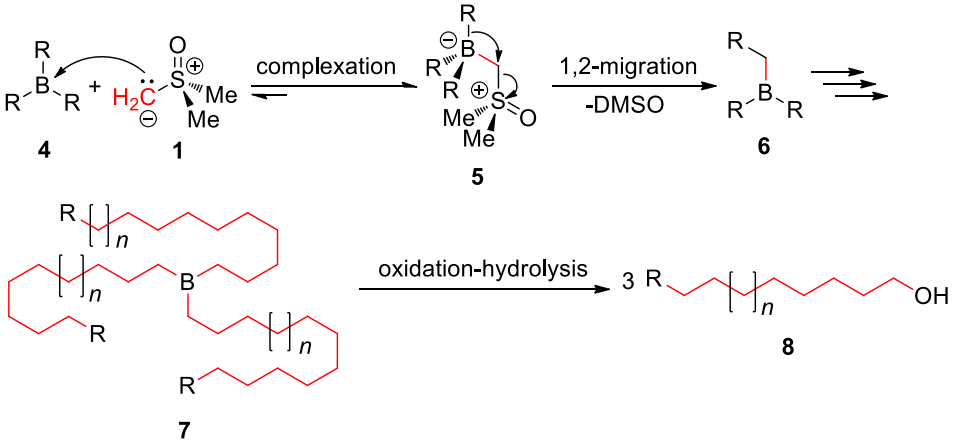

The mechanism of polyhomologation reaction was supported by variable temperature ^{11}B NMR studies (Figure 1.3).[15,18] In the absence of coordinating solvents, tri-*n*-hexylborane **4** shows a ^{11}B chemical shift of approximate 88 ppm at 40 ℃ (Figure 1.3a). When a stoichiometric amount of methylide **1** was added at −78 ℃ followed by warming the mixture to −15 ℃, the initial peak disappeared and a new resonance emerged at −13.4 ppm due to formation of the borate complex **5** (Figure 1.3b). This complex is stable at −15 ℃ with no observable 1,2-migration. After the mixture was warmed to 40 ℃, the peak shifted back to 82 ppm which corresponds to the homologated organoborane **6**. The ^{11}B NMR study indicated that the complexation step is a fast pre-equilibrium which strongly prefers the formation of borate **5**. The equilibrium between ylide and organoborane was also supported by the fact that the

homologation of trialkylborane with an equal molar of ylide will afford small amounts of the double-homologated product. The subsequent 1,2-migration is a rate-limiting step that undergoes at higher temperature than −15 ℃. This is consistent with the fact that the polyhomologation reaction only proceeds at an appreciable rate at 40 ℃.

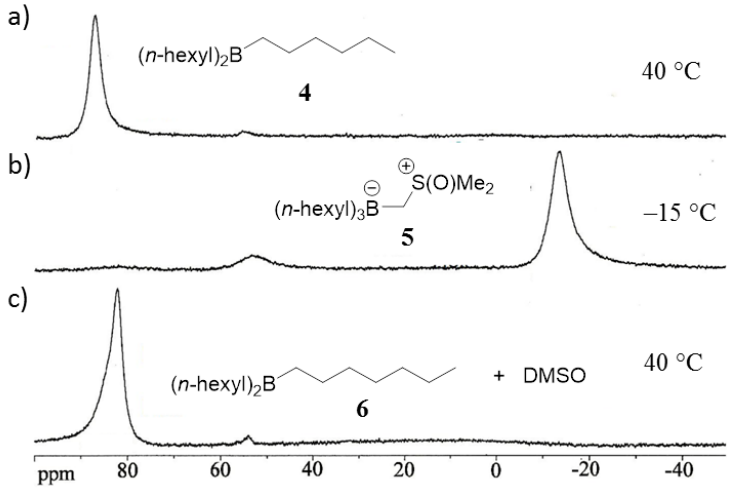

Figure 1.3. ^{11}B NMR of a) tri-*n*-hexylborane at 40 ℃; b) tri-*n*-hexylborane·methylide complex **5** at −15 ℃; c) homologated trialkylborane **6** with DMSO byproduct at 40 ℃. The small peak at 48 ppm is a borinic acid impurity (< 2%).[7]

Experimental kinetic studies were also carried out to support that the 1,2-migration is the rate-limiting step.[15] Plots of the ylide consumption versus time are linear for over three half-lives, indicating the accumulated byproduct DMSO has no obvious influence on the polyhomologation reaction. The reaction was found to be first order in organoborane and zero order in ylide **1** under pseudo first-order conditions with an excess of ylide **1**. The result corroborates the ^{11}B NMR studies and is consistent with the proposed two-step mechanism (Scheme 1.4).

In addition, computational studies were employed to further investigate the 1,2-migration step. The ground state geometry of the starting complex ylide·BMe_3 **9** was calculated to have all-staggered conformation at B3LYP/6-311G(d,p) level.[19] The calculation positions the migrating methyl group on boron *anti* to the sulfoxonium substructure with the B–C σ orbital (HOMO)

aligned *anti*-periplanar to the C–S σ* orbital (LUMO) and the weakened C–S bond (Figure 1.4a). The S–O bond of complex **9** is aligned *anti* to the CH_2–B bond as well with a stabilizing interaction between the filled B–C σ orbital and the empty S–O σ* orbital (Figure 1.4b). Such a ground state geometry foreshadows the transition state of 1,2-migration and was experimentally confirmed by single crystal X-ray analysis of a stable and isolable complex ylide·BF_3.[20]

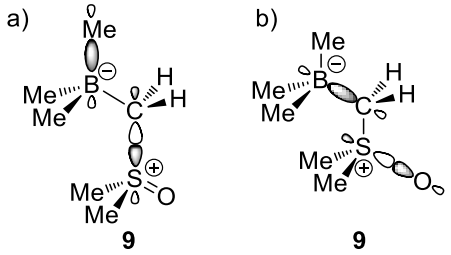

Figure 1.4. Proposed molecular orbital interactions of complex **9** deduced from single crystal X-ray analysis and the calculated ground state geometry. a) The migrating group (HOMO: σ_{C-B}) aligns *anti*-periplanar to the sulfoxonium leaving group (LUMO: σ^*_{C-S}). b) The filled B–C σ orbital aligns *anti*-periplanar to the empty S–O σ* orbital for stabilization.

The activation energy was calculated to be 11.6 kcal/mol at 368 K in toluene with B3LYP/6-311G(d,p) level of theory (Figure 1.5).[19] It is lower than the experimentally determined value of 23.8 kcal/mol measured in toluene at room temperature[15] as a result of the underestimation of the energy of transition state **10** with DFT functionals.

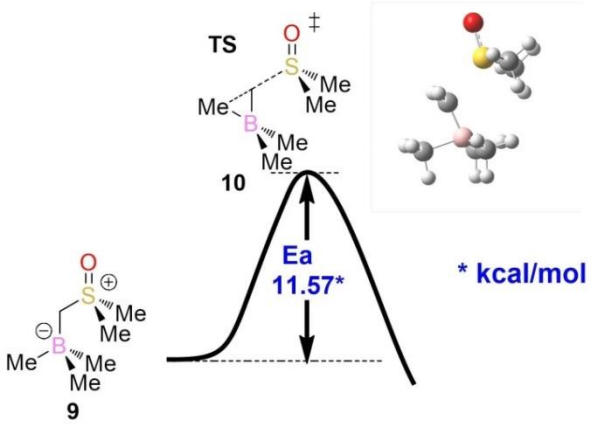

Figure 1.5. DFT calculations of the ground and transition states in the 1,2-migration step at B3LYP/6-311G(d,p) level of theory.

1.4. Polymer Composition Control

1.4.1. Telechelic polymethylene

With proper design of functionalized catalysts, the polyhomologation reaction can be used to prepare telechelic polymethylenes which are functionalized linear long–chain hydrocarbons on both chain ends. As the polyhomologation reaction affords organoboranes with three polymer arms, it guarantees the introduction of one functional group on the ω-chain end (the one from cleavage of B–C bond) by oxidation or other chemical reactions to convert the boron of the B–C bond with some other atom. The introduction of a functional group on the α-chain end requires additional reaction steps.

Functionality on the α-termini of polymethylene can be achieved with a pre-installed functional group on the organoborane catalyst. The functionalized catalysts can be readily obtained by hydroboration of functional α-olefins **11a**–**j** or by the boron–metal exchange reaction of **11k** (Scheme 1.5).[21,22] ω-Hydroxypolymethylenes **14a**–**k** were synthesized by a standard polyhomologation–oxidation sequence. In all cases, the incorporation of functional groups was estimated to be quantitative on both chain ends by ^{1}H NMR and GPC analysis. The resulting polymers have a narrow PDI ranging from 1.01 to 1.19. The well control of MW and PDI are not compromised by the presence of functional groups on the initiators.

Functional groups can also be engineered at the ω-chain end of polymethylene. In addition to the oxidation–hydrolysis process, a number of other synthetic transformations can be applied to replace boron with functionalities including amino groups, halogens, and carbon–metal bonds.[18]

Scheme 1.5. Synthesis of α-functionalized-ω-hydroxypolymethylenes **12a**–**k** from functional trialkylboranes.

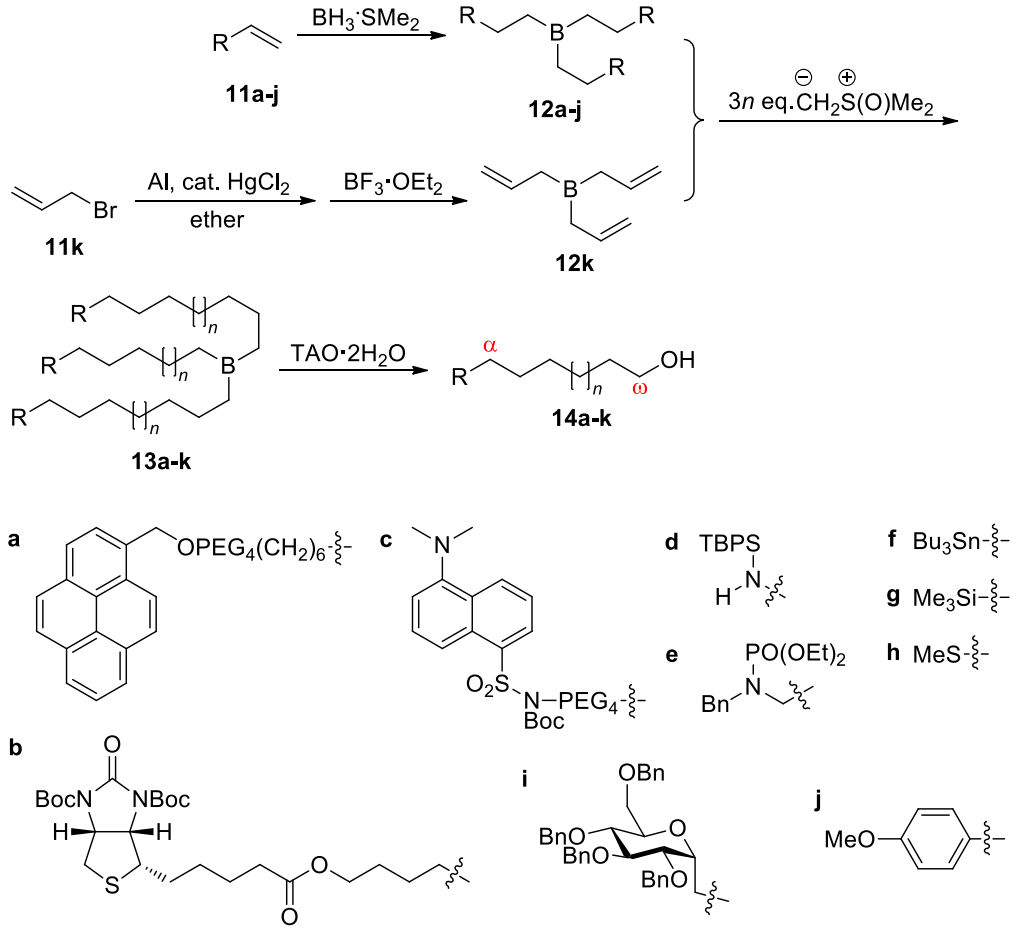

1.4.2. Substituted hydrocarbon chains

The introduction of substituents onto simple hydrocarbon chains has been used to tailor polymer properties, such as melting point, glass transition temperature, adhesion, and mechanical properties.[23] These polymer structures can be synthesized from the polyhomologation reaction with the additional use of substituted ylides in the monomer mix. The design and preparation of the secondary or tertiary ylides must meet several criteria: (1) the ylide must be thermally stable that it can survive the polymerization conditions; (2) the ylide must have reasonable reactivity with sufficient nucleophilicity and a good leaving group; (3) the byproduct does not inhibit the

polymerization; (4) the ylide should have no additional acidic hydrogens that can undergo proton exchange and relocate the nucleophilic center; (5) the ylide should be synthetically available without use of high-cost reagents. Based on these requirements, (dimethylamino)aryl-oxosulfonium alkylides **15** were found to be one of the most appropriate candidates (Figure 1.6).[24-27] Other types of ylides such as trimethylsilyl diazomethane **16**[28] and allylic arsonium ylides **17**[8,29] were also employed in the polyhomologation reaction.

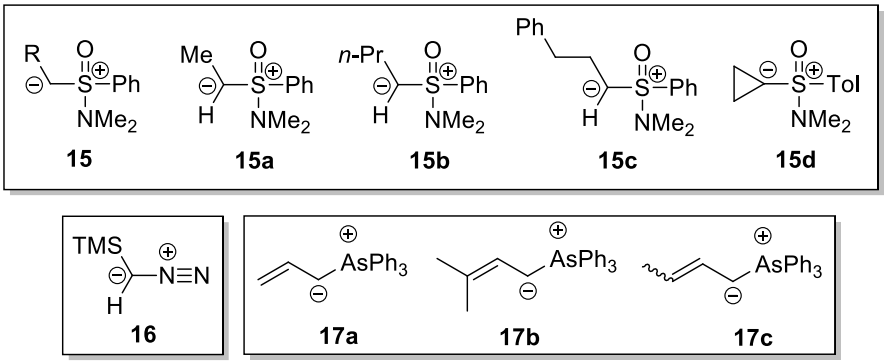

Figure 1.6. Secondary and tertiary ylides that were employed in the polyhomologation reaction for incorporation of branch and functionality including (dimethylamino)aryloxosulfonium alkylide derivatives **15a**–**d**, trimethylsilyl diazomethane **16**, and allylic arsonium ylide derivatives **17a**–**c**.

Several polymethylenes with incorporation of branch and functional groups were synthesized using methylide **1** and ylide **15a**–**d** *via* the polyhomologation reaction (Scheme 1.6). For ylide **15a**–**c**, the obtained random copolymers **18** at 60 ℃ have controlled branch incorporation in addition to the controlled polymer MW and PDI.[24,26-27] The composition of copolymers can be tuned by the feed ratio of the comonomers. For ylide **15d** and **16**, the reaction temperature was lowered to 0 ℃ to suppress the decomposition of monomers. Copolymers were obtained with increased PDI (~1.5) and lower incorporation ratios of cyclopropylidene or trimethylsilyl methylidene compared to the monomer feed ratios.[25,28] Two possible factors could account for this result. First, both ylides are thermally less stable and prone to α-elimination. And

second, they have higher activation energy for the 1,2-migration step than the secondary ylides **15a**–**c** due to the presence of sterically hindered groups.

Scheme 1.6. Branched hydrocarbon chains **18** synthesized *via* the polyhomologation reaction using methylide **1** with (dimethylamino)aryloxosulfonium alkylide derivatives **15a**–**d** or trimethylsilyl diazomethane **16**.

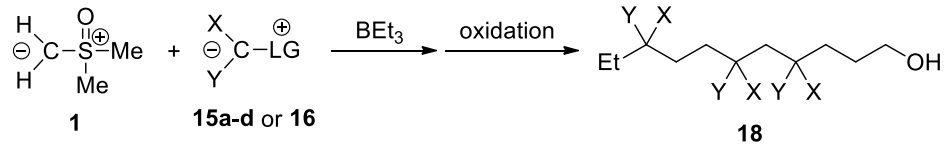

Attempts to homopolymerize ylides **15a**, **15d** and **16** were unsuccessful.[24-25,28] After a few homologations, the boron center becomes sterically crowded with tertiary or quaternary carbons. Its reactivity would be dramatically reduced towards addition of the next substituted ylide. This can be visualized by molecular models on the inactive boron species (Figure 1.7). The short B–C bond renders the boron atom inaccessible for the subsequent secondary/tertiary ylide.

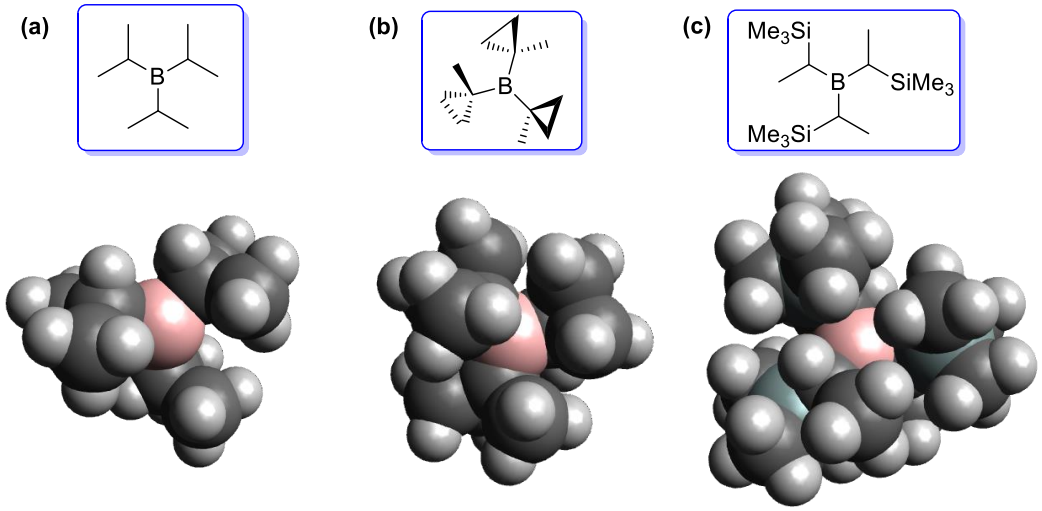

Figure 1.7. Space filling models of (a) triisopropylborane; (b) tris(1-methylcyclopropyl)borane; (c) tris(1-trimethylsilyl-ethyl)borane, the putative catalytic centers during homopolymerization of ylide **15a**, **15d** and **16**.

Allylic arsonium ylides **17a**–**c** were also reported to undergo polyhomologations with organoboranes. They have lower thermal stability compared to ylide **15a**–**c**. When treated with

triethylborane at 0 ℃, ylide **17a** with no substitutions on the allyl group could produce random copolymers with incorporation of C1 and C3 units (Scheme 1.7a).[29] The polymers **19a** were afforded with ratios of C3/C1 contents around 2.0 and well control on both MW and PDI. The C3 unit originates from the [1,3]-sigmatropic rearrangement of allylic boron species after homologation of the C1 unit (Scheme 1.8). To inhibit the rearrangement, ylide **17b** was designed with two methyl groups on the terminal carbon (Scheme 1.7b).[29] Using this ylide, oligomers **19b** with up to 14 C1 units were produced but with loss of MW and PDI control. Recently, it was found that ylide **17c** with only one methyl substitution can afford homopolymers **19c** with incorporation of exclusively C3 units (Scheme 1.7c).[8] Random and block copolymers were also demonstrated using ylide **17c** in combination with methylide **1**. However, the polymers from use of **17c** have almost double-massed MW and PDI around 1.2. Furthermore, the use of arsonium ylides would produce stoichiometric quantities of hazardous organoarsine byproducts which limited their applications.

Scheme 1.7. Branched hydrocarbon chains synthesized *via* the polyhomologation reaction using allylic arsonium ylides **17a**–**c**. a) C1/C3 polymerization of ylide 17**a**; b) C1 polymerization of ylide 17**b**; c) C3 polymerization of ylide 17**c**.

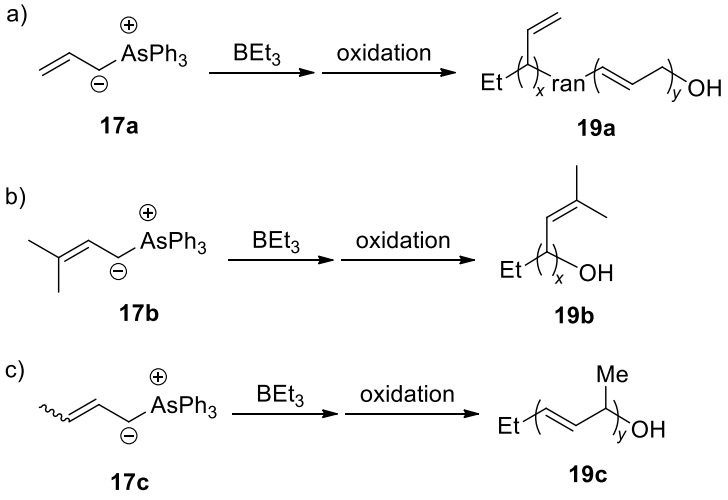

Scheme 1.8. Incorporation of allylic arsonium ylides as C1 or C3 unit interconverted by [1,3]-sigmatropic rearrangement.

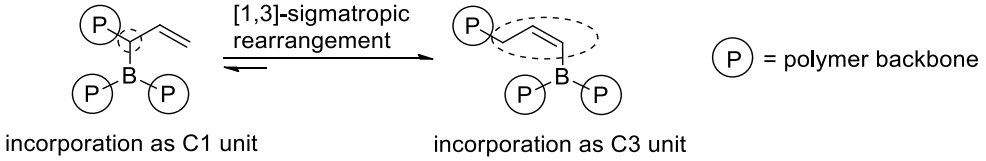

1.5. Polymer Topological Control

The polymer topology relates to the way of branching that leads to deviations from a linear polymer chain. It affects the physical properties of the material including solubility, density, crystallinity, glass transition temperature, diffusion rate, melt rheology, and mechanical strength.[30-32] Many polyethylene-based polymer architectures have been demonstrated including cyclic structures by ring-opening metathesis polymerization (ROMP)[31], star, comb, H-shape, and pom-pom polyethylenes produced by anionic polymerization[30]. These polymers have broad MW distributions and branching defects. As an alternative method, the polyhomologation reaction can provide polymers with unique structures by post-polymerization or from well-designed cyclic organoboranes.

Organoboranes with three polymer chains can be subjected to reactions that are capable of connecting the polymer chains. By use of a 'three-arm stitch' reaction, three-arm star polymers can be obtained (Scheme 1.9).[33] With three potential leaving groups in dichloromethoxy methyl ether, all three polymer arms on organoborane **7** are able to migrate to the same carbon from $CHCl_2OMe$ aided by the base $LiOCEt_3$. And several three-arm star polymethylenes **20** were prepared with well-controlled MW and low PDI. By use of organoboranes with other functionalities, different functional groups could also be incorporated at all three polymer chain ends.

Scheme 1.9. Synthesis of tris(polymethylene)carbinol **20**.

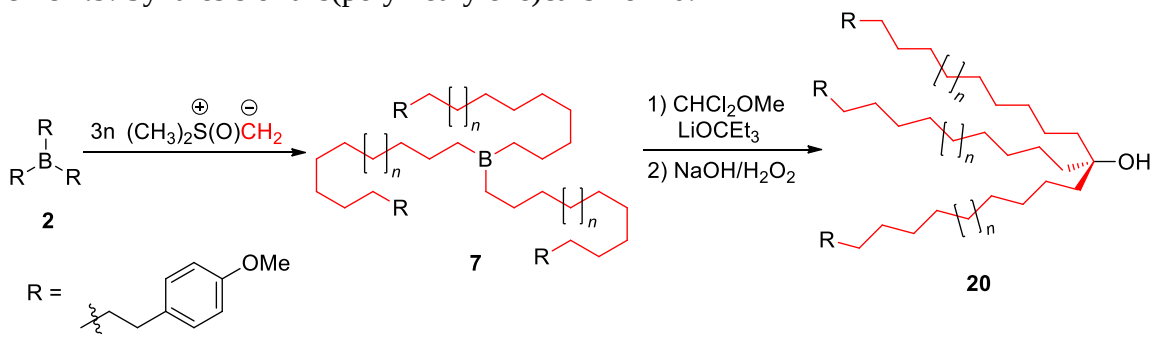

Unique structures of organoborane initiators can also produce novel polymer architectures *via* the polyhomologation reaction. For example using 1-boraadamantane·THF **21** as the catalyst, 'giant tubelike' macropolycyclic organoborane **22** can be generated in solution after polymerization with the methylide **1** (Scheme 1.10).[34,35] Further oxidation afforded a regular three-arm star polymethylene **23**. The MW of polymer **23** was found to be three times as large as the theoretical value from the stoichiometry of the monomer/initiator, yet the polymer PDI was kept below 1.12. Both experimental and computational analyses pointed out that two-thirds of the propagating catalytic species became inactive during the early stage of polymerization. The inactive catalytic centers arise from a few monomer insertions and are specific isomeric caged tricyclic geometries with inverted pyramidal boron centers.[34] They have high activation energies for further addition of the monomer. The polymers were mainly from one active boron intermediate found after approximate six insertions. This isomer can proceed rapidly to expand all rings. At a later stage of the polymerization, each branch migrates with equal probability in a manner similar to acyclic trialkylboranes.

Scheme 1.10. Synthesis of three-arm star polymer **23** with a *cis,cis*-1,3,5-trisubstituted cyclohexane core from 1-boraadamantane·THF **21**.

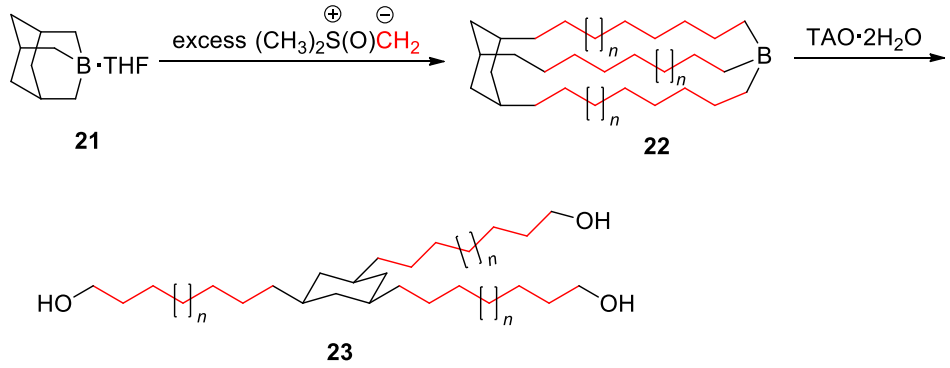

In combination of both cyclic borane initiators and post-polymerization modification, macrocyclic polymethylene can be synthesized. For this purpose, a 'two-arm stitch' reaction is required with a non-migrating group on the third arm of an organoborane. With *B*-thexylborocane catalyst **24** and excess of methylide **1**, boracycle **25** was prepared (Scheme 1.11).[36] The thexyl group on boron is known to resist the 1,2-migration below 10 ℃. After further sequential treatment of **25** using sodium cyanide, benzyl chloride and hydrogen peroxide basic solution, cyclic ketones **26** were revealed with narrow MW distribution.

Scheme 1.11. Synthesis of oligomeric cyclic ketone from *B*-thexylborocane **24**.

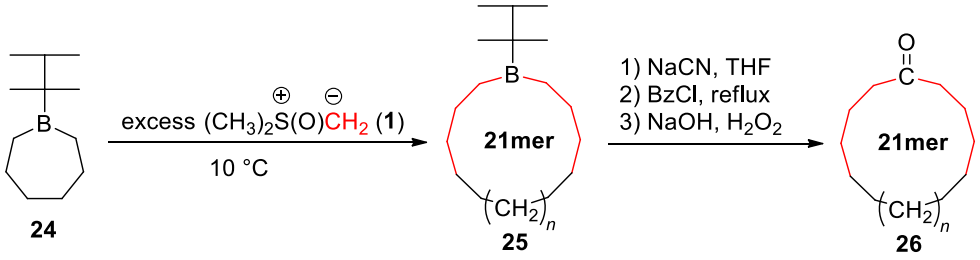

1.6. Combination of Polyhomologation with Other Polymerizations

Applications of nonpolar PE are limited because of its high degree of crystallinity, poor adhesion properties and incompatibility with many materials. These disadvantages can be overcome by construction of block copolymers containing a polymethylene block that can

interact with PE. As the polyhomologation reaction has well control of polymer MW, PDI and polymer chain end functionalization, it has been further applied to prepare block copolymers in combination with other polymerization methods including nitroxide-mediated radical polymerization (NMP), atom transfer radical polymerization (ATRP), reversible addition-fragmentation chain-transfer (RAFT) polymerization, living anionic polymerization and ring-opening polymerization (ROP).[37]

Using the hydroboration/polyhomologation and NMP strategy, well-defined block copolymer polystyrene-*b*-polymethylene (PS-*b*-PM) was prepared (Scheme 1.12a).[38] The PS block was built from initiator **27** *via* nitroxide mediated polymerization (a living polymerization) of styrene. The polymer chain end hydroxyl group was allylated and hydroborated to afford the macroinitiator organoborane **30**. Polyhomologation–oxidation reactions gave the desired diblock copolymer **31**. This copolymer was evaluated as the compatibilizer for immiscible blends of PE and PS.

In order to combine the polyhomologation reaction and ATRP or RAFT polymerization, the most common strategy is to prepare the macroinitiator bearing the chemically inert hydrocarbon chains. For examples, α-bromo ester **32** and trithiocarbonate terminated macroinitiator **35** were synthesized from ω-hydroxy-polymethylene **8** (Scheme 1.12b–c).[39,40] The polymerization of the second block (PS) was performed with standard protocols. Due to the living nature of all the involved polymerization methods (polyhomologation, ATRP, RAFT), these PS-*b*-PM copolymers **33** and **36** can be obtained with control of chain lengths on both blocks and narrow MW distribution.

Scheme 1.12. Representative examples of block copolymers synthesized *via* the polyhomologation reaction with a) NMP; b) ATRP; c) RAFT; d) ROP; e) anionic polymerizations.

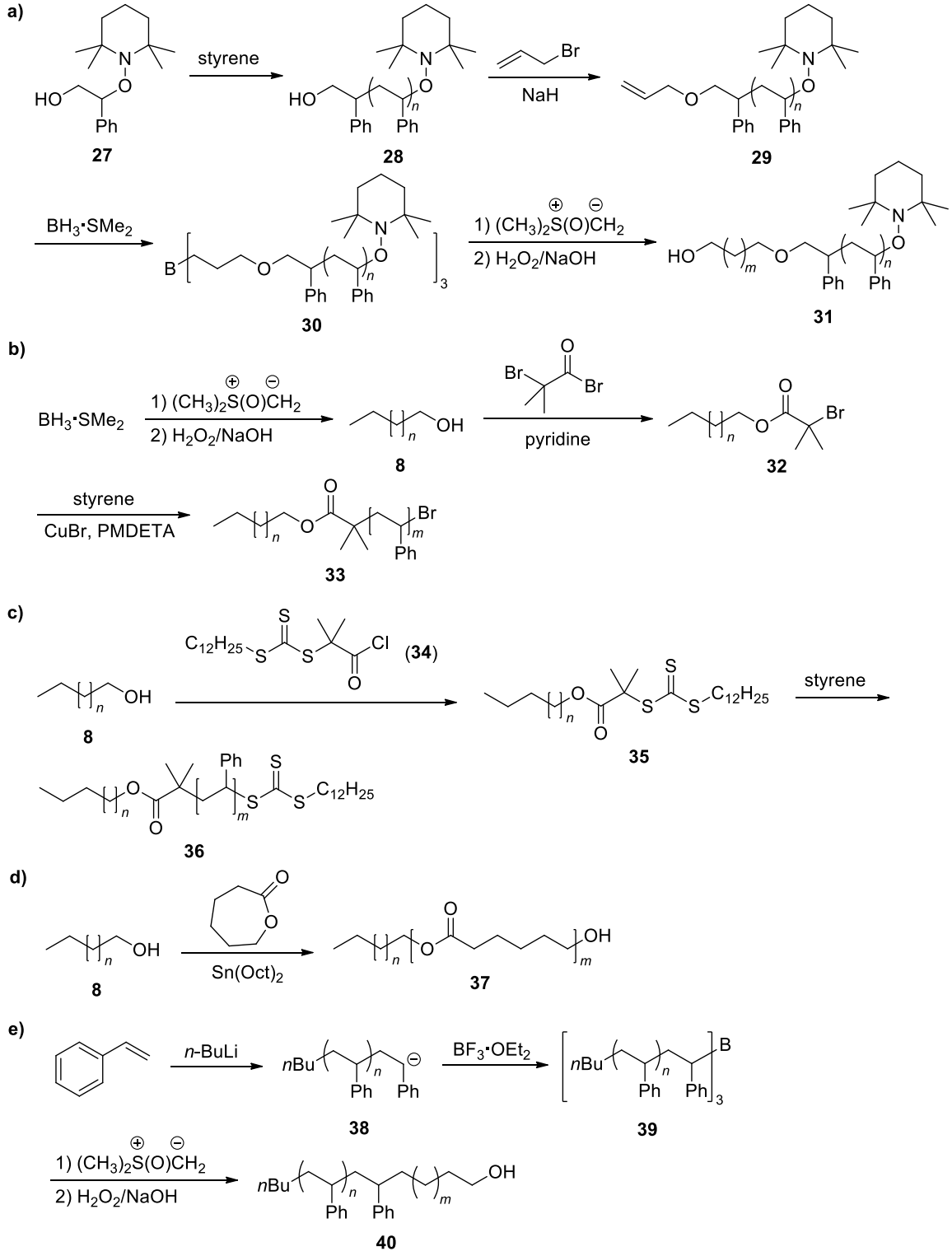

As the polyhomologation reaction can readily produce polymer chains with ω-hydroxyl group, the resulting polymer can directly serve as the macroinitiator for ring-opening polymerization of lactones. In the presence of ω-hydroxypolymethylene **8** and a coinitiator tin(II) 2-ethylhexanoate, ε-caprolactone was polymerized to afford polymethylene-*b*-polycaprolactone **37** (Scheme 1.12d).[41] The copolymer MW is as high as 17400 g/mol with PDIs less than 1.2 and content of PCL ranging from 51.7% to 87.0%. The synthesized PM-*b*-PCL can serve as a good compatibilizer for blending PM and PCL.

Since organoboranes can be synthesized *via* carbanions and $BF_3{\cdot}OEt_2$[18], the living anionic polymerization can be directly carried on to the polyhomologation reaction. With this strategy, polystyrene was first prepared by the living anionic polymerization (Scheme 1.12e).[42] Addition of $BF_3{\cdot}OEt_2$ converted the living chains to organoborane **39** *in-situ*. A subsequent standard polyhomologation reaction resulted in PS-*b*-PM with low PDI.

1.7. The Aqueous Polyhomologation Reaction

The conventional polyhomologation reaction requires preparation of the Corey ylide **1** or Johnson ylide **15a-c**. The syntheses of these ylides as well as the subsequent polymerizations need to be carried out under strictly anhydrous conditions in organic solvents at elevated temperatures. Development of a mild hydrocarbon production process is imminent that is more environmentally friendly and less energy consuming.

Recently, the polyhomologation reaction was extended to an aqueous system. The Corey ylide precursor, commercially available trimethylsulfoxonium iodide **41**, was polymerized in 50% sodium hydroxide aqueous solution at room temperature in an inert atmosphere (Scheme 1.13).[43] The organoborane initiators can be the same as the ones for conventional polyhomologation

reactions. To this reaction mixture, small amount of organic solvent dichloromethane (DCM) or toluene was introduced to solubilize the hydrocarbon oligomers at the early stage of polymerization. A phase-transfer catalyst, tetrabutylammonium iodide (TBAI), was also added to facilitate the migration of active reactants from the aqueous phase to the organic phase leading to an increased efficiency of initiation. After consumption of the monomer salt in 48 h, the reaction was open to air and filtered to afford a flocculent white material. Spectroscopic analysis of the white solid such as NMR and IR established its identity as polymethylene. Without a formal oxidation step, the polymer chain end consists of boronic and boric acids/esters, and their hydroxy complexes. The polymerization rate can be greatly accelerated at slightly higher temperature (40 ℃) with production of hydrocarbon polymers in near quantitative yield in 2 h.

Scheme 1.13. Polymerization of trimethylsulfoxonium iodide **41** initiated by tri-*n*-hexylborane in an aqueous base *via* the polyhomologation reaction.

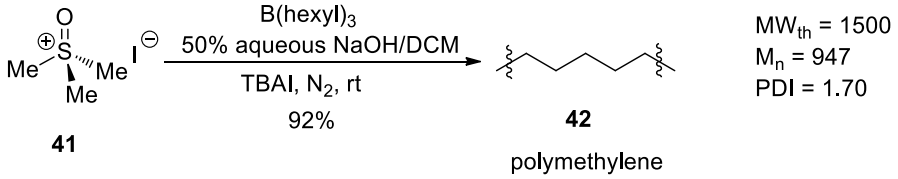

The aqueous polyhomologation is not a living polymerization, as broader MW distributions were observed compared to the traditional polyhomologation method, especially for high MW polymer synthesis (MW > 3 kDa). When the polymerization was carried out at higher temperatures (i.e., 40 ℃), polymers can be obtained with better control of MW and PDI up to the MW of 5–6 kDa.[26]

In this multi-phase reaction system, the polymerization mechanism can be complicated. The proposed mechanism involves production of the active ylide monomer and trivalent organoborane initiator (Scheme 1.14). Without use of concentrated base, sulfoxonium salt **41** does not undergo polymerization. Although sulfoxonium salt **41** has been reported to have a higher pK_a (~18)[44] than water, small amounts of ylide **1** can still be generated *in-situ* with a high

concentration of hydroxide (Scheme 1.14a). If the concentration of aqueous base was lowered, the polymer yield would drop to below 50% with loss of MW control.[26] In addition, organoboranes are Lewis acidic and do not stay intact under basic conditions. In the concentrated NaOH solution, most of trivalent organoborane **4** would be complexed by the abundant hydroxide to form the inactive tetravalent borate **42** (Scheme 1.14b). The complexation of **4** with hydroxide competes with the polyhomologation reaction using ylide **1**. However, this complexation reaction is in equilibrium and small amount of organoborane **4** can be released and transferred to the organic phase.

Scheme 1.14. Competing equilibrium reactions that influence the aqueous polyhomologation reaction. a) Production of the active ylide monomer **1**; b) Production of the active trivalent organoborane initiator **4**.

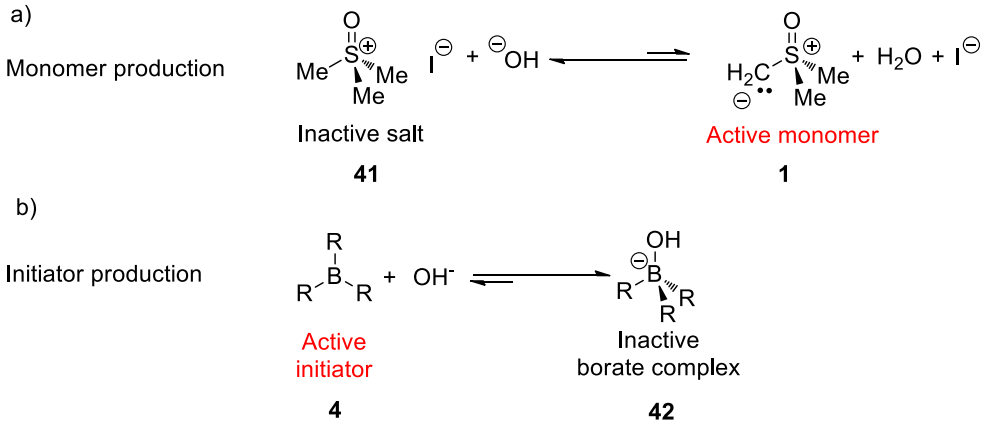

With both ylide and organoborane initiator present in the organic phase, the polymerization takes place and polymer grows with an irreversible 1,2-migration. This drives the equilibrium towards production of the active monomers and initiator until the complete consumption of salt **41**.

It should be noted that the starting sulfoxonium salt **41** has very poor solubility in both concentrated NaOH solution and dichloromethane, and mostly stays in its solid form. The proposed stepwise pathway explains how salt **41** is transferred to ylide **1** in organic phase (Scheme 1.15). The heterogeneous suspension functions as a monomer reservoir and the rapid

(but unfavorable) equilibrium between the dormant monomer **41** and the active monomer **1** is established in aqueous base creating a low but steady-state concentration of **1**. The *in-situ* generated ylide then partitions to the organic phase where the polymerization is initiated. The presence of TBAI can greatly facilitate these processes.

Scheme 1.15. Proposed pathway for sulfoxonium salt **41** transferred from the solid phase to ylide **1** in the organic phase.

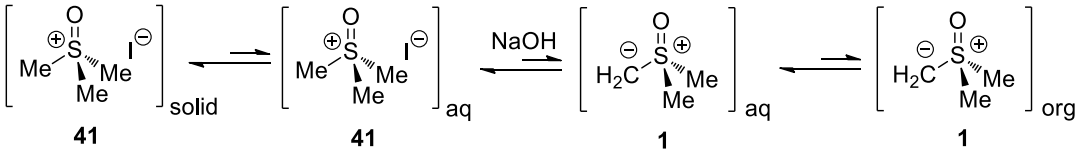

1.8. Research objectives

The polyhomologation reaction using organoborane catalysts and sulfoxonium ylides has been developed for synthesis of carbon backbone polymers by a mechanism that adds one carbon at a time to the growing polymer chain. The polymerization proceeds *via* complexation and rate-limiting 1,2-migration steps. The living character of the polyhomologation provides accurate control of polymer MW with low PDI. The polymer composition including chain-end and branch functionalization as well as polymer architecture can be finely tuned by the living polyhomologation reaction. In addition, this polymerization can be combined with many other living polymerization methods including NMP, ATRP, RAFT, ROP and living anionic polymerization to build well-defined block copolymers.

My thesis focused on three major objectives. First, my goal is to explore applications of the aqueous polyhomologation reaction. With the ability to control polymer chain length and PDI, this environmentally friendly reaction can be combined with other polymerization methods to readily produce commercialized polymers such as polyester, polycaprolactone-*b*-polymethylene and polyethylene glycol-*b*-polymethylene copolymers. Second, I aim to demonstrate the

sequence control in the carbon backbone polymers using the polyhomologation reaction. And lastly, I attempt to synthesize fully substituted carbon backbone polymers. This would require the development of single-site catalysts.

There are many other challenges left in this research field. Most involve synthetic challenges and require further efforts. For example, design of new ylide platforms that can incorporate functional groups (i.e., hydroxyl, carbonyl, amino and carboxyl) will help extend the application of the polyhomologation reaction. Further investigations on tuning the reaction energy profile are also necessary to achieve the ultimate polymer sequence control in which the complexation reaction became the rate-limiting step. Moreover, development of a living aqueous polyhomologation reaction can fully liberate our reliance on the traditional polyhomologation reaction to achieve control of polymer MW with low PDI.

1.9. References

(1) Peacock, A. J. *Handbook of Polyethylene: Structure, Properties, and Applications*; CRC Press: New York, 2000.

(2) Simmons, H. E.; Smith, R. D. *J. Am. Chem. Soc.* **1959**, *81*, 4256.

(3) Ihara, E.; Wake, T.; Mokume, N.; Itoh, T.; Inoue, K. *J. Polym. Sci., Part A: Polym. Chem.* **2006**, *44*, 5661.

(4) Ihara, E.; Kobayashi, K.; Wake, T.; Mokume, N.; Itoh, T.; Inoue, K. *Polym. Bull.* **2008**, *60*, 211.

(5) Noels, A. F. *Angew. Chem. Int. Ed.* **2007**, *46*, 1208–1210.

(6) Jellema, E.; Jongerius, A. L.; Reek, J. N. H.; de Bruin, B. *Chem. Soc. Rev.* **2010**, *39*, 1706–1723.

(7) Luo, J.; Shea, K. J. *Acc. Chem. Res*. **2010**, *43*, 1420–1433.

(8) Wang, D.; Zhang, Z.; Hadjichristidis, N. *ACS Macro Lett.* **2016**, *5*, 387–390.

(9) Landauer, S. R.; Rydon, H. N. *J. Chem. Soc.* **1953**, 2224–2234.

(10) Olah, G. A. Goeppert, A. Prakash, G. K. S. *Beyond Oil and Gas: The Methanol Economy*, 2nd ed.; Wiley-VCH: Federal Republic of Germany, 2009.

(11) Maruoka, K.; Oishi, M.; Yamamoto, H. *Macromolecules* **1996**, *29*, 3328.

(12) Hetterscheid, D. G. H.; Hendriksen, C.; Dzik, W. I.; Smits, J. M. M.; van Eck, E. R. H.; Rowan, A. E.; Busico, V.; Vacatello, M.; Van Axel Castelli, V.; Segre, A.; Jellema, E.; Bloemberg, T. G.; de Bruin, B. *J. Am. Chem. Soc*. **2006**, *128*, 9746.

(13) (a) Tufariello, J.; Lee, L. *J. Am. Chem. Soc.* **1966**, *88*, 4757–4759. (b) Tufariello, J.; Wojtkowski, P.; Lee, L. *J. Chem. Soc., Chem. Commun.* **1967**, 505–506. (c) Tufariello, J.; Lee, L.; Wotjkowski, P. *J. Am. Chem. Soc.* **1967**, *89*, 6804.

(14) Shea, K. J.; Walker, J. W.; Zhu, H.; Paz, M.; Greaves, J. *J. Am. Chem. Soc.* **1997**, *119*, 9049–9050.

(15) Busch, B. B.; Paz, M. M.; Shea, K. J.; Staiger, C. L.; Stoddard, J. M.; Walker, J. R.; Zhou, X.-Z.; Zhu, H. *J. Am. Chem. Soc.* **2002**, *124*, 3636–3646.

(16) Zhou, X. Z. Ph.D. Thesis, University of California, Irvine, 2002.

(17) Hicks, F.; Brookhart, M. *Organometallics* **2001**, *20*, 3217.

(18) Brown, H. C. *Organic Syntheses via Boranes*; Wiley: New York, 1975.

(19) Luo, J.; Zhao, R.; Shea, K. J. *Macromolecules* **2014**, *47*, 5484−5491.

(20) Stoddard, J. M.; Shea, K. J. *Organometallics* **2003**, *22*, 1124–1131.

(21) Busch, B. B.; Staiger, C. L.; Stoddard, J. M.; Shea, K. J. *Macromolecules* **2002**, *35*, 8330–8337.

(22) Wagner, C. E.; Rodriguez, A. A.; Shea, K. J. *Macromolecules* **2005**, *38*, 7286–7291.

(23) Odian, G. *Principles of Polymerization*, 4th ed.; Wiley: Hoboken, NJ, 2004.

(24) Zhou, X. Z.; Shea, K. J. *J. Am. Chem. Soc.***2000**, *122*, 11515–11516.

(25) Sulc, R.; Zhou, X.-Z.; Shea, K. J. *Macromolecules* **2006**, *39*, 4948–4952.

(26) Luo, J. Ph.D. Thesis, University of California, Irvine, 2012.

(27) Lu, F. Ph.D. Thesis, University of California, Irvine, 2012.

(28) Bai, J.; Shea, K. J. *Macromol. Rapid Commun.* **2006**, *27*, 1223–1228.

(29) Mondière, R.; Goddard, J.-P.; Huiban, M.; Carrot, G.; Gall, T. L.; Mioskowski, C. *Chem. Commun.* **2006**, 723–725.

(30) Lohse, D. J.; Milner, S. T.; Fetters, L. J.; Xenidou, M.; Hadjichristidis, N.; Mendelson, R. A.; Garcia-Franco, C. A.; Lyon, M. K. *Macromolecules* **2002**, *35*, 3066–3075.

(31) Bielawski, C. W.; Benitez, D.; Grubbs, R. H. *Science* **2002**, *297*, 2041–2044.

(32) McLeish, T. *Science* **2002**, *297*, 2005–2006.

(33) Shea, K. J.; Busch, B. B.; Paz, M. M. *Angew. Chem., Int. Ed*. **1998**, *37*, 1391–1393.

(34) Wagner, C. E.; Kim, J.-S.; Shea, K. J. *J. Am. Chem. Soc*. **2003**, *125*, 12179–12195.

(35) Wagner, C. E.; Shea, K. J. *Org. Lett*. **2001**, *3*, 3063–3066.

(36) Shea, K. J.; Lee, S. Y.; Busch, B. B. *J. Org. Chem*. **1998**, *63*, 5746–5747.

(37) Zhang, H.; Alkayal, N.; Gnanous, Y.; Hadjichristidis, N. *Macromol. Rapid Commun.* **2014**, *35*, 378−390.

(38) Zhou, X. Z.; Shea, K. J. *Macromolecules* **2001**, *34*, 3111–3114.

(39) Zhao, L.; Chen, J.; Shi, L.; Chen, W.; Li, G.; Wang, Y.; Ma, Z. *Acta Chim. Sin.* **2011**, *69*, 591.

(40) Wang, X.; Gao, J.; Zhao, Q.; Huang, J.; Mao, G.; Wu, W.; Ning, Y.; Ma, Z. *J. Polym. Sci., Part A: Polym. Chem*. **2013**, *51*, 2892.

(41) Li, Q.; Zhang, G.; Chen, J.; Zhao, Q.; Lu, H.; Huang, J.; Wei, L.; Dágosto, F.; Boisson, C.; Ma, Z. *J. Polym. Sci., Part A: Polym. Chem*. **2011**, *49*, 511.

(42) Zhang, H.; Alkayal, N.; Gnanou, Y.; Hadjichristidis, N. *Chem. Commun.* **2013**, *49*, 8952.

(43) Luo, J.; Lu, F.; Shea, K. J. *ACS Macro Lett.* **2012**, *1*, 560–563.

(44) Bordwell, F. G. *Acc. Chem. Res*. **1988**, *21*, 456−463.

Chapter 2. Convenient Controlled Aqueous C1 Synthesis of Long-chain Aliphatic AB, AA and BB Macromonomers for the Synthesis of Long-chain Aliphatic Polyesters

2.1. Introduction

Increasing worldwide demand for plastics has driven their exponential growth since the 1950s. Most of the worlds' synthetic plastics are derived from petroleum feedstock. Due to concerns of fossil fuel reserves, it is now important to focus on more abundant and/or renewable carbon sources for these vital materials. Biomass-derived monomers such as diacids, diols and ω-hydroxyacids from lignin, suberin and vegetable oils are being developed as sources of renewable building blocks for the preparation of medium-chain aliphatic polyesters.[1] Indeed, several biomass-based polyesters containing short and medium hydrocarbon chain segments have been commercialized. For example, polylactic acid (PLA) has found applications for packaging and biomedical uses. However, due to the low glass transition temperature of PLA and the low melting point of medium-chain aliphatic polyesters, these materials have figures of merit that limit their use as replacements for petroleum-based plastics such as polyethylene (PE) and polypropylene (PP). By incorporating longer hydrocarbon chains into the monomer unit, polymer crystallinity can be modulated and enhanced with performance that approaches high-density polyethylene (HDPE).[2] Long-chain aliphatic polyesters (LCAPs) therefore, are potential candidates to replace petroleum-based plastics.

Aliphatic polyesters comprised of long-chain fatty acids have been extensively studied.[2-4]

α,ω-Diacid/ester and ω-hydroxyacid/ester monomers for polycondensation can be chemically synthesized via alkoxycarbonylation[3], olefin metathesis[4] and thio-ene reactions[5] from natural fatty acid sources including oleic acid, 10-undecenoic acid and erucic acid. In addition to polycondensation, acyclic diene metathesis (ADMET) polymerization was also employed to synthesize LCAPs.[4a,5b,6] To date, these methods require the use of Pd, Ru or Co catalysts. In several examples, enzymatic ω-oxidation was employed to synthesize building blocks for LCAPs from naturally occurring fatty acids.[7] A decided advantage is that many of these diols and diacid/esters are available from renewable sources. However, their preparation involves multistep reactions using transition metal catalysts or enzymes. Nevertheless, this can be somewhat limiting since the range of hydrocarbon chain lengths is dependent on the diversity of naturally occurring acids and esters that biology provides. There remains a challenge to synthesize long-chain aliphatic building blocks with variable lengths of hydrocarbon chain segments using either renewable or more abundant carbon sources by synthetic pathways that avoid hazardous and/or toxic substances.

In this chapter, I will describe a convenient synthesis of long-chain aliphatic macromonomers including ω-hydroxyacid esters (AB), α,ω-diols (AA) and α,ω-diacids (BB) for use as precursors to long-chain aliphatic polyesters. The synthesis of these telechelic macromonomers utilizes C1 carbon sources, which are derived from more abundant, non-petroleum feedstocks. The polymerization provides control over the average aliphatic chain length and is regulated only by the stoichiometric ratio of monomer/initiator. The AB macromonomers are produced as suspensions in aqueous base in a one-pot reaction without the use of transition metal catalysts. This reaction is ideally suited for synthesis of telechelic polymers with well controlled average molecular weight (MW) and polydispersity (PDI).

Polyesters obtained by a subsequent condensation polymerization of AB macromonomers exhibit indistinguishable thermal and mechanical properties to those of comparable LCAPs prepared from AA and BB type monomers derived from biomass.

In contrast to the conventional C2 olefin polymerization, C1 polymerizations utilize sulfoxide ylides and diazo compounds as monomers.[8] For sulfoxide ylide polymerizations, trialkylboranes serve as a Lewis acid catalyst/initiator for the nexus of three propagating hydrocarbon chains. Following consumption of the ylide, the hydrocarbon chains are oxidatively cleaved from boron to yield a hydroxyl terminated linear polymethylene chain. This living polymerization provides precise control of MW and the opportunity to introduce functional groups on the carbon backbone.[8a] The reactions are carried out in an inert atmosphere using anhydrous organic solvents. Recently, an aqueous variant of this C1 polymerization was developed for the preparation of linear hydrocarbon waxes.[9] The reaction is run at or near ambient temperature in an aqueous base suspension of the ylide precursor, trimethylsulfoxonium halide, and proceeds rapidly with MW control in the range of 500–7000 g/mol. The active ylide monomer **2** generated *in–situ* by deprotonation of the sulfoxonium salt **1** in the aqueous base partitions to the organic phase where it homologates the organoborane initiator (Scheme 2.1). Each homologation was accomplished by complexation of ylide monomer with the initiator followed by a subsequent 1,2-migration. The B–C bond was eventually cleaved during oxidation to produce α-hydroxypolymethylene **6**.

Scheme 2.1. Mechanism of the polyhomologation reaction with trimethylsulfoxonium iodide **1** in aqueous base.

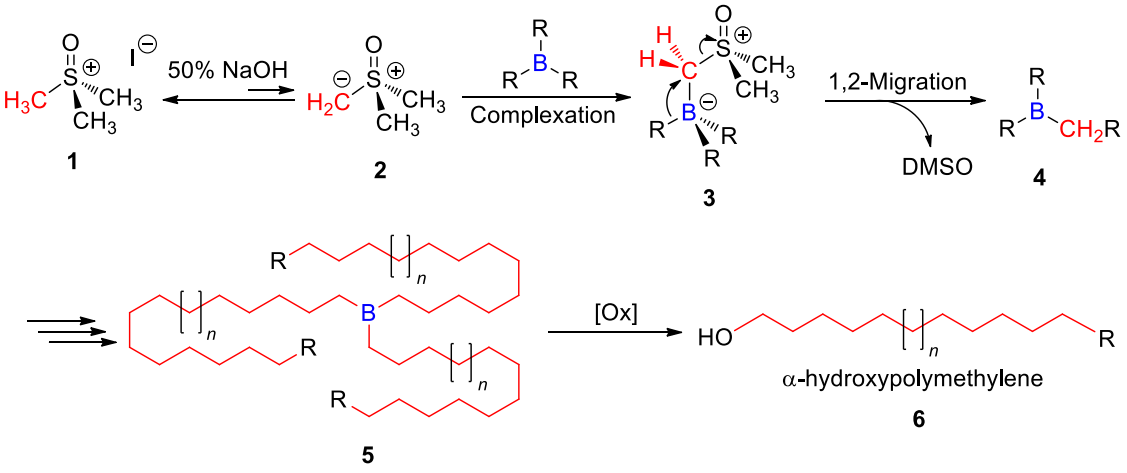

The monomer precursor, trimethylsulfoxonium halide, is synthesized from a functional C1 molecule (e.g., methyl halide) and dimethylsulfoxide (DMSO), a byproduct of the paper industry. DMSO serves as a carrier for the active C1 fragment and is not consumed (Scheme 2.2). It can be recovered and recycled from the polymerization. The polymer building blocks, C1 molecules, are derived from abundant non-petroleum sources including coal, natural gas and biomass. For example, methanol can be made from a variety of feedstocks, and is one of the most versatile chemical commodities and energy sources available today. Syngas as one source to produce methanol is comprised primarily of carbon monoxide and hydrogen gas and can be derived from biomass via steam gasification. In addition, CO_2 can be converted into methanol by hydrogenation, a technology that is already commercially being used.[10]

Scheme 2.2. A simplified schematic of the materials cycle for production of polymethylene from biomass or carbon dioxide via C1 polymerization.

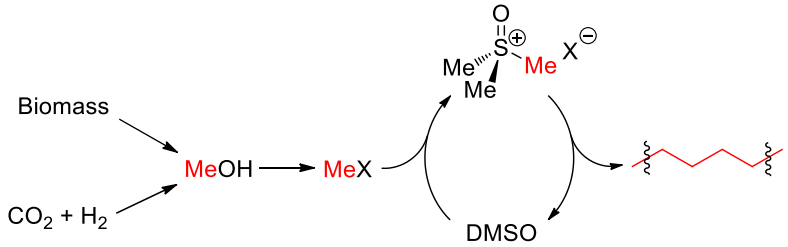

2.2. Results and Discussion

My objective is to develop versatile, efficient and practical methods to synthesize telechelic macromonomers using C1 polymerization. These long-chain aliphatic AB, AA and BB macromonomers are telechelic polymers for the synthesis of LCAPs. Several telechelic linear polymethylenes have been synthesized via the traditional non aqueous C1 polymerization.[11-12] α-Chain end functionality is realized by the use of α-functional organoborane initiators (Scheme 2.3). These initiators are typically synthesized via hydroboration of functional α-olefins. To obtain an α-carboxyl-ω-hydroxypolymethylene, the most direct application of this strategy would be by incorporating a pre-installed carboxyl or ester group on the organoborane initiator. The success of this approach requires selection of the functional group to be compatible with the hydroboration reaction. The oxidative cleavage of the carbon–boron bond following polymerization introduces the ω-hydroxyl group.

Scheme 2.3. Synthesis of telechelic polymethylenes from functional α-olefins.

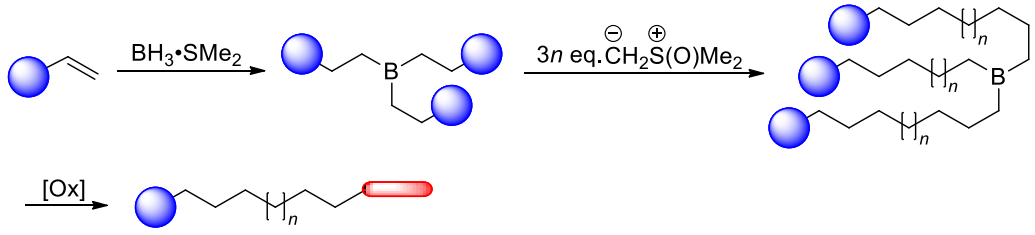

2.2.1. Synthesis of the AB macromonomer

Since carboxylic acids and many acid esters react with borane,[13] they must be protected to survive the hydroboration and subsequent aqueous C1 polymerization. The *tert*-butyl ester was selected as it is stable against borane and many common bases at ambient temperatures. In the event, the initiator was prepared first for synthesis of the long-chain aliphatic AB macromonomers (Scheme 2.4). I chose the readily available 5-hexenoic acid **7** as the precursor

for synthesis of the initiator. The carboxylic acid **7** was protected as the *tert*-butyl ester **8** followed by hydroboration to obtain the organoborane initiator **9**. A small amount (< 15%) of methyl branch side products arises from the less than perfect regioselectivity of the hydroboration reaction. The combined yield of the major and side product of the hydroboration reaction was quantitative. Other ω-ene linear carboxylic acids such as 4-pentenoic acid would also function to serve as starting materials for synthesis of telechelic AB macromonomers.

Scheme 2.4. Preparation of *tert*-butyl ester functionalized organoborane **9** for synthesis of telechelic macromonomers.

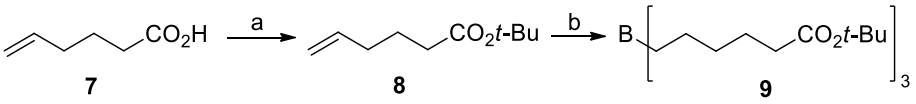

Reagents and conditions: (a) *tert*-butanol, dicyclohexylcarbodiimide, 4-dimethylaminopyridine, rt, 71%; (b) $BH_3 \cdot SMe_2$, 0 ℃ to rt, quantitative.

To achieve the polymer MW control, the amount of initiator introduced to the polymerization solution must be accurate. A common employed strategy was to dissolve a known quantity of the organoborane in a given volume of solvent to have an accurate concentration. The amount of the injected initiator can be calculated based on the actual volume of injection. This method, however, requires purified organoboranes. The organoboranes with three *tert*-butyl ester functions have both high boiling points and low tendency to crystallize which made a challenge for their purifications.

One solution is to determine the concentration of the organoborane *in-situ* via ^{1}H NMR with an internal standard. Here a chemically inert compound, 1,4-dioxane, with distinctive ^{1}H chemical shifts was chosen as the internal standard. A ^{1}H NMR example is shown below with all peaks assigned to the related structures (Figure 2.1). The total amount of organoboranes, regardless of regioisomers, can be calculated by Equation 2.1.

$$\frac{n_{BR_3}}{n_{1,4\text{-dioxane}}} = \frac{I_a / 6}{I_{1,4\text{-dioxane}} / 8} \qquad \text{Eq. (2.1)}$$

where *I* stands for the integration value of a certain peak.

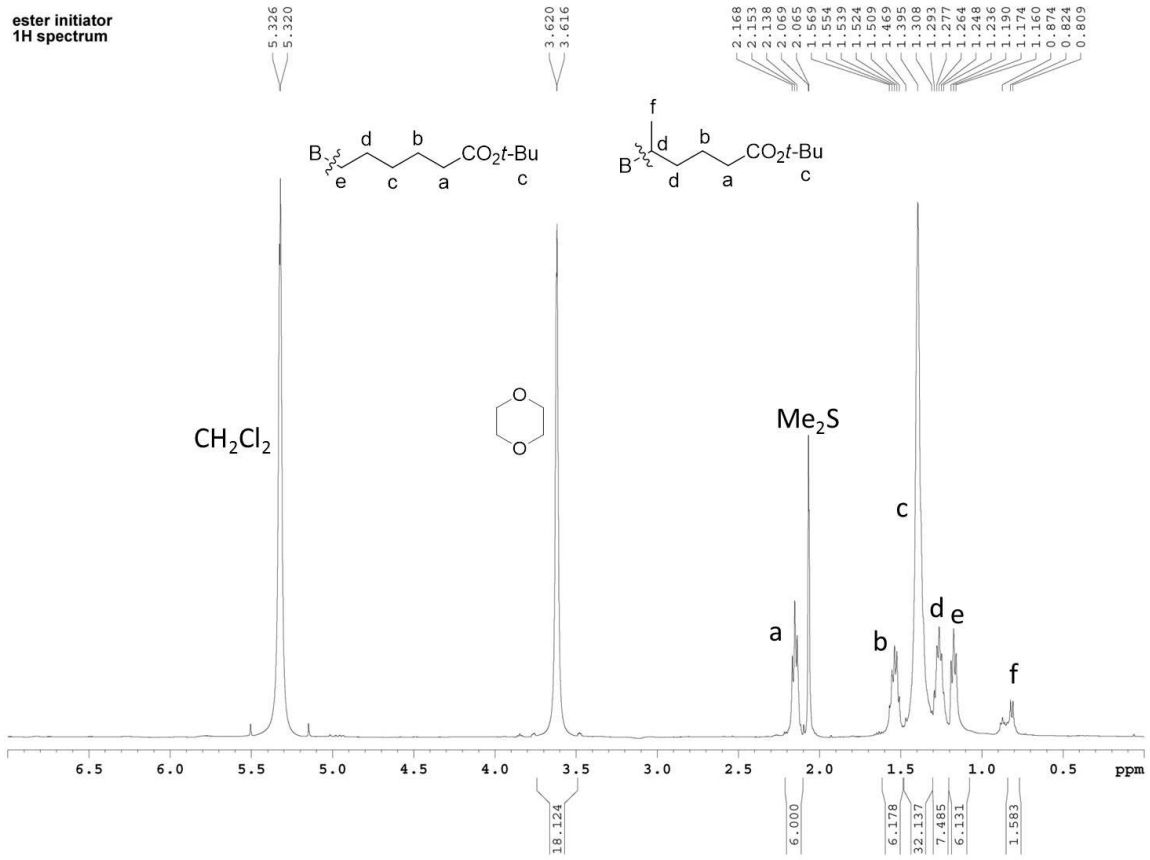

Figure 2.1. Determination of the concentration of organoborane **9** via ^{1}H NMR with 1,4-dioxane as the internal standard.

Aqueous C1 polymerizations were carried out using organoborane **9** with ratios of monomer **1**: initiator **9** ranging from 15 to 55 carbons (Scheme 2.5, Table 2.1). The polymers **10** were obtained after an overnight reaction in high yield with MW control and relatively low PDI. The *tert*-butyl protecting group was found to remain intact during the polymerization. The degree

of polymerization (DP) by end group analysis from ^{1}H NMR well corroborates the theoretical values calculated from the feed ratio of monomer **1**: initiator **9**.

Scheme 2.5. Synthesis of AB macromonomers **10** via the aqueous C1 polymerization.

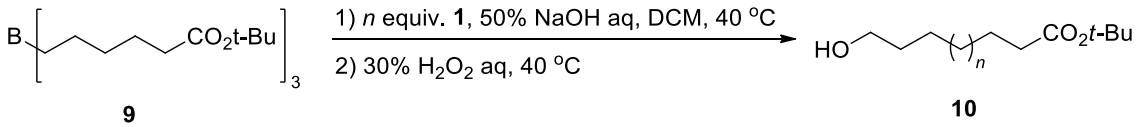

9 **10**

Table 2.1. Synthesis of AB macromonomers **10** via the aqueous C1 polymerization.

sample[a]	yield (%)	MW_{th}[b] (g/mol)	DP_{th}[b]	DP_{NMR}[c]	M_n[d] (g/mol)	M_w[d] (g/mol)	PDI[d]
PM20	76	398	15	19	413	422	1.02
PM30	87	538	25	29	539	581	1.08
PM40	88	678	35	38	701	876	1.25
PM50	92	818	45	42	821	1142	1.39
PM60	92	958	55	54	1058	1861	1.76

a. The samples were named after the theoretical number of methylene units present in the polymer chain based on reaction stoichiometry and takes into account the 5 CH_2 units from the initiator.
b. DP_{th} is the theoretical degree of polymerization based on reaction stoichiometry. MW_{th} is the theoretical MW calculated as $MW_{th} = (DP_{th} + 5) \times M_{CH2} + M_{OH} + M_{COOtBu}$.
c. DP_{NMR} is degree of polymerization (excluding the 5 CH_2 units from the initiator) obtained by end-group analysis via ^{1}H NMR.
d. M_n, M_w and PDI were obtained from GPC analysis using low MW hydrocarbon and polyethylene standards.

After consumption of the monomer, the B–C bond was oxidatively cleaved by addition of hydrogen peroxide to the basic solution. Routine oxidation of polymer-based organoboranes **5** using trimethylamine-*N*-oxide (TAO) requires a high temperature of at least 60 ℃ to achieve a quantitative conversion of polymer chain ends to terminal hydroxyl groups.[14] These criteria can be accomplished with ease in the conventional polyhomologation reaction, in part because the crude medium-chain polymer is soluble in toluene at 60 ℃ or above. In the aqueous C1 polymerization, the polymer is insoluble in the concentrated aqueous base. In addition, the *tert*-butyl group cannot survive the aqueous base for a long time at elevated temperatures. In contrast, the oxidation method with H_2O_2 is efficient at ambient temperatures. Although it would introduce small amounts of other polymer chain ends such as –H and –CHO as well as polymers

with double MW[15], these impurities do not inhibit the polycondensation reaction. Also, oxidation using H_2O_2 requires the presence of an aqueous base which complies with the aqueous polyhomologation reaction condition. Therefore H_2O_2 instead of TAO was employed to carry out the oxidation. The long-chain aliphatic AB macromonomer, ω-hydroxyacid *t*-butylester **10**, was isolated by filtration in excellent yield.

The PDI of macromonomers increases slightly as the polymer chain increases from PM20 to PM60. As mentioned previously, the reaction system is heterogeneous. During the initial stage of the reaction, methylene insertions in the organoborane are taking place in the organic phase. However, very soon after, they precipitate as the linear hydrocarbon chains grow. The hydrocarbon polymer rapidly solidifies due to the much lower polymerization temperature than its melting point (~ 120 ℃). These precipitates are polycrystalline particles located at the solvent interface containing catalytic boron centers, some embedded in the crystalline domains that are stacked lamella (Figure 2.2).[9] The remaining polymerization takes place in the solid polycrystalline hydrocarbon polymer phase. Growth continues by diffusion of ylide from the aqueous basic phase through the amorphous domains in the polycrystalline hydrocarbon polymer. As the particle and crystalline domain size increases, polymer growth slows and an increasing fraction of catalytic boron centers becomes inaccessible and no longer active resulting in a gradual increase on the polymer PDI at higher MWs.

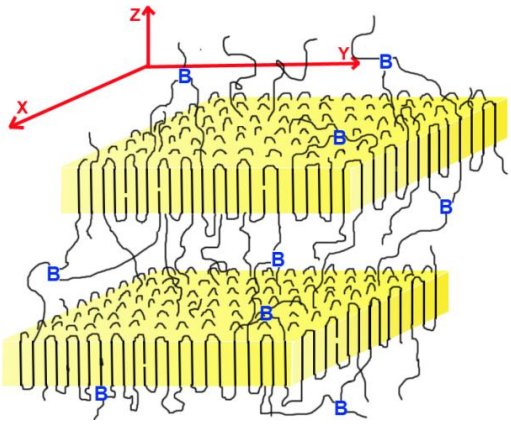

Figure 2.2. Schematic representation of the orientation of lamellae and organoborane initiator/catalysts in the crystalline/amorphous domains.

*2.2.2 Attempted removal of the t-butyl protecting group on macromonomer **10***

Hydrolysis of the AB macromonomer **10** to the deprotected long-chain ω-hydroxyacid **11** presented several unanticipated challenges (Scheme 2.6). The low solubility of long-chain hydrocarbons **10** in common organic solvents such as dichloromethane, acetonitrile and THF at room temperature made many popular hydrolysis methods inapplicable and resulted in low conversions. The first method tested was adopted from a recent report using aqueous phosphoric acid (85 wt %).[16] The reaction conditions are mild and offer good selectivity in the presence of other acid-sensitive groups. The hydrolysis reaction was carried out by adding H_3PO_4 to a solution of polymer **10** in toluene at various temperatures. The reaction has a conversion of 58% at 50 ℃ for overnight and only 68% even at 100 ℃ for an additional 12 h. The hydrolysis using H_3PO_4 failed to give high conversions after several attempts. This is probably due to the heterogeneity of the reaction that the phosphoric acid is immiscible with the polymer solution in toluene.

Scheme 2.6. Attempted removal of *tert*-butyl group in AB macromonomers **10** using phosphoric acid.

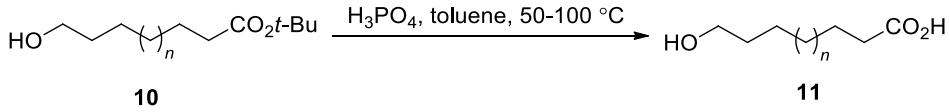

A second method was employed with the routine procedure to remove the *tert*-butyl group on an ester. Trifluoroacetic acid (TFA) was added to the polymer solution in toluene at 70 ℃ (Scheme 2.7). A complete removal of the *tert*-butyl group was observed with disappearance of the sharp singlet peak at 1.38 ppm (Figure 2.3). However, most hydroxyl groups were converted to trifluoroacetate evidenced by ^{1}H chemical shift from 3.35 to 3.87 ppm.

Scheme 2.7. Attempted removal of *tert*-butyl group in AB macromonomers **10** using trifluoroacetic acid.

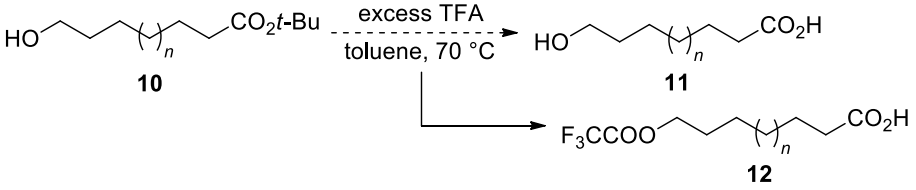

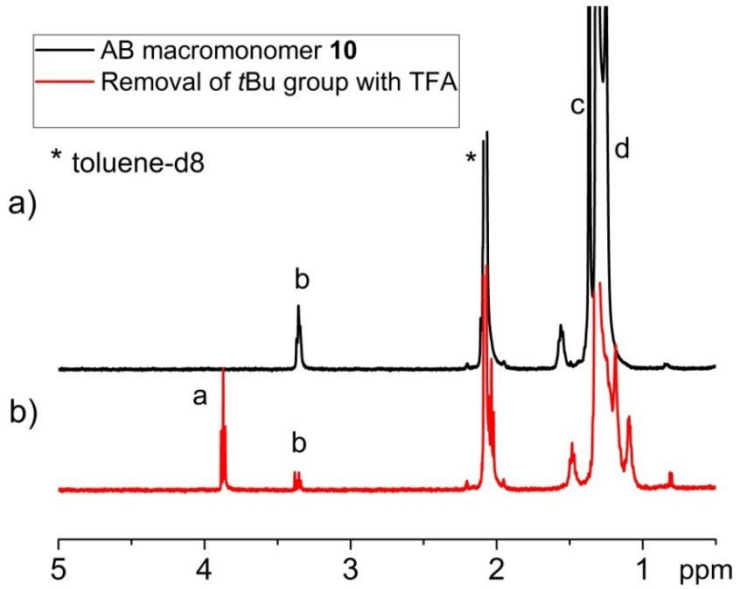

Figure 2.3. Stacked ^{1}H NMR spectra of a) starting AB macromonomer **10** and b) its hydrolysis products using TFA. For all spectra, the peak intensities at 1.4 and 2.1 ppm were truncated for clarity. Only major diagnostic peaks were labelled for analysis. Peak assignments are: a = $CF_3COO–C\underline{\mathbf{H}}_2–$, b = $–C\underline{\mathbf{H}}_2–OH$, c = $–COO–C(C\underline{\mathbf{H}}_3)_3$, d = $R–C\underline{\mathbf{H}}_2–R$.

TFA is widely used to hydrolyse *tert*-butyl ester at or below room temperature where hydroxyl groups do not become esterified. Due to the low solubility of macromonomer **10**, the reaction has to be carried out at elevated temperatures to achieve homogeneity. This results in competing esterification reactions between the hydroxyl group and TFA. To minimize the esterification, one set of experiments were set up to monitor the product distribution using increasing amount of TFA at 70 ℃ (Table 2.2). Preliminary results indicated that the hydroxyl group is esterified by TFA to a very low degree before removal of the *tert*-butyl group. With slight excess of TFA (entry 2, 1.05 eq.), only a small fraction of **10** was reacted. A large excess of TFA completely removed all *tert*-butyl groups but meanwhile esterified most of the hydroxyl groups (entry 3). Further investigations are required to achieve a clean hydrolysis by tuning the reaction time and ratio between TFA and macromonomer **10**.

Table 2.2. Removal of *tert*-butyl group in macromonomer **10** with different amounts of TFA.

entry	TFA (equiv.)	time (h)	conversion (%)	n_{11}:n_{12}[a]
1	< 0.1	9	26	1 : 0
2	1.05	10	31	1 : 0
3	5.2	6	100	0 : 1

a. Molar ratio of polymer **11** : **12** calculated by ^{1}H NMR end group analysis after the hydrolysis with TFA.

With the TFA ester **12** in hand, hydrolysis conditions were also studied to deprotect hydroxyl groups. Removal of the TFA protecting group was performed using aqueous NaOH solution (Scheme 2.8). The hydrolysis was carried out under basic conditions at 90 ℃ to dissolve the starting material **12**. After 24 hours of reaction, a subsequent protonation of the carboxylate was performed with HCl solution at room temperature overnight. The final macromonomer product was obtained as a solid with low solubility in many solvents including even toluene. GPC analysis on the products showed a very broad MW distribution, and in some cases multimodal MW distribution. Careful inspections via ^{1}H NMR spectra revealed contamination of

11 with ester oligomers (Figure 2.4), which is consistent with the observed broad MW distributions.

Scheme 2.8. Attempted removal of the trifluoroacetyl group in long-chain TFA ester **12**.

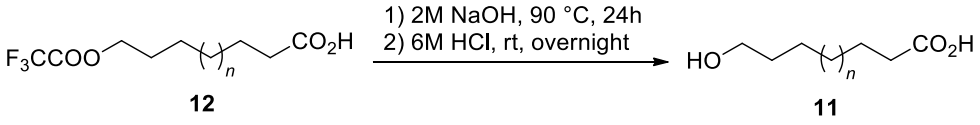

12 **11**

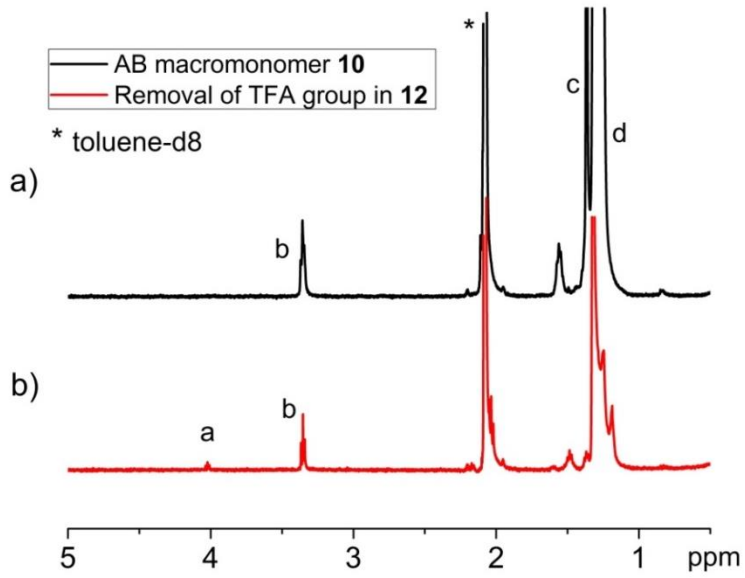

Figure 2.4. Stacked ^{1}H NMR spectra of a) a sample of AB macromonomer **10** and b) the hydrolysis products of **12** using NaOH. For all spectra, the peak intensities at 1.4 and 2.1 ppm were truncated for clarity. Only major diagnostic peaks were labelled for analysis. Peak assignments are: a = $RCH_2COO–C\underline{\mathbf{H}}_2–$, b = $–C\underline{\mathbf{H}}_2–OH$, c = $–COO–C(C\underline{\mathbf{H}}_3)_3$, d = $R–C\underline{\mathbf{H}}_2–R$.

*2.2.3. Synthesis and characterization of polyesters from AB macromonomers **10***

Although a clean removal of the *tert*-butyl protecting group in AB macromonomer **10** was not achieved, I was pleased to learn that these telechelic macromonomer *tert*-butylesters can be directly used in the polyester synthesis. The polycondensations were carried out at high temperatures in the presence of Ti(O-*n*Bu)$_4$ catalyst (Scheme 2.9). The LCAPs **13** were obtained in near quantitative yield with moderate MW and PDI (Table 2.3). For GPC analysis,

polyethylene standards were used instead of the commonly used polystyrene standards, because the latter one overestimates MW for polymers with linear hydrocarbon chain segments.[17] For further verification, I tested the thermal and physical behaviour of the LCAPs **13**.

Scheme 2.9. Synthesis of LCAPs **13** by polycondensation of AB macromonomers **10**.

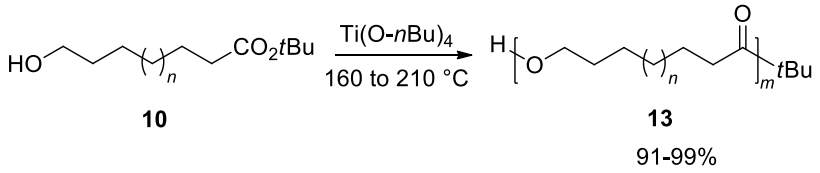

10 **13**

91-99%

Table 2.3. Results of polyesters **13** synthesized from AB macromonomers **10**.

sample[a]	yield (%)	M_n[b] (g/mol)	M_w[b] (g/mol)	PDI[b]	T_m[c] (°C)	ΔH_m[c] (J/g)
P(PM20)	91	10.9K	19.3K	1.76	102.0	164.1[d]
P(PM30)	91	11.5K	18.0K	1.57	111.7	153.7
P(PM40)	95	10.3K	17.7K	1.73	116.0	155.9
P(PM50)	99	11.0K	18.0K	1.63	115.5,124.2[e]	184.9
P(PM60)	94	11.9K	17.7K	1.48	121.5,124.3[e]	184.9

a. Samples were named after the macromonomer **10**. P(PM20) represents the polyester synthesized from PM20.
b. Determined using GPC analysis with polyethylene standards.
c. Measured using DSC analysis.
d. This high enthalpy of melting is because of the very low PDI of the macromonomer (1.02) which gives a uniform distribution of ester groups along the polymer chain.
e. The presence of two melting peaks is probably due to different lengths of hydrocarbon chain segments in the polyester caused by the increased PDI of the corresponding macromonomer **10**.

Thermal analysis revealed that the LCAPs have an increased melting point with an increasing length of the hydrocarbon chain segment (Figure 2.5a), in agreement with the reported trends.[6b,18] Next I examined the mechanical properties of the materials. All polymers exhibited a stress–strain behavior of brittle materials (Figure 2.5b). The stress increased rapidly with strain prior to brittle fracture at a percentage strain of approximately 2% (Table 2.4). The values of elongation at break (EB) are in the same range as reported for medium-chain aliphatic polyesters of similar MW.[19] With an increasing length of hydrocarbon chain segment from P(PM20) to P(PM60), the polyesters exhibited an increased tensile strength (TS) and Young's modulus. The TSs are lower compared to literature values due to the lower M_n of our samples as discussed by

Narine et al.[19] The polyester with short hydrocarbon chain length as P(PM20) has similar Young's modulus as those prepared from pure ω-hydroxyacids originated from biomass.[19] The polyester with the longest hydrocarbon chain segment, P(PM60), achieved an average Young's modulus of 876 MPa, close to the value of 900–1200 MPa for typical high MW HDPE.[20]

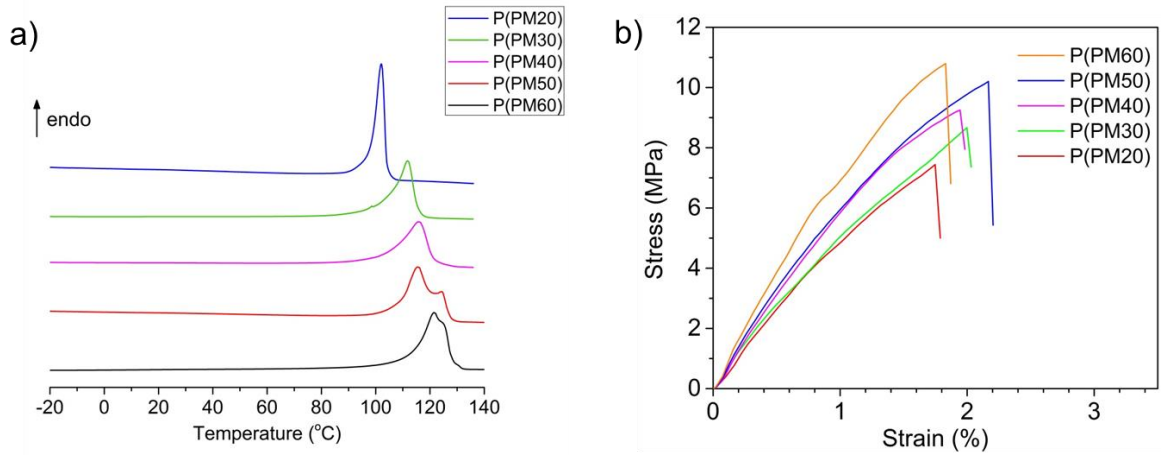

Figure 2.5. a) Stacked DSC traces of LCAPs over the temperature range of −20–140 ℃. b) Stacked stress–strain curves of LCAPs as a function of hydrocarbon chain length.

Table 2.4. Tensile analysis results of polyesters **13**.

sample	M_n (g/mol)	EB[a] (%)	TS[a] (MPa)	E[a] (MPa)
P(PM20)	10.9K	1.8 ± 0.2	7.5 ± 1.0	626 ± 30
P(PM30)	11.5K	2.0 ± 0.4	8.0 ± 0.6	641 ± 25
P(PM40)	10.3K	2.1 ± 0.3	8.4 ± 0.9	693 ± 28
P(PM50)	11.0K	2.0 ± 0.3	9.0 ± 0.9	747 ± 44
P(PM60)	11.9K	1.9 ± 0.3	10.1 ± 0.7	876 ± 25

a. EB = elongation at break; TS = tensile strength; E = Young's modulus.

*2.2.4. Synthesis of long-chain aliphatic α,ω-diol (AA) and α,ω-diacid (BB) from **10***

In addition to serve as AB macromonomers for LCAP synthesis, the ω-hydroxyacid *t*-butylester **10** can also be used as precursors for AA and BB macromonomers. These α,ω-diols and diacids are synthetic bolaamphiphiles with a fascinating chemistry all of their own.[21] The AA and BB macromonomers are also valuable precursors for preparation of long-chain aliphatic

α,ω-diene, acetals, dithiols, esters and amides. Importantly, they can be used as additives in AA–BB polycondensations to modulate the physical properties of the polyesters.

Long-chain aliphatic α,ω-diols **14** and diacids **15** were synthesized by reduction or oxidation of the AB macromonomers **10** in high yield (Scheme 2.10). Reduction to α,ω-diols **14** was achieved by use of lithium aluminum hydride ($LiAlH_4$). However, the oxidation of **10** to the corresponding α,ω-diacids **15** was found to be not as straightforward.

Several one-step oxidation methods were investigated.[22-24] Although these reactions work well for small organic molecules in polar solvents, the same conditions gave low conversion of **10** due to its low solubility in polar solvents. Elevated temperatures (> 60 ℃) in toluene or decalin solvent can dissolve the macromonomers. Furthermore, contamination was observed with byproducts arising from oxidation of hemiacetals, intermediates by reaction between –CHO and the unreacted –OH group, as evidenced by NMR absorptions at 4.1 ppm (–COO–CH_2–). A successful strategy was found by carrying out the oxidation in two steps. The use of stabilized 2-iodoxybenzoic acid (SIBX) can convert the hydroxyl group to an aldehyde in high yield.[25] Following removal of the *tert*-butyl protecting group with TFA, the α,ω-diacid **15** was obtained by oxidation with sodium chlorite.[26] NMR analysis indicated pure product without ester or acetal contamination (Figure 2.6). IR and elemental analysis were also performed to confirm the result (Chapter 2.5 experimental and Appendix D).

Scheme 2.10. Synthesis of AA and BB macromonomers from AB macromonomers **10**.

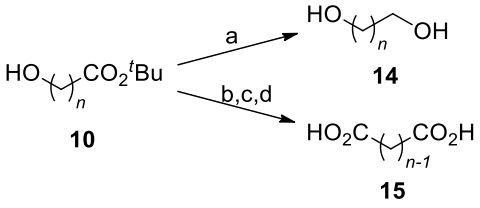

Reagents and conditions: a) $LiAlH_4$, THF, 85%; b) SIBX, toluene; c) TFA, toluene; d) $NaClO_2$, 30% H_2O_2 aq, NaH_2PO_4, toluene/acetonitrile/H_2O, 74% in 3 steps.

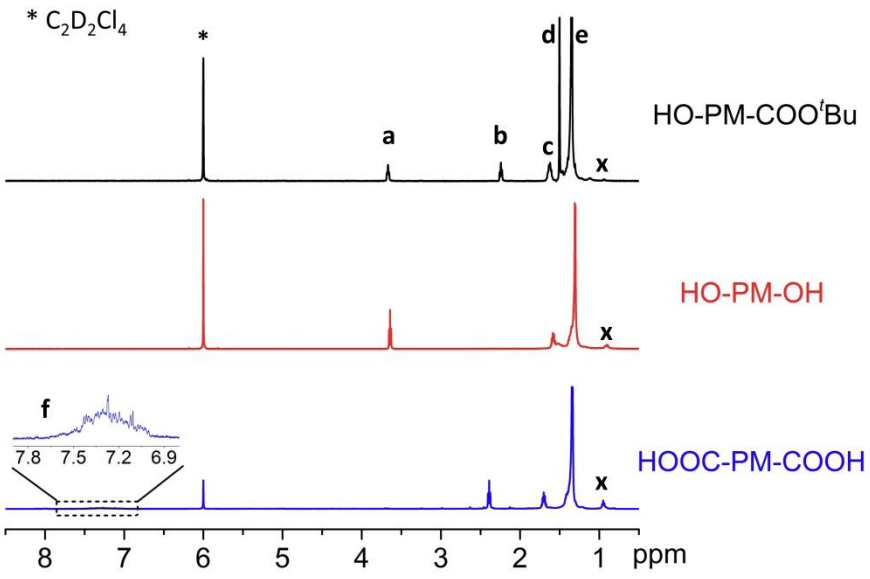

Figure 2.6. Stacked ^{1}H NMR spectra of the AB, AA and BB macromonomers. For all spectra, the peak intensity at 1.4 ppm was truncated for clarity. Peak assignments are: a = –C**H**$_2$–OH, b = –C**H**$_2$–COO–, c = –C**H**$_2$–CH$_2$OH and –C**H**$_2$–CH$_2$COO–, d = –COO–C(C**H**$_3$)$_3$, e = –C**H**$_2$– in the polymer chain, f = –COO**H** in $C_2D_2Cl_4$ that matches the literature report[4a], x = methyl branch from regioisomer of hydroboration.

2.3. Conclusion

In summary, I have developed a simple, convenient low-tech synthesis of AB, AA and BB long chain aliphatic macromonomers. ω-Hydroxy long-chain aliphatic acid *t*-butylesters with hydrocarbon chain lengths ranging from C20–C60 were synthesized by the aqueous C1 polymerization. Although a perfect deprotection of the carboxyl group was not achieved, the ω-hydroxy aliphatic acid *t*-butylesters can still be polymerized *via* polycondensation. These telechelic macromonomers were used to produce long-chain aliphatic polyesters with comparable thermal and mechanical properties to those with similar aliphatic chain lengths synthesized from biomass. The length of hydrocarbon chain segment was precisely tuned over a wide range of carbon numbers by adjusting the ratio of monomer/initiator. With this strategy, one can prepare AB macromonomers with various hydrocarbon chain lengths using readily

available reagents in a one-pot aqueous C1 polymerization. The length of hydrocarbon chain segments can go beyond the limit of long-chain fatty acids/esters that nature provides. This method utilizes C1 monomers from abundant and non-petroleum based C1 sources under eco-friendly conditions with no transition metals. Moreover, the AB type macromonomers can be readily converted to the corresponding α,ω-diols and diacids for use as co-monomers with medium- or short-chain diols and diacids.

2.4. References

(1) Vilela, C.; Sousa, A. F.; Fonseca, A. C.; Serra, A. C.; Coelho, J. F. J.; Freirea, C. S. R.; Silvestre, A. J. D. *Polym. Chem.* **2014**, *5*, 3119–3141.

(2) Stempfle, F.; Ortmann, P.; Mecking, S. *Chem. Rev.* **2016**, *116*, 4597–4641.

(3) (a) Quinzler, D.; Mecking, S. *Chem. Commun.* **2009**, 5400–5402; (b) Quinzler, D.; Mecking, S. *Angew. Chem., Int. Ed.* **2010**, *49*, 4306–4308; (c) Stempfle, F.; Quinzler, D.; Heckler, I.; Mecking, S. *Macromolecules* **2011**, *44*, 4159–4166.

(4) (a) Trzaskowski, J.; Quinzler, D.; Bährle, C.; Mecking, S. *Macromol. Rapid Commun.* **2011**, *32*, 1352–1356; (b) Vilela, C.; Silvestre, A. J. D.; Meier, M. A. R. *Macromol. Chem. Phys*. **2012**, *213*, 2220–2227; (c) Winkler, M.; Meier, M. A. R. *Green Chem.* **2014**, *16*, 3335–3340.

(5) (a) Samuelsson, J.; Jonsson, M.; Brinck, T.; Johansson, M. *J. Polym. Sci. A Polym. Chem.* **2004**, *42*, 6346–6352; (b) Türünç, O.; Meier, M. A. R. *Macromol. Rapid Commun.* **2010**, *31*, 1822–1826; (b) Türünç, O.; Meier, M. A. R. *Green Chem.* **2011**, *13*, 314–320.

(6) (a) Warwel, S.; Tillack, J.; Demes C.; Kunz, M. *Macromol. Chem. Phys*. **2001**, *202*, 1114–1121; (b) Ortmann, P.; Mecking, S. *Macromolecules* **2013**, *46*, 7213–7218.

(7) For selected reports: (a) Kusunose, M.; Kusunose E.; Coon, M. J. *J. Biol. Chem*. **1964**, *239*, 1374–1380; (b) Picataggio, S.; Rohrer, T.; Deanda, K.; Lanning, D.; Reynolds, R.; Mielenz, J.; Eirich, L. D. *Nat. Biotechnol*. **1992**, *10*, 894–898; (c) Eschenfeldt, W. H.; Zhang, Y.; Samaha, H.; Stols, L.; Eirich, L. D.; Wilson, C. R.; Donnelly, M. I. *Appl. Environ. Microbiol*. **2003**, *69*, 5992–5999; (d) Lu, W.; Ness, J. E.; Xie, W.; Zhang, X.; Minshull, J.; Gross, R. A. *J. Am. Chem. Soc*. **2010**, *132*, 15451–15455.

(8) (a) Luo, J.; Shea, K. J. *Acc. Chem. Res*. **2010**, *43*, 1420–1433; (b) Jellema, E.; Jongerius, A. L.; Reek, J. N. H.; de Bruin, B. *Chem. Soc. Rev*. **2010**, *39*, 1706–1723.

(9) Luo, J.; Lu, F.; Shea, K. J. *ACS Macro Lett*. **2012**, *1*, 560–563.

(10) Olah, G. A. *Angew. Chem. Int. Ed*. **2013**, *52*, 104–107.

(11) Busch, B. B.; Staiger, C. L.; Stoddard, J. M.; Shea, K. J. *Macromolecules* **2002**, *35*, 8330–8337.

(12) Wagner, C. E.; Rodriguez, A. A.; Shea, K. J. *Macromolecules* **2005**, *38*, 7286–7291.

(13) Wuts, P. G. M.; Greene, T. W. *Greene's Protective Groups in Organic Synthesis,* 4th ed.; John Wiley & Sons: Hoboken, 2006.

(14) Soderquist, J. A.; Najafi, M. R. *J. Org. Chem*. **1986**, *51*, 1330-1336.

(15) Busch, B. B.; Paz, M. M.; Shea, K. J.; Staiger, C. L.; Stoddard, J. M.; Walker, J. R.; Zhou, X.-Z.; Zhu, H. *J. Am. Chem. Soc.* **2002**, *124*, 3636–3646.

(16) Li, B.; Berliner, M.; Buzon, R.; Chiu, C. K.-F.; Colgan, S. T.; Kaneko, T.; Keene, N.; Kissel, W.; Le, T.; Leeman, K. R.; Marquez, B.; Morris, R.; Newell, L.; Wunderwald, S.; Witt, M.; Weaver, J.; Zhang, Z.; Zhang, Z. *J. Org. Chem.* **2006**, *71*, 9045–9050.

(17) Mecking *et al*. compared the GPC MW of polyesters using polystyrene and polyethylene. Stempfle, F.; Schemmer, B.; Oechsle, A-L.; Mecking, S. *Polym. Chem.* **2015**, *6*, 7133–7137.

(18) Pepels, M. P. F.; Hansen, M. R.; Goossens, H.; Duchateau, R. *Macromolecules* **2013**, *46*, 7668–7677.

(19) Jose, J.; Pourfallah, G.; Leao, A. L.; Narine, S. S. *Polym. Int.* **2014**, *63*, 1902–1911.

(20) Mihaies, M.; Olaru, A. Mechanical Properties and Parameters of Polyolefins. In *Handbook of Polyolefins*, 2nd ed.; Vasile, C., Ed.; Marcel Dekker: New York, 2000; pp 267–275.

(21) (a) Fuhrhop, J-H.; Wang, T. *Chem. Rev*. **2004**, *104*, 2901–2937; (b) Nuraje, N.; Bai, H.; Su, K. *Prog. Polym. Sci.* **2013**, *38*, 302–343.

(22) Zhao, M.; Li, J.; Song, Z.; Desmond, R.; Tschaen, D. M.; Grabowski, E. J. J.; Reider, P. J. *Tetrahedron Lett*. **1998**, *39,* 5323–5326.

(23) Thottumkara, A. P.; Bowsher, M. S.; Vinod, T. K. *Org. Lett*. **2005**, *7*, 2933–2936.

(24) Schmidt, A-K. C.; Stark, C. B. W. *Org. Lett*. 2011, **13**, 4164–4167.

(25) (a) More, J. D.; Finney, N. S. *Org. Lett*. **2002**, *4*, 3001–3003; (b) Ozanne, A.; Pouységu, L.; Depernet, D.; François, B.; Quideau, S. *Org. Lett*. **2003**, *5*, 2903–2906.

(26) Dalcanale, E.; Montanari, F. *J. Org. Chem*. **1986**, *51*, 567–569.

(27) Ogibin, Y. N.; Starostin, E. K.; Aleksandrov, A. V.; Pivnitsky, K. K.; Nikishin, G. I. *Synthesis*, **1994**, *9*, 901–903.

2.5. Experimental

General considerations. Appendix A. 5-Hexenoic acid **7** was prepared according to literature.[27]

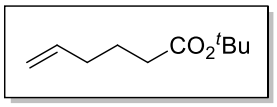

***tert*-Butyl 5-hexenoate (8)**. 5-hexenoic acid **7** (6.745 g, 59.1 mmol), dry *tert*-butanol (12.2 mL, 128.5 mmol), 4-dimethylaminopyridine (DMAP, 0.591 g, 4.84 mmol) and dichloromethane (DCM, 30 mL) were mixed in a round bottom flask equipped with a drying tube at 10 ℃. *N*,*N*'-Dicyclohexylcarbodiimide (DCC, 13.450 g, 65.2 mmol) was dissolved in 50 mL DCM. The DCC solution was slowly added to the acid and alcohol mixture at 10 ℃. The resulting mixture was then stirred at room temperature for one day. After the reaction, the mixture was filtered through celite and the residue was washed with DCM (3 × 10 mL). The collected filtrate was sequentially washed with 0.5 M HCl (3 × 30 mL), saturated $NaHCO_3$ (30 mL), H_2O (30 mL) and brine (30 mL). The organic solution was dried over $MgSO_4$ before concentration and evaporation to dryness in *vacuo*. The obtained liquid was further distilled under vacuum to give a colorless oil (7.12 g, 41.8 mmol, yield 71 %). ^{1}H NMR (500 MHz, $CDCl_3$) δ 5.76 (ddt, *J* = 16.5, 10.0, 7.0 Hz, 1H), 4.96–5.12 (m, 2H), 2.21 (t, *J* = 7.5 Hz, 2H), 2.06 (q, *J* = 7.0 Hz, 2H), 1.67 (quin, *J* = 7.5 Hz, 2H), 1.43 (s, 9H); ^{13}C NMR (125 MHz, $CDCl_3$) δ 173.1, 138.0, 115.3, 80.1, 35.0, 33.2, 28.2, 24.4. HRMS (ESI) calcd for $C_{10}H_{18}O_2Na$ $[M+Na]^+$ 193.1205, found 193.1201.

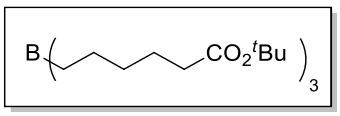

***tert*-Butyl ester functionalized organoborane initiator (9)**. To a N_2 purged round bottom flask containing *tert*-Butyl 5-hexenoate **8** (3.996 g, 23.47 mmol, 3.1 equiv) was added $BH_3{\cdot}SMe_2$ (1.0 M in DCM, 7.60 mL, 7.6 mmol, 1.0 equiv) dropwise at 0 ℃. The solution was stirred at 0 ℃ for 30 minutes before leaving at room temperature overnight. The

resulting solution was used directly for polymerization without any post process. The accurate concentration of organoborane **8** was determined as below. Meanwhile NMR characterization was performed with the presence of 1,4-dioxane. ^{1}H NMR (500 MHz, CD_2Cl_2) δ 2.14 (t, J = 7.5 Hz, 6H), 1.47–1.60 (m, 6H), 1.30–1.45 (m, 33H), 1.20–1.29 (m, 6H), 1.12–1.28 (m, 6H); ^{13}C NMR (125 MHz, CD_2Cl_2) δ 172.9, 79.5, 67.1 (1,4-dioxane), 35.5, 32.5, 27.9, 25.1, 24.2, 17.8.

Determination of the concentration of initiator 9. To an NMR tube was added 1,4-dioxane (47.4 mg, 0.538 mmol), an aliquot of freshly prepared organoborane **9** solution (0.350 mL) and degassed CD_2Cl_2 (~0.3 mL) under N_2. A ^{1}H NMR example is shown with all peaks assigned to the related structures (Figure 2.1). The total mole of organoboranes including all regioisomers can be calculated by Equation 2.1. Here I used the isolated signal at 2.2 ppm (peak a) for an accurate calculation. The mole of organoborane that was sampled out is calculated to be 0.24 mmol. The concentration was calculated in Equation 2.2.

$$[BR_3] = \frac{n}{V} = \frac{0.24}{0.35} = 0.686\ (M) \qquad \text{Eq. (2.2)}$$

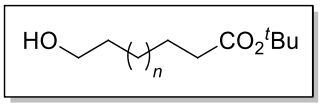

General procedure for synthesis of AB macromonomers 10 (Table 2.1, sample PM20). To a two-neck round bottom flask equipped with a condenser was added trimethylsulfoxonium iodide (18.373 g, 83.5 mmol, 45 equiv.) and tetrabutylammonium iodide (0.924 g, 2.50 mmol). The system was switched to N_2 atmosphere by vacuum–N_2 cycle for 3 times. DCM (12 mL) and 50% NaOH aqueous solution (80 mL) were degassed under N_2 and added to the reaction flask. The mixture was vigorously stirred and pre-heated at 40 ℃ followed by a fast injection of organoborane **9** (0.686 M in DCM, 2.70 mL, 1.85 mmol, 1.0 equiv.). After

stirring overnight, the reaction was cooled to room temperature and added 30% H_2O_2 aqueous solution (3.8 mL, 37.2 mmol, 20 equiv.). The reaction was further stirred at 40 ℃ for 1 d. After the oxidation, the mixture was poured into 200 mL deionized (DI) water and vacuum filtered. The solid was washed with DI water (3 × 20 mL) and methanol (3 × 20 mL). After drying under vacuum overnight, ω-hydroxyacid *t*-butyl ester was obtained as white solid (1.691 g, 76%). For polymers with high MW or in large quantities, incomplete oxidations were observed and repeated oxidation is required using 30% H_2O_2 (1 mL) and NaOH (1 M, 1 mL) in toluene at 80 ℃. ^{1}H NMR (500 MHz, $C_2D_2Cl_4$, 90 °C) δ 3.63 (t, J = 5.5 Hz, 2H, C**H**$_2$OH), 2.22 (t, J = 7.0 Hz, 2H, C**H**$_2$COO^{t}Bu), 1.54–1.73 (m, 4H, C**H**$_2$CH$_2$OH and C**H**$_2$CH$_2$COOH), 1.47 (s, 9H, C(C**H**$_3$)$_3$), 1.10–1.43 (m, 40H, C**H**$_2$); ^{13}C NMR (125 MHz, $C_2D_2Cl_4$, 90 ℃) δ 173.0 (**C**=O), 79.6 (COO**C**(CH$_3$)$_3$), 62.8 (**C**H$_2$OH), 35.5 (**C**H$_2$COO^{t}Bu), 32.7 (**C**H$_2$CH$_2$OH), 29.50, 29.45, 29.41, 29.3, 29.2, 29.1, 28.9 (**C**H$_2$), 28.0 (C(**C**H$_3$)$_3$), 25.6 (**C**H$_2$CH$_2$CH$_2$OH), 25.0 (**C**H$_2$CH$_2$COO^{t}Bu); GPC analysis: M_n = 413, M_w = 422, PDI = 1.02.

A second batch (denoted as **PM25**) was also performed for purposes of reduction and oxidation studies. GPC analysis: M_n = 426, M_w = 440, PDI = 1.03; Anal. Calcd. for $C_{29}H_{58}O_3$: C: 76.59%; H: 12.86%, Found; C: 76.22%; H: 12.97%.

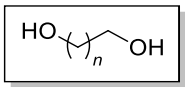

Synthesis of long-chain α,ω-diol (14). Lithium aluminum hydride (LAH, 0.125 g, 3.3 mmol) was added in 10 mL dry THF at room temperature. The AB macromonomer **10** (**PM25**, M_n = 426, 0.419 g, 0.98 mmol) was pre-dissolved in 20 mL dry THF at 60 ℃. After being cooled down to room temperature, the macromonomer solution was added dropwise to the LAH suspension. The mixture was then heated to reflux for 24 hours. The reaction was stopped by cooling down and addition of H_2O (1 mL) dropwise. Then NaOH solution (1 M in H_2O, 2 mL) and toluene (20 mL) were added sequentially. The mixture was heated to 60 ℃ for 30 min

before filtration through celite at the same temperature. The celite was further washed with toluene at 80 ℃ (3 × 10 mL). The filtrate was evaporated to dryness and the obtained crude solid was extracted with hot toluene (3 × 20 mL). After evaporation to dryness, the α,ω-diol was obtained as white solid (0.298 g, 85%). ^{1}H NMR (500 MHz, $C_2D_2Cl_4$, 60 °C) δ 3.64 (t, J = 6.5 Hz, 4H, C**H**$_2$OH), 1.58 (quin, J = 7.0 Hz, 4H, C**H**$_2$CH$_2$OH), 1.51 (br, 2H, O**H**), 1.15–1.43 (m, 60H, C**H**$_2$); ^{13}C NMR (125 MHz, toluene-d$_8$, 60 °C) δ 63.0 (**C**H$_2$OH), 33.6 (**C**H$_2$CH$_2$OH), 30.3, 30.2, 30.1 (**C**H$_2$), 26.4 (**C**H$_2$CH$_2$CH$_2$OH); GPC analysis: M_n = 331, M_w = 363, PDI = 1.10; Anal. Calcd. for $C_{25}H_{52}O_2$: C: 78.05%; H: 13.63%, Found; C: 77.92%; H: 13.60%.

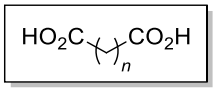

Synthesis of long-chain α,ω-diacid (15).

First oxidation. Dissolve the AB macromonomer **10** (**PM25**, M_n = 426, 78 mg, 0.18 mmol) in 8 mL toluene at 80 ℃. Add stabilized 2-iodoxybenzoic acid (SIBX 45 wt%, 350 mg, 0.56 mmol) to the macromonomer solution. The reaction was stirred at 80 ℃ overnight before filtration through celite at the same temperature. The celite was further washed with toluene at 80 ℃ (3 × 10 mL). The filtrate was concentrated to ~ 10 mL and washed in a vial using glass pipette with NaOH (1 M in H_2O, 10 mL) and H_2O (3 × 10 mL) sequentially. The organic layer was evaporated to dryness to give white power (69 mg). The product was directly used for the subsequent hydrolysis.

Hydrolysis. The white powder from first oxidation was dissolved in 10 mL toluene at 80 ℃. Then trifluoroacetic acid (0.2 mL) was added. The mixture was stirred at 80 ℃ for 3 hours before concentration *in vacuo*. After evaporation to dryness, the solid was washed with H_2O (3 × 10 mL) and methanol (2 × 10 mL). The obtained white solid was directly used for the second oxidation.

Second oxidation. All the product from the hydrolysis was dissolved in 10 mL toluene at 80 ℃. After the solution was cooled down to room temperature, NaH_2PO_4 (161 mg in 2 mL H_2O, 1.34 mmol) and H_2O_2 (30% in H_2O, 0.1 mL, 0.98 mmol) were added. The mixture was stirred vigorously before addition of $NaClO_2$ (80% purity, 30 mg in 1 mL H_2O, 0.27 mmol) dropwise in 5 min. After 1 h, additional $NaClO_2$ (30 mg) was added to the mixture. After the reaction was stirred overnight, the bottom clear aqueous solution was removed with a glass pipette. Then Na_2SO_3 solution (0.05 g in 1 mL H_2O) was added and stirred to destroy the remaining peroxides. After the aqueous layer was removed, the organic layer was added 0.05 mL trifluoroacetic acid and washed with H_2O (3 × 10 mL) in a vial using glass pipette. The toluene solution was evaporated to dryness and further washed with methanol (3 × 5 mL). After vacuum dry, the α,ω-diacid was obtained as white solid (52 mg, 74% in total). ^{1}H NMR (500 MHz, $C_2D_2Cl_4$, 90 °C) δ 7.28 (br, 2H, COO**H**), 2.39 (t, *J* = 7.5 Hz, 4H, C**H**$_2$COOH), 1.70 (quin, *J* = 7.5 Hz, 4H, C**H**$_2$CH$_2$COOH), 1.15–1.50 (m, 58H, C**H**$_2$); ^{13}C NMR (125 MHz, $C_2D_2Cl_4$, 90 °C) δ 176.3 (**C**=O), 33.33, 33.26 (**C**H$_2$COOH), 29.42, 29.40, 29.2, 29.1, 29.0, 28.92, 28.86, 28.83 (**C**H$_2$), 24.6 (**C**H$_2$CH$_2$COO), the peaks at 31.7, 22.4 and 13.8 ppm belong to the methyl branch region originated from regioisomer of hydroboration; Anal. Calcd. for $C_{25}H_{48}O_4$: C: 72.76%; H: 11.73%, Found; C: 73.15%; H: 11.33%.

Attempted removal of *tert*-butyl group in 10 using H_3PO_4. AB macromonomer **10** (190 mg, M_n = 542) was dissolved in 6 mL toluene at 70 ℃ in a round bottom flask. After addition of H_3PO_4 aqueous solution (85%, 0.23 mL), the mixture was stirred at 70 ℃ for 18 h. Then the reaction was cooled down to room temperature and added 10 mL H_2O. The resulting suspension was filtered to afford white solids followed by washing with H_2O (3 × 10 mL) and methanol (3 ×

10 mL). After drying under vacuum for 24 h, white powder (148 mg) was obtained. ^{1}H NMR analysis revealed remaining *t*-butyl group at 1.38 ppm. The conversion of **10** was calculated to be 58% based on the integration ratio of CH_2/*t*-butyl before and after hydrolysis.

Attempted removal of *tert*-butyl group in 10 using TFA. AB macromonomer **10** (298 mg, M_n = 468) was dissolved in 10 mL toluene at 70 ℃ in a round bottom flask. After addition of trifluoroacetic acid (0.98 mL, 12.8 mmol), the mixture was stirred at 70 ℃ for 24 h. Then the reaction was cooled down to room temperature and added 20 mL methanol. The resulting suspension was filtered to afford white solids followed by washing with H_2O (3 × 5 mL) and methanol (3 × 10 mL). After drying under vacuum at 50 ℃ for 24 h, white powder (278 mg) was obtained. ^{1}H NMR analysis revealed complete removal of *t*-butyl group and presence of CF_3COOCH_2– in large quantities (Figure 2.3).

Attempted removal of the trifluoroacetyl group in 12 using NaOH. AB macromonomer **10** (270 mg, M_n = 452) was dissolved in 10 mL toluene at 90 ℃ in a round bottom flask. After addition of NaOH aqueous solution (2 M, 1.2 mL), the mixture was stirred at 90 ℃ for 24 h. Then the reaction was cooled down to room temperature and added HCl aqueous solution (6 M, 2 mL). The mixture was stirred at room temperature overnight and the resulting suspension was filtered to afford white solids. The solid was washed with H_2O (3 × 10 mL) and methanol (3 × 10 mL). After drying under vacuum at room temperature for 24 h, white powder (205 mg) was obtained. ^{1}H NMR analysis revealed complete removal of the trifluoroacetyl group and presence of –CH_2COOCH_2– in small quantities (Figure 2.4).

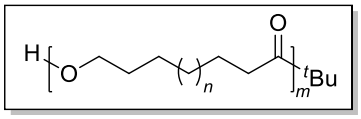

General procedure for synthesis of polyesters 12 (Table 2.3, sample P(PM20)). To a round bottom flask was added AB macromonomer **10** (**PM20**, 1.566 g) and titanium *n*-butoxide Ti(O-*n*Bu)$_4$ (12 mg, 0.035 mmol). The reaction was purged with N_2 before heating to 160 ℃ under atmospheric pressure. After 6 hours, the reaction was further heated to 210 ℃ at 300 mTorr for 24 hours. After cooling down to room temperature, the brown solid was dissolved in 50 mL toluene at 110 ℃ and precipitated by pouring into 150 mL methanol. The suspension was filtered and the white solid was washed with methanol (3 × 10 mL). The obtained purified material was dried under vacuum as white solid (1.199 g, 91%). ^{1}H NMR (500 MHz, $C_2D_2Cl_4$, 90 °C) δ 4.11 (t, *J* = 6.0 Hz, 2H, COOC**H**$_2$), 2.33 (t, *J* = 7.0 Hz, 2H, C**H**$_2$COO), 1.60–1.75 (m, 4H, COOCH$_2$C**H**$_2$ and C**H**$_2$CH$_2$COO), 1.15–1.50 (m, 44H, C**H**$_2$); ^{13}C NMR (125 MHz, $C_2D_2Cl_4$, 90 °C) δ 173.3 (**C**=O), 64.1 (COO**C**H$_2$), 34.2 (**C**H$_2$COO), 29.4, 29.33, 29.29, 29.24, 29.20, 29.0, 28.9 (**C**H$_2$), 28.6 (COOCH$_2$**C**H$_2$), 25.8 (COOCH$_2$CH$_2$**C**H$_2$), 24.8 (**C**H$_2$CH$_2$COO); GPC analysis: M_n = 10939, M_w = 19284, PDI = 1.76.

Chapter 3. Gradient Methylidene-Ethylidene Copolymers *via* the Living Polyhomologation Reaction: an Ersatz Gradient Ethylene–Propylene Copolymer

3.1. Introduction

Carbon backbone polymers, especially polyethylene (PE) and polypropylene (PP), are ubiquitous in contemporary society, serving as components for paints, lubricants, printing inks, packaging materials and surface coatings. Ethylene–propylene block copolymers are used as the compatibilizer for PE/PP blends. These blends have improved tensile and impact strength and expand the potential applications of these abundant, inexpensive materials.[1,2] In contrast to conventional random and block copolymers, gradient copolymers are materials where the instantaneous composition varies continuously from one end of the polymer chain to the other (Figure 3.1). Theoretical calculations indicate that gradient copolymers can undergo microphase separation with a blurred interface region between chemically different components.[3] These gradient copolymers are expected to have unique thermal properties,[4] particularly a broad glass transition temperature (T_g) range in situations where the corresponding homopolymers have very different T_gs.[5] Experimental studies provided examples of materials containing incompatible comonomers with a very broad T_g range.[6]

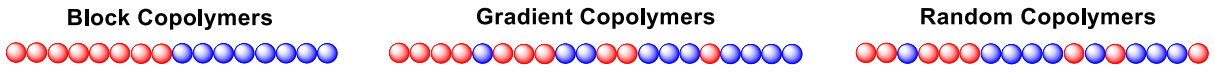

Figure 3.1. Schematic illustration of compositional change in block, gradient and random copolymers.

Generation of gradient contents along the polymer chain relies on different monomer reactivities or a gradual change of monomer concentrations during the polymerization.[7] The former method is spontaneous gradient that utilizes batch copolymerizations, while the latter one is forced gradient achieved by semi-batch copolymerizations. In order to achieve a homogeneous gradient copolymer, all polymer chains must be initiated simultaneously and survive until the end of polymerization. This requires a living polymerization. For non-living polymerizations, attempts on synthesis of gradient copolymers will result in polymer mixtures with various monomer contents among different polymer chains. This is because the polymer chain initiated at an early time will have high contents of one monomer but those initiated late will have the other monomer in abundance. Well-defined gradient copolymers have been synthesized from controlled/living polymerizations such as NMP (nitroxide mediated polymerization)[8], ATRP (atom transfer radical polymerization)[9,10] and RAFT (reversible addition-fragmentation chain transfer radical polymerization)[11]. Many gradient copolymers are produced from functionalized olefin monomers, e.g., poly(styrene-*grad*-butadiene)[12] and poly(styrene-*grad*-butyl acrylate)[9]. Very few gradient copolymers based on non-functionalized hydrocarbon monomers have been reported. For example, ethylene–norbornene gradient copolymers were obtained *via* Pd–diimine-catalyzed copolymerization.[13] A somewhat related simple triblock ethylene–propylene copolymer, PE-*b*-poly(ethylene-*co*-propylene)-*b*-PP, was first reported *via* living olefin polymerization with a fluorine-containing titanium catalyst bearing phenoxy–imine ligands.[14] Well-defined ethylene–propylene gradient copolymers, the simplest gradient hydrocarbon polymers, have not been reported and their properties have yet to be studied.

The living C1 polymerization allows for the production of linear hydrocarbon polymers with controlled molecular weight (MW), polydispersity (PDI) and well-defined topology. We

have previously reported a sp^3–sp^3 carbon–carbon bond forming polyhomologation reaction which produces a carbon backbone polymer by sequential insertion of C1 building blocks.[15] Here we report the synthesis of a gradient methylidene–ethylidene copolymer *via* the living polyhomologation reaction.

3.2. Results and Discussion

The synthesis of gradient copolymers using the polyhomologation reaction requires development of a convenient source of the ethylide monomer. We have previously demonstrated that (dimethylamino)phenyloxosulfonium alkylides can be employed to synthesize substituted carbon backbones.[16] However, its synthesis involves at least four synthetic steps with long reaction time and use of hazardous reagents such as sodium azide. The ethylide monomer with a simple design, e.g., diethylsulfoxonium ethylide, has not been employed in the polyhomologation reaction. This is because its synthesis requires high-cost reagents in large quantities such as $AgBF_4$[17] and $RuCl_3$[18] or as a perchlorate salt using $NaClO_4$[19] which is potentially explosive and incompatible with the subsequent deprotonation reaction. The preparation of these ylides usually requires the corresponding sulfoxonium salts as the precursors.

3.2.1. Synthesis of diethylsulfoxonium ethylide

There are mainly two different strategies to synthesize alkyl or arylsulfoxonium salts. One is the alkylation of alkyl sulfoxide **2** and the other is oxidation of the sulfonium salt **3** (Scheme 3.1). Compared to the readily S-alkylation of dimethyl sulfoxide with methyl iodide, the S-alkylation of other alkyl sulfoxides proved to be very challenging.[20]

Scheme 3.1. Two different methods to synthesize sulfoxonium salts **4**.

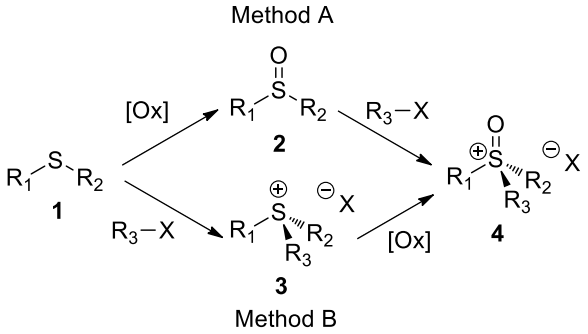

My first plan was to synthesize the triethylsulfoxonium iodide **6** by S-alkylation of diethyl sulfoxide **5** with iodoethane in the same way as the synthesis of trimethylsulfoxonium iodide (Scheme 3.2). The reaction was carried out by heating of **5** and an excess of iodoethane in a sealed tube at 110 ℃. After 2 d, however, triethylsulfonium iodide **7** was obtained with no formation of sulfoxonium salt **6**. A lower temperature at the boiling point of iodoethane (70 ℃) under atmospheric pressure gave no reaction. Purification of **7** is challenging due to the large amounts of I_2 generated in the reaction and its low thermal stability during recrystallization. To be compatible with the subsequent oxidation step, the iodide needs to be exchanged with a stable anion, e.g., chloride. To simplify the purification process and avoid side reactions in the oxidation, an efficient anion exchange reaction was performed to convert iodide **7** to chloride **8** with the phase-transfer agent benzyl tri-*n*-butylammonium chloride.

Scheme 3.2. Synthesis of triethylsulfoxonium iodide **6** *via* ethylation of diethyl sulfoxide.

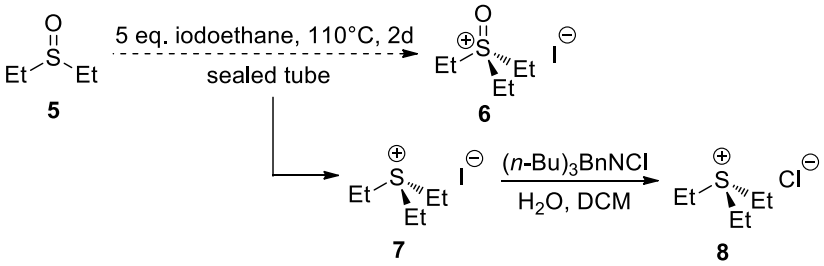

The ethylation of sulfoxide **5** was also studied with different equivalent of iodoethane (Table 3.1). As product **7** is difficult to isolate and quantify, the reaction was characterized with

the chloride salt **8** after the anion exchange. An excess of iodoethane with at least three equivalents is necessary to achieve a high reaction yield. Using one equivalent of iodoethane (entry 1), diethyl sulfide, ethanol as well as iodine were observed as the major byproducts in the reaction mixture.

Table 3.1. Reaction of diethyl sulfoxide **5** with different ratios of iodoethane.

entry	iodoethane (eq.)	yield of **8** (%)
1	1.0	43
2	2.0	75
3	3.0	88

Since the sulfoxide alkylation will give the sulfide intermediate before formation of the sulfonium salt, I decided to synthesize the triethylsulfonium salt **7** directly from diethyl sulfide. A common synthesis of alkyl or aryl sulfonium salts was reported using alcohols under strong acidic conditions as the tetrafluoroborate, perchlorate or trifluoroacetate salts.[21] Other methods include using more reactive alkylating reagents such as allyl bromides[22] and the addition of soluble silver salts to drive the reaction to completion *via* precipitation.[23] But a direct alkylation of dialkyl sulfide with alkyl iodide has been poorly developed. Therefore, the reaction between diethyl sulfide **9** and iodoethane was examined (Scheme 3.3). In addition to the alkylation with iodoethane, the anion exchange reaction was also carried out to quantify and compare the results.

Scheme 3.3. Synthesis of triethylsulfonium chloride **8** from diethyl sulfide **9**.

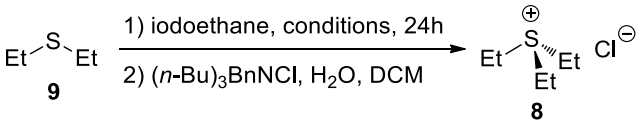

A direct alkylation of sulfide **9** with iodoethane was inefficient, even with an excess of the alkylating reagent (Table 3.2, entry 1–2). These results are inconsistent with the high percent yield from alkylation of the sulfoxide **5** under the same conditions (Table 3.1, entry 2–3). However, since I_2 was generated during the sulfoxide alkylation, a possible explanation could be

that I_2 will promote the alkylation of sulfide. With an increasing amount of I_2, the yield of the sulfonium salt **8** was increased dramatically (Table 3.2, entry 3–5). Moreover, this reaction could take place even at room temperature without significant drop on the percent yield (entry 7).

Table 3.2. Screening conditions for alkylation of diethyl sulfide **9** in Scheme 3.3.

entry	temperature (°C)	iodoethane (eq.)	I_2 (mol%)	yield% of **8**
1	110	1.0	0	3
2	110	2.0	0	12
3	110	1.0	10	32
4	110	1.0	20	45
5	110	1.0	50	92
6	70	1.0	50	94
7	25	1.0	50	81

With triethylsulfonium chloride **8** in hand, a following simple oxidation was performed and modified based on reports by Kobayashi and coworkers to obtain the desired triethylsulfoxonium chloride.[24] In my case, the oxidant sodium *m*-chloroperbenzoate was not prepared separately but rather generated *in-situ* from *m*-chloroperoxybenzoic acid (*m*CPBA). The reaction is clean with the desired sulfoxonium salt **10** over 95% in the crude product which can be readily purified by recrystallization.

Scheme 3.4. Synthesis of triethylsulfoxonium chloride by oxidation of the sulfonium salt **8**.

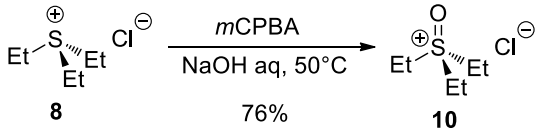

8 **10**

To serve as the secondary ylide in the traditional polyhomologation, the ylide must be prepared separately under strictly anhydrous conditions. *In-situ* generation of sulfoxonium ylides at or below room temperature, as a popular method, is not compatible with the polyhomologation reaction due to the low solubility of hydrocarbon polymers under these conditions. Moreover, the rate of chain propagation can be influenced by the rate of ylide production and the introduced extra bases. Therefore, the deprotonation reaction of **10** was examined using different bases.

My first attempt was to follow the reported protocol for preparing a structural similar ylide, dimethylsulfoxonium methylide **2**, which requires NaH as the base in high yields.[20b] This method would produce a solution of ylide free of other byproducts. The reaction was carried out at elevated temperatures with toluene or THF as solvents (Scheme 3.5, Table 3.3). No reaction was found to occur at a temperature lower than the boiling point of the corresponding solvent by titration of an aliquot of the clear solution. The reaction was found to have a low yield with poor reproducibility after several attempts (Table 3.3).

Scheme 3.5. Synthesis of ethylide **11** with NaH.

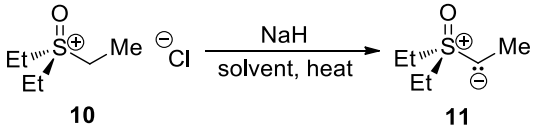

Table 3.3. Results of the ethylide **11** prepared with NaH.

entry	solvent	NaH (eq.)	temperature (ºC)	rxn time (h)	yield (%)
1	Toluene	2.1	110	1	16
2	Toluene	2.0	110	1.5	10
3	Toluene	3.0	110	1.5	25
4	Toluene	3.6	110	0.5	40
5	Toluene	3.6	90	2.5	NR
6	Toluene	4.1	110	2~5	NR
7	THF	1.2	reflux	4	27

The low reaction yield is probably due to the low thermal stability of **11** at elevated temperatures. Sulfoxonium ylides are known to undergo α-elimination to afford sulfoxides and carbene intermediates. The half-life of ethylide **11** in toluene at 110 ℃ was measured to be only about 1 h! Therefore, the deprotonation of sulfoxonium salt **10** using NaH is abandoned due to the required elevated temperatures incompatible with the low thermal stability of ethylide **11**. A deprotonation method at lower temperatures needs to be developed.

For deprotonation of the sulfoxonium salt **10**, a non-nucleophilic base must be used to avoid the competing ethylation reaction. A common base used in organic synthesis, lithium diisopropylamide (LDA), was thus employed (Scheme 3.6). The deprotonation reaction was found to proceed very fast under mild conditions in near quantitative yield of the ethylide. This resulting solution contains byproducts such as diisopropylamine and lithium chloride. Complexation between diisopropylamine and trialkylborane is not of concern because of the bulkiness of the Lewis base. Since it is anticipated that none of these byproducts will exert an influence on the polyhomologation reaction, the ethylide solution was used for polymerization studies.

Scheme 3.6. Synthesis of ethylide **11** with LDA.

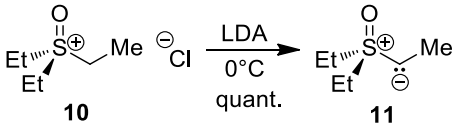

The only disadvantage of using LDA to prepare ethylide **11** is that the concentration of ethylide cannot be obtained directly *via* titration due to the presence of diisopropylamine byproducts in large quantity. Currently my strategy is to calculate ethylide concentration from ^{1}H NMR analysis of a sample mixed with a known concentration of dimethylsulfoxonium methylide. Both methylide and ethylide can be protonated to the corresponding sulfoxonium salts which have distinctive chemical shifts in ^{1}H NMR.

For deprotonation reactions using either NaH or LDA method, the identity of ethylide **11** was not obtained by NMR analysis due to the abundant byproducts present in the reaction. A cyclopropanation reaction with (*E*)-chalcone **12** was used instead to identify the deprotonation products (Scheme 3.7). Ethylide **11** prepared from both methods exhibited same products with similar ratios (Table 3.4).

Scheme 3.7. Identification of ethylide **11** *via* cyclopropanation reaction with (*E*)-chalcone **12**.

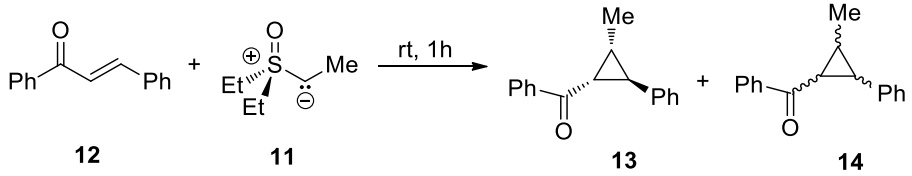

12 **11** **13** **14**

Table 3.4. Cyclopropanation of (*E*)-chalcone with ethylide **11** prepared using different bases.

entry	base[a]	**11** (eq.)	solvent	**13**	**14**
1	NaH	1.10	toluene	60%	36%
2	LDA	1.03	THF	61%	30%

a. The base refers to the method to prepare diethylsulfoxonium ethylide **11**.

In summary, I developed an efficient and economical protocol to synthesize the diethylsulfoxonium ethylide **11** which can function as an ethylidene monomer in the polyhomologation reaction. Its synthesis starts from diethyl sulfide **9** (Scheme 3.8). Following alkylation with iodoethane and an anion exchange, sulfide **9** was converted to triethylsulfonium chloride **8**. Oxidation of **8** with *m*CPBA under basic conditions gave the ylide precursor Et_3SOCl **10**. Deprotonation of **10** using LDA at 0 ℃ results in near quantitative conversion to the ethylide **11**. With a high yield three-step synthesis of ethylide **11**, I then explored its ability to serve as a secondary monomer in the polyhomologation reaction.

Scheme 3.8. Summary of synthesis of diethylsulfoxonium ethylide **11**.

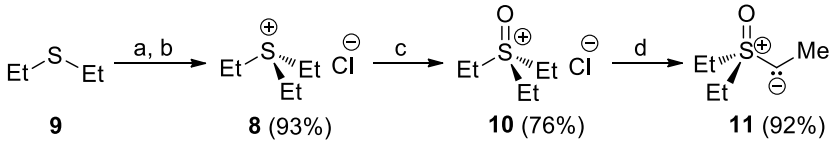

9 **8** (93%) **10** (76%) **11** (92%)

Reagents and conditions: (a) iodoethane, 0.5 equiv. I_2, 70 ℃, overnight; (b) $(n\text{-Bu})_3BnNCl$, H_2O/DCM, rt, overnight; (c) *m*CPBA, NaOH aq, 50 ℃, 0.5 h; (d) LDA, 0 ℃, 10 min.

*3.2.2. Use of triethylsulfoxonium chloride **10** in the aqueous polyhomologation*

Due to convenience without preparation of the ylide, I first explored the applications of triethylsulfoxonium salt **10** in the aqueous polyhomologation reaction. In this event, the active ethylide monomer was produced *in-situ*. Concerns were made on whether ethylide **11** can be generated in an aqueous base, as the pK_a value of triethylsulfoxonium chloride **10** is higher than that of trimethylsulfoxonium salts (pK_a ~18)[25].

Exposure of **10** to small amount of NaOD/D_2O resulted in rapid deuterium exchange of all protons within 5 min at room temperature (Figure 3.2). The disappearance of peak at 3.93 ppm and the splitting pattern change of peak at 1.47 ppm indicate that triethylsulfoxonium chloride **10** is rapidly converted to its deuterium form **10-d_6** in 0.3% NaOD/D_2O solution. Diethylsulfoxonium ethylide **11** is the intermediate in this exchange reaction (Scheme 3.9). The fast H–D exchange of **10** indicates that the active ethylide monomer can be generated in the aqueous polyhomologation reaction.

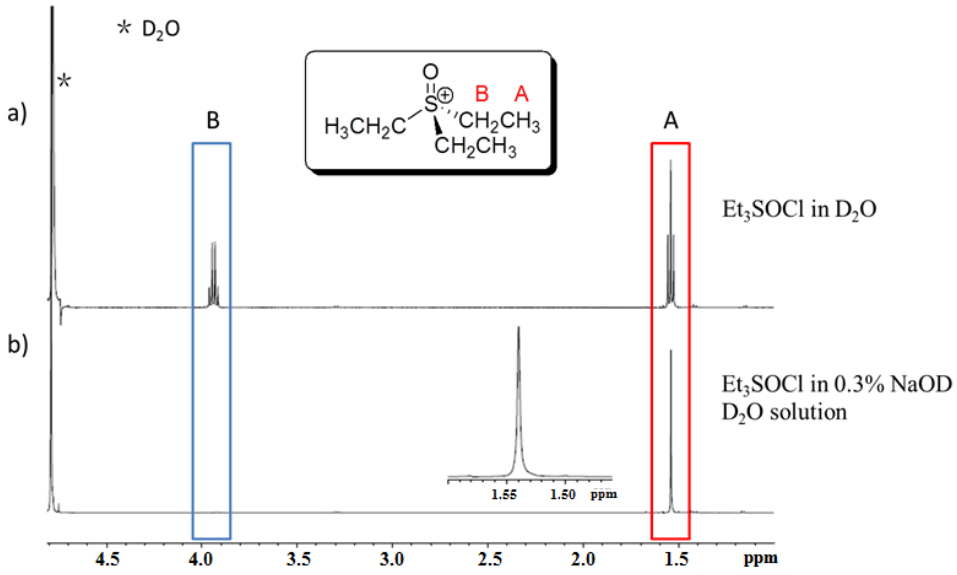

Figure 3.2. ^{1}H NMR spectra of a) triethylsulfoxonium chloride **10** in D_2O and b) triethyl-sulfoxonium chloride **10** in 0.3% NaOD D_2O solution. Inset is the enlarged spectra of spectra b at 1.5 ppm. Both spectra were recorded immediately after the samples were prepared at room temperature.

Scheme 3.9. Schematic illustration for H–D exchange between triethylsulfoxonium salt **10** and its deuterium form **10-d$_6$**.

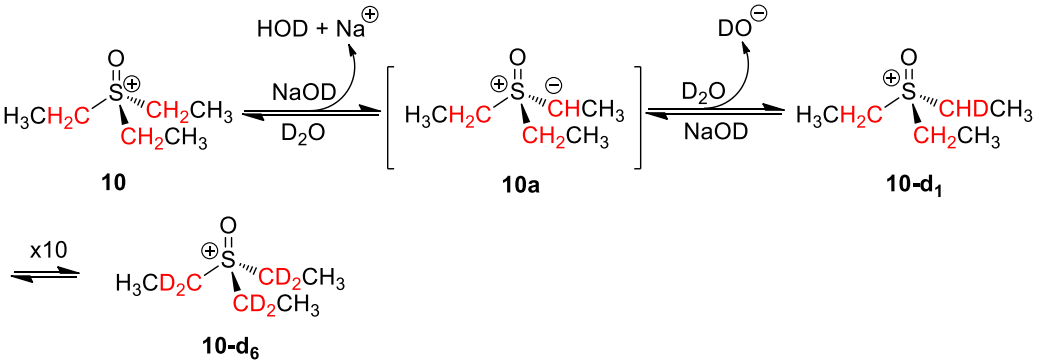

To evaluate the efficiency in the polymer branch incorporation using triethylsulfoxonium salt **10**, copolymerization of **10** with trimethylsulfoxonium iodide **15** was carried out in different feed ratios under the standard polymerization condition (Scheme 3.10). All polymers were obtained after filtration without a formal oxidation step. The polymer content was determined from ^{1}H NMR and polymer MW and PDI were characterized *via* GPC analysis (Table 3.5).

Scheme 3.10. Copolymerization of trimethylsulfoxonium iodide **15** and triethylsulfoxonium chloride **10** in the aqueous polyhomologation reaction.

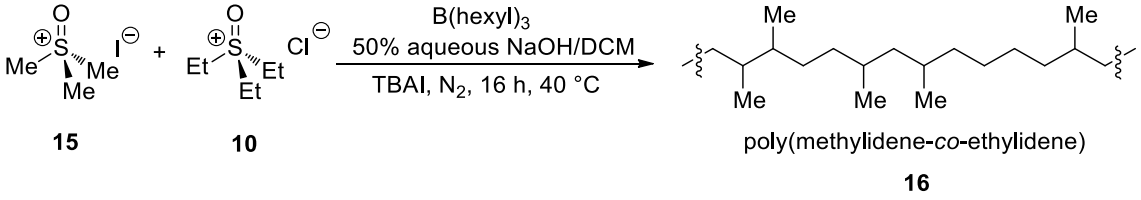

Table 3.5. Poly(methylidene-*co*-ethylidene) **16** synthesized from copolymerization of **10** and **15**.

entry	theoretical		experimental				
	[M]/[E]^a	MW$_{th}$ (g/mol)	yield (%)	[M]/[E]^b	M_n^{c} (g/mol)	M_w^{c} (g/mol)	PDI^c
1	8.99 : 1	1488	88	9.28 : 1	1921	20716	10.8
2	6.05 : 1	1558	89	6.52 : 1	2107	12531	5.9
3	3.01 : 1	1502	87	3.02 : 1	1337	8140	6.1
4	2.00 : 1	1502	84	2.08 : 1	1209	5377	4.4
5	1.00 : 1	1488	72	1.33 : 1	913	1561	1.7

a. [M]/[E] represents the molar ratio of methylidene to ethylidene [CH_2]/[$CHCH_3$]. Theoretical [M]/[E] and MW$_{th}$ were calculated from feed molar ratio of Me_3SOI and Et_3SOCl.

b. [M]/[E] was calculated from ^{1}H NMR in toluene-d_8.

c. M_n, M_w and PDI were obtained from high temperature GPC analysis.

The experimental ethylidene incorporation ratio is close to the theoretical feed ratio (Table 3, entry 1–5). However, the PDI of most samples are much higher than that of a typical aqueous polyhomologation reaction below 2.0 (entry 1–4). With an increased ratio of the secondary monomer, the polymerization yield, the polymer MW and PDI all decreased (entry 1–5). To obtain kinetic characters of the polymerization, the reaction needs to be monitored. Due to the heterogeneity of the aqueous polyhomologation, a direct monitoring of the reaction progress by measuring the rate of monomer consumption is very challenging. To obtain information on the rate of polymerization, several separate polymerizations were set up with different reaction times (Table 3.6).

Table 3.6. Copolymerization of **10** and **15** for different reaction times.[a]

		theoretical		experimental				
entry	time (h)	Et%[b]	MW_{th} (g/mol)	yield (%)	Et%[b]	M_n[c] (g/mol)	M_w[c] (g/mol)	PDI[c]
1	1	10.0	1488	33	19.0	884	2026	2.29
2	2	10.0	1488	68	10.5	1538	11094	7.21
3	4	10.0	1488	88	8.6	1961	24008	12.2
4	16	10.0	1488	88	9.7	1921	20716	10.8
5	1	24.8	1502	36	47.2	---[d]	---[d]	---[d]
6	2	24.8	1502	55	32.5	798	1266	1.6
7	4	24.8	1502	65	23.5	1123	8123	7.2
8	16	24.8	1502	72	24.9	1337	8140	6.1

a. All reactions were carried out at 40 ℃.
b. Et% is the mole percentage of ethylidene in the copolymer. The theoretical value was determined based on the feed ratio of two monomers; while the experimental value was calculated from ^{1}H NMR in toluene-d_8.
c. M_n, M_w and PDI were obtained from high temperature GPC analysis.
d. The sample was not analyzed by GPC due to the very low polymer chain length.

The copolymerization with a lower ratio of monomer **10** (Et% = 10%) can run into completion within 4 h (Table 4, entry 3–4), while the one starting from a higher secondary monomer ratio (Et% = 24.8%) was still incomplete after 4 h (entry 7–8). With an increased feed ratio of monomer **10**, the polymerization rate was lowered. Additionally, a decrease of the branch content (Et%) in the polymer composition was observed during the polymer chain growth

until it reached close to the monomer feed ratio (entry 1–4, 5–8). The growing polymers at an early stage of polymerization have higher branch content compared to the monomer feed ratio with a relative low PDI. As the polymers grow, PDIs increased to high values (entry 3–4, 7–8).

The polymerization at the early stage is believed to occur in the organic phase where the actual concentrations of both monomer ylides are unknown. To acquire this information, an experiment without adding the initiator was carried out under the same condition to determine the actual concentration ratio of the ylides in the dichloromethane (DCM) phase (Scheme 3.11).

Scheme 3.11. Determination on the actual ratio of ylide monomers **11** : **17** in the organic phase.

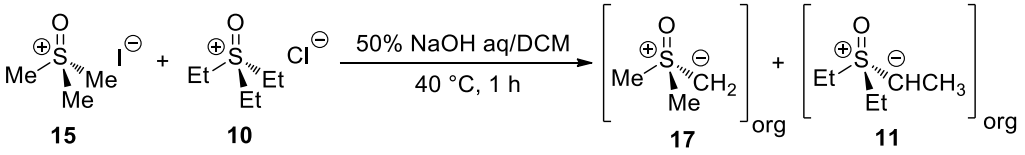

15 **10** **17** **11**

During the early stage of polymerization, both monomer salts are not completely consumed especially in the case where high feed ratio of **10** was introduced (Table 3.6, entry 5). Therefore at an early stage of polymerization, both ylides are saturated in the organic phase with the same concentrations as determined in the control experiment described above (Scheme 3.11). If ethylide **11** had the same reactivity as methylide **17** in the polyhomologation reaction, we would have observed the same monomer contents in the copolymer compared to the ylides ratio in DCM. When a 3:1 feed ratio of Me_3SOI **15** : Et_3SOCl **10** was employed, the copolymer obtained after a 1 h of polymerization has a slightly lower methylidene incorporation ratio than the ylide concentration ratio in DCM (Table 3.7, entry 2). In the case where 9:1 feed ratio of Me_3SOI **15** : Et_3SOCl **10** was introduced, a higher methylidene (or lower ethylidene) content was observed (entry 1). This is because most of monomer **10** was consumed before 1 h of polymerization and the ethylide **11** in DCM is much less than the abundant methylide **17**. These

observations conclude that the ethylide **11** has a slightly higher reactivity than the methylide **17** in the aqueous polyhomologation reaction.

Table 3.7. The ylides concentration in comparison with the monomer incorporation ratio at an early stage (1 h) of polymerization.

entry	salt feed **15** : **10**	ylide in DCM **17** : **11**	polymer [M] : [E][a]
1	8.99 : 1	2.37 : 1	4.38 : 1
2	3.03 : 1	1.35 : 1	1.12 : 1

a. The ratio of methylidene/ethylidene content in the copolymer was measured after 1 h of polymerization and is the same as Table 3.6, entry 1 and 5.

In addition, both partitions of ylides **11** and **17** in the organic phase were also measured separately in common aprotic solvents in the same way as described in Scheme 3.11 (Table 3.8). With both ylide precursors **10** and **15** in excess, ethylide **11** was found to have a much higher concentration (or partition) in DCM compared to methylide **17**.

Table 3.8. A comparison between methylide **17** and ethylide **11** on the partition in common aprotic organic solvents.

entry	solvent	[**17**] (mol/L)	[**11**] (mol/L)	$[OH^-]^a$ (mol/L)
1	DCM	0.066	0.79	0
2	THF	0.020	0.56	0
3	toluene	0.005	0.01	0

a. This is the control experiment with only 50% NaOH aq and DCM.

The aqueous polyhomologation does not provide control of PDI in the copolymerization of monomer salts **10** and **15**. This is a result of the non-living polymerization from different types of propagating chain ends (catalytic sites). As a consequence, the rate of chain growth varies largely among all propagating chain ends. The polymer chains with a faster propagation rate have higher ethylidene contents; while the slow growing chains have lower ethylidene contents as evidenced by a decrease of ethylidene content in the copolymer as the polymerization proceeds (Table 3.6). Therefore, the aqueous copolymerization of **10** and **15** afforded polymer

mixtures rather than homogeneous gradient copolymers, with part of polymers abundant in branch content and the others resemble polymethylene.

3.2.3. Synthesis and characterization of gradient methylidene–ethylidene copolymers using the traditional polyhomologation reaction

To evaluate the utility of ethylide **11** as a secondary ylide monomer for the traditional polyhomologation reaction, batch copolymerizations of ethylide **11** with methylide **17** were studied first. The polymerization starts with a pool of pre-mixed monomers **11** and **17** followed by injection of the organoborane initiator, tri-*n*-hexylborane, at 75 ℃ (Scheme 3.12). After oxidation and hydrolysis, an α-hydroxyl terminated hydrocarbon copolymer **18** was obtained in high yield. The ^{1}H NMR spectrum exhibited two diagnostic regions at 0.7–1.1 ppm (CH_3) and 1.1–2.0 ppm (CH_2 + CH). The obtained polymer had the chemical composition of an ethylene–propylene copolymer. Poly(methylidene-*co*-ethylidene) **18** were obtained with monomer incorporation ratios [CH_2]/[$CHCH_3$] ranging from 8.0 to 2.0 (Table 3.9). All copolymers have a low PDI in the range of 1.02–1.17 with the monomer composition close to the feed ratio.

Scheme 3.12. Poly(methylidene-*co*-ethylidene) **18** synthesized from batch copolymerization of methylide **17** and ethylide **11**.

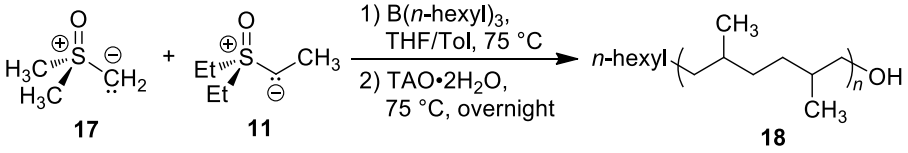

Table 3.9. Batch copolymerization of methylide **17** and ethylide **11**.

sample	$(M/E)_{feed}$[a]	$(M/E)_{NMR}$[a]	yield (%)	MW_{th}[b] (g/mol)	M_n[c] (g/mol)	M_w[c] (g/mol)	PDI[c]	T_g[d] (°C)	T_m[d] (°C)	cryst.[d] (%)
r1	90:10	88:12	99	1614	1744	1782	1.02	---[e]	99	36
r2	86:14	85:15	92	2340	2070	2144	1.04	−56	97	25
r3	80:20	80:20	91	1782	1575	1646	1.05	−53	80	21
r4	67:33	67:33	80	1502	1364	1594	1.17	−38	55	3

a. $(M/E)_{feed}$ was calculated from the molar feed ratio of monomers [**2**]/[**10**]. $(M/E)_{NMR}$ is the cumulative monomer incorporation ratio in the copolymer determined from the polymer ^{1}H NMR in toluene-d_8 at 363 K.
b. Theoretical MW is calculated as $MW_{th} = M_{hexyl\text{-}OH} + M_{CH2} \times [\mathbf{2}]/3[B(hexyl)_3] + M_{CH\text{-}CH3} \times [\mathbf{10}]/3[B(hexyl)_3]$.
c. M_n, M_w and PDI were determined from GPC analysis.
d. T_g, T_m and crystallinity were determined from DSC analysis.
e. T_g was not observed in the range of −80 to 180 ℃.

To obtain monomer compositions along the chain of copolymer **18**, several polymerizations were carried out as a function of time with the same monomer feed ratio. At 75 ℃, the polymerization proceeds near completion in 5 min which is difficult to monitor any compositional change on the polymer backbone (Table 3.10, entry 1–2). To slow down the reaction rate and monitor the polymerization progress, a second series of reactions were carried out at room temperature (entry 3–5). ^{1}H NMR shows similar monomer incorporation ratios of polymers with a relatively low PDI obtained from different reaction times. This indicates that the copolymers **18** synthesized from the batch polymerization are random copolymers.

Table 3.10. Batch polymerizations using methylide **17** and ethylide **11** as a function of time.

	theoretical		experimental						
entry	[M]/[E][a]	MW_{th} (g/mol)	temperature (ºC)	time (min)	yield (%)	[M]/[E][b]	M_n[c] (g/mol)	M_w[c] (g/mol)	PDI[c]
1	6.76 : 1	1600	75	5	90	5.92 : 1	1139	1405	1.23
2	6.76 : 1	1600	75	10	96	5.89 : 1	-	-	-
3	4.28 : 1	1418	25	6	44	3.08 : 1	1059	1366	1.29
4	4.36 : 1	1292	25	10.5	83	2.90 : 1	826	1126	1.36
5	4.22 : 1	1292	25	20	81	2.87 : 1	874	1160	1.33

a. [M]/[E] represents the molar ratio of methylidene to ethylidene [CH_2]/[$CHCH_3$]. Theoretical [M]/[E] and MW_{th} were calculated from the feed molar ratio of methylide **17** and ethylide **11**;
b. [M]/[E] was calculated from ^{1}H NMR in toluene-d_8;
c. M_n, M_w and PDI were from high temperature GPC analysis.

There have been no previous reports of gradient ethylene–propylene copolymers. To achieve a compositional equivalent as poly(methylidene-*grad*-ethylidene), I examined semi-batch copolymerizations of methylide **17** and ethylide **11**. A first strategy was carried out by injection of the tri-*n*-hexylborane initiator to a pool of methylide **17** followed by continuously addition of ethylide **11** in a controlled manner (Scheme 3.13). However after several attempts, it was found that the reaction proceeds so fast that most methylide was consumed in 1–2 min before the full addition of ethylide **11**.

Scheme 3.13. Semi-batch copolymerization by controlled addition of ethylide **11** to the polymerization reaction of methylide **17**.

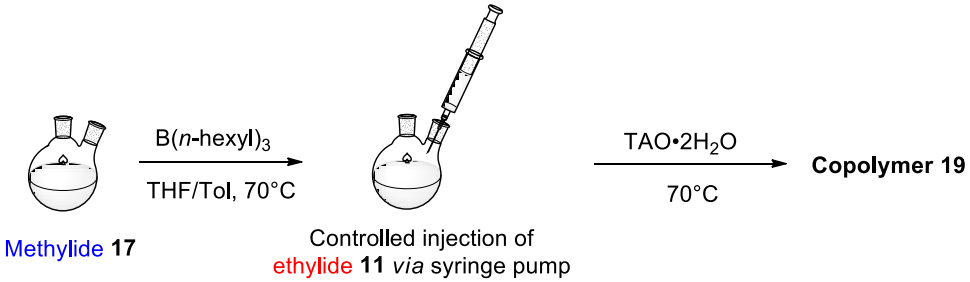

A different strategy of semi-batch copolymerization was carried out by injection of methylide **17** to a pre-mixed solution of tri-*n*-hexylborane and ethylide **11** (Scheme 3.14). The ethylide **11** was found not able to homopolymerize with B(*n*-hexyl)$_3$. Then methylide **17** was continuously added in a controlled manner *via* a syringe pump. To characterize the gradient copolymer, the monomer incorporation needs to be monitored as a function of the polymer chain growth. And most importantly a living polymerization with low PDI must be demonstrated to rule out the possibility on a polymer mixture with very different monomer contents. Polymerization kinetics are usually measured by sampling the reaction mixture as a function of time which are subjected to ^{1}H NMR analysis. It can be readily accomplished if the monomer and polymer show different diagnostic peaks with no interference from byproducts. However,

the presence of large quantities of sulfoxide byproducts as well as the sensitivity of ylide monomers towards moisture impede a direct monitor on the progress of the polymerization.

Scheme 3.14. Semi-batch copolymerization by controlled addition of methylide **17** to the polymerization reaction of ethylide **11**.

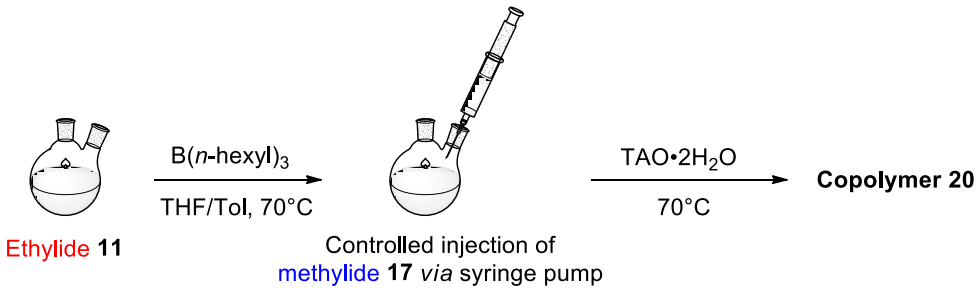

Due to the difficulty in monitoring the conversion of each monomer, parallel polymerizations were set up to obtain information regarding the composition and molecular weight of the polymer as a function of reaction time (Table 3.11). Parallel reactions quenched at different times will give results close to sampling one reaction at the corresponding time. The parallel reactions were carried out under the same conditions with the only difference in the actual injection volume of methylide **17**.

Table 3.11. Semi-batch copolymerizations with methylide **17** and ethylide **11** (M/E = 4/1).

	theoretical		experimental				
entry	[M]/[E]^a	MW_{th}^{a} (g/mol)	yield^b (%)	[M]/[E]^c	M_n^{d} (g/mol)	M_w^{d} (g/mol)	PDI^d
1	0.80 : 1	1278	27.6	1.67 : 1	650	1235	1.90
2	1.60 : 1	1614	58.8	1.83 : 1	1209	2257	1.87
3	2.40 : 1	1950	72.8	2.58 : 1	1536	2946	1.92
4	3.20 : 1	2286	87.0	3.57 : 1	1805	4085	2.26
5	3.84 : 1	2552	98.5	4.62 : 1	2976	7871	2.65

a. [M]/[E] represents the molar ratio of methylidene to ethylidene [CH_2]/[$CHCH_3$]. Theoretical [M]/[E] and MW_{th} are calculated from the feed molar ratio of methylide **17** and ethylide **11**;
b. This is the normalized yield% assuming that all polymerizations are targeting at a full injection of all methylide **17** as in entry 5.
c. [M]/[E] was calculated from ^{1}H NMR in toluene-d_8;
d. M_n, M_w and PDI were from high temperature GPC analysis.

However, all attempts resulted in polymers with a multimodal MW distribution (Table 3.11). The chain propagation between ethylide **11** and tri-*n*-hexylborane lead to formation of organoboranes containing 2–3 2 ° carbons adjacent to the boron center rendering them less (or non) reactive, compared to boron species with zero or only one adjacent 2 ° carbon. The sterically congested boron centers result in kinetically distinct propagating species and a broadened or bimodal MW distribution.

Ylides are used as monomers for the polyhomologation reaction and their rate of incorporation is quite fast. This presents a challenge to monitor the monomer consumption during chain growth. As a practical matter to verify the compositional gradient during the course of polymerization, gradient copolymers were synthesized by sequential addition of monomer mixtures to the polymerization reaction (Scheme 3.15). This allowed sampling the composition of the growing polymer chain at various stages of growth. The final gradient copolymer was synthesized from six incremental additions of the methylide and ethylide monomers starting with a segment of linear polymethylene and ending up with a segment rich in methyl branches. Each increment of added monomers contained a greater proportion of ethylide **11** than the previous one. The polymerization progress was monitored by removing, quenching and oxidizing an aliquot of the reaction prior to addition of the next increment of monomers.

Scheme 3.15. Semi-batch copolymerization by sequential addition of mixtures of ylides **11** and **17** with an increasing ratio of ethylide **11**.

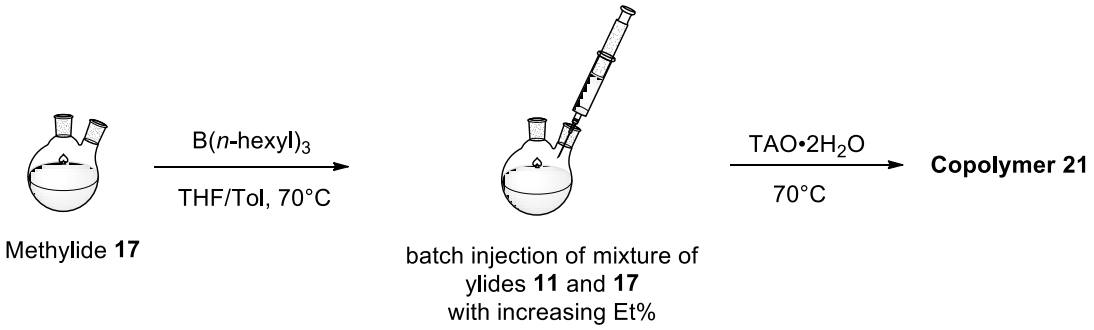

The MW distribution of the isolated polymers, measured by GPC, remained narrow and shifted to higher MW as the polymerization proceeded (Figure 3.3 and Table 3.12). The cumulative ethylidene content increased with an increase of ethylide **11** in the monomer feed (Table 3.12). Progress of gradient polymerizations is traditionally tracked by monitoring monomer consumptions with *in-situ* ^{1}H NMR. The practical challenges of measuring the monomer conversion by this method necessitate estimation of the polymer compositions in order to calculate the instantaneous monomer content. This was accomplished by determining the average number of monomer units in the polymer at different polymerization stages. The instantaneous monomer content was then calculated based on the polymer compositions at the beginning and the end of each segment.

Table 3.12. Monitoring the formation of gradient copolymers **21** with the chemical composition of poly(ethylene-*grad*-propylene).

sample	N[a]	$(M/E)_{feed}$[b]	$(M/E)_{cum}$[b]	Et_{cum}%[c]	M_n[d] (g/mol)	M_w[d] (g/mol)	PDI[d]	T_g[e] (°C)	T_m[e] (°C)	cryst.[e] (%)
g1	1	100:0	100:0	0	451	458	1.02	—[f]	82,71[g]	70
g2	2	93.8:6.2	92.0:8.0	8.0	784	837	1.07	—[f]	65	41
g3	3	88.2:11.8	87.5:12.5	12.5	1314	1400	1.07	−35	58	32
g4	4	83.0:17.0	82.9:17.1	17.1	1912	2103	1.10	−37	50	22
g5	5	78.3:21.7	78.9:21.1	21.1	2613	2933	1.12	−38	46	15
g6	6	72.1:27.9	72.0:28.0	28.0	3081	3483	1.13	−32	45	10

a. N is the number of segments in the gradient copolymer **21**.
b. $(M/E)_{feed}$ is the cumulative feed ratio of monomers **17**:**11**. $(M/E)_{cum}$ is the cumulative monomer incorporation ratio in the polymer calculated from ^{1}H NMR in toluene-d_8.
c. Et_{cum}% represents the cumulative ethylidene content in the copolymer determined as $Et_{cum}\% = 1/[1 + (M/E)_{cum}] \times 100\%$.
d. Determined using GPC analysis.
e. Determined using DSC analysis.
f. Not observed in the range of –80 to 140 ℃.
g. The melting peak at 71 ℃ of sample g1 is from small portions of methyl branched polymethylene. The terminal *sec*-hexyl group from regioisomers of B(*n*-hexyl)$_3$ accounts for the defect structure of linear PE and can interrupt its perfect chain packing. This phenomenon can only be observed in low MW polymethylene using the organoborane initiators prepared *via* hydroboration.

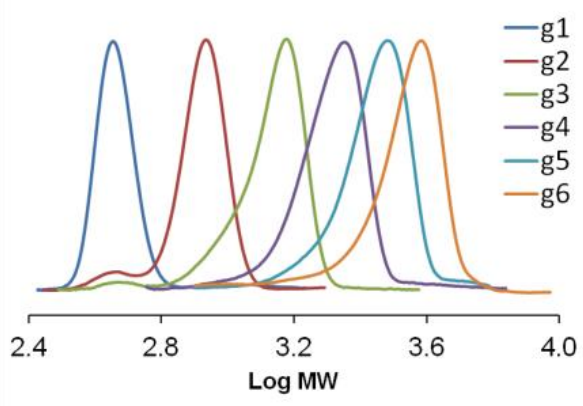

Figure 3.3. GPC traces of the gradient copolymers **g1**–**g6** sampled during the copolymerization. The small low MW peak in polymer **g2**–**g5** belongs to a small amount of **g1** with active chain terminated by trace O_2 introduced during sampling periods. It can be easily removed in the final polymer **g6**.

Based on the polymer molecular weight and monomer incorporation ratio, I assigned the number of both methylidene and ethylidene units for all polymers sampled during the course of the copolymerization (Figure 3.4). Both the calculated polymer MW and monomer incorporation ratio based on these numbers are very close to the experimental values (Table 3.13).

Table 3.13. Determination of the average numbers of monomer units per polymer chain and calculation of instantaneous ethylidene contents of the gradient copolymer **21**.

sample	N_{CH2}[a]	N_{CH3}[a]	Et_{inst}%[b]	Et_{feed}%[b]	$(CH_2/CH_3)_{exp}$[c]	$(CH_2/CH_3)_{cal}$[d]	M_p[e] (g/mol)	M_{cal}[f] (g/mol)
g1	30	1	0	0	23.4:1	30.0:1	453	452
g2	56	5	13.3	11.9	11.5:1	11.2:1	864	928
g3	84	12	20.0	20.5	6.97:1	7.00:1	1513	1516
g4	112	23	28.2	27.7	4.85:1	4.87:1	2268	2216
g5	142	38	33.3	33.4	3.75:1	3.74:1	3055	3056
g6	155	60	62.9	44.4	2.57:1	2.58:1	3858	3854

a. N_{CH2} and N_{CH3} are the average quantities of CH_2 and CH_3 units per polymer chain determined from polymer peak MW and CH_2/CH_3 ratio by NMR analysis. All samples contains at least one CH_3 unit that is from the polymer chain end rather than –(CH)CH_3–.

b. Et_{inst}% is the calculated instantaneous ethylidene content in the last segment of each polymer. $(Et_{inst}\%)_{g4} = (\Delta N_{CH3})_{g3\rightarrow g4}/[(\Delta N_{CH2})_{g3\rightarrow g4} + (\Delta N_{CH3})_{g3\rightarrow g4}] \times 100\%$ where $(\Delta N)_{g3\rightarrow g4} = N_{g4} - N_{g3}$. Et_{feed}% is the experimental ethylide content in the monomer feed for the very last segment of each polymer determined from ^{1}H NMR.

c. $(CH_2/CH_3)_{exp}$ is the monomer incorporation ratio of the copolymer calculated from ^{1}H NMR in toluene-d_8 at 363K.

d. $(CH_2/CH_3)_{cal}$ is the calculated monomer incorporation ratio based on N_{CH2} and N_{CH3}. $(CH_2/CH_3)_{cal} = N_{CH2}/N_{CH3}$.

e. M_p is the polymer peak molecular weight determined by GPC analysis.

f. M_{cal} is the calculated polymer MW based on N_{CH2} and N_{CH3}; $M_{cal} = M_{CH2} \times N_{CH2} + M_{CH\text{-}CH3} \times (N_{CH3} - 1) + M_{CH3\text{-}OH}$.

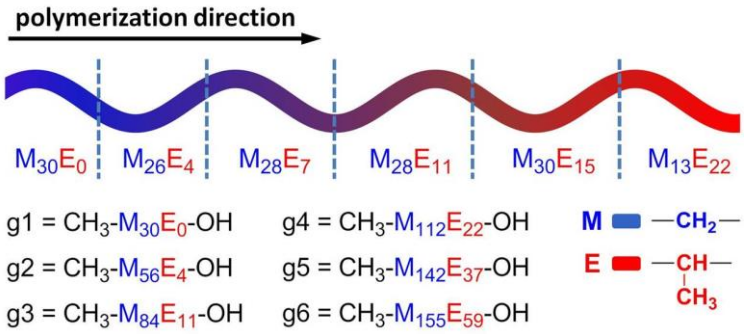

Figure 3.4. Experimentally determined methylidene–ethylidene compositions in the gradient copolymer. The colored ribbon represents the final gradient copolymer color scaled using the experimentally determined M/E units in each segment (e.g., $M_{30}E_0$, $M_{26}E_4$, etc). **g1** = CH_3–$M_{30}E_0$–OH to **g6** = CH_3–$M_{155}E_{59}$–OH represents the cumulative number of M/E units for the copolymers isolated at each stage of polymer growth. **g6** = CH_3–$M_{155}E_{59}$–OH is the final composition of the gradient copolymer.

The instantaneous ethylidene content calculated with this method is also very close to the experimental ethylide ratio in the monomer feed at each stage (Figure 3.5a) and increases progressively as the polymerization reaction proceeded (Figure 3.5b). The high ethylidene content (over 60%) in the last segment of the polymer indicates that this copolymer possesses a significant number of adjacent ethylidene substructures –CH(CH3)–CH(CH3)– and, in the extreme, ethylidene triads –CH(CH3)–CH(CH3)–CH(CH3)–.

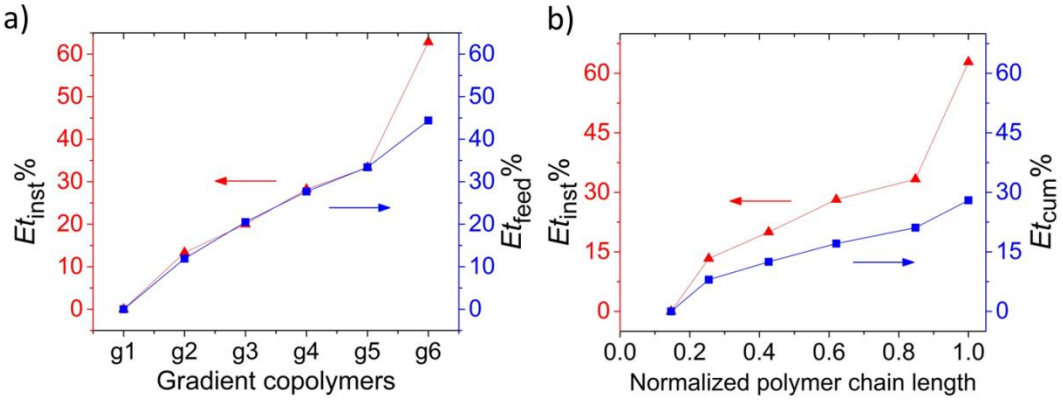

Figure 3.5. a) Comparison between the instantaneous ethylidene content in the copolymer and the ethylide ratio in each monomer feed.[26] b) The instantaneous and cumulative ethylidene contents as a function of the polymer chain length.

The presence of ethylidene dyads and triads is also supported by ^{13}C NMR analysis. Distribution of branch along the carbon chain is described by the nomenclature proposed by Randall and Carman.[27,28] Carbons on polymer branches are named as iB_n, with *n* represents the length of the branch and *i* tells the position of the carbon on the branch numbered from the branch terminal carbon as "1" ($1B_1$ = methyl branch). The methine carbons at the branch point on the polymer backbone are named as "br". To describe the relative location of a substituent to the nearest branch point, a pair of Greek letters is added as subscript to indicate the number of CH_2 units in between from either direction. For example, $1B_{1\alpha\gamma}$ represents the carbon atom on a methyl branch located in between two nearest branch points spaced by zero and two CH_2 units, respectively.

Microstructures with relatively isolated methyl branches such as $1B_{1\beta\delta+}$, $1B_{1\gamma\delta+}$ and $1B_{1\delta+\delta+}$ fall in the range of 18.5–20.5 ppm. In the gradient copolymer **g6**, $1B_{1\alpha\delta+}$ was assigned as 14.22 and 16.04 ppm (Figure 3.6b) which corroborate the values at 14.69 and 16.75 ppm suggested by Fr êche for 7,8-dimethyltetradecane[29]. In addition, $br_{\alpha\delta+}$ was observed at 36.44 and 37.27 ppm that also matches reported values.[29] These peaks indicate that the ethylidene dyad is present in polymer **g6**.

The identification of an ethylidene triad microstructure is challenging due to the lack of appropriate models. A structural similar compound, 3,4,5-trimethyloctane, was employed to identify ethylidene triads in the gradient copolymer **g6**. The observed peaks at 14.7, 15.2 and 17.3–17.7 ppm (Figure 3.6b) are in accord with those reported for the methyl groups of 3,4,5-trimethyloctane at 14.6, 15.4–15.6, 17.3 and 17.8–18.5 ppm.[30] Resonances at 34.5–35.4, 36.3 and 37.2 ppm are also close to the values from 3,4,5-trimethyloctane which were assigned to

$br_{\alpha\delta+}$. The diagnostic $br_{\alpha\alpha}$ can be found at 40.7 and 41.6 ppm, also close to values at 40.4 and 41.3–41.5 ppm as reported for 3,4,5-trimethyloctane.

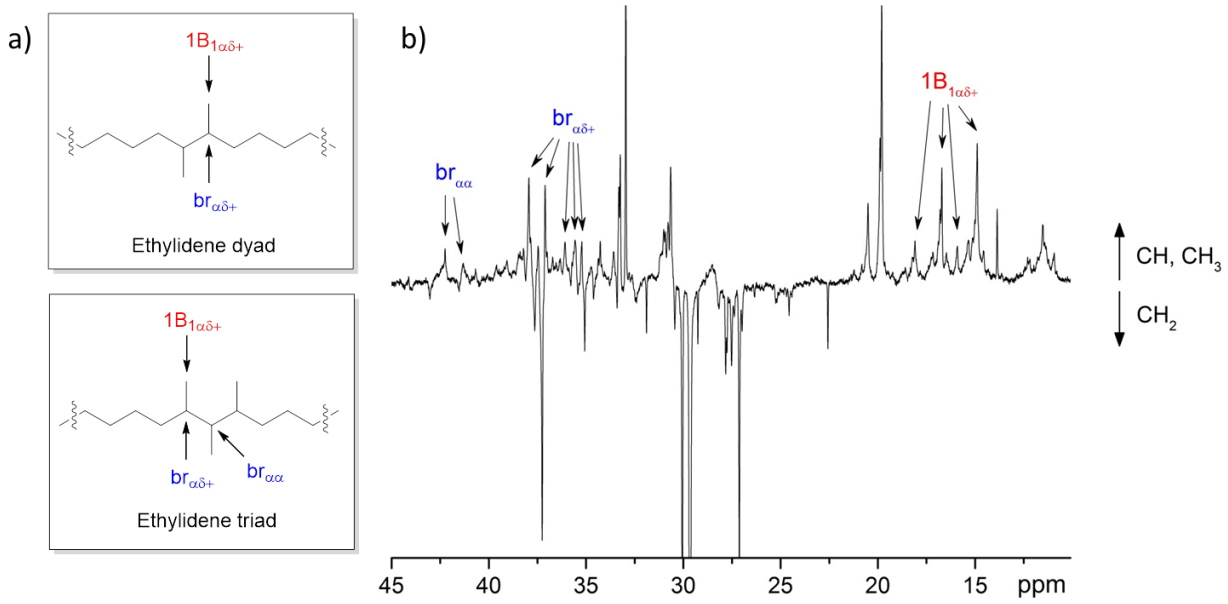

Figure 3.6. a) Illustration of the diagnostic carbons $1B_{1\alpha\delta+}$, $br_{\alpha\alpha}$, $br_{\alpha\delta+}$ in ethylidene dyad and triad on a carbon chain. b) DEPT135 spectrum of poly(methylidene-*grad*-ethylidene) **g6** produced from copolymerization of methylide **17** and ethylide **11**.

These ethylidene dyad and triad substructures have a higher ethylidene content than polypropylene and cannot be obtained by C2 polymerization of propylene. The living C1 polymerization therefore is able to continuously tune the content of methyl branches along the polymer chain over a wider range than what can be achieved by ethylene–propylene copolymerization.

Thermal analyses of all polymer samples revealed that the polymer crystallinity decreased with increasing methyl branch content (Figure 3.7 and Table 3.9, 3.12). The T_g of random copolymers **r2** to **r4** increases from −56 to −38 ℃ as the ethylidene content increased (Figure 3.8a and Table 3.9). The gradient copolymers **g3** to **g6** have similar T_g in the range of −32 to −38 ℃ (Table 3.12 and Figure 3.8b), in between the values of linear PE (T_g = −78 ±

10 ℃)[31] and atactic PP with similar MW (T_g = −24 ℃, M_n = 3800)[32]. A broad T_g range, as proposed for some gradient copolymers, was not observed in these materials due to the chemical similarity between the comonomers.

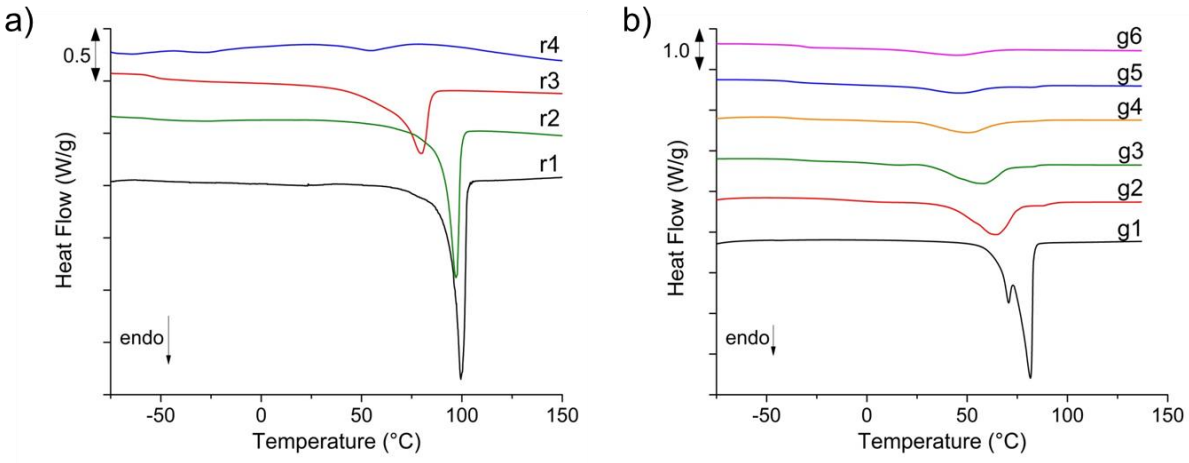

Figure 3.7. Stacked DSC traces of a) random copolymers **18** and b) gradient methylidene–ethylidene copolymers **21** at a temperature range of −75 to 150 ℃. We believe that the melting peak at 71 ℃ of sample **g1** is from small portions of methyl branched polymethylene. The terminal *sec*-hexyl group from regioisomers of B(*n*-hexyl)$_3$ accounts for the defective structure of linear PE and can interrupt its perfect chain packing. This phenomenon can only be observed in low MW polymethylene using the organoborane initiators prepared *via* hydroboration.

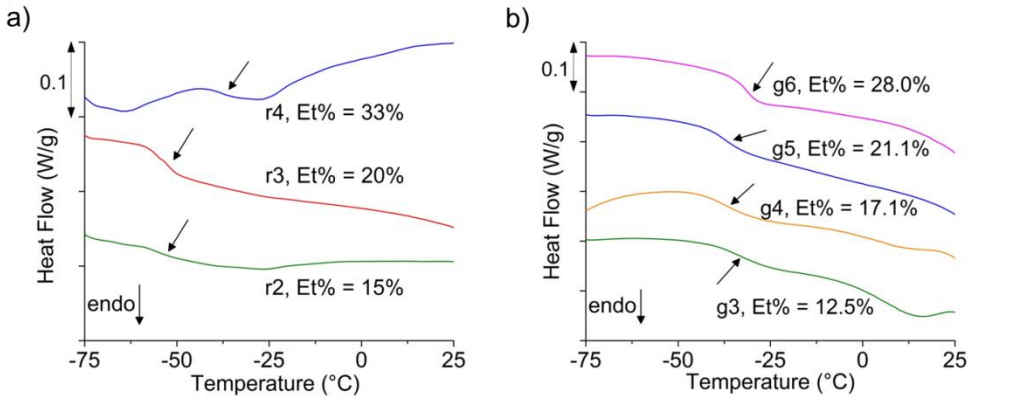

Figure 3.8. Stacked DSC traces of a) random copolymers **18** and b) gradient methylidene–ethylidene copolymers **21** expanded in the temperature range of −75 to 25 ℃.

3.3. Conclusion

In conclusion, I have developed a convenient protocol to prepare diethylsulfoxonium ethylide. This ethylide is used in the polyhomologation reaction for the controlled synthesis of poly(methylidene-*co*-ethylidene) copolymers. The aqueous copolymerization of sulfoxonium salts **10** and **15** does not have a control on polymer MW as well as PDI, because the partitions of two ylides in the organic phase are very different which generates a variety of different catalytic propagating chain ends. The structurally unique hydrocarbon polymer, gradient methylidene–ethylidene copolymer, an ersatz gradient ethylene–propylene copolymer, can be realized *via* the traditional living polyhomologation reaction permitting investigation of the physical and thermal properties of this material. This methodology can be used for the synthesis of multi-segment hydrocarbon copolymers with control of monomer content and allows for the insertion of functionality at any location on the linear polyethylene chain.

3.4. References

(1) Flaris, V.; Stachurski, Z. H. *J. Appl. Polym. Sci.* **1992**, *45*, 1789–1798.

(2) Wang, L.; Huang, B. *J. Polym. Sci., Part B: Polym. Phys.* **1990**, *28*, 937–949.

(3) Aksimentiev, A.; Hołyst, R. *J. Chem. Phys.* **1999**, *111*, 2329–2339.

(4) Buzin, A. I.; Pyda, M.; Constanzo, P.; Matyjaszewski, K.; Wunderlich, B. *Polymer* **2002**, *43*, 5563–5569.

(5) Lefebvre, M. D.; Olvera de la Cruz, M.; Shull, K. R. *Macromolecules* **2004**, *37*, 1118–1123.

(6) Kim, J.; Mok, M. M.; Sandoval, R. W.; Woo, D. J.; Torkelson, J. M. *Macromolecules* **2006**, *39*, 6152–6260.

(7) Beginn, U. *Colloid. Polym. Sci.* **2008**, *286*, 1465–1474.

(8) Grubbs, R. B. *Polym. Rev.* **2011**, *51*, 104–137.

(9) Matyjaszewski, K.; Ziegler, M. J.; Arehart, S. V.; Greszta, D.; Pakula, T. *J. Phys. Org. Chem.* **2000**, *13*, 775–786.

(10) Matyjaszewski, K.; Xia, J. *Chem. Rev.* **2001**, *101*, 2921–2990.

(11) Moad, G.; Rizzardo, E.; Thang, S. H. *Aust. J. Chem.* **2005**, *58*, 379–410.

(12) Hashimoto, T.; Tsukahara, Y.; Tachi, K.; Kawai, H. *Macromolecules* **1983**, *16*, 648–657.

(13) Xiang, P.; Ye, Z. *J. Polym. Sci., Part A: Polym. Chem.* **2013**, *51*, 672–686.

(14) Saito, J.; Mitani, M.; Mohri, J.-i.; Yoshida, Y.; Matsui, S.; Ishii, S.-i.; Kojoh, S.-i.; Kashiwa, N.; Fujita, T. *Angew. Chem. Int. Ed.* **2001**, *40*, 2918–2920.

(15) Luo, J.; Shea, K. J. *Acc. Chem. Res.* **2010**, *43*, 1420–1433.

(16) Zhou, X.-Z.; Shea, K. J. *J. Am. Chem. Soc.* **2000**, *122*, 11515–11516.

(17) Doi, J. T.; Luehr, G. W. *Tetrahedron Lett*. **1985**, *26*, 6143–6146.

(18) Edwards, M. G.; Paxton, R. J.; Pugh, D. S.; Whitwood, A. C.; Taylor, R. J. K. *Synthesis* **2008**, *20*, 3279–3288.

(19) Aggarwal, V. K.; Thompson, A.; Jones, R. V. H. *Tetrahedron Lett*. **1994**, *35*, 8659–8660.

(20) (a) Kuhn, R.; Trischmann, H. *Liebigs*. *Ann. Chem.* **1958**, *611*, 117; (b) Corey, E. J.; Chaykovsky, M. *J. Am. Chem. Soc.* **1965**, *87*, 1957; (c) Kamiyama, K.; Minato, H.; Kobayashi, M. *Bull. Chem. Soc. Jpn.*, **1973**, *46*, 3895.

(21) Badet, B.; Julia, M. *Tetrahedron Lett*. **1979**, *20*, 1101–1104.

(22) Chigboh, K.; Nadin, A.; Stockman, R. A. *Synlett* **2007**, *18*, 2879.

(23) (a) Brajeul, S.; Delpech, B.; Marazano, C. *Tetrahedron Lett*. **2007**, *48*, 5597–5600; (b) Chigboh, K.; Morton, D.; Nadin, A.; Stockman, R. *Tetrahedron Lett*. **2008**, *49*, 4768–4770.

(24) Mori, M.; Takeuchi, H.; Minato, H.; Kobayashi, M.; Yoshida, M.; Matsuyama, H.; Kamigata, N. *Phosphorus Sulfur Silicon Relat. Elem.* **1990**, *47*, 157–164.

(25) Bordwell, F. G. *Acc. Chem. Res*. **1988**, *21*, 456−463.

(26) Please see Chapter 3 experimental section for detailed results.

(27) Randall, J. C. *J. Macromol. Sci., Rev. Macromol. Chem. Phys.* **1989**, *C29(2,3)*, 201–317.

(28) Carman, C. J.; Harrington, R. A.; Wilkes, C. E. *Macromolecules* **1977**, *10*, 536–544.

(29) Fr ĉhe, P.; Grenier-Loustalot, M.-F.; Metras, F. *Makromol. Chem*. **1983**, *184*, 569–583.

(30) Lachance, P.; Brownstein, S.; Eastham, A. M. *Can. J. Chem*. **1979**, *4*, 367–376.

(31) Boyer, R. F. *Macromolecules* **1973**, *6*, 288–299.

(32) Burfield, D. R.; Doi, Y. *Macromolecules* **1983**, *16*, 702–704.

(33) Davies, D. M.; Deary, M. E. *Analyst*, **1988**, *113*, 1477–1479.

(34) Brown, H. C.; Kramer, G. W.; Levy, A. B.; Midland, M. M. *Organic Syntheses via Boranes*; WILEY-VCH: New York, 1975; pp 26–27.

(35) Corey, E. J.; Chaykovsky, M., *Org. Synth., Coll. Vol*. **1973**, *5*, 755.

3.5. Experimental

General considerations. Appendix A. The commercial *m*CPBA was titrated before use to determine the amount of the active oxidant according to literature.[33] Tri-*n*-hexylborane was synthesized according to literature.[34] Dimethylsulfoxonium methylide **17** was prepared according to literature.[35] The methylide was purged under N_2 and titrated with standardized hydrochloric acid to give an accurate concentration before use.

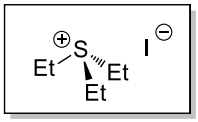

Synthesis of triethylsulfonium iodide 7 by alkylation of diethyl sulfoxide 5. A neat solution of diethyl sulfoxide **5** (6.078 g, 57.24 mmol) and iodoethane (10.1 mL, 125.6 mmol, 2.2 eq) was heated at 110 ℃ in a sealed tube for 2 d. The reaction vessel was protected against light with aluminum foil. After cooling down to room temperature, the black liquid mixture was concentrated *in vacuo* at 40 ℃ to give the crude product as black oil. The crude product could be used for the subsequent anion exchange without any purification (details please refer to synthesis of **8** below). To obtain the pure product, the black oil needs to be added 10% $Na_2S_2O_3$ aqueous solution (9 mL) and washed with DCM (9 mL × 3). The aqueous layer was separated and a light yellow solid could be obtained after concentration *in vacuo*. Then 2-propanol (10 mL) was added to extract the product. A recrystallization in 2-propanol gave the pure product as a white powder. ^{1}H NMR (500 MHz, DMSO-d_6) δ 3.33 (q, *J* = 7.5, 6H), 1.36 (t, *J* = 7.5, 9H); ^{13}C NMR (125 MHz, DMSO-d_6) δ 31.8, 8.6. HRMS (ESI) calcd for $C_6H_{15}S$ $(M–I)^+$ 119.0894, found 119.0899.

Formal synthesis of diethylsulfoxonium ethylide 11

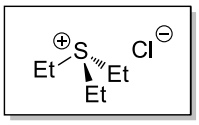

Triethylsulfonium chloride (8). Diethyl sulfide (4.0 mL, 37.1 mmol), iodoethane (3.0 mL, 37.3 mmol) and iodine (4.80 g, 18.9 mmol) were heated at 70 ℃ in a sealed tube protected against light for 1 d. The resulting mixture was then transferred to an Erlenmeyer flask containing H_2O (115 mL) and CH_2Cl_2 (75 mL). After the addition of benzyltri(*n*-butyl)ammonium chloride (11.62 g, 37.3 mmol), the reaction was allowed to stir in air overnight at room temperature. The aqueous layer was separated from the mixture and washed thoroughly with CH_2Cl_2 (5 × 30 mL). After evaporation of all solvents in *vacuo*, the product was obtained as a white hygroscopic solid (5.34 g, 34.5 mmol, 93 % overall for 2 steps). ^{1}H NMR (500 MHz, D_2O) δ 3.33 (q, *J* = 7.5 Hz, 6H), 1.47 (t, *J* = 7.5 Hz, 9H); ^{13}C NMR (125 MHz, DMSO-d_6) δ 31.7, 8.5. HRMS (ESI) calcd for $C_6H_{15}S$ $(M–Cl)^+$ 119.0894, found 119.0899.

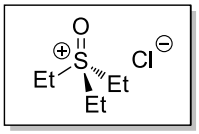

Triethylsulfoxonium chloride (10). Triethylsulfonium chloride (9.310 g, 60.18 mmol) was dissolved in 300 mL deionized water and the solution was cooled to 0 ℃. Then NaOH (14.48 g, 362.1 mmol, 6.0 eq) was slowly added and the solution was kept stirring until homogeneity. After adding *m*-chloroperoxybenzoic acid (titrated before use, 70%, 51.94 g, 210.7 mmol, 3.5 eq.), the resulting suspension was stirred vigorously at 50 ℃. After 30 min, the clear colorless solution was cooled to 0 ℃ and quenched with 6 M hydrochloric acid until pH = 1. The large amount of white precipitate was filtered off and washed with DI water (20 mL × 3). The filtrate was concentrated in *vacuo* to ~100 mL and further washed with CH_2Cl_2 (20 mL). The pH of the aqueous solution was adjusted to 5~6 with saturated sodium bicarbonate solution. After evaporation of the aqueous solution to dryness, the resulting solid mixture was dispersed in 2-

propanol (60 mL) and sonicated for 10 min. The suspension was allowed to pass through a syringe filter (0.2 μm PVDF w/GMF) to remove NaCl. The clear solution was then concentrated in *vacuo* and the crude product was obtained as a white solid. The pure product could be obtained after recrystallization in 2-propanol as white crystals (7.796 g, 45.7 mmol, 76 %). ^{1}H NMR (500 MHz, D_2O) δ 3.96 (q, *J* = 7.0 Hz, 6H), 1.58 (t, *J* = 7.5 Hz, 9H); ^{13}C NMR (125 MHz, DMSO-d_6) δ 42.3, 4.7. HRMS (ESI) calcd for $C_6H_{15}SO$ $(M\text{-}Cl)^+$ 135.0844, found 135.0838. Anal. Calcd. for $C_6H_{15}SOCl$: C: 42.22%; H: 8.86%; S: 18.79%; Cl: 20.77%, Found; C: 42.07%; H: 8.90%; S: 18.53%; Cl: 21.05%.

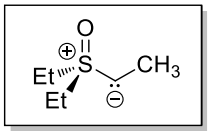

Diethylsulfoxonium ethylide (11) using LDA. To a 50 mL round bottom flask containing triethylsulfoxonium chloride **10** (2.435 g, 14.3 mmol) was added 10 mL degassed anhydrous THF under N_2. The flask was then cooled in an ice bath before addition of freshly prepared lithium diisopropylamide solution (0.67 M in THF, 20.8 mL, 13.9 mmol). The reaction was stirred at 0 ℃ for 10 min and then warmed to room temperature. The resulting light yellow solution can be stored in refrigerator for at least 2 weeks. The concentration was determined as 0.414 M (30.8 mL, 12.8 mmol, 92%) from ^{1}H NMR with a known concentration of the methylide **17** (Figure 3.8). The identity of this ylide was confirmed by reaction with (*E*)-chalcone.

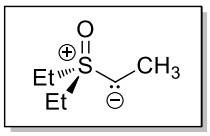

Diethylsulfoxonium ethylide (11) using NaH. To a flame dried, N_2 purged, 50 mL two-neck round bottom flask fitted with a condenser was added NaH (60% dispersion in mineral oil, 0.550 g, 13.7 mmol). The NaH-oil dispersion was washed with 3 × 15 mL of anhydrous hexane. Powdered and vacuum dried triethylsulfoxonium chloride (0.654 g, 3.83

mmol) was added to the flask. After the system was evacuated and backfilled with N_2 three times, anhydrous toluene (10 mL) was then added into the flask under N_2. The reaction mixture was vigorously stirred and heated at reflux for 30 min. After cooling down to room temperature, the ylide solution was cannulated under N_2 to an oven dried Schlenk filter containing Celite 545. The ylide solution was allowed to pass through the filter and collected in a 25 mL flask. An ylide solution aliquot (1.50 mL) was treated with 2 drops of phenolphthalein in H_2O and titrated with 0.1000 M HCl (2.325 mL). The concentration was calculated as 0.155 M. The ylide solution was stored at –20 ℃ and remained stable over several weeks.

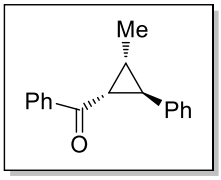

Cyclopropanation of (*E*)-chalcone with diethylsulfoxonium ethylide 11; synthesis of (1RS,2RS,3RS)-1-(3-methyl-2-phenylcyclopropyl)-1-phenylmethanone (12). A 10 mL round bottom flask containing (*E*)-chalcone (103 mg, 0.50 mmol) was purged with N_2. After addition of degassed anhydrous THF (3 mL) to dissolve the solid, diethylsulfoxonium ethylide **11** (0.40 M, 1.20 mL, 0.48 mmol) was injected dropwise to the flask at room temperature. The reaction was stirred overnight and quenched with HCl (1 M, 2 mL). The resulting mixture was diluted with H_2O (20 mL) and extracted with CH_2Cl_2 (1 × 20 mL). The organic phase was washed with H_2O (3 × 20 mL) and dried over $MgSO_4$. After evaporation to dryness, the crude product was purified on silica gel (CH_2Cl_2−Hexane 1:4) to afford **12** as a white solid 71 mg (yield 61%); mp 79–80 ℃. The configuration was determined from NOE experiments (Appendix C). ^{1}H NMR (500 MHz, $CDCl_3$) δ 8.02 (d, *J* = 7.5 Hz, 2H), 7.56 (t, *J* = 7.5 Hz, 1H), 7.47 (t, *J* = 7.5 Hz, 2H), 7.29 (t, *J* = 7.5 Hz, 2H), 7.22–7.16 (m, 3H), 3.00 (dd, *J* =

9.5, 5.0 Hz, 1H), 2.82 (dd, *J* = 6.0, 5.0 Hz, 1H), 2.05 (dqd, *J* = 9.5, 6.5, 6.0 Hz, 1H), 1.29 (d, *J* = 6.5 Hz, 3H); ^{13}C NMR (125 MHz, $CDCl_3$) δ 197.5, 141.1, 138.9, 132.8, 128.7, 128.6, 128.2, 126.42, 126.39, 34.9, 33.0, 29.0, 11.8. HRMS (CI) calcd for $C_{17}H_{17}O$ $(M+H)^+$ 237.1279, found 237.1284.

Determination of the concentration of diethylsulfoxonium ethylide 11. Dimethylsulfoxonium methylide **17** (0.762 M, 0.200 mL, 0.152 mmol) and diethylsulfoxonium ethylide **11** (0.200 mL) were mixed and quenched with 2 mL deionized H_2O. All ylides were protonated to their corresponding sulfoxonium salts. The basic aqueous phase was washed with CH_2Cl_2 (3 × 2 mL) and then acidified with 1 mL 6 M HCl. The aqueous solution was concentrated in *vacuo* followed by addition of D_2O and analyzed by ^{1}H NMR. The ratio of $[Me_3SO^+]/[Et_3SO^+]$, equal to [methylide **17**]/[ethylide **11**], can be calculated from the integration ratio of the singlet peak at 3.86 ppm (I_a) over the quartet peak at 3.96 ppm (I_b) by Equation 3.1.

$$\frac{[M]\times V_M \times 9}{[E]\times V_E \times 6} = \frac{I_a}{I_b} \qquad \text{Eq. (3.1)}$$

Where,

[*M*] ([*E*]) = Concentration of the methylide (or ethylide);

V_M (V_E) = Volume of the methylide (or ethylide);

I_a (I_b) = Integration value of $C\underline{\mathbf{H}}_3SO$ ($CH_3C\underline{\mathbf{H}}_2SO$).

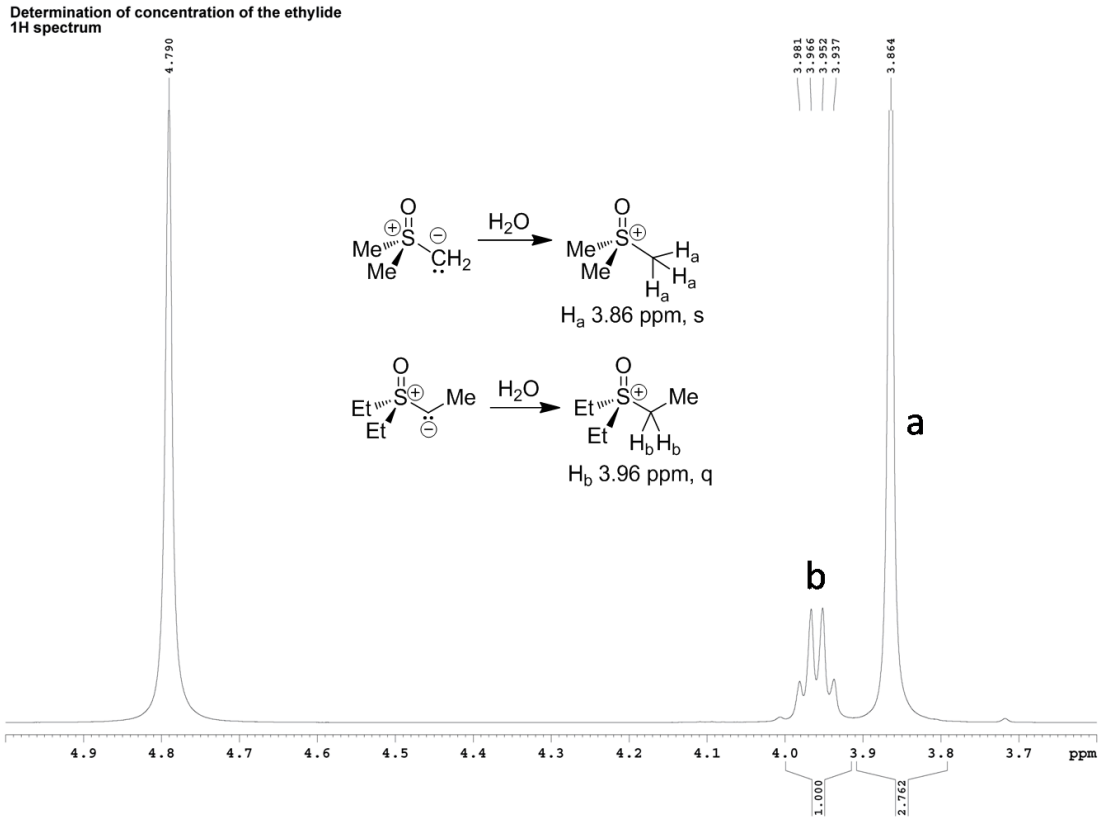

Figure 3.9. Determination of the concentration of diethylsulfoxonium ethylide from ^{1}H NMR with a known concentration of dimethylsulfoxonium methylide.

Representative procedure for measurement of partition of ylides from Me_3SOI 15 and Et_3SOCl 10 (M/E = 9/1) in DCM (Table 3.7, entry 1). To a two-neck round bottom flask equipped with a condenser and stir bar was charged with trimethylsulfoxonium iodide **15** (1.536 g, 6.98 mmol) and triethylsulfoxonium chloride **10** (0.132 g, 0.77 mmol). The system was evacuated and backfilled with N_2 for three times. Then the degassed NaOH (50% in water, 14.4 mL) and DCM (4.8 mL) were added to the flask. The mixture was vigorously stirred under N_2 and gradually warmed up to 40 ℃. After 1 h, the mixture was centrifuged and an aliquot of the top DCM layer was quenched with 1 M HCl solution. The ylides dissolved in DCM were recovered as the chloride salts. The ratio of **15**:**10** can be calculated via ^{1}H NMR the same way as determination of the ethylide concentration by Equation 3.1.

Calculation of monomer incorporation ratio in copolymers from ^{1}H NMR. In the methyl branched linear carbon chain, the number of methine protons is assumed equal to one third of the number of methyl protons. This assumption is based on that the methyl group on polymer chain end was ignored compared to the number of branch methyls per polymer chain, as the monomers were in large excess compared to the initiator B(*n*-hexyl)$_3$ and the resulting copolymer has a M_n for at least 1.0×10^3 g/mol. The methine and methylene protons are both in the range of 1.90–1.08 ppm, while the methyl protons are in the range of 1.08–0.70 ppm. To calculate the amount of methylene protons, the amount of methine protons need to be subtracted from the total integration values in the range of 1.90–1.08 ppm. The composition ratio is calculated as below. The ratio of methylidene over ethylidene in the copolymer can be calculated as Equation 3.2.

$$[M]/[E] = (\frac{I_{[CH_2]}}{2}) / (\frac{I_{[CH_3]}}{3}) = (\frac{I_{[CH+CH_2]} - I_{[CH_3]}/3}{2}) / (\frac{I_{[CH_3]}}{3}) \qquad \text{Eq. (3.2)}$$

Where,

[M]/[E] stands for the ratio of methylidene to ethylidene;

$I_{[CH+CH2]}$ and $I_{[CH3]}$ represents the integration value for CH + CH_2 and CH_3, respectively.

H–D exchange for triethylsulfoxonium chloride 10. Triethylsulfoxonium chloride **10** (10 mg) and D_2O (0.7 mL) were added to an NMR tube. Then an aqueous NaOD solution (30% in D_2O, 70 μL) was added to the NMR tube. ^{1}H NMR (500 MHz, D_2O) δ 1.58 (s).

Representative procedure for aqueous copolymerization of trimethylsulfoxonium iodide 15 and triethylsulfoxonium chloride 10 (Table 3.5, entry 1). To a two-neck round bottom flask equipped with a condenser and stir bar was charged with tetrabutylammonium iodide (68 mg, 0.18 mmol, 4.1 equiv.), trimethylsulfoxonium iodide **15** (2.396 g, 10.89 mmol, 246 equiv.) and

triethylsulfoxonium chloride **10** (206 mg, 1.21 mmol, 27.2 equiv.). The system was evacuated and backfilled with N_2 for three times. Then the degassed NaOH (50% in water, 24 mL) and DCM (8 mL) were added to the flask. The reaction mixture was vigorously stirred and gradually warmed up to 40 ℃ followed by immediately injecting a solution of trihexylborane (42 mg/mL in DCM, 0.280 mL, 11.7 mmol, 1.0 equiv.). After 16 h at 40 ℃, the reaction was cooled down to room temperature and quenched with a mixture of DI water (200 mL) and methanol (200 mL). The mixture was stirred in the open air for 30 min. After filtration and washing with methanol, the product was vacuum dried to afford a white solid (185 mg, 92%).

Representative procedure for batch copolymerization of dimethylsulfoxonium methylide 17 and diethylsulfoxonium ethylide 11 (Table 3.9, sample r2). To a two-neck round bottom flask equipped with a condenser and purged under N_2 was charged with degassed dimethylsulfoxonium methylide **17** (0.776 M, 7.14 mL, 5.54 mmol), diethylsulfoxonium ethylide **11** (0.462 M, 2.00 mL, 0.924 mmol) and toluene (9 mL). The mixture was preheated on an oil bath at 75 ℃ for 3 min followed by a quick injection of tri-*n*-hexylborane (23.3 mg/mL in toluene, 0.176 mL, 0.0154 mmol). After the reaction being stirred for 15 min, a degassed solution of trimethylamine *N*-oxide dihydrate (73 mg/mL in H_2O, 0.22 mL, 0.141 mmol) was injected. The reaction was stirred at 75 ℃ for 24 h followed by addition of 1 M NaOH aqueous solution (1 mL) in air. After stirring for another 3 h at 75 ℃, the reaction was cooled down and quenched with 1 mL 6 M HCl. The mixture was concentrated in *vacuo* and precipitated with 50 mL methanol. After filtration, the precipitate was washed with deionized water (3 × 10 mL) and methanol (3 × 10 mL). Purification by reprecipitation in toluene/methanol afforded a purified white polymer (100 mg, 92%). GPC analysis: M_n = 2070, M_w = 2144, PDI = 1.04.

Representative procedure for semi-batch synthesis of the gradient copolymer (21).

Preparations. Prepare five dry and N_2 flushed round bottom flasks labeled from A to E. Dimethylsulfoxonium methylide **17** (0.547 M) and diethylsulfoxonium ethylide **11** (0.300 M) were mixed in different ratios in flask A to E. The actual concentration ratio of ylides in each flask was determined from ^{1}H NMR with an aliquot quenched by H_2O. The final concentration of methylide in each mixture was calculated from its original concentration and the volume change of solution, while the ethylide concentration was determined from the concentration of methylide and concentration ratio of ylides (Table 3.14).

Table 3.14. The concentration, injection volume and reaction time of each ylide solution.

solution	[M]^a (mol/L)	[E]^a (mol/L)	[M]/[E]^b	V_{inject}^{c} (mL)	$n_{Me,in}$^{d} (mmol)	$n_{Et,in}$^{d} (mmol)	rxn time (min)
A	0.439	0.0592	7.42 : 1	15	6.585	0.888	20
B	0.372	0.0957	3.89 : 1	18	6.696	1.723	30
C	0.322	0.1234	2.61 : 1	21	6.762	2.591	40
D	0.285	0.1434	1.99 : 1	24	6.840	3.442	60
E	0.222	0.178	1.25 : 1	30	6.660	5.340	180

a. [M] and [E] is the concentration of methylide and ethylide in each ylide mixture.
b. [M]/[E] is the concentration ratio of methylide over ethylide determined from ^{1}H NMR by quenching of an aliquot of ylide mixture with H_2O.
c. V_{inject} is the volume of each ylide solution injected into the reaction.
d. $n_{Me,in}$ and $n_{Et,in}$ represent the mole of methylide and ethylide monomer that was injected to the polymerization reaction at each stage. $n_{Me,in(A)} = [M]_{(A)} \times V_{inject(A)}$.

Polymerization to afford 21. To a 250 mL two-neck round bottom flask equipped with a condenser was added degassed toluene 70 mL and dimethylsulfoxonium methylide **17** (0.547 M, 14.0 mL, 7.66 mmol). The solution was preheated at 70 ℃ for 5 min followed by an injection of tri-*n*-hexylborane (51.9 mg/mL in toluene, 0.546 mL, 0.106 mmol). After stirring for 15 min, an aliquot of the reaction (8 mL) was transferred to a N_2 purged flask containing trimethylamine *N*-oxide dihydrate (TAO) solution (20 mg/mL in DMSO, 1 mL, 0.18 mmol). And the original reaction was added ylide mixture A (15 mL) and stirred for 20 min. Aliquots of the reaction were sampled out and quenched by TAO in the same way as mentioned above before addition of the

subsequent ylide mixture. The volumes of ylide solutions added to the polymerization and aliquots for sample analysis, as well as the polymerization time for each segment, were summarized in Table 3.14. All reactions quenched by TAO were stirred at 75 ℃ overnight before addition of 1 mL 6M HCl. After concentrated on a rotary evaporator and added 30 mL MeOH at 0 ℃, all reaction mixtures were filtered and washed with H_2O (3 × 10 mL) and MeOH (3 × 10 mL). Purification by reprecipitation in toluene/methanol afforded purified polymers from white powder (**g1** to **g3**) to colorless transparent solid (**g4** to **g6**). The final gradient copolymer **g6** was afforded as a tough transparent rubbery material (803 mg). GPC analysis: M_n = 3081, M_w = 3483, PDI = 1.13.

Calculation of monomer content in polymer 21. As all gradient copolymers were performed in the same reaction flask and aliquots were sampled out continually, the actual quantities of monomers (as well as monomer feed ratio) for each polymer do not equal to simply adding up the injected quantities. Thus the cumulative monomer feed ratio for each gradient copolymer has to be recalculated in consideration of the material lost during monitoring the polymerization progress. The calculation of the cumulative monomer feed ratio for each gradient copolymer are summarized in Table 3.15.

Table 3.15. Calculation of the cumulative monomer feed ratio for each gradient copolymer.

sample	solution[a]	$n_{Me,in}$[b] (mmol)	$n_{Et,in}$[b] (mmol)	V_{inject}[b] (mL)	$V_{aliquot}$[c] (mL)	$V_{rxn,I}$[d] (mL)	$V_{rxn,II}$[d] (mL)	$n_{Me,sol}$[e] (mmol)	$n_{Et,sol}$[e] (mmol)	$(M/E)_{feed}$[f]
g1	—	7.658	0	14	8	84	76	6.929	0	1:0
g2	A	6.585	0.888	15	9	91	82	12.177	0.800	15.2:1
g3	AB	6.696	1.723	18	10	100	90	16.986	2.271	7.48:1
g4	ABC	6.762	2.591	21	11	111	100	21.395	4.380	4.88:1
g5	ABCD	6.840	3.442	24	12	124	112	25.503	7.065	3.61:1
g6	ABCDE	6.660	5.340	30	—	142	—	32.163	12.405	2.59:1

a. each gradient polymer sample was prepared based on solutions of ylide mixtures as described in table 3.14. For example, g4 was prepared based on the gradient copolymer g3 and subsequent reaction with ylide solution C.

b. $n_{Me,in}$, $n_{Et,in}$ and V_{inject} are from Table 3.14.

c. $V_{aliquot}$ is the volume of aliquot removed from the reaction for analysis at each stage.

d. $V_{rxn,I}$ represents the reaction volume at the end of each stage of polymerization before an aliquot was removed for analysis. $V_{rxn,II}$ is the reaction volume after an aliquot was removed for analysis and before an injection of the subsequent ylide solution. $V_{rxn,I}$ at each stage was calculated based on $V_{rxn,II}$ at the previous stage and the volume of newly injected ylide solution. $V_{rxn,I(g2)} = V_{rxn,II(g1)} + V_{inject(g2)}$. $V_{rxn,II}$ at each stage was calculated based on $V_{rxn,I}$ at current stage and the volume of aliquot removed from the reaction. $V_{rxn,II(g2)} = V_{rxn,I(g2)} - V_{aliquot(g2)}$.

e. $n_{Me,sol}$ and $n_{Et,sol}$ are the cumulative mole of methylide and ethylide units that remained in the reaction at each stage after consideration of an aliquot removed from the system. For example, $n_{Me,sol(g3)} = (n_{Me,sol(g2)} + n_{Me,in(g3)}) \times V_{rxn,II(g3)}/V_{rxn,I(g3)}$.

f. $(M/E)_{feed}$ is the cumulative monomer feed ratio of the gradient copolymer calculated based on the total amount of monomer feed. The copolymer sample obtained from quenching an aliquot of the polymerization reaction has the same monomer feed ratio as the one remained in the reaction at the same stage. $(M/E)_{feed,g2} = n_{Me,sol(g2)}/n_{Et,sol(g2)}$

Chapter 4. Precise Insertion of Phenyl Groups on a Linear Carbon Chain

4.1. Introduction

Biological polymers such as DNA employ a simple set of four nucleic acids to encode the replication or peptides that utilize dozens of amino acids to embed specific functionalities. These sequence controlled biopolymers possess information density that can exceed those of modern computers by many orders of magnitude.[1] The precise control of chemical structures and its attendant information content endows biopolymers with complex function that can be traced ultimately to all vital processes of life. The biosynthesis of these biopolymers in nature can now be mimicked via several chemical approaches, including Merrifield solid phase peptide synthesis,[2] and related variants[3] and phosphoramidite chemistry for oligonucleotide synthesis.[4] In biopolymers, the linkages between monomers are usually amide, phosphate ester or glycosidic bonds. The monomers are designed with two different reactive sites, one of which is protected. After each monomer addition, deprotection reveals a new reactive site for addition of the next monomer. As a consequence, discrete monomers can be incorporated into the growing polymer chain one by one. Thus biopolymers are synthesized via a step growth polymerization in an automated fashion.

In comparison, synthetic carbon backbone polymers lack specific control of sequence; therefore their information content is low and unable to carry out complex tasks on the molecular level. The ability to control sequence in synthetic carbon backbone copolymers can result in truly transformative macromolecular properties.[5] During the past two decades, considerable progress has been made on controlling the sequence of synthetic polymers. Sequence-regulated vinyl

copolymers with periodic chemical structures can be obtained in a step growth radical polymerization by use of a designed monomer with specific chemical properties.[6] For chain growth polymerization, polymer chains can be encrypted with various functional groups via time-controlled addition of acceptor monomers during the living polymerization of a donor monomer.[7,8] In addition, preformed polymer or oligomer templates have been employed to transcribe weak intermolecular interactions between template and monomer to orchestrate the sequence of polymerization.[9] However, complete control of the location of specific monomers in the polymer chain in chain growth polymerizations remains an elusive goal.

One measure of a truly controlled polymerization is the ability to insert a functional monomer at a specific location on the polymer chain. To achieve this goal, several methods have been developed including time-controlled addition of discrete amounts of monomers during the course of a living polymerization[10] and the use of donor–acceptor monomer couples[11]. However, these ingenious approaches are far from perfect. In addition, they present challenges to validate the precise location of the insertion site due in part to the chemical complexity of the functional polymer chains and the chain-to-chain distribution of composition that is inherent in most, even living, polymerizations.[12]

In this chapter I focus on the controlled introduction of a functional group at precise locations on a simple linear polymethylene chain. Here the polymerization is investigated with the focus on monomer design using a conventional polyhomologation initiator triorganoborane. A different approach for the sequence control will be discussed by evaluation of a unique initiator platform in Chapter 5.

Scheme 4.1. Proposed introduction and validation of phenyl groups at the precise location of a polymer chain.

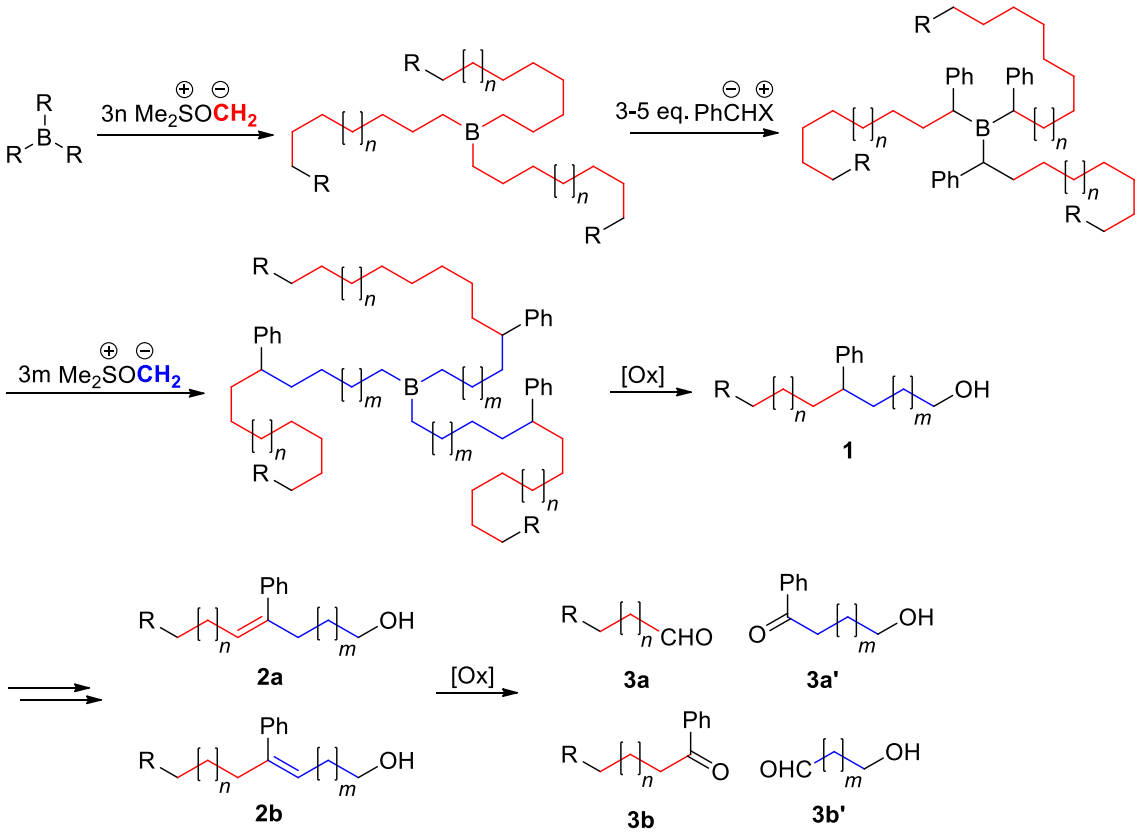

As a proof of concept, the phenyl group is selected to help 'visualize' the insertion location on the polymer chain. A mild 'cutting' of the polymer backbone then becomes possible as there are several methods to cleave the C–C bond incorporating a benzylic carbon. In addition, the aromatic ring can be functionalized for future introduction of various functional groups. As a living polymerization, the polyhomologation reaction is able to control molecular weight (MW) and achieve low polydispersity. By addition of monomers in a sequential manner, the phenyl group can be attached to the terminus of a growing polymethylene chain (Scheme 4.1). Following insertion of the benzylic carbon, controlled growth of the polymer chain can be resumed. The resulting designed polymer **1** could be obtained after oxidation to cleave the boron–carbon bond. The location of benzyl insertion can be revealed by formation of an unsaturated carbon–carbon bond as in polymer **2** via reactions such as bromination followed by

elimination. A further oxidation on the C=C bond will cleave the polymer chain into fragments **3**. The chain lengths can be calculated and compared based on the measured MW from GPC analysis between the intact parent polymer and the resulting polymer fragments. The position of insertion on the polymer chain can thus be determined to prove the level of control.

4.2. Results and Discussion

To insert the phenyl group on a carbon chain via the polyhomologation reaction, a benzylide with sufficient reactivity and a good leaving group is required. With triorganoborane as the initiator, choices on the type of monomers are quite limited to sulfoxonium ylides and diazo compounds. In my study, the more reactive sulfonium ylide was chosen instead of the commonly used sulfoxonium ylide. The latter one is not ideal due to its low reactivity as well as the difficulties in preparation of the (dimethylamino)phenylsulfoxonium benzylide **9** (Scheme 4.2a). The conjugation of the carbanion with both the adjacent aromatic ring and S=O bond made the pair of electrons on carbon further delocalized and much less nucleophilic compared to the case in the sulfonium ylide without S=O bond. In contrast, synthesis of sulfonium benzylide based on tetrahydrothiophene **12** can be readily achieved (Scheme 4.2b). The only disadvantage with sulfonium ylides is that they are thermally much less stable than the sulfoxonium ylides. Most of the sulfonium ylides are known to decompose above 0 ℃ and are often introduced to reactions at low temperatures or generated *in-situ*.[13] This factor conflicts with the traditional polyhomologation using sulfoxonium ylides which requires reaction temperatures above 0 ℃ to undergo the 1,2-migration.

Scheme 4.2. Comparison of the synthetic routes between a) sulfoxonium benzylide **9** and b) sulfonium benzylide **12**.

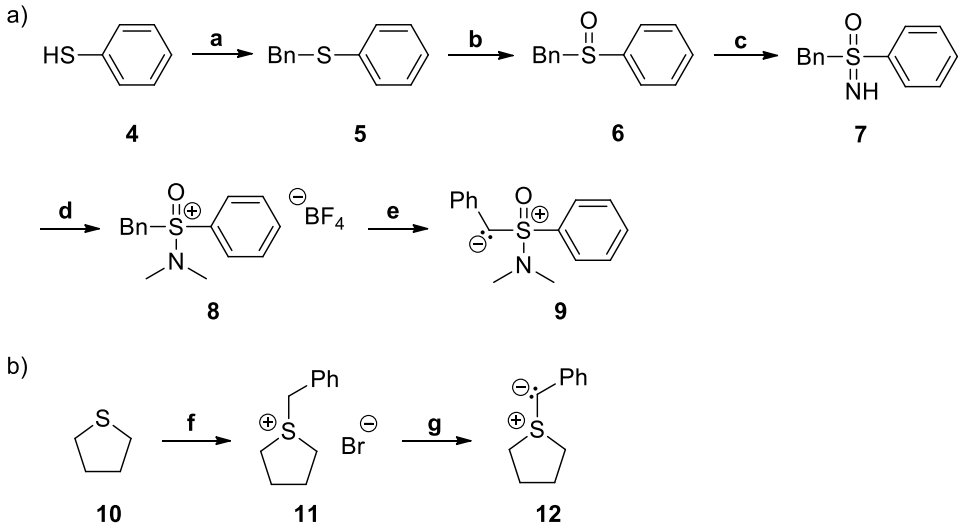

Reagents and conditions: a) NaH, THF, reflux then benzyl bromide; b) 30% H_2O_2, cat. CF_3COCH_3, CH_2Cl_2, 0 ℃ to rt; c) NaN_3, H_2SO_4, $CHCl_3$, reflux, 3 d; d) Me_3OBF_4, Na_2CO_3, CH_2Cl_2, rt, 5 d; e) LiHMDS, 0 ℃; f) benzyl bromide, rt, 20 min; g) LiHMDS, −78 ℃, 1 h.

One of the challenges to the goal of precise insertion is to guarantee the insertion on every single polymer chain. The polyhomologation is a two-step reaction: complexation of the catalytic site with the monomer and 1,2-migration step. As each organoborane initiator has three propagating arms, the ylide monomers will be added one by one statistically distributed on the three arms of the same initiator (Scheme 4.3). In addition, the complexation is a reversible reaction. During the 1,2-migration step, small portions of the borate complex can undergo decomplexation to generate the monomer ylide. As a result, some polymer chains will have two benzyl insertions. that can react with organoboranes to generate different numbers of insertions among all polymer chains.

Scheme 4.3. The random monomer incorporations due to the three active catalytic sites per initiator.

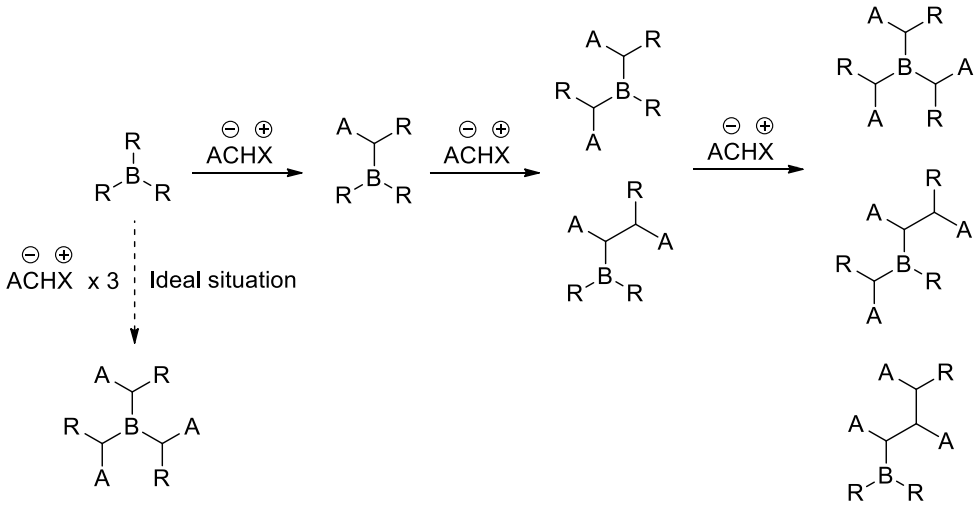

With an excess of the secondary ylide, at least one insertion can be guaranteed on all polymer chains. In this case, multiple insertions of the same secondary ylide will be expected to occur on a single polymer chain. This is not of concern because the substituted ylides do not polymerize without the presence of the simple dimethylsulfoxonium methylide. Based on my studies in Chapter 3, even just consecutive three insertions of substituted monomers are rather rare due to the steric hindrance that impedes the monomer on further complexation with the catalytic site. With only two insertions on the polymer backbone, the following chain cleavage reactions including bromination and oxidation can still proceed. And the resulting polymer fragments will have the chain length near identical to those from the single insertion which is indistinguishable by GPC analysis.

4.2.1. Model studies with small molecules

As a model study, the efficiency of the benzyl insertion was evaluated by reaction of organoborane **13** with *in-situ* generated benzylide **12** (Scheme 4.4). The presence of *p*-methoxyphenyl group is important to help characterization during separation and NMR analysis

as well as to help avoid loss of the final products due to the low vapor pressure with low MW components.

Scheme 4.4. Benzyl insertion on tris(*p*-methoxyphenylethyl)borane **13** carried out at different conditions using benzylide **12**. Stereo- and regio-isomers are not shown.

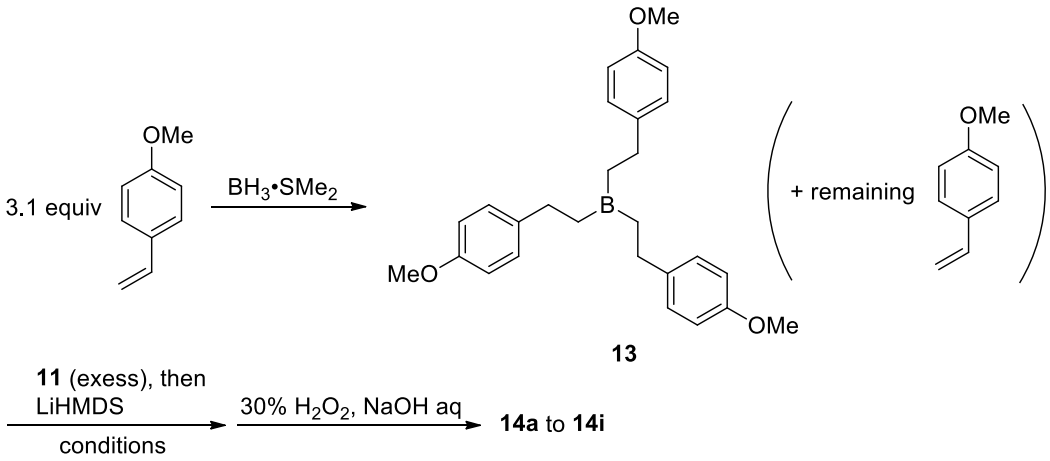

Major products of concern:

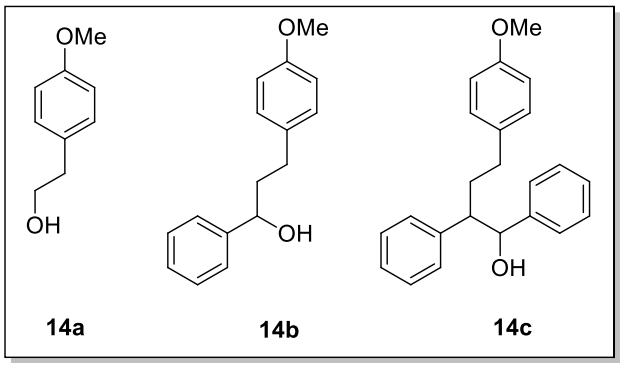

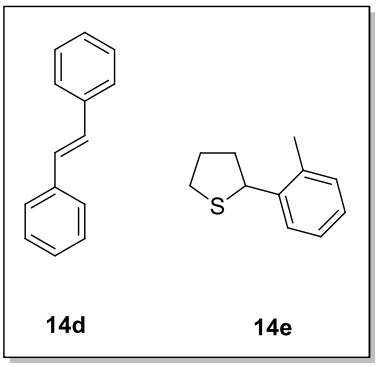

Other compounds observed:

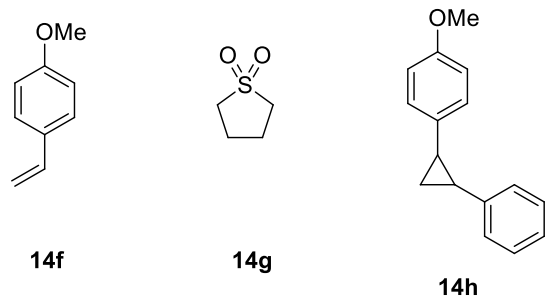

Organoborane **13** was prepared by hydroboration of *p*-methoxystyrene and directly used without further purification. To minimize decomposition of the benzylide, organoborane **13** was

first mixed with the ylide precursor **11** followed by addition of the base lithium bis(trimethylsilyl)amide (LiHMDS) to produce **12** *in-situ*. After oxidation to cleave the boron–carbon bond, the mixtures were extracted with CH_2Cl_2 and dried before subjected to GC-MS analysis. Further chromatographic separations followed by GC-MS and NMR analyses were also performed to identify every component.

Efforts have been taken to identify most of the products except for two unidentified products (15%) at m/Z of 226 and 316 (Scheme 4.4). Five major products from **14a** to **14e** account for 70~75% of the mixture. Other GC traces indicated the presence of unreacted *p*-methoxystyrene **14f**, oxidation product **14g** from the homologation byproduct tetrahydrothiophene, cyclopropanation product **14h** which arises from reaction of **14f** with the benzylide, and the dimerization product **14i** from ·OH racial addition of **14f** (a well-known oligomerization for styrene derivatives). Most of **14f** to **14i** originate from the use of an excess of *p*-methoxystyrene and will not be discussed here, because the *p*-methoxyphenyl substructure only serves as the marker in the model study and will not be employed in an actual polymerization. Compound **14a** is the product from organoborane **13** with no participation in the homologation. And its amount is an important indicator of the efficiency of benzyl insertions. Compound **14b** and **14c** are products from single-insertion and double-insertion, respectively.

To help identify all major products, two control reactions were also performed with one to identify the decomposition products of the benzylide and the other to discover whether the benzylide can react with hydrocarbon compounds bearing aromatic moieties (Scheme 4.5). Thermal decomposition of the ylide **12** by α-elimination was always present with its product identified as stilbene **14d**. In addition, thermal induced rearrangement of the benzylide, known as the Sommelet–Hauser rearrangement[14,15], was also observed as product **14e** (Scheme 4.5a). The

benzylide was found to have no reaction at all with tetralin **15** (Scheme 4.5b). Thus there should be no concern on insertions at aliphatic C–H, aromatic C–H and benzylic C–H.

Scheme 4.5. Control reactions on a) decomposition of the benzylide **12** and b) possible side reaction between ylide and hydrocarbon compound.

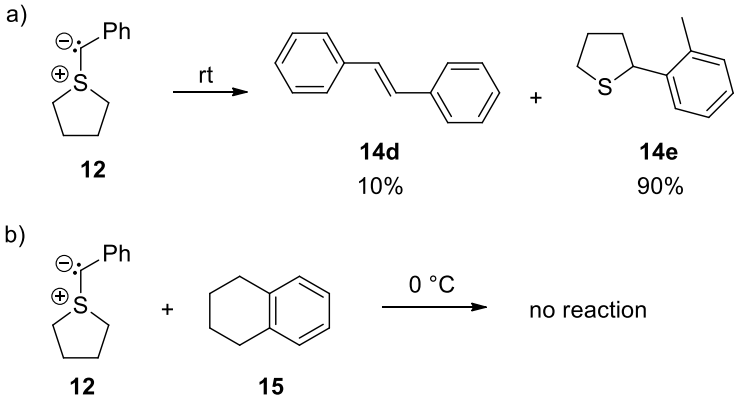

The benzyl insertion in Scheme 4.4 was investigated under two reaction conditions (Table 4.1). The results are normalized to have a total of 100% for compound **14a**–**e**. In my first attempt, the reaction was carried out at 0 ℃ with 6 equivalent of the benzylide (entry 1). To ensure enough ylide present for insertion, the amount of benzylide introduced is doubled compared to the theoretical three equivalence. A large portion of the benzylide was found to undergo decomposition and rearrangement with a total of 40% in the products. Due to these competing side reactions, the actual amount of benzylide participated in the insertion is lowered. While only focusing on **14a**–**c** as the destiny of the organoborane **13**, the product **14a** with no insertion was present to be almost 12% even with an excess of ylide **12**. This is not ideal in an actual polymerization as over 10% of the polymer will not be cleaved in the post-modification process. And an extra purification process will be required to remove the uncleaved polymer chains. The double-insertion product **14c** was found to be in majority among **14a**–**c** due to the use of benzylide in excess.

Table 4.1. Benzyl insertion on tris(*p*-methoxyphenylethyl)borane **13** carried out under different conditions.

entry	LiHMDS (eq.)	temp (˚C)	time (h)	**14a** (%)	**14b** (%)	**14c** (%)	**14d** (%)	**14e** (%)	**14a**[a] (% in **14a**–**c**)
1	6	0	0.5	7.4	21.1	31.4	22.3	17.8	11.6
2	4.2	−20	1.5	4.7	71.8	21.2	1.0	1.3	4.8

a. The last column is calculated as **14a**%/(**14a**% + **14b**% + **14c**%) to highlight the distribution of the organoboranes.

I also carried out the insertion reaction at lower temperature with lower amounts of ylides (Table 4.1, entry 2). The decomposition and rearrangement products of **12** are reduced to less than 3%. The no-insertion product **14a** is less than 5% which is tolerable for the polymerization study. And the single-insertion product **14b** appears to be in majority because of the slight excess of benzylide **12**. These conditions are close to an ideal situation.

4.2.2. Polymerization studies

With these preliminary findings, the insertion of a benzyl group in a polymer chain was then investigated. The polymerization was carried out with addition of monomers in three steps under different conditions (Scheme 4.6). First, one part of the polymer backbone was built from sulfoxonium methylide **16** initiated by tri-*n*-hexylborane (Step A). The methylide can be fully consumed within 30 min at 60 ℃ indicated by titration of an aliquot of the reaction solution. Then the mixture was cooled down to −20 ℃ to minimize the decomposition of the benzylide in the next step. After addition of the freshly and separately prepared benzylide **12**, the mixture was heated back to 60 ℃ to destroy all the remaining benzylide (Step B). The polymer living chain end was further propagated with methylide **16** (Step C). A final oxidation was carried out to cleave all polymer chains from boron. The results are summarized in Table 4.2.

Scheme 4.6. Synthesis of benzylidene incorporated polymethylene.

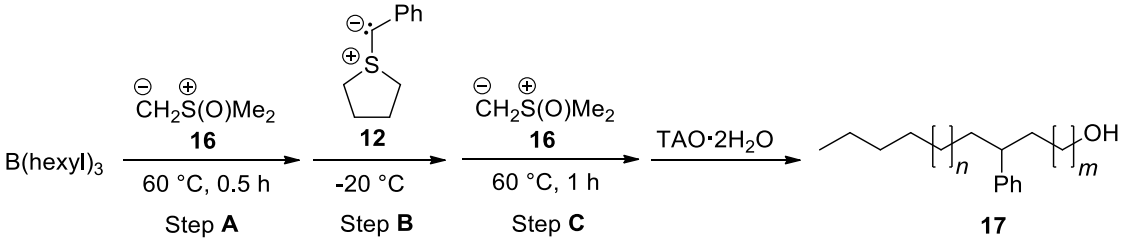

Table 4.2. Benzyl insertion on linear carbon chains.

entry	A[a]	B[a]		C[a]					
	16 (eq.)	**11** (eq.)	time (h)	**16** (eq.)	yield (%)	MW_{th}[b] (g/mol)	M_n[c]	PDI[c]	ratio[c]
1	45	4.3	1	60	75	682	2271 298	1.07 1.07	27 73
2	72	8.0	4	90	83	948	1889 394	1.13 1.04	62 38
3	9	6.6	4	60	81	514	964	1.05	100[d]

a. The equivalence of monomers is provided here. Each theoretical degree of polymerization (DP) can be easily calculated as DP = equivalence/3.
b. MW_{th} is the theoretical MW of the polymer. $MW_{th} = M_{CH2} \times (DP_A + DP_C) + M_{C7H6} + M_{hexyl} + M_{OH.}$
c. Determined by GPC analysis.
d. The polymer is partially contaminated (~14%) with very low MW chains (M_n ~ 210) which can be washed away during the filtration process.

In my first attempt, both hydrocarbon segments before and after the insertion were designed to have short chains with a theoretical degree of polymerization of 15 and 20, respectively (entry 1). The optimized insertion condition was applied to the benzyl insertion with 4.3 equivalents of benzylide at −20 ℃. After the final product was obtained, GPC analysis shows a bimodal MW distribution with 27% for high MW fraction (M_n = 2271) and the remaining majority for the low MW polymers (M_n = 298). A comparison of the sample MW with the theoretical value indicates that there are two types of catalytic sites. The more reactive one gave a faster propagation with MW over twice the MW of the expected theoretical value; while the less reactive one produced the polymer fraction with only half of the theoretical MW.

To identify the two catalytic sites with distinct reactivities, analysis is required on all possible propagating chain ends after the benzyl insertion. To simplify the discussion, the double-insertion will not be taken into considerations because I expect it will not differ in reactivity from the catalytic site with single-insertion. With the benzylide in excess, a triorganoborane will end up with a distribution among all three possible products **18a**–**c** (Scheme 4.7). These new boron species can still undergo polymerization with the methylide having different propagation rates ranked as **18a** > **18b** > **18c**. If the triorganoborane was the same as the one in the model study (section 4.2.1), **18c** would represent almost all boron species as there is very small amount of no-insertion products (< 5%). If the same result occurred to an actual polymerization, high MW polymers from no-insertion catalytic sites would be no more than 5%. Although subsequent homologations of the methylide will transform **18c** to species **18b**, **18a** or even **18**, it will be a gradual process with no sudden change in distributions of the boron species. As a result, the polymer MW would be obtained as unimodal distribution with slightly increased polydispersity. In reality, two very different catalytic sites are present in which the boron species are probably mainly **18** and **18c**, meaning that part of the boron species has benzyl inserted on none of the three arms; while most of those reacted has benzyl inserted on all three arms. The much faster propagation rate of **18** compared to **18c** allows it to quickly consume all methylides before **18c** could catch up by only a few insertions. This hypothesis was also supported by my observations below.

Scheme 4.7. Possible propagating chain ends after the benzyl insertion.

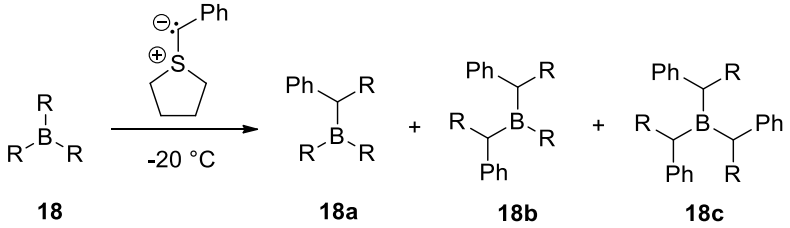

The first possible factor is an inadequate reaction time for the benzyl insertion at −20 ℃. Raising the insertion time from 1 h to 4 h together with more benzylide gave the polymer with 38% in low MW which is much lower compared to the previous 73% (Scheme 4.6, entry 2). With longer reaction time, a higher percentage of **18c** as well as **18a** and **18b** were formed and the amount of polymer from **18** was significantly reduced, leaving more methylides polyhomologated with boron species containing benzyl groups. The observed MW of the high MW polymer fraction was only twice as large as the theoretical value compared to the case in entry 1. A longer reaction time was not investigated, as the benzylide decomposition/rearrangement is not completely suppressed at −20 ℃.

For the second factor, one observation during the reaction setup caught my attention. After formation of the first polymethylene segment (Step A), the reaction mixture was a colorless and transparent solution. But during the cooling process, cloudiness was observed before addition of the benzylide. This indicates low solubility of the long hydrocarbon chains at −20 ℃. As the reaction became heterogeneous, some part of the catalytic sites may become inaccessible, leading to an incomplete benzyl insertion. Even though the benzylide was in large excess, some of the insoluble catalytic sites may not engage in the insertion at all, leading to the distribution of boron species as stated above (Scheme 4.7). The incomplete benzyl insertion was also supported by the measured MW of the low MW polymer fraction (entry 1, M_n = 298) which is very close to the theoretical value for the polymer fraction after step A with a designed formula of *n*-hexyl–$(CH_2)_{15}$–OH (MW = 312). This also applies to the second trial with M_n = 394 *vs.* *n*-hexyl–$(CH_2)_{24}$–OH (MW = 438) (entry 2). As the polyhomologation reaction is a living polymerization with no chain-termination reactions, polymer chains with no benzyl insertion during step B will resume for further propagations in step C. Therefore the low MW fraction

should be identified as phenyl terminated polymethylenes with their origins from the low-reactive catalytic sites that resemble **18c**. Having the benzyl insertion will theoretically add an additional MW of 90 to the polymer. However, using GPC analysis with the refractive index (RI) detector, such a benzyl inserted polymer can hardly be distinguished from long hydrocarbon chains of the same length with none phenyl groups.

To verify the influence of polymer solubility, a third polymerization was carried out with design of a much shorter chain for step A (Scheme 4.6, entry 3). In this case, only 9 equivalence (DP = 3) of methylide was added. Not surprisingly, all the three reactions remained homogeneous and transparent until the very end. And the polymer was obtained with a unimodal distribution of MW. As there are still differences on the reactivity among all boron species, part of **18c** did not engage in further homologation. As a result, the actual amount of initiator is less than expected with a higher MW than the calculated value. This was also evidenced by the GPC trace with a long tail for the low MW fractions. However, the use of a very short chain greatly limits the outcome and is far from satisfactory.

From the above study, the limitation of benzylide **12** is quite clear. Its low thermal stability requires a low insertion temperature at which some of the catalysts are no longer soluble. As a result, there is a fraction of catalysts that have no benzyl inserted leading to a bimodal MW distribution. Although a very short chain could resolve this issue, the comparison between the parent polymer and its fragments will be made challenging via GPC analysis after chain cleavage. In summary, the low solubility of the organoboranes attached by three polymer chains at low temperatures should be responsible for the bimodal MW distribution. Some of the propagating chain ends became inactive after the benzyl insertion and failed to participate in step C.

4.2.3. Alternative solutions to the single insertion challenge

To solve the above problem, the first idea is to increase the solubility of the first polymer segment at −20 ℃. However, very few choices on the solvent could be made, since the reaction media for ylide preparations is quite limited. Sulfonium and sulfoxonium ylides do not dissolve in nonpolar solvents such as decalin, great solvents for hydrocarbon polymers. Even when decalin or toluene is used, linear hydrocarbon chains with more than 20 carbons in the backbone are no longer soluble at −20 ℃. A different approach was explored by changing from a linear hydrocarbon chain into a more soluble methyl branched carbon chain (Scheme 4.8). Branching on a linear polymer backbone is known to increase its solubility and lower the melting point due to the disrupted chain to chain interactions.[16] To examine this possibility, the reactions were the same as Scheme 4.6 except for the additional use of ethylide **18** to introduce a methyl branch on the polymer backbone.

Scheme 4.8. Benzyl insertion on branched carbon chains.

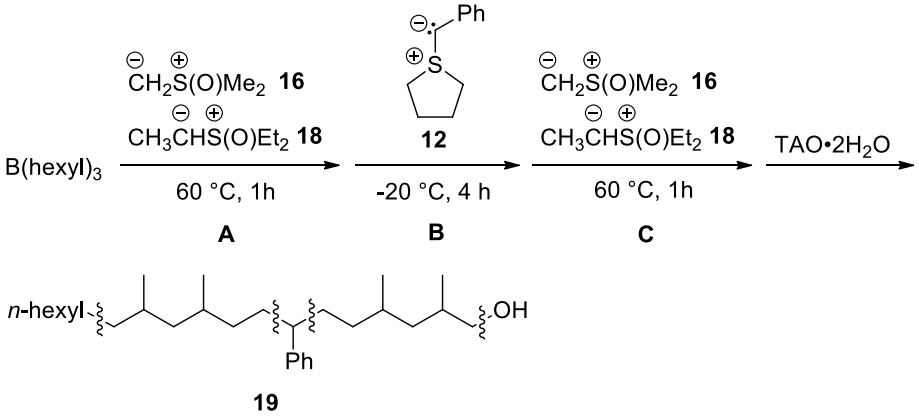

With methyl branch of approximately 33% in the first polymer segment close to the limit of methyl incorporation[16], the final material still had bimodal MW distributions (Table 4.3, entry 1–2) with near equal amount for both high and low MW fractions. Cloudiness was also observed for both reactions. The introduction of the methyl branch is still insufficient to increase the solubility of short-chain hydrocarbon polymers due to the low reaction temperature at −20 °C.

Table 4.3. Benzyl insertion on branched carbon chains.

entry	A[a]		C[a]		yield	MW_{th}[b]	M_n[c]	PDI[c]	ratio[c]
	16 (eq.)	**18** (eq.)	**16** (eq.)	**18** (eq.)	(%)	(g/mol)	(g/mol)		
1	60	30	108	12	95	1368	1973 652	1.05 1.10	59 41
2	60	30	120	0	97	1312	2248 659	1.07 1.11	58 42

a. The equivalence of monomers is provided here. Each theoretical degree of polymerization (DP) can be easily calculated as DP = equivalence/3.
b. MW_{th} is the theoretical MW of the polymer. $MW_{th} = M_{CH2} \times (DP_{A(16)} + DP_{C(16)}) + M_{CH3CH} \times (DP_{A(18)} + DP_{C(18)}) + M_{C7H6} + M_{hexyl} + M_{OH.}$
c. Determined by GPC analysis.

Another solution is to search for a different benzylide with sufficient stability that can withstand room temperature at which most short- and medium-chain aliphatic organoboranes are soluble. Further studies are necessary to focus on the design of stable benzylide monomers. Having the phenyl group in the benzylide, it brings opportunities to tune the stability and reactivity by incorporation of various functionalities at different locations on the aromatic ring. The synthetic method can be adapted from the one for sulfonium salt **11** by simply mixing a benzyl bromide derivative with tetrahydrothiophene at room temperature. In my preliminary study, substrates with electron donating groups such as methyl and methoxy on the para position in benzyl bromide can easily undergo the desired substitution reaction (Scheme 4.9). Those with electron withdrawing groups CF_3 or $CO_2{}^tBu$ did not proceed well. Additional studies are required to optimize the reaction conditions for successful synthesis on all substrates. The corresponding ylides after deprotonation can be carried for stability tests at room temperature.

Scheme 4.9. Synthetic attempts of other benzyl sulfonium salts based on tetrahydrothiophene.

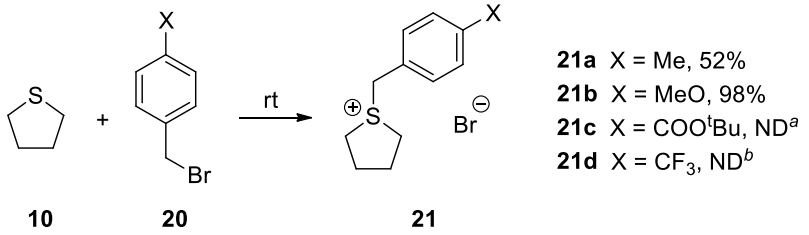

a. ND = not determined. The *tert*-butyl group was not found in the obtained solid.
b. The CH_2 between sulfur and aromatic group was not observed on both ^1H and ^{13}C NMR.

An alternative strategy is to replace the substituted benzyl sulfonium bromide salts **21** with the tetrafluoroborate salts. They can be synthesized in the same way as **21** with an additional use of $NaBF_4$.[17] The tetrafluoroborate salt is also thermally more stable than the sulfonium bromide without the reversed reaction between the anion and one of the three substituents on sulfur during its synthesis.[18] In addition, the possibility of benzyl insertions with (dimethylamino)phenylsulfoxonium benzylide **9** has not yet been completely ruled out. This sulfoxonium ylide has higher thermally stability than sulfonium benzylide **12**.

4.3. Conclusion

The precise single insertion of a functional monomer in a simple hydrocarbon chain is an ultimate level of control as the first step to achieve the complete sequence control of a carbon backbone polymer. As a proof of concept, the benzyl insertion is preferred because of the ease to cut the polymer backbone at the insertion point for analysis. It also allows the benzyl insertion to be a superior choice because of the capability of embedding various functional groups on the aromatic ring to bring diversity to the polymers. For this purpose, the sulfonium benzylide **12** based on tetrahydrothiophene was evaluated. A low temperature (−20 ℃) is required to suppress the decomposition and rearrangement of ylide **12**. The benzyl insertion was found to be only

effective when the first polymer segment was short in length. The first stage in this process requires sufficient solubility of the organoborane bearing three aliphatic polymer chains at low temperatures to guarantee a complete benzyl insertion on all chains. The non-benzylated propagating chains will rapidly grow the polymer at elevated temperatures after the insertion step and produce materials with bimodal MW distribution. The change to a different solvent or incorporation of branches on the linear backbone did not effectively solve the problem. The best choice is to increase the insertion temperature to room temperature at which most polymers with less than 50 carbons in length are soluble.

In the future, efforts should be made on search of a benzyl ylide that is stable at room temperature. Once the desired polymer structure was obtained, the following bromination and oxidation would be straightforward with no interference from other parts of the polymer because those are aliphatic hydrocarbons. Analysis of the MW of the resulting polymer fragments compared to the one of the intact polymer can provide unambiguous validation on the site of functional monomer introduction.

4.4. References

(1) Church, G. M.; Gao, Y.; Kosuri, S. *Science* **2012**, *337*, 1628–1628.

(2) Merrifield, R. B. *J. Am. Chem. Soc*. **1963**, *85*, 2149–2154.

(3) Pfeifer, S.; Zarafshani, Z.; Badi, N.; Lutz, J.-F. *J. Am. Chem. Soc.* **2009**, *131*, 9195–9197.

(4) Gryaznov, S. M.; Letsinger, R. L. *J. Am. Chem. Soc*. **1991**, *113*, 5876–5877.

(5) Lutz, J.-F.; Ouchi, M.; Liu, D. R.; Sawamoto, M. *Science* **2013**, *341*, 628–635.

(6) Satoh, K.; Ozawa, S.; Mizutani, M.; Nagai, K.; Kamigaito, M. *Nat. Commun.* **2010**, *1*.

(7) Lutz, J.-F. *Acc. Chem. Res.* **2013**, *46*, 2696–2705.

(8) Zhang, J.; Matta, M. E.; Hillmyer, M. A. *ACS Macro Lett.* **2012**, *1*, 1383–1387.

(9) (a) Połowiński, S. John Wiley & Sons, Inc.: 2002. (b) Akashi, M.; Ajiro, H. (eds Kobayashi, S.; Müllen, K.) Springer Berlin Heidelberg: 2015.

(10) Zamfir, M.; Lutz, J.-F. *Nat. Commun*. **2012**, *3*, 1138.

(11) Srichan, S.; Chan-Seng, D.; Lutz, J.-F. *ACS Macro Lett*. **2012**, *1*, 589–592.

(12) Voit, B. *Angew. Chem, Int. Ed.* **2000**, *39*, 3409.

(13) Corey, E. J.; Chaykovsky, M. *J. Am. Chem. Soc*. **1965**, *87*, 1353–1364.

(14) Block, E. The Chemistry of the Sulfonium Group, eds. Stirling C. J. M. and Patai, S. Wiley, New York, 1982, p. 673; I. E. Marko, Comprehensive Organic Synthesis, eds. Trost, B. M. and Fleming, I. Pergamon, Oxford, 1991, vol. 3, p. 913.

(15) Aggarwal, V. K.; Smith, H. W.; Hynd, G.; Jones, R. V. H.; Fieldhouse, R.; Spey, S. E. *J. Chem. Soc., Perkin Trans.* **2000**, *1*, 3267–3276.

(16) Zhao, R.; Shea, K. J. *ACS Macro Lett.* **2015**, *4*, 584–587.

(17) Aggarwal, V. K.; Fang, G. Y.; Schmidt, A. T. *J. Am. Chem. Soc*. **2005**, *127*, 1642.

(18) Aggarwal, V. K.; Thompson, A.; Jones, R. V. H. *Tetrahedron Lett*. **1994**, *35*, 8659–8660.

(19) Khartulyari, A. S.; Kapur, M.; Maier, M. E. *Org. Lett.* **2006**, *8*, 5833–5836.

(20) Shea, K. J.; Zhu, H. D.; Walker, J.; Paz, M.; Greaves, J. *J. Am. Chem. Soc*. **1997**, *119*, 9049–9050.

(21) Blumberg, S.; Martin, S. F. *Tetrahedron Lett*. **2015**, *56*, 3674–3678.

4.5. Experimental

General and materials. In addition to those described in Chapter 2, the following starting materials were prepared according to literature reports: benzylide **12**,[17] *p*-methoxybenzyl bromide[19] and tris(*p*-methoxyphenylethyl)borane **13**.[20] Preparation of diethylsulfoxonium ethylide **18** was described in Chapter 3. The amount of benzylide **12** was approximated by the amount of LiHMDS added (assuming 100% conversion). Lithium bis(trimethylsilyl)amide (LiHMDS) was titrated before use.[21] Note that any CH_2Cl_2 must be removed before addition of ylide monomers if it was involved in synthesis of the organoborane **13**. Otherwise $[CHCl_2]^-$ ylide would be generated and homologated to **13** which was observed in GC-MS.

Representative procedure for synthesis of sulfonium salts (11). To an Erlenmeyer flask containing 5 mL dichloromethane was added tetrahydrothiophene (2.5 mL, 28.4 mmol) and benzyl bromide (3.4 mL, 28.6 mmol). The mixture was stirred at room temperature for 20 min with appearance of large amounts of white precipitate. The reaction was cooled down to 0 ℃ and filtered with addition of another portion of dichloromethane (10 mL) to help transfer the solid. After washed with dichloromethane (3 × 10 mL), the white solid was dried under vacuum at room temperature to afford the desired product **11** (6.794 g, 26.2 mmol, 92%).

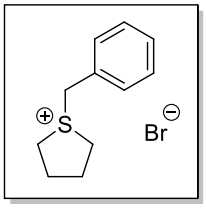

(11) ^{1}H NMR (600 MHz, methanol-d_4) δ 7.48–7.57 (m, 5H), 4.57 (s, 2H), 3.43–3.57 (m, 4H), 2.23–2.41 (m, 4H); ^{13}C NMR (150 MHz, methanol-d_4) δ 131.6, 131.2, 130.8, 130.3, 47.1, 43.8, 29.6.

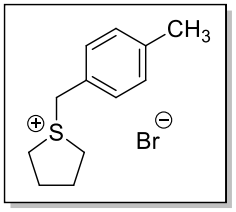

(21a). ^{1}H NMR (600 MHz, methanol-d_4) δ 7.43 (d, *J* = 9.6 Hz, 2H), 7.31 (d, *J* = 9.6 Hz, 2H), 4.54 (s, 2H), 3.42–3.55 (m, 4H), 2.38 (s, 3H), 2.22–2.38 (m, 4H); ^{13}C NMR (150 MHz, methanol-d_4) δ 141.7, 131.5, 131.4, 127.1, 47.0, 43.6, 29.6, 21.3.

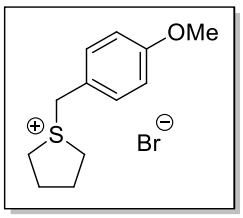

(21b). ^{1}H NMR (600 MHz, D_2O) δ 7.48 (d, *J* = 9.6 Hz, 2H), 7.10 (d, *J* = 9.6 Hz, 2H), 4.50 (s, 2H), 3.88 (s, 3H), 3.39–3.55 (m, 4H), 2.22–2.31 (m, 4H).

Representative procedure for benzyl insertion on tris(*p*-methoxyphenylethyl)borane 13 (Table 4.1, entry 2). To a round-bottom flask containing sulfonium salt **11** (1.334 g, 5.12 mmol) and THF (20 mL) was charged the freshly prepared organoborane **13** (1.1 mmol). The suspension was stirred at −20 ℃ with dropwise addition of LiHMDS (1.0 M, 4.6 mL, 4.6 mmol) in 40 min. The original colorless mixture turned to light yellow upon addition of LiHMDS. After completion of LiHMDS addition, the reaction was stirred at −20 ℃ for another 1 h before slowly warmed to room. After an overnight stir at room temperature, the reaction mixture was added a solution of H_2O_2 (30% w/w, 2 mL) and NaOH (1 M, 2 mL). After stirred at 40 ℃ for 3 h, the reaction was cooled down and concentrated *in vacuo*. The resulting mixture was added H_2O (10 mL) and extracted with ethyl acetate (3 × 10 mL). The organic layer was dried over $MgSO_4$ and evaporated to dryness before subjected to GC-MS analysis. Chromatographic column separations were also performed to obtain four fractions of products on silica gel with eluents gradually

change in an order of hexane/EtOAc = 10/1, hexane/EtOAc = 6/1, hexane/EtOAc = 2/1 and EtOAc. These fractions were further separated on preparative TLC plates (1000 μm) to obtain individual major component for NMR analysis and HRMS to further confirm their identities.

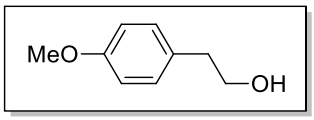

(**14a**) ^{1}H NMR (500 MHz, $CDCl_3$) δ 7.15 (d, *J* = 8.5 Hz, 2H), 6.86 (d, *J* = 8.5 Hz, 2H), 3.82 (t, *J* = 6.5 Hz, 2H), 3.79 (s, 3H), 2.81 (t, *J* = 6.5 Hz, 2H), 1.59 (br, 1H); ^{13}C NMR (125 MHz, $CDCl_3$) δ 158.4, 130.5, 130.1, 114.1, 63.9, 55.4, 38.4. HRMS (CI) calcd for $C_9H_{16}O_2N$ $[M+NH_4]^+$ 170.1181, found 170.1174.

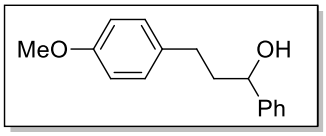

(**14b**) ^{1}H NMR (500 MHz, $CDCl_3$) δ 7.36 (d, *J* = 4.5 Hz, 4H), 7.27–7.31 (m, 1 H), 7.11 (d, *J* = 8.5 Hz, 2H), 6.83 (d, *J* = 8.5 Hz, 2H), 4.58 (dd, *J* =7.5, 5.5 Hz, 1H), 3.79 (s, 3H), 2.59–2.72 (m, 2H), 1.96–2.15 (m, 2H); ^{13}C NMR (125 MHz, $CDCl_3$) δ 157.9, 144.7, 133.9, 129.5, 128.7, 127.8, 126.1, 113.9, 74.0, 55.4, 40.8, 31.3. HRMS (CI) calcd for $C_{16}H_{18}O_2$ M^+ 242.1307, found 242.1309.

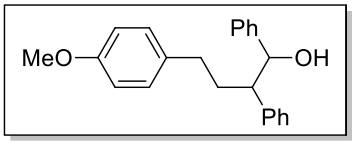

(**14c**) Two diastereomers were found with a ratio ~1:1 from analysis of ^{1}H NMR. Currently the peaks were not assigned for each individual diastereomer. The data were all tabulated here. ^{1}H NMR (500 MHz, $CDCl_3$) δ 7.17–7.40 (m, 16H), 7.11 (d, *J* = 6.5 Hz, 2H), 7.07 (d, *J* = 7.0 Hz, 2H), 6.96 (d, *J* = 8.5 Hz, 2H), 6.84 (d, *J* = 8.5 Hz, 2H), 6.78 (d, *J* = 8.5 Hz, 2H), 6.74 (d, *J* = 8.5 Hz, 2H), 4.79 (d, *J* = 6.5 Hz, 1H), 4.73 (d, *J* = 8.5 Hz, 1H), 3.78 (s, 3H), 3.76 (s, 3H), 2.95 (ddd, *J* = 10.5, 6.5, 3.5 Hz, 1H), 2.85–2.90 (m, 1H), 2.15–2.36 (m, 4H), 1.67–1.94 (m, 4H); ^{13}C NMR (125 MHz, $CDCl_3$) δ 157.8, 142.9, 142.6, 141.3, 141.2, 134.5, 134.1,

129.4, 129.3, 129.1, 129.0, 128.9, 128.5, 128.4, 128.1, 128.0, 127.4, 127.22, 127.16, 126.7, 126.6, 113.8, 113.7, 79.0, 78.6, 55.38, 55.37, 53.7, 53.1, 33.8, 32.8, 32.6, 31.8. HRMS (CI) calcd for $C_{23}H_{24}O_2$ M^+ 332.1776, found 332.1776.

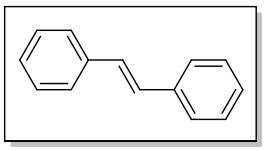

(**14d**) ^{1}H NMR (500 MHz, $CDCl_3$) δ 7.52 (d, *J* = 7.0 Hz, 2H), 7.36 (t, *J* = 7.5 Hz, 2H), 7.26 (t, *J* = 7.5 Hz, 1H), 7.12 (s, 1H); ^{13}C NMR (125 MHz, $CDCl_3$) δ 137.4, 128.8, 127.8, 126.6. HRMS (CI) calcd for $C_{14}H_{12}$ M^+ 180.0939, found 180.0945.

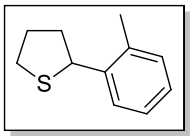

(**14e**) ^{1}H NMR (500 MHz, CD_2Cl_2) δ 7.58 (d, *J* = 8.0 Hz, 1H), 7.16–7.19 (m, 1H), 7.09–7.13 (m, 2H), 4.74 (dd, *J* = 8.0, 7.0 Hz, 1H), 3.11–3.17 (m, 1H), 2.97–3.02 (m, 1H), 2.37 (s, 3H), 2.24–2.35 (m, 2H), 1.94–2.01 (m, 2H); ^{13}C NMR (150 MHz, CD_2Cl_2) δ 141.4, 136.3, 130.5, 126.94, 126.92, 126.5, 48.8, 38.9, 33.5, 31.2, 19.8. HRMS (CI) calcd for $C_{11}H_{18}SN$ $[M+NH_4]^+$ 196.1160, found 196.1162.

Determination of the percentage of every component in the reaction mixture of Scheme 4.4 via GC-MS. Two instruments were involved for GC-MS analysis with EI or CI mode (Appendix A). Assignments of the peaks from GC-MS(CI) were readily achieved by comparison with the isolated pure samples under the same instrumentation condition (Appendix E). The isolated pure samples were not subjected to GC-MS(EI). Assignments of the peaks from GC-MS(EI) were performed based on the measured low resolution mass for each peak and the assumption that the sequence of retention time of peaks do not change between the two instruments equipped with the same type of column for GC. Detailed results of benzyl insertion on tris(*p*-

methoxyphenylethyl)borane **13** at two different temperatures are listed below (Table 4.4, 4.5). Two components were not identified at retention time (EI) of 16.7 and 21.8 min. They are probably decomposition products from the known compounds at high GC temperatures.

Table 4.4. GC-MS results of benzyl insertion on tris(*p*-methoxyphenylethyl)borane **13** at 0 ℃ (Table 4.1, entry 1)

Compound	Retention time (CI, min)	Retention time (EI, min)	Integration values (EI)	NMR, HRMS confirmed?	LRMS
14f	9.3	7.7	---	Y	
14g[a]	10.8	8.5	79702779	**N**	120
14a	12.4	11.1	88790921	Y	
14e	14.7	12.5	214016435	Y	
14d	16.5	14.5	267926098	Y	
---[b]	18.5	16.7	55910752	**N**	226
14h[c]	18.6	17.8	79183299	Y	224
14b	20.6	18.6	253226571	Y	
14i	22.2	19.8	125576508	**N**	286
---[b]	24.2	21.8	148456067	**N**	316
X[c,d]	26.0	22.8	11687191	Y	
14c	26.0	23.2	376884561	Y	

a. Compound 14g can be observed in crude products without H_2O wash. After washing with H_2O for several times, it was difficult to locate at10~11 min.
b. Not identified.
c. ^1H NMR showed diagnostic resonances for the claimed structures. The spectra have lots of impurities due to the very small quantity of these isolated compounds.
d. Compound X was isolated and fully characterized as 1,5-bis(4-methoxyphenyl)pentan-3-ol. Its presence is due to the mistakenly use of CH_2Cl_2 in the synthesis of initiator **13** (see general considerations in chapter 4.5 experimental).

Table 4.5. GC-MS results of benzyl insertion on tris(*p*-methoxyphenylethyl)borane **13** at −20 °C (Table 4.1, entry 2)

Compound	Retention time (CI, min)	Retention time (EI, min)	Integration values (EI)	NMR, HRMS confirmed?	LRMS
14f	9.3	7.3	210156421	Y	
14g[a]	10.8	8.7	588823578	**N**	120
14a	12.4	11.3	236177260	Y	
14e	14.7	12.6	65745627	Y	
14d	16.5	14.7	48598927	Y	
---[b]	18.5	16.6	104593494	**N**	226
14h[c]	18.6	17.5	98859750	Y	224
14b	20.6	18.6	3583940182	Y	
14i	22.2	19.9	635811301	**N**	286
---[b]	24.2	21.9	297931059	N	316
X[c,d]	26.0	22.8	89129635	Y	
14c	26.0	23.5	1058972249	Y	

a. Compound 14g can be observed in crude products without H_2O wash. After washing with H_2O for several times, it was difficult to locate at10~11 min.
b. Not identified.
c. ^1H NMR showed diagnostic resonances for the claimed structures. The spectra have lots of impurities due to the very small quantity of these isolated compounds.
d. Compound X was isolated and fully characterized as 1,5-bis(4-methoxyphenyl)pentan-3-ol. Its presence is due to the mistakenly use of CH_2Cl_2 in the synthesis of initiator **13** (see general considerations in chapter 4.5 experimental).

Representative procedure for synthesis of benzylidene incorporated polymers 17 and 19 (Table 4.3, entry 1). To a round-bottom flask equipped with a condenser and purged under N_2 was charged with toluene (20 mL), dimethylsulfoxonium methylide **16** (0.655 M, 9.2 mL, 6.03 mmol) and diethylsulfoxonium ethylide **18** (0.275 M, 11.0 mL, 3.02 mmol). The mixture was preheated on an oil bath at 60 ℃ for 5 min followed by a quick injection of tri-*n*-hexylborane (73 mg/mL in toluene, 0.365 mL, 0.10 mmol). After 1 h of reaction, an aliquot was titrated against phenolphthalein to indicate no remaining ylides. Then the reaction was cooled down to −20 °C and added freshly prepared benzylide solution (0.66 mmol) via cannula. The reaction was stirred for another 4 h at −20 °C before slowly warming up to room temperature. After raising the temperature and heating at 60 ℃ for 10 min, methylide **16** (16.5 mL, 10.8 mmol) and ethylide **18** (4.5 mL, 1.24 mmol) were added to the reaction. The reaction mixture turned to milky and was stirred at 60 ℃ for additional 1 h before addition of a degassed solution of trimethylamine *N*-oxide dihydrate (73 mg/mL in H_2O, 1.6 mL, 1.05 mmol). The reaction was stirred at 70 ℃ overnight before cooling down and concentrated *in vacuo*. The resulting sticky solid was washed with deionized water (3 × 20 mL) and methanol (3 × 20 mL) to afford colorless gel-like solid (418 mg, 95% assuming two benzyl insertion per polymer chain). All the GPC and NMR results are summarized in Table 4.2 and 4.3. Synthesis of polymer **17** employed the same procedure but without addition of ethylide **18**.

Chapter 5. Evaluation of 9-Borafluorene Derivatives as Single-site Catalysts in the Polyhomologation Reaction and the Synthesis of Polyethylidene

5.1. Introduction

Advances in 'living' or controlled polymer synthesis over the past 20 years have had a profound impact on many branches of science. Control of the average molecular weight (MW), polydispersity (PDI), composition and functionality have allowed tailoring synthetic carbon backbone polymers with properties and functions that were inconceivable in earlier times. One of the remaining challenges in the synthesis of carbon backbone polymers is sequence control. To achieve full sequence control of every single carbon on a linear carbon chain, an ideal strategy will be to use reactions that can add a single carbon atom to a growing carbon chain. With a self-reacting bifunctional C1 monomer XY, the polymer chain can be fabricated in a specific order with various functionalities (Scheme 5.1). To avoid the repeated incorporation of the same monomer, one of the reactive functions in the XY monomer needs to be temporarily protected/deactivated. The use of main-chain protecting groups requires extra protection and deprotection steps. These additional steps increase the possibility of reduced yields and side products requiring extensive purification at the end. The yield of monomer addition must be near quantitative to avoid sequence defects especially in the case of the long-chain polymer synthesis.

Scheme 5.1. Sequential building of a carbon backbone polymer with C1 monomers.

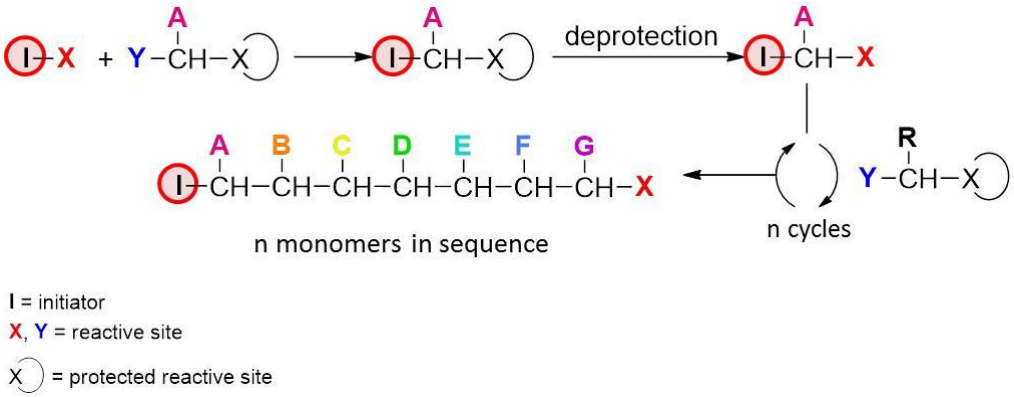

Nevertheless, considerable progress has been made in pursuit of this goal. Although the one–carbon addition was not employed, Burke and coworkers demonstrated the syntheses of many linear polyene natural products from bifunctional *N*-methyliminodiacetic acid (MIDA) boronate building blocks in a sequence-specific manner.[1] The method can even be expanded to synthesis of C_{sp3}-rich cyclic and polycyclic natural products.[2] By use of the lithiation–borylation methodology, Aggarwal and coworkers reported stereocontrolled synthesis of substituted carbon chains via reagent-controlled asymmetric homologation of boronic esters.[3] All these success belongs to small-molecule organic synthesis.

Up to now, one example that most resembles a carbon backbone polymer synthesis is the fabrication of ethylidene decamer derivatives with full control on all stereocenters (Scheme 5.2a).[4] This iterative molecular assembly-line synthesis was achieved via homologation of boronic esters with lithiated benzoates. The heteroatoms (oxygen) do not undergo 1,2-migration due to the high activation energies. Each monomer insertion is regulated by complexation at a low temperature (−78 ℃) followed by 1,2-migration at room temperature (Scheme 5.2b). However, this method cannot be applied for polymer synthesis. Polymerization will not take place by simply mixing the boronic ester initiator with an excess amount of organolithium monomers, because the chain migration requires a temperature at which the excess

organolithium reagents with good leaving groups will instantaneously decompose. Additionally, building a long-chain polymer in a 'one carbon at a time' fashion with post-process every 3–5 steps is tedious and inefficient, as these complexation-migration reactions for building C–C bond need to be repeated over hundreds of thousands of times and are vulnerable to moisture and oxygen.

Scheme 5.2. a) Synthesis of ethylidene decamer derivatives with lithiated benzoates; and b) its homologation mechanism.

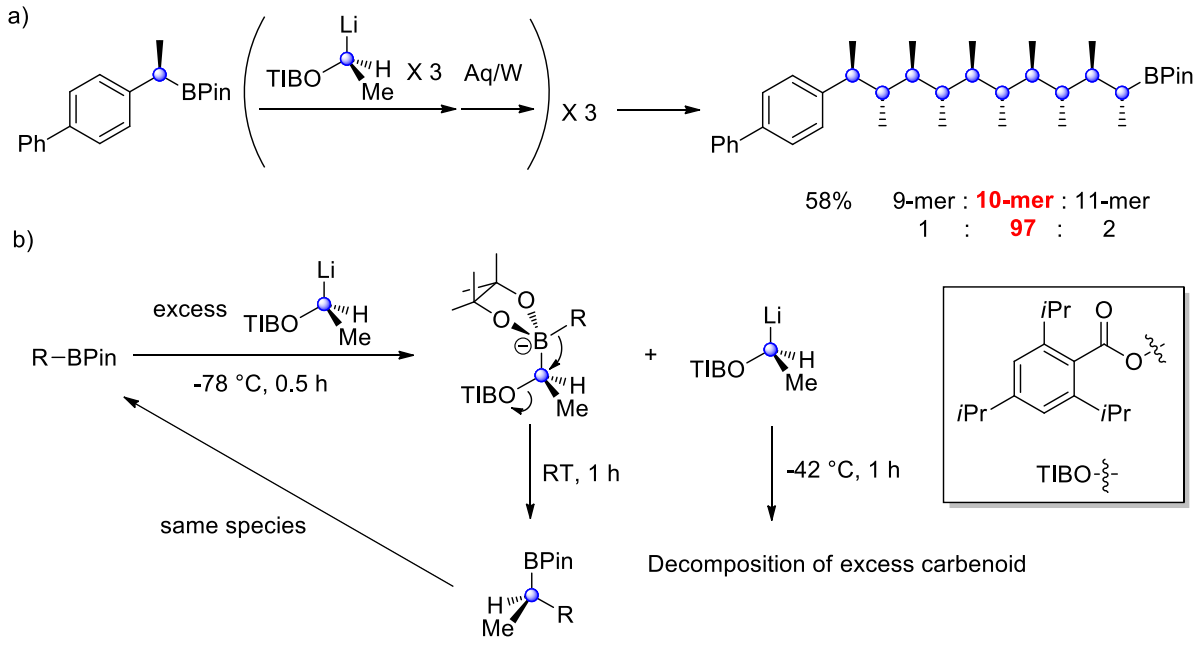

Compared to the abovementioned examples, the polyhomologation reaction developed in the Shea lab is an ideal method for the full sequence control on a linear polymer chain with a carbon backbone.[5] Each monomer addition is composed of two stages, complexation and 1,2-migration, both in quantitative yield. The use of monomers with good leaving groups such as dialkyl sulfoxides avoids the extra protection and deprotection steps. And the sulfoxonium ylide monomers are thermally stable that most can survive the chain-migration conditions even at 100 ℃.

Much of our prior work utilized triorganoborane catalysts. In these cases all three alkyl/aryl groups are polyhomologated. These catalysts are not suitable for precise sequence control as the monomer incorporations are randomly distributed among all three chains. Another challenge with the triorganoborane catalyst is that it does not allow for synthesis of unique, sterically crowded as yet unknown polymer structures such as polyethylidene and polycyclopropylidene (Figure 5.1). Although several early reports studied the synthesis of polyethylidene via decomposition of diazoalkanes,[6-8] such a method was made impractical and questionable by the use of explosive diazoalkane monomers as well as lack of evidences to exclude the azo group incorporation and NMR analysis to fully demonstrate the proposed ideal structure.

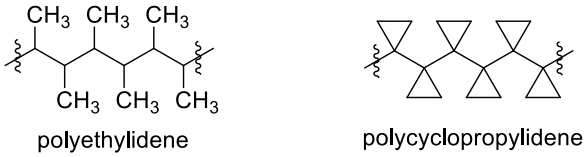

Figure 5.1. Examples of highly substituted polymer chains as polyethylidene and polycyclopropylidene.

Attempts to synthesize these highly substituted carbon chains using triorganoborane catalysts with secondary ylides (Scheme 5.3a), resulted in polymerizations that were terminated at early stages with a trimer as the longest chain. The three propagation sites around boron quickly became congested with three secondary alkyl groups and inaccessible for the next ylide monomer. Precise sequence control, as well as synthesis of highly substituted carbon backbone polymers, can be realized with an organoborane catalyst that only allows for a single–chain migration (Scheme 5.3b).

Scheme 5.3. Attempted C1 polymerization of secondary ylides by a) three–chain versus b) single–chain migration.

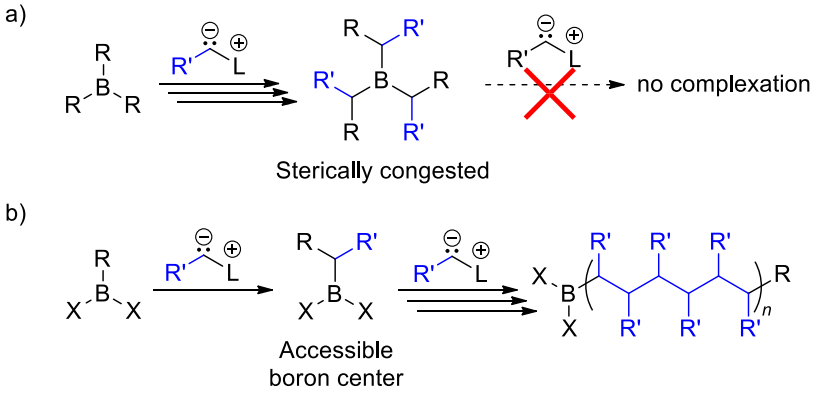

Many efforts have been made on searching for a single-site organoborane catalyst (Figure 5.2).[9-12] Tuning steric effects or introducing heteroatoms directly bonded to boron do not provide a single-site catalyst. These observations were also corroborated by computational studies.[11-13] The thexyl group could serve as the non-migrating group at a low temperature (5 ℃), but it cannot be used for polymerization of substituted ylides due to the large steric hindrance around the boron center.

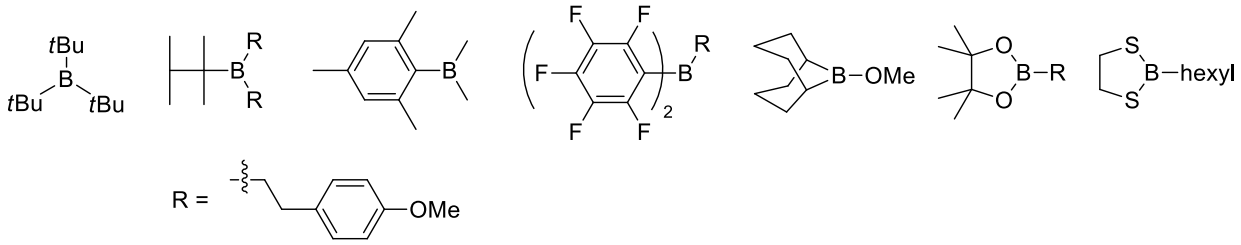

Figure 5.2. Previously investigated organoboranes in the Shea lab in search of non-migrating blocking groups on boron.

Instead of the catalyst designs with boron bonded to sp^3–carbon, heteroatoms or aromatic derivatives, direct incorporation of the boron atom into an organic π-system has yet to be examined. These boron-doped π-systems, such as boroles and borepins, have been studied for applications as luminophores, organic cells, organic light-emitting devices and anion sensors.[14-16] We believe these are promising catalyst platforms for propagating a single polymer chain. The

synthesis of these catalysts will allow us to realize polymer sequence control and synthesis of highly substituted carbon backbone polymers.

5.2. Results and Discussion

Boroles have a strained planar five-membered ring containing four π-electrons, making them antiaromatic. They can be stabilized by either phenyl substitution on every atom of the five-membered ring or ring fusion with other aromatics (Figure 5.3). The former, also referred as nonannulated or antiaromatic boroles, are strongly electrophilic with unusual electronic properties[17]; while some of the latter annulated boroles are even air-stable with selected sterically congested substitutions on boron and have been employed in many applications.[14-16] For this study, I chose the annulated borole platform due to its diversity on the aromatic rings which could be utilized to tune the reactivity of the catalyst.

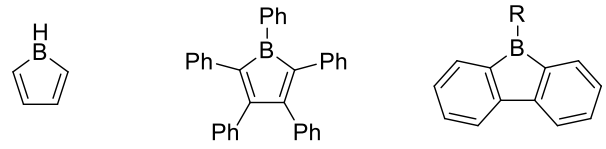

Figure 5.3. Borole and its two stabilized forms as antiaromatic and annulated boroles.

One of the most common annulated boroles is dibenzoborole, also known as 9-H-9-borafluorene. It easily undergoes dimerization followed by ring-opening oligomerization.[18] However, this can be avoided by an alkyl substitution on the boron atom. With two tethered aromatic groups on boron, I hope to use this design as a single site polyhomologation catalyst for the propagation of the sp^3 alkyl group on boron in preference over the two sp^2 carbons on the aromatic rings (Scheme 5.4). The relative migratory aptitudes of the sp^3 and sp^2 carbons can be

further tuned with different substitutions on the aromatic rings to alter stereoelectronic factors around the boron center.

Scheme 5.4. Proposed selectivity between sp^3 alkyl and sp^2 phenyl 1,2-migration in the borate complex from dibenzoborole derivatives.

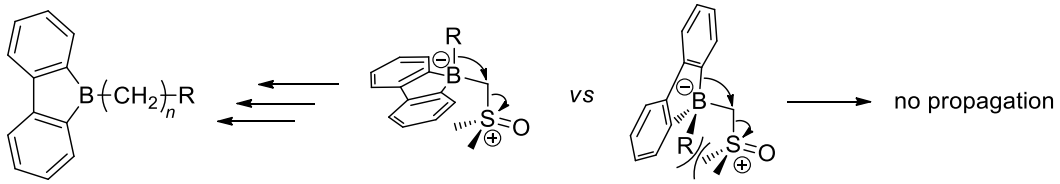

In this research it is of interest whether a single–chain migration can be achieved using 9-borafluorenes and sulfoxonium ylides. I undertook a computational study of this problem. Three catalysts were designed for evaluation (Figure 5.4). Having a methyl group on boron can simplify the synthesis and reduce the computational cost. The dimethyl substituted derivative **cat-Me** was designed to increase the steric hindrance for the sp^2 phenyl migration compared to the prototype **cat-H** and increase the electron density on boron by introducing two adjacent methyl groups; while **cat-F** is designed to greatly decrease the electron density on boron by replacing all hydrogens with fluorines on the aromatic ring. This was intended to reduce the migration aptitudes of the sp^2 carbons.

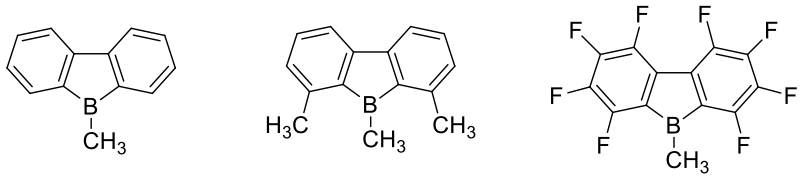

1a **cat-H** **1b** **cat-Me** **1c** **cat-F**

Figure 5.4. Designed 9-borafluorene catalysts for the polyhomologation study.

5.2.1. Computational studies

The task is to compare migratory aptitudes between the methyl and phenyl migration of the borate complexes **3** formed from the catalysts **1a–c** and dimethylsulfoxonium methylide **2**

(Scheme 5.5). The desired methyl migration will afford **5** with the 9-borafluorene core intact while the competing phenyl migration will result in the ring-expansion to produce structure **7**. To determine which pathway is kinetically preferred, activation energies can be calculated for both migrations with the available computational tools.

Scheme 5.5. Reaction mechanisms of methyl and phenyl migrations in a borate complex between 9-borafluorene and dimethylsulfoxonium methylide.

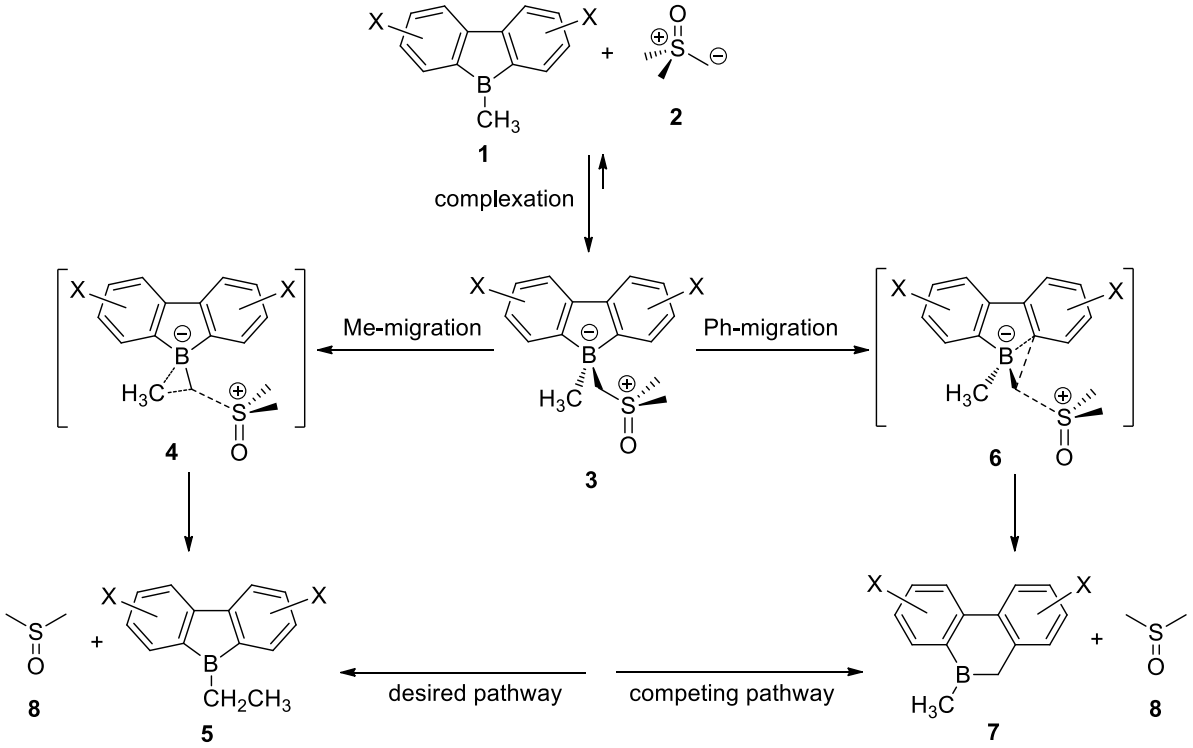

5.2.1.1. System evaluations with density functional theory (DFT) using TPSS functional

The computation of energies relies on good geometries of global minimum for all the key intermediates. To find the global minimum, a conformational search was performed with Optimized Potential for Liquid Simulations (OPLS_2005) force fields.[19] Such a task is straightforward for ground state (GS) **3** using Systematic Torsional Sampling with no constraints applied. However, for transition states (TS) **4** and **6**, a constrained optimization needs to be

carried out first with only one fixed internal coordinate. A following strain-release optimization with transition vector of 1 generated the desired TS which was verified by frequency analysis. When using this strategy to search for ALL possible transition states of 1,2-migration, the conformational search is also required for the constrained geometry with the carefully selected one internal coordinate. Use of an inappropriate internal coordinate in the constrained conformational search will result in some geometries collapse to either starting materials or the products during the subsequent strain-release optimization. After screening most possible parameters involved in the migration including the B–C bond (1.8–2.1 Å with stepsize of 0.1 Å), C–C bond (1.8–2.1 Å with stepsize of 0.1 Å), C–S bond (2.3–2.5 Å with stepsize of 0.1 Å) and C–C–B angle (78–83 ° with stepsize of 1.0 °), it was found that the only effective internal coordinate to search for a transition state is the fixed C–S bond around 2.3–2.4 Å. With dozens to hundreds of local minima pre-screened during the conformational search, the more accurate DFT optimizations were applied to these geometries at a cheap cost with a double-ζ basis set SVP to rectify and confirm the results. Belonging to the class of meta–generalized gradient approximation (meta-GGA), the non-empirical TPSS functional is popular for its accuracy with small numbers of empirical parameters and low computational cost.[20-21] Due to the similarities of these two migrations, it is safe to use TPSS to calculate and compare the differences of activation energies. The global minimum geometries were further refined for GS **3**, TS **4** and TS **6** of all catalysts at TPSS-D3BJ/def2-TZVP level. As suggested by Grimme etc., the DFT dispersion correction D3 was selected together with Becke-Johnson damping.[22-23] In addition to the gas phase calculation, solvent such as THF was also taken into consideration with a continuum solvation model as Conductor-like Screening Model (COSMO).[24]

The frequency analyses were performed at TPSS-D3BJ/def2-TZVP level to guarantee zero imaginary frequency for GS and one for every TS. The enthalpy and Gibbs free energy for every geometry was obtained with zero-point energy (ZPE) and thermal corrections at 298 K. The calculated energy profile in THF solvent is listed in figure 5.5.

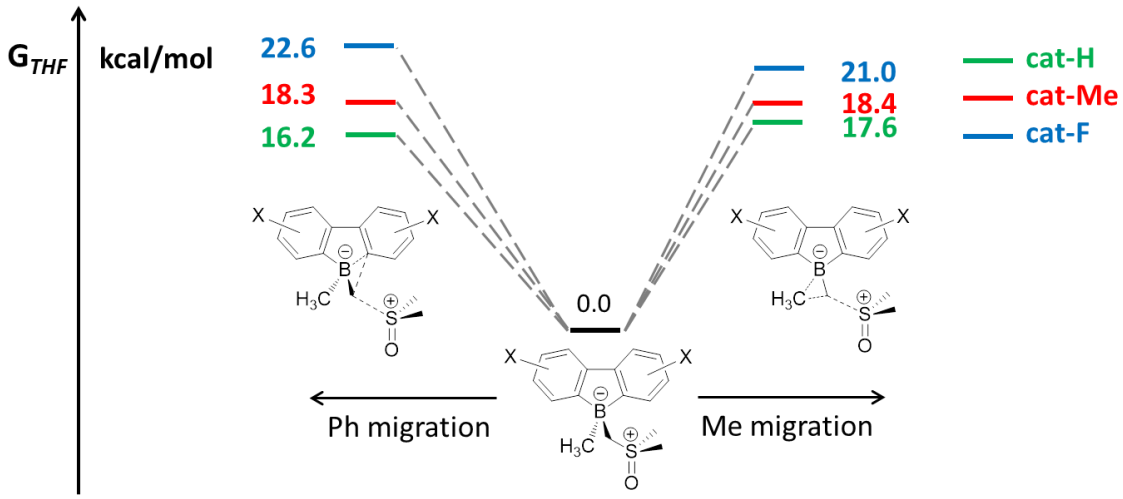

Figure 5.5. Activation energies of methyl and phenyl migrations in THF solvent for all three catalysts.

With no substitutions on the borafluorene core, the borate complex **cat-H**·ylide has a lower activation energy for phenyl migration compared to methyl migration ($\Delta\Delta G^{\neq}$ = 1.4 kcal/mol). The phenyl migration proceeds with a shortened B–C distance and an elongated C–S bond (~ 2.4 Å) in the transition state. The central carbon involved in both bond-forming and bond-breaking events resembles a carbocation. The preferred phenyl migration is probably due to the stabilization of this carbocation by the *p*-orbital of the migrating C_{sp2}. Still, the phenyl migration proceeds only by breaking and formation of B–C σ bond without participation of the π bond from the aromatic ring. With two methyls on the ortho position of the aromatic rings in **cat-Me**, there is no longer a preference between the two migration pathways due to the introduced steric hindrance. However, this modification also increases the electron density on the migrating

C_{sp2} which did not result in a preferred methyl migration. With the best performance of the three, **cat-F** is a promising candidate which has a calculation of lower $\Delta\Delta G^{\neq}$ for methyl migration than the phenyl migration by 1.6 kcal/mol.

Several other 9-methyl-9-borafluorene derivatives were designed to further evaluate the influences of both steric and electronic factors on $\Delta\Delta G^{\neq}$ of the two competing migrations (Figure 5.6, Table 5.1). The calculations were performed in the same way as above except for excluding the solvent environment to reduce the computational cost.

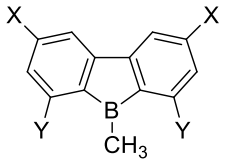

H: X = Y = H

***o*-Me**: X = H, Y = Me

***o*-*t*Bu**: X = H, Y = *t*Bu

***o*-CF$_3$**: X = H, Y = CF_3

***o*,*p*-di-CF$_3$**: X = Y = CF_3

***p*-NMe$_2$**: X = NMe_2, Y = H

***p*-Me**: X = Me, Y = H

***p*-Cl**: X = Cl, Y = H

***p*-NO$_2$**: X = NO_2, Y = H

Figure 5.6. 9-methyl-9-borafluorene derivatives for computational evaluations of steric and electronic effects on the two migrations.

Table 5.1. Differences of activation energies between methyl and phenyl migration for various 9-methyl-9-borafluorene derivatives.[a]

catalyst	**H**	***o*-Me**	***o*-*t*Bu**	***p*-NMe$_2$**	***p*-Me**	***p*-Cl**	***p*-NO$_2$**	***o*-CF$_3$**	***o*,*p*-di-CF$_3$**
$\Delta\Delta G^{\neq}$[b]	-0.39	0.93	-0.73	-1.75	-1.15	-0.58	-0.05	2.83	3.60

a. Calculations were performed at TPSS-D3BJ/def2-TZVP level in gas phase.
b. $\Delta\Delta G^{\neq} = \Delta G^{\neq}$ (Ph migration) – $\Delta G^{\neq}$ (Me migration), unit: kcal/mol.

With steric hindrance as the major factor, ***o*-Me** shows a preferred methyl migration over phenyl migration compared to the unsubstituted catalyst **cat-H**. However with ***o*-tBu**, the methyl migration is no longer favored. The giant ortho *tert*-butyl groups blocked the path for methyl migration while the phenyl migration can still proceed with a slightly twisted geometry (Figure 5.7). To completely exclude the steric factors, electronic factors were examined by installation of para-substituents. Although the phenyl migration is preferred for all substrates include ***p*-NMe$_2$**, ***p*-Me**, ***p*-Cl** and ***p*-NO$_2$**, the absolute value of $\Delta\Delta G^{\neq}$ ($|\Delta\Delta G^{\neq}|$) was observed in an order of ***p*-**

NMe$_2$ > ***p*-Me** > ***p*-Cl** > ***p*-NO$_2$**. As the electron density on the migrating C_{sp2} decreased in an order of ***p*-NMe$_2$** > ***p*-Me** > ***p*-Cl** > ***p*-NO$_2$**, the activation energy of phenyl migration is increased resulting in a lower selectivity on phenyl migration in ***p*-NO$_2$** compared to ***p*-NMe$_2$**. Employment of both steric hindrance and low electron densities at the migrating C_{sp2}, i.e. ***o*-CF$_3$**, exhibits a $\Delta\Delta G^{\neq}$ of 2.83 kcal/mol with a high selectivity on the methyl migration. To further increase $\Delta\Delta G^{\neq}$ as well as gain synthetic convenience, ***o,p*-di-CF$_3$** is calculated to have $\Delta\Delta G^{\neq}$ of 3.60 kcal/mol. It is an ideal catalyst with a selectivity of over 100:1 on the methyl over phenyl migration at 298 K.

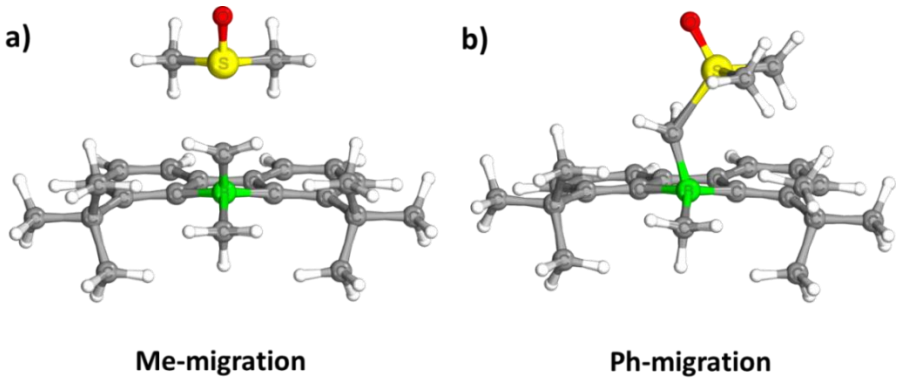

Figure 5.7. Optimized transition state geometries of a) methyl and b) phenyl migration for the borate complex of catalyst ***o*-tBu**.

The calculation of activation energies employed global minimum geometries of both ground and transition states. In all possible ground states, only the global minimum positions the methyl group anti-periplanar to the leaving sulfoxide group (Cs symmetry) which corresponds to the subsequent methyl migration. Many of other local minima, however, position the phenyl group anti-periplanar to the leaving sulfoxide group. If the transformation between different conformers via bond rotations required more energy than the activation energy of 1,2-migration, the GS might be locked at a specific geometry other than the global minimum and underwent the 1,2-phenyl migration. To compare the differences between activation energy of 1,2-migration and rotational barrier of GS, the latter one was then investigated.

5.2.1.2. Estimation of rotational barriers between local minima of ground states

In the borate complex **3**, the 9-borafluorene subunit has a nearly planar geometry. The transformation between conformers can thus be simplified due to the rigidity of the 9-methyl-9-borafluorene subunit. Based on the 3D model, various conformational isomers can be distinguished by only two dihedral angles as Φ(O–S–C–B) and Φ(S–C–B–Me) (Figure 5.8). The symbol C here refers to the carbon bonded to both boron and sulfur. And a 2D potential energy surface (PES) can be generated as a function of Φ(O–S–C–B) and Φ(S–C–B–Me) to help locate the approximate transition state of the rotational transformation.

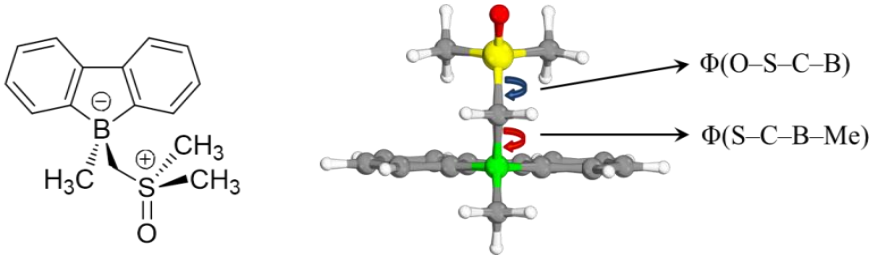

Figure 5.8. Characteristic internal coordinates for different conformations of the borate complex. (White: H, Grey: C, Red: O, Yellow: S and Green: B)

As the B3LYP hybrid functional[26-29] performed well in generating geometries for 9-borofluorene based structures[30-31], it was employed for PES scan with def2-TZVP basis set. Due to the presence of one mirror plane in the 9-methyl-9-borafluorene substructure, a complete scan can be accomplished by scanning Φ(O–S–C–B) in the range of –180° to +180° while Φ(S–C–B–Me) from 0 ° to 180 °. The PES for all borate complexes from catalysts **1a-c** is shown below (Figure 5.9).

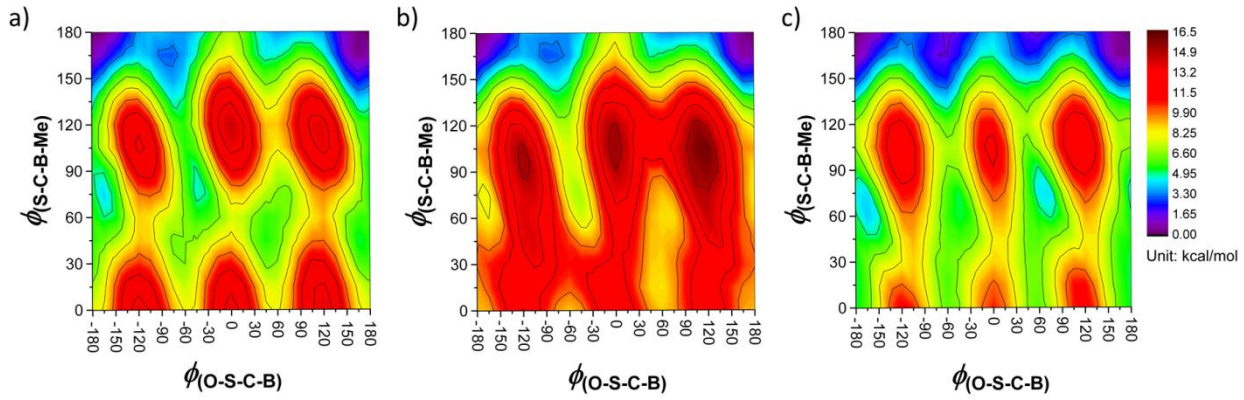

Figure 5.9. Potential energy surface of the borate complex **3a-c** from a) **cat-H**, b) **cat-Me** and c) **cat-F** as a function of two dihedral angles. Relaxed scan with freezing on two internal coordinates Φ(O–S–C–B) and Φ(S–C–B–Me) was performed for all geometries. Optimization was performed at RI-B3LYP-D3BJ/def2-TZVP level. Each dihedral angle was scanned at an increment of 15 °.

From the above heat maps, every valley point was further optimized with tighter convergence criteria to precisely locate all the local minima. The results of the corresponding complexes **3a** from **cat-H**, **3b** from **cat-Me** and **3c** from **cat-F** are summarized in table 5.2. The global minimum of complex **3a–c** has Cs symmetry with the aromatic groups *syn* to the methyl groups from the DMSO subunit because of the stabilizing electrostatic interactions (Figure 5.10). This was also observed in 1,2-migration of organoborate with the phenyl substituent.[25]

Table 5.2. Local minima identified and characterized with the two dihedral angles.

	O-S-C-B (°)	S-C-B-Me (°)		O-S-C-B (°)	S-C-B-Me (°)		O-S-C-B (°)	S-C-B-Me (°)
3a-1	180.0	180.0	**3b-1**	180.0	180.0	**3c-1**	180.0	180.0
3a-2	−165.1	81.4	**3b-2**	−169.2	73.3	**3c-2**	−164.8	68.7
3a-3	167.2	45.8	**3b-3**	−52.6	77.9	**3c-3**	73.6	73.2
3a-4	−46.4	85.7	**3b-4**	73.4	64.3	**3c-4**	−48.7	60.9
3a-5	46.5	45.8	**3b-5**	62.9	13.1			

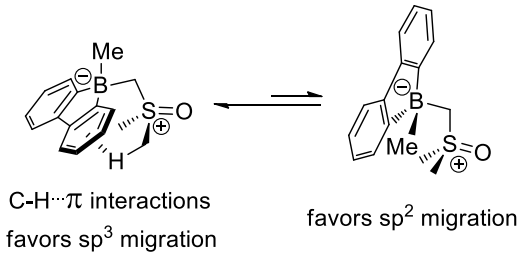

Figure 5.10. Conformational equilibrium of the borate complex **3**.

The transition states between rotational conformers can be approximated as the saddle points on these PES maps. The appearance of the PES map is mainly influenced by steric hindrance during the bond rotation. The PES of complex **3a** is very close to **3c** (Figure 5.9a and 5.9c), because of the similarity of steric effects between **cat-H** and **cat-F**. Many of the conformers are accessible from the global minimum by only 5–6 kcal/mol. In the case of **3b**, the rotational barriers (> 8 kcal/mol) are higher with two isolated conformers **3b-4** and **3b-5** due to the presence of two ortho methyl groups. The values of all rotational barriers can be estimated based on the grid points of PES maps from Appendix B. To obtain accurate values, the transition states need to be precisely located first which could start from the approximate locations of saddle points found in the PES scan in figure 5.9.

All the rotational barriers (< 12 kcal/mol) were found to be much lower than the activation energy of 1,2-migration (> 16 kcal/mol). The distribution of ground state geometries is not important in studying the kinetics of 1,2-migration.

*5.2.1.3. Calibration of DFT functionals on the methyl migration of borate **3***

In comparing the competing pathways of a reaction, DFT calculations do not offer guaranteed accuracy on the activation energies. Various DFT functionals do not give the same results while working on certain problems. As different DFT functionals use diverse

approximations, high level *ab initio* calculations are often required as reference for DFT calibration. The 1,2-migration of common organoborates has been well studied computationally and calibrated by high level *ab initio* methods.[25] An extension to the 9-borafluorene system has not been investigated. For closed-shell systems without serious multiconfigurational character, CCSD(T), known as the coupled cluster method with single and double excitations and a perturbative treatment of triple excitations, is often chosen as a 'golden standard' in modern quantum chemistry.[32-33] To reduce the work load, one series of reactions including complexation and 1,2-migration were set as the model reactions for study. Here the sp^3 carbon migration of **cat-H·ylide** was chosen because it has the least heavy atoms and more importantly, high symmetry Cs (Scheme 5.6). For the sp^2 carbon migration, calculations with high level *ab initio* methods were not performed due to the low symmetrized geometries (C1 symmetry) which require much more computation resources that are currently impractical and unavailable.

Scheme 5.6. The model reactions for calibration of reaction and activation energies in the complexation and 1,2-migration steps.

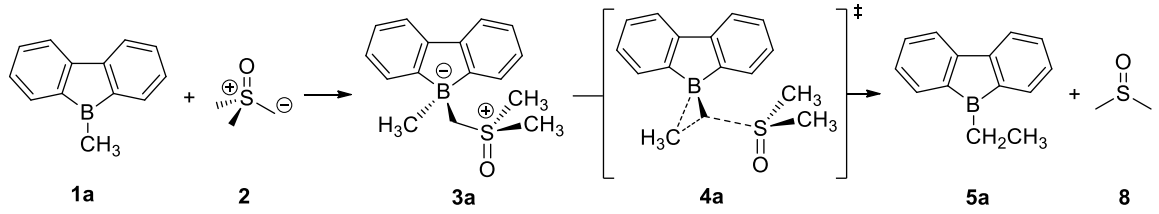

Single-point energies were calculated with the coupled cluster (CC) methods as references based on the optimized geometries at level of B3LYP-D3BJ/def2-TZVP (Table 5.3). The recently developed explicitly correlated CC methods CCSD(T)-F12 was employed which can alleviate the basis set dependence of the conventional CC methods.[34] With the explicitly correlated double-ζ basis set (VDZ-F12), the results can be as accurate as the ones using conventional CC methods with quadruple-ζ basis set. Due to the huge computational costs, I did not proceed on further calculations with the triple-ζ (VTZ-F12) basis set. The T1 diagnostic

values in CCSD(T) calculations are all below 0.02 which indicated that multiconfigurational characters can be ignored (Table 5.4). The CCSD(T) calculations are thus reliable for all the closed-shell systems in this section.

Table 5.3. Results of reaction and activation energies of complexation and 1,2-migration using *ab initio* methods and double hybrid density functionals.[a]

method	ΔE(complexation)[b] (kcal/mol)	$\Delta E^{\neq}$(migration)[b] (kcal/mol)	ΔE(migration)[b] (kcal/mol)
DF-MP2-F12/VDZ-F12	−40.39	33.23	3.44
DF-MP2-F12/VTZ-F12	−40.30	33.05	3.13
DF-MP2-F12/(D,T)	−40.40	32.93	3.03
B2GPPLYP-D3BJ/A'VTZ	−35.53	26.99	−5.31
B2GPPLYP-D3BJ/A'VQZ	−34.74	27.58	−5.34
B2GPPLYP-D3BJ/(T,Q)	−34.35	27.69	−5.53
DF-LCCSD(T)-F12b/VDZ-F12	−36.95	30.54	−2.41
DF-LCCSD(T)-F12b/VTZ-F12	−37.31	31.05	−2.52
CCSD(T)-F12b/VDZ-F12	−35.03	28.84	−4.83
CBS-QB3	−38.22	27.69	−3.16

a. ZPE corrections were not included. The details of calculations and extrapolations can be found in the experimental section 5.5.
b. ΔE(complexation) = E(3a) – E(2) – E(1a); $\Delta E^{\neq}$(migration) = E(4a) – E(3a); ΔE(migration) = E(5a) + E(8) – E(3a).

Table 5.4. T1 Diagnostic of CCSD(T)-F12 calculations.

Structure	**1a**	**2**	**3a**	**4a**	**5a**	**8**
T1-diagnostic	0.012	0.015	0.013	0.014	0.012	0.015

In addition to the CC method, several other ab initio methods as well as a double hybrid density functional and composite method were also employed to compare the reaction and activation energies of complexation and methyl migration reactions (Table 5.3). Compared to the reference values calculated with CCSD(T)-F12b/VDZ-F12, the explicitly correlated second order Møller–Plesset calculations (MP2-F12)[35] with use of density fitting (DF) scheme[36] showed an overestimation of the complexation energy by about 5 kcal/mol and the activation energy of 1,2-migration by 4.1 kcal/mol. Even larger errors are present for the exothermic 1,2-migration by over 7 kcal/mol. This is probably due to the underestimated energy level of the borate complex **3a**. The popular double hybrid DFT functional B2GP-PLYP[37] showed values close to the

references. Calculations with the explicitly correlated local coupled cluster method with single and double excitations and a perturbative treatment of triple excitations (DF-LCCSD(T)-F12)[38] exhibited an overestimation of around 2 kcal/mol for all energies. One composite method, Complete Basis Set Extrapolation (CBS-QB3)[39], was also performed for another comparison using high-level computation with high accuracy.

Based on the calculation results with CCSD(T)-F12b/VDZ-F12, the complexation reaction is quite downhill due to the strong Lewis acidity of the 9-borafluorene subunit (Table 5.3). Compared to the case with traditional tri(*n*-hexyl)borane[40], the stable borate complex with lower energy also slightly increases the activation energies of 1,2-migration. This indicated that a higher temperature is required for the 1,2-migration in borate **3**.

With the standard setup, DFT calculations were then investigated. To mitigate basis set incompleteness error (BSIE), basis set convergence tests were carried out to choose the optimal basis set using B3LYP functional for the model reactions. Single-point DFT calculations of reaction energies and activation energies were performed using B3LYP functional with nZ (cc-pVnZ[41] for B, C, H, O and cc-pV(n+d)Z[42] for S, n = T, Q) basis sets (Table 5.5). For the activation energy $\Delta E^{\neq}$ of the 1,2-migration, the difference between TZ and QZ is less than 0.2 kcal/mol which indicates convergence and thus a safe use with the QZ basis set. For the reaction energies ΔE of both complexation and 1,2-migration, the QZ basis set is insufficient. After further calculations with augmented functions, these two reaction energies converged with a difference close to 0.2 kcal/mol between ATZ and AQZ. Thus AQZ should be used as the basis set for reaction energies ΔE of both complexation and 1,2-migration.

Table 5.5. Evaluation of basis set convergence for the model reactions at B3LYP level.

Reaction	TZ	QZ	|QZ-TZ|	ATZ	AQZ	|AQZ-ATZ|
ΔE(complexation)[a]	−18.80	−18.32	0.48	−18.27	−18.03	0.24
ΔE(migration)[a]	−22.99	−23.29	0.30	−23.90	−23.74	0.16
$\Delta E^{\neq}$(migration)[a]	19.31	19.44	0.13	---	---	---

a. ΔE(complexation) = E(3a) – E(2) – E(1a); $\Delta E^{\neq}$(migration) = E(4a) – E(3a); ΔE(migration) = E(5a) + E(8) – E(3a).

Table 5.6. Energy differences between DFT/QZ calculations with dispersion corrections and the reference values at CCSD(T)-F12/VDZ-F12 level.[a]

Type	Functional	DFT-D3BJ				DFT-D3			
		ΔE(GS)	ΔE(TS)	ΔE(pdt)	$\Delta E^{\neq}$	ΔE(GS)	ΔE(TS)	ΔE(pdt)	$\Delta E^{\neq}$
GGA	BP86	2.99	9.68	1.27	6.70	2.36	9.57	0.46	7.21
	B97D	16.41	21.42	0.07	5.01	14.44	20.86	1.43	6.42
	OLYP	4.05	7.19	2.84	3.14	1.06	6.67	0.37	5.61
	BLYP	2.85	8.62	0.85	11.47	4.44	8.11	1.97	12.55
	MPWLYP	6.51	6.50	1.42	13.01	7.67	5.95	1.84	13.63
meta-GGA	TPSS	0.14	8.93	0.07	8.79	0.77	8.68	0.48	9.46
	M06-L	6.43	0.39	0.35	6.03	6.43	0.39	0.35	6.03
hybrid GGA	PBE0	2.49	2.66	0.79	0.17	1.78	2.45	0.43	0.68
	B1B95	2.95	3.44	0.82	0.49	2.56	3.35	0.11	0.78
	B3PW91	3.97	5.28	0.80	1.31	2.69	4.89	0.08	2.20
	B3LYP	1.58	4.20	1.02	5.79	3.40	3.57	1.94	6.97
	O3LYP	20.68	12.23	0.30	8.45	20.68	12.23	0.30	8.45
hybrid meta-GGA	TPSSh	0.96	7.08	0.11	6.12	0.10	6.64	0.61	6.74
	BMK	9.07	9.58	4.30	0.51	9.35	9.65	5.14	0.30
	MPWB1K	2.29	0.07	0.08	2.36	2.12	0.34	0.30	2.46
	MPW1B95	0.73	1.50	0.32	0.77	1.04	1.62	0.05	0.58
	PW6B95	1.52	1.75	0.48	3.28	1.56	1.69	0.78	3.24
	M06	5.28	0.62	1.63	5.90	5.28	0.62	1.63	5.90
	M06-2X	0.19	0.71	1.97	0.51	0.19	0.71	1.97	0.51
range-separated	LC-ωPBE	5.71	1.23	0.25	6.93	5.10	1.53	0.21	6.63
	CAM-B3LYP	1.88	0.35	1.26	1.53	2.08	0.47	1.65	1.61
	ωB97XD	0.52	0.73	1.78	0.21	0.52	0.73	1.78	0.21

a. Functionals ωB97XD, O3LYP and the Minnesota series (M06, M06-L, M06-2X) were not added the dispersion corrections. GS, TS and pdt represent the complex **3a**, transition state **4a** and the final products **5a** + **8** respectively. ΔE = E(DFT/QZ) – E(CCSD(T)-F12/VDZ-F12); E(GS) = E(3a) – E(2) – E(1a); E(TS) = E(4a) – E(2) – E(1a); E(pdt) = E(5a) + E(8) – E(2) – E(1a).

With these results, several commonly used DFT functionals were evaluated with QZ basis set for reaction and activation energies. The AQZ basis set was not used due to the limit of computational resources. Two different dispersion corrections, D3zero and D3BJ, were also evaluated. The preliminary results are summarized below (Table 5.6). Based on these results, M06-2X showed one of the best performances.

However, the highly parameterized M06-2X functional only exhibits its accuracy on the methyl migration but does not guarantee the same effect on the phenyl migration. The non-empirical basis set TPSS, on the other hand, cancels out such an effect. The most important task here is to obtain the accurate values of differences of activation energies ($\Delta\Delta G^{\neq}$) between methyl and phenyl migrations. As for semi-quantitative demonstration, it is safe to use the data from section 5.2.1.1 for analysis and validation of the experimental results. It should be noted that the absolute activation energies from either TPSS or M06-2X single-point energy calculations are much lower compared to the reference value 28.8 kcal/mol. To achieve a full calibration of DFT functionals on all the reactions including both complexation and 1,2-migration, additional studies are required to calibrate the phenyl migration with high level *ab initio* methods and employ augmented basis set AQZ in DFT calculations as indicated in table 5.5.

5.2.2. Synthesis of 9-borafluorene derivatives

To synthesize the 9-borafluorene derivatives, one common and simple strategy is to prepare the 2,2'-dihalo-1,1'-biphenyl derivatives followed by dilithiation and ring closure with organotin reagents (Scheme 5.7). The boron atom can be installed by a final boron–tin exchange reaction. Post modifications on the aromatic rings after construction of the borole core are quite challenging. The 4e five-membered borole ring is sensitive to many chemical reactions such as

Lewis acid-base reaction, Diels-Alder reaction and two electron reductions.[17] After several attempts, all three designed catalysts were synthesized with satisfactory yields and high purities (Scheme 5.8).

Scheme 5.7. A common synthetic strategy to build the 9-borafluorene core.

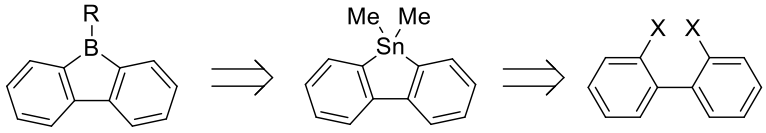

Scheme 5.8. Synthesis of 9-borafluorene derivatives a) **cat-H 1a**, b) **cat-Me 1b** and c) **cat-F 1c**.

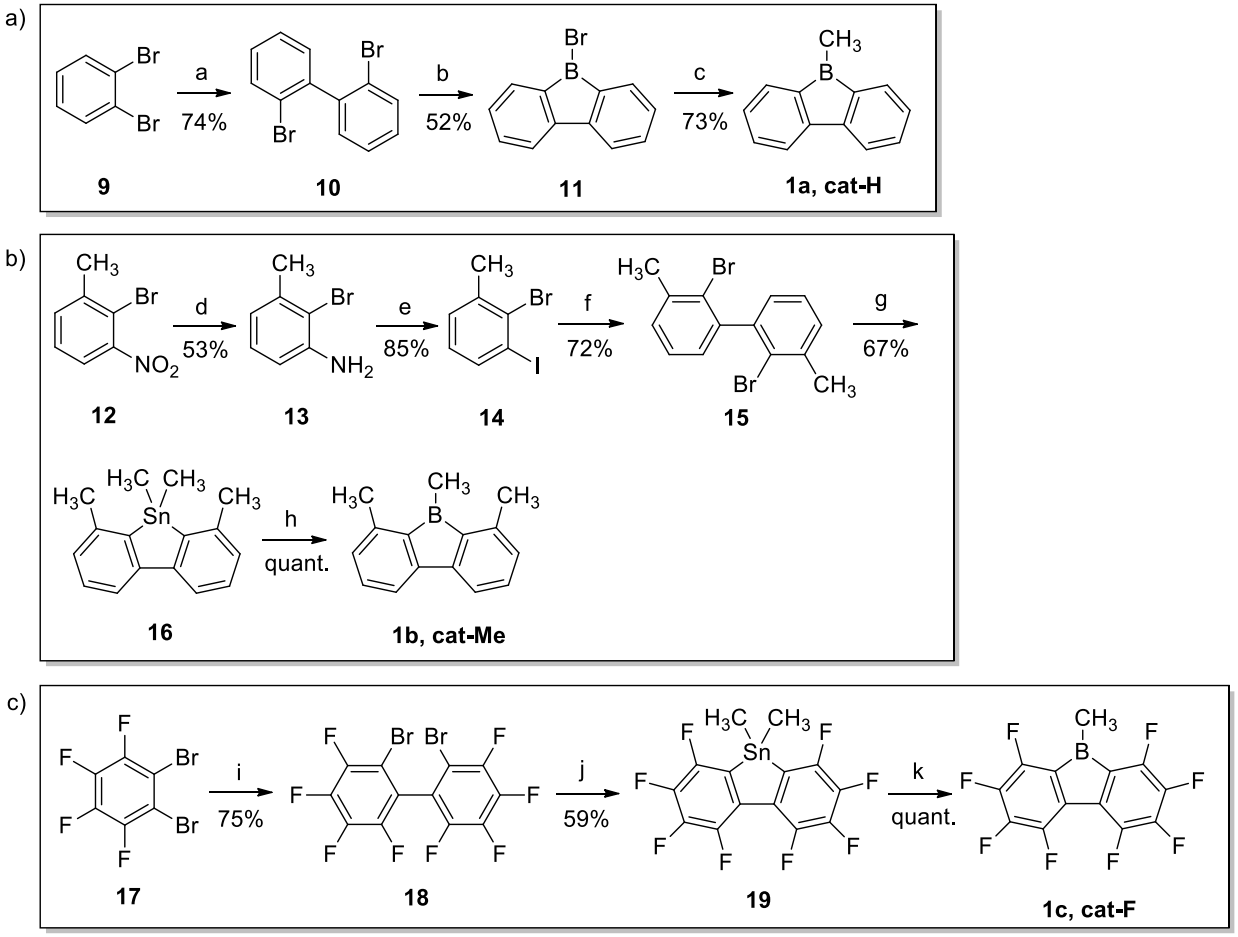

Reagents and conditions: a) 0.5 eq. *n*-BuLi, THF, –78 ℃ to rt; b) 2.2 eq. *n*-BuLi, hexane, rt, 2 d; then BBr_3, 0 ℃, overnight; c) 0.5 eq. Cp_2ZnMe_2, hexane, rt, 1 d; d) Fe, HOAc/EtOH, reflux, 3.5 h; e) p-TsOH, KI, $NaNO_2$, MeCN, rt, overnight; f) $(Bpin)_2$, K_3PO_4, $Pd(dppf)Cl_2$, DMSO, 100 ℃, 20 h; g) *n*-BuLi, THF, –78 ℃, 1 h; then Me_2SnCl_2, –78 ℃ to rt, overnight; h) $MeBBr_2$, hexane, rt, overnight; i) *n*-BuLi, Et_2O, –78 ℃, 15 min; then $TiCl_4$, –78 ℃ to rt, overnight; j) *n*-BuLi, Et_2O, –78 ℃; then Me_2SnCl_2, –78 ℃ to rt; k) $MeBBr_2$, C_6H_6, sealed tube, 120 ℃.

To obtain 2,2'-dihalo-1,1'-biphenyl derivatives, the most efficient strategy is the homocoupling of 1,2-dihalobenzene derivatives. The two halogen substituents can be either the same or different depending on whether a selective coupling on a specific location is required. For substrates with symmetrical substitutions such as **9** and **17**, homocoupling was carried out by formation of benzyne intermediates or aided by $TiCl_4$.[43-44] For target molecule **15**, halogen substituents were designed with the more reactive iodine placed on the meta position to the methyl group for an initial coupling before the ring closure via the bromine substituent on the ortho position. The reaction proceeded via a one-pot, two-step homocoupling catalyzed by $Pd(dppf)Cl_2$[45] with both the Miyaura borylation and Suzuki–Miyaura cross-coupling.[46-47]

Different from the other two, catalyst **1a** was first synthesized with use of BBr_3 for ring closure to avoid the use of toxic dimethyltin dichloride. However, there are several disadvantages of using boron reagents directly for ring closure. For compound **11** synthesized from **10**, the most practical purification method is vacuum distillation. Other methods such as recrystallization and chromatography are not an option due to the presence of many side products as well as the vulnerability of **11** towards air and moisture. Therefore to avoid impurities in vacuum distillation, compound **10** should be completely consumed where the dilithiation process requires alkyllithium in slight excess. Additional process is necessary to wash away the extra alkyllithium from the generated insoluble dilithiated aromatics during which the reaction could suffer from the unintentional introduced trace amount of moisture and oxygen.

By comparison, the organotin products such as **16** and **19** are air- and moisture-stable compounds that can be readily purified via chromatography. The subsequent boron–tin exchange is a quantitative reaction with easy purification protocols. The only disadvantage of ring closure

with Me_2SnCl_2 is the toxicity which could be minimized by handling with suggested protective equipments and strict handling and cleaning procedures.

To obtain catalyst **1a**, the final methylation step was carried out by use of dimethylzirconocene (Cp_2ZnMe_2) adopted from the literature report on a similar substrate.[48] This synthetic method starting from 9-bromo-9-borafluorene derivatives, however, was abandoned for other similar substrates. First, vacuum distillation is not applicable for many 9-bromo-9-borafluorene derivatives due to observed decomposition at a required high temperature under high vacuum condition. Second, the use of an uncommon and expensive zirconocene reagent in quantitative amounts is not economical. Lastly, it is challenging and impractical for products containing the moisture- and air-sensitive borole subunit subjected to the repeated purifications both before and after the methylation reaction.

In contrast, **cat-Me** and **cat-F** were synthesized in one step from **16** and **19** via a direct boron–tin exchange with $MeBBr_2$. Such an organodihaloborane reagent could be prepared readily from boron–tin exchange or hydroboration of olefins with $HBBr_2$ in high purity.[49] With the pre-installed methyl (or other alkyls) group, the borole subunit was built only in the last step with a single purification. Benefited from the quantitative boron–tin exchange, the final products can be obtained after high static vacuum under heat to sublime and remove the side product Me_2SnBr_2.

The reaction conditions of boron–tin exchange were found to be quite different between the synthesis of **cat-Me** and **cat-F**. The exchange reaction for **16** occurred readily at –78 ℃ with use of only one equivalent of the boron reagent. However, for substrate **19**, no reaction took place even at 60 ℃ due to the low reactivity of **19** resulting from the low electron density around the Sn–C_{sp2} bond. After several attempts, I found that the reaction did not occur until the

temperature reached 80 ℃ at which a sealed tube is required due to the low boiling point of $MeBBr_2$. Moreover, prolonged reaction time at high temperatures would result in dark brown solids from side reactions. The exchange reaction for **19** was eventually optimized to be clean and quantitative, after screening the reaction time, temperature and number of equivalents of $MeBBr_2$.

Final purification was not performed for either **cat-Me** or **cat-F** due to the lack of static vacuum that could be used inside the glove box. Purification attempts using a dynamic or static vacuum outside the glove box resulted in oxidized products. Without purification, the reaction mixture is only composed of the desired catalysts and byproduct Me_2SnBr_2 with no observed impurities by NMR analysis. The latter organotin compound proved to have no reactivity in the polyhomologation reaction by a control experiment. Thus it is safe to use the unpurified **cat-Me** and **cat-F** for polymerization studies.

Another 9-borafluorene derivative, 9-(*n*-hexyl)-9-borafluorene, was also synthesized by a different method (Scheme 5.9). The synthesis requires a first preparation of the 9-bromo-9-borafluorene **11**. In the presence of the reducing agent triethylsilane, **11** can be converted to 9-H-9-borafluorene **20** and trapped *in-situ* with olefin or terminal alkynes via hydroboration.[18]

Scheme 5.9. Synthesis of 9-(*n*-hexyl)-9-borafluorene **1d**.

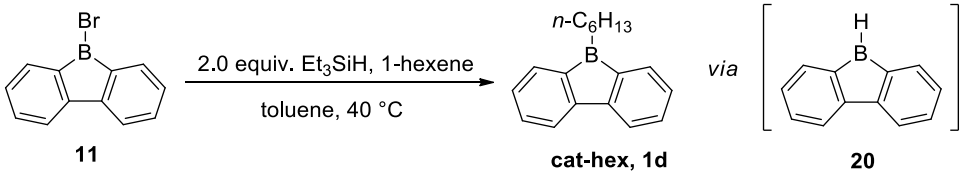

11 **cat-hex, 1d** **20**

5.2.3. Polymerization studies

With various synthesized 9-borafluorene derivatives, the polyhomologation reaction was carried out using methylide **2** to evaluate their performances (Scheme 5.10). The polymerizations

were carried out at both room temperature and THF reflux temperatures. After the oxidation reaction, polymers were filtered and characterized via ^{1}H NMR and GPC. Two types of polymers with **21** from methyl migration and **22** from phenyl migration were identified. The results are summarized in table 5.7.

Scheme 5.10. Polymerization of sulfoxonium methylide **2** with various 9-borafluorene derivatives.

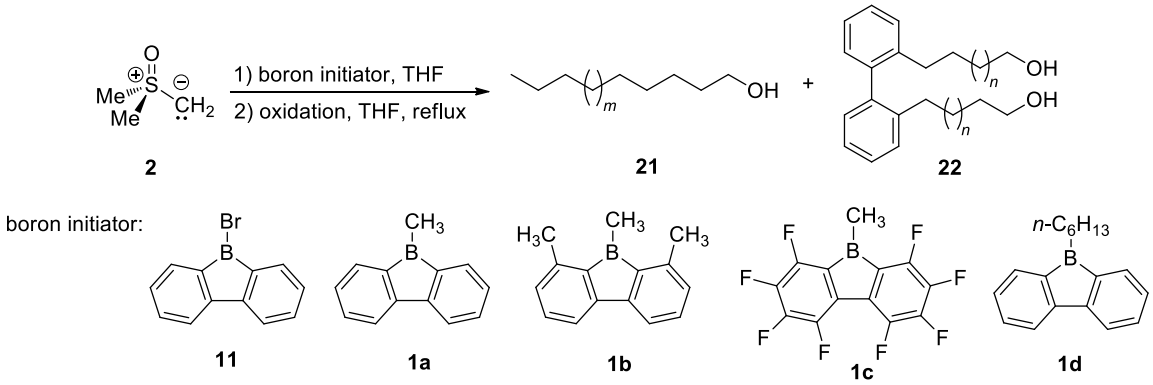

Table 5.7. Evaluation of catalysts performances with methylide **2**.[a]

entry	initiator	temp (˚C)	time (h)	yield (%)	**21** : **22**	DP_{th}[c]	MW_{th}[c] (g/mol)	M_n[d] (g/mol)	M_w[d] (g/mol)	PDI[d]
1	**11**	25	24	NR	ND	25	368	ND	ND	ND
2	**11**	reflux	0.3	64	ND[b]	25	368	4531	5518	1.22
3	**1a**	25	20	100	1 : 0.11	36	536	2469	3568	1.44
4	**1a**	reflux	0.3	95	1 : 0.14	36	536	631	1346	2.13
5	**1b**	25	15	95	1 : 0.07	36	536	682	1384	2.03
6	**1b**	reflux	0.5	94	1 : 0.14	36	536	1064	2275	1.73
7	**1c**	25	24	NR	ND	36	536	ND	ND	ND
8	**1c**	reflux	13	36	ND[b]	36	536	11292	35473	3.14
9	**1d**	25	14	48	1 : 0.20	16	326	490	662	1.35
10	**1d**	reflux	0.2	50	1 : 0.58	29	508	914	1170	1.28

a. NR = no polymerization; ND = not determined.
b. The ratio of two polymers cannot be calculated from ^{1}H NMR, due to difficulties with end group analyses resulted from high MW.
c. Calculated based on the stoichiometry of ylide **2** assuming growth of a single chain. DP_{th} = [**2**]/[**cat**.]; MW_{th} = $M_{CH2} \times DP_{th} + M_{CH3} + M_{OH.}$
d. Obtained from GPC analysis.

The 9-bromo-9-borofluorene catalyst **11** was investigated first. Upon mixing with large excess of ylide **2**, cloudiness was observed immediately in the reaction solution at room

temperature. No consumption of the ylide was found after stirring for 2 hours at room temperature (Table 5.7, entry 1). The observed cloudiness could probably be attributed to the dissociation of the weak Lewis base bromide from the borate complex **23** (Scheme 5.11). Such phenomenon was also observed during the study of catalyst **1b** and **1c**, which might be ascribed to the reactions between methylide **2** and the remaining Me_2SnBr_2 from the unpurified catalysts. The polymerization with catalyst **11** could still undergo reaction at elevated temperatures with rapid consumption (10 min) of ylide **2** (entry 2). GPC analysis on the obtained material exhibits much higher MW than expected. Only a small portion of the catalyst underwent initiation and chain propagation, regardless of methyl or phenyl migration. In consequence, the polymer end groups cannot be recognized from ^{1}H NMR to determine the ratio between polymer **21** and **22**.

Scheme 5.11. Proposed explanation on the initial precipitation in the polymerization using catalyst **11**.

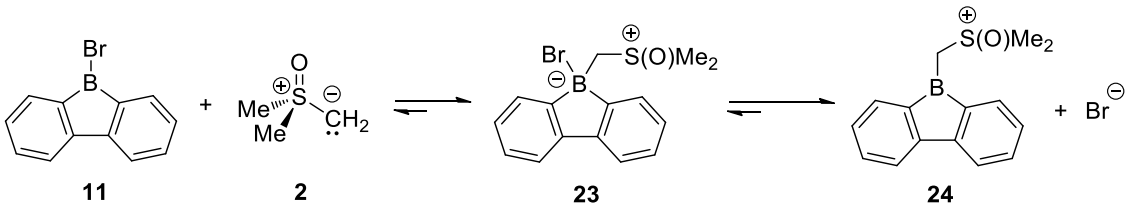

Next catalysts **1a**–**d** with alkyl substitutions on boron were studied (entry 3–10). All obtained polymers had evidence of phenyl migrations from the diagnostic benzylic H and aromatic H by ^{1}H NMR. The mole ratio of polymer **21** over **22** can be calculated by end-group analysis. Importantly, the polymerization lost its living feature for most cases as evidenced by the multimodal MW distributions. There are several reasons to account for these results. First, the calculated activation energies for sp^3 and sp^2 migrations are close to each other. Second, the reaction rates are quite different for further ring expansions of the homologated borole **25** during the early stage of polymerization (Scheme 5.12). It involves competing migrations among alkyl, phenyl and benzyl groups. After the first phenyl migration, various catalytic species were

generated with different reactivities. Thus polymer chains would grow at different rates leading to broad and multimodal MW distributions. Once enough methylene units had inserted on all three chains around boron, the propagation would proceed as a common trialkylborane. As the reaction rate for early homologation is still unknown, a full explanation requires identification of all intermediates and comparison of their related activation energies.

Scheme 5.12. Some of the possible catalytic species generated at early polymerization stage after the first phenyl migration.

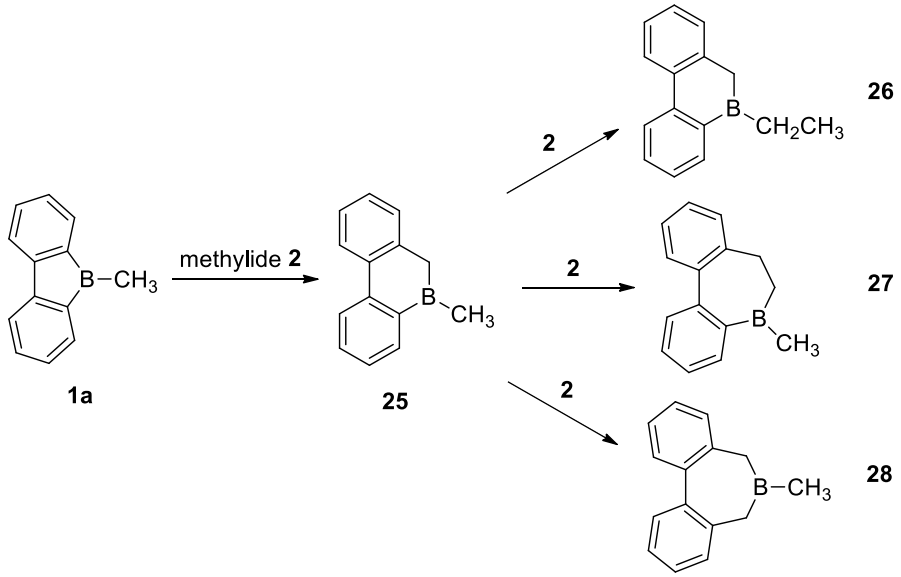

When the reaction temperature was raised from 25 ℃ to near 70 ℃, the ratio of polymer **22** by phenyl insertion also increased (entry 3–6, 9–10). The introduced extra energy by temperature elevation reduced the preferences between methyl and phenyl migration.

In addition, the catalyst **1c** is a bit different from the others (entry 7–8). As its calculated methyl migration is 1.6 kcal/mol lower than that of the phenyl migration, control of the initiation site should be achieved by low reaction temperatures. However, no consumption of ylide was observed after stirring at room temperature for over 12 h. The higher activation energy of 1,2-migration (by 3.4 kcal/mol than **1a**) made catalyst **1c** slower at room temperature to undergo homologation with ylide **2**. Even at elevated temperatures, only a fraction of ylide was consumed

by catalyst **1c** in the first 1–2 hours. An overnight polymerization was carried out instead; while ylide was consumed within 30 minutes with catalyst **1a**, **1b** and **1d** under the same condition.

In summary, the preferred methyl migration was designed by installation of electron withdrawing groups to decrease the electron density of the migrating C_{sp2}. On the other hand, these electron withdrawing groups increased the Lewis acidity of the catalyst and resulted in a more stable borate complex. By lowering the energy level of the borate complex, such a design would increase the activation energy of 1,2-migration. As a result, a higher reaction temperature is necessary for homologation which would, in turn, reduce its selectivity for methyl migration. In this sense, the catalyst ***o,p*-di-CF_3** was not synthesized and investigated due to the calculated high activation energy of 18.7 kcal/mol for methyl migration (comparable to **cat-F** 18.8 kcal/mol in gas phase), although it demonstrated an activation energy difference between sp^3 and sp^2 carbon migrations of 3.6 kcal/mol.

To further investigate the 9-borafluorene derivatives in the polyhomologation reaction, polymerizations were carried out with sulfoxonium ethylide **29** for synthesis of polyethylidene (Scheme 5.13). In addition to the catalysts **1a**–**c**, control polymerizations were also carried out with Me_2SnCl_2 (analogous to Me_2SnBr_2 that was not removed from boron–tin exchange) and catechol boronate **32** that was recently reported to have only single-chain migration with methylide **2**.[50]

Scheme 5.13. Polymerization of sulfoxonium ethylide **29** with various 9-borafluorene derivatives.

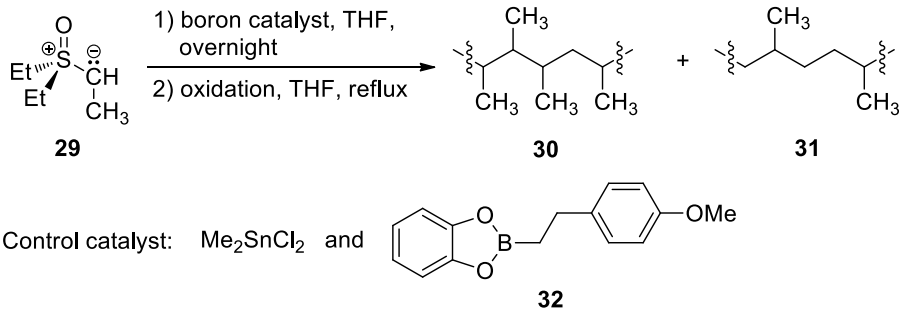

All polymerizations including the control reactions were found to have almost no consumption of ethylide **29** at room temperature overnight. Full consumption of ethylide was not achieved even after an overnight reflux in THF. Other solvents with higher boiling points were not investigated due to the limited choices on solvents for the ethylide synthesis. After removal of volatile solvents, all residues were washed with water and methanol resulting in sticky gel-like materials in low yield (< 60%). ^{1}H NMR analysis indicated long-chain hydrocarbons with only CH_3, CH_2 and CH present and absence of phenyl, hydroxyl or other functional groups.

Surprisingly, in the control reaction in the absence of Lewis acids, ethylide **29** treated with Me_2SnCl_2 gave polymeric materials with low MW but unimodal distributions (Table 5.8, entry 1). However, NMR analysis revealed the presence of large contents of CH_2 in the polymer chain which in theory should not be generated when only ethylide was present. The same results were also found for polymerizations with small ratio of [ethylide **29**]:[cat. **32** or **1a**–**c**] depicted by low theoretical degree of polymerization (DP_{th}) (entry 2–5). The low MW polymers are not originated from Me_2SnCl_2 (byproducts Me_2SnBr_2 in catalysts **1b** and **1c**), as catalyst **32** and **1a** were prepared in high purity. These observations indicated that the obtained polymers were not produced by the polyhomologation reaction. Considering the decreased thermal stability of ethylide **29** compared to methylide **2**, the origin of CH_2 is probably from the decomposition of

ethylide **29** at elevated temperatures. Further studies are required to confirm the instability of ethylide **29** and elucidate the pathway to generate the CH_2 unit.

Table 5.8. Attempts at synthesizing polyethylidene using ethylide **29** catalyzed by 9-borafluorene derivatives.

entry	catalyst	DP_{th}[a]	MW_{th}[a]	M_n[b]	M_w[b]	PDI[b]	ratio[b]	N(CH_2)%[c]	N*(CH_2)%[d]
1	**Me_2SnCl_2**	29	---	369	378	1.02	100	76	76
2	**32**	21	740	410	444	1.08	100	60	60
3	**1a**	36	1040	390	402	1.03	100	71	71
4	**1b**	30	872	387	395	1.02	100	76	76
5	**1c**	45	1292	329	381	1.16	100	68	68
6	**1a**	150	4232	2942 419	4015 462	1.36 1.10	52 48	50	30 71
7	**1b**	492	13808	1926 360	3207 370	1.66 1.03	65 35	40	21 76
8	**1c**	500	14032	3647 364	4375 375	1.20 1.03	20 80	58	18 68

a. Calculated based on the stoichiometry of ylide **29** assuming growth of a single chain. DP_{th} = [**29**]/[**cat**.]; MW_{th} = $M_{CH3CH} \times DP_{th} + M_{CH3} + M_{OH.}$

b. Obtained from GPC analysis.

c. Percentage of CH_2 units in the polymer chain calculated from ^{1}H NMR.

d. Recalculated percentage of CH_2 units in the polymer chain with the assumption that the low MW polymer fraction in polymerization of **29** in high DP_{th} has the same composition as the polymer from **29** in low DP_{th} using the same catalyst.

When ethylide **29** was present in large excess (high DP_{th}), polymers were obtained having bimodal MW distributions (entry 6–8). The percentage of CH_2 content is lower compared to polymerizations using the same catalyst but with low DP_{th} (entry 3–5). In these runs, at least two types of polymers were produced as evidenced by GPC traces (Figure 5.11). Attempts at fractional precipitation or chromatography failed to separate these two materials. In the polymer mixtures, the low MW fractions have a MW very close to those from the control reactions and polymerizations with low DP_{th}. Thus it should be identified as the same material as entry 1–5 with high content of CH_2 units perhaps due to the decomposition of ylide under the same reaction conditions. In consequence, the high MW fraction would have even a lower amount of

CH_2 units than the measured overall CH_2 contents determined by NMR analysis. Therefore at high DP_{th}, the CH_2 content for each polymer fraction can be determined by comparison of the ratio between the two polymer fractions and assuming that the low MW fraction has the same CH_2 content as the polymers obtained with the same catalyst and small amounts of ylide (low DP_{th}). Using this assumption, the CH_2 content of the high MW polymer fraction was calculated to be below 30% (entry 6–8). This remaining low amount of CH_2 units could be a contribution of both monomer decomposition and polyhomologation of ethylide **29** during the polymer chain growth (Scheme 5.14).

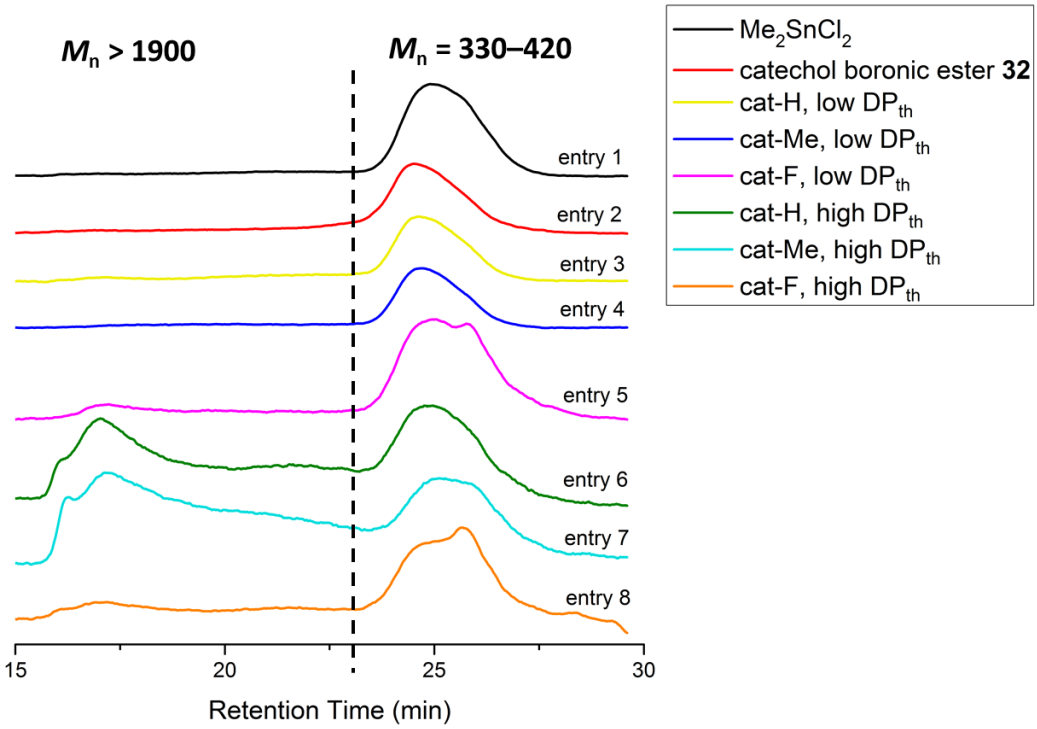

Figure 5.11. Stacked GPC traces of polymers obtained from homopolymerization of ethylide **29**.

Scheme 5.14. Proposed explanation on the origin of the two polymer fractions.

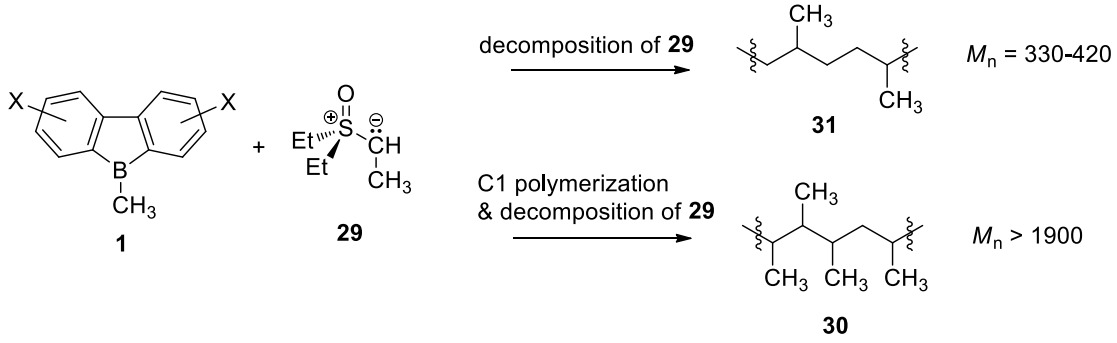

Due to the possibility of both methyl and phenyl migrations, catalyst **1a**–**c** could be saturated by three secondary alkyl chains preventing the next ethylide addition. A further study needs to be carried out with only small amount of ethylide such as three equivalents to directly prove the migration of the phenyl groups. An enforced polymerization at high temperatures for long reaction time would result in the competing decomposition of ethylide. With small amounts of ethylide (low DP_{th}), most of it would decompose to give low MW polymer with high CH_2 content and a low PDI. At high DP_{th}, there is evidence that the ethylide undergoes polymerization but requires the release of the accessible boron site by CH_2 (or CH_2CH_2) insertion via unidentified mechanisms. As a result, high MW polymer fraction was produced with low CH_2 contents. As the thermal decomposition of ethylide is always present, polymers were obtained as a mixture of the two competing reactions. Without an effective separation method, it is impossible to verify the content of each fraction.

5.3. Conclusion

Development of a single-site initiator is important for the polyhomologation reaction for the controlled growth of carbon backbone polymers and to build highly substituted linear carbon chains. With direct incorporation of the boron atom into an organic π-system, 9-borafluorene

derivatives were examined both computationally and experimentally. Computational studies established that the phenyl migration can be suppressed by installation of electron withdrawing groups on the aromatic rings on ortho and para positions of the boron catalyst. A preferred methyl migration could be readily achieved and $\Delta\Delta G^{\neq}$ can be as high as 3.6 kcal/mol with catalyst ***o,p*-di-CF_3**. However, such designs also increased the activation energy for the 1,2-migration step leading to low reactivity of the migration. A high reaction temperature is then required for monomer insertion which would reduce the selectivity of migration. With the stable methylide **2**, polymers were obtained that incorporated aromatic residues indicating migration of both sp^3 and sp^2 carbons. While using the unstable ethylide **29**, polymerizations were quite slow probably due to formation of a sterically congested boron center. In this case, the monomer decomposition is in dominant. Polymer fraction with low content of CH_2 can be obtained with very high DP_{th}.

I am still optimistic that it is possible to design single-site boron initiators for such tasks in the C1 polymerization. As has been demonstrated for small molecule synthesis, the single chain growth has been achieved using the combination of boronic esters and lithiated carbamates or benzoates. Future work might also require the engineering of new ylide monomers.

5.4. References

(1) Woerly, E. M.; Roy, J.; Burke, M. D. *Nat. Chem.* **2014**, *6*, 484–491.

(2) Li, J.; Ballmer, S. G.; Gillis, E. P.; Fujii, S.; Schmidt, M. J.; Palazzolo, A. M. E.; Lehmann, J. W.; Morehouse, G. F.; Burke, M. D. *Science* **2015**, *347*, 1221–1226.

(3) Leonori, D.; Aggarwal, V. K. *Acc. Chem. Res*. **2014**, *47*, 3174−3183.

(4) Burns, M.; Essafi, S.; Bame, J. R.; Bull, S. P.; Webster, M. P.; Balieu, S.; Dale, J. W.; Butts, C. P.; Harvey, J. N.; Aggarwal, V. K. *Nature* **2014**, *513*, 183-188.

(5) Luo, J.; Shea, K. J. *Acc. Chem. Res*. **2010**, *43*, 1420–1433.

(6) Buckley, G. D.; Cross, L. H.; Ray, N. H. *J. Chem. Soc.*, **1950**, 2714–2718.

(7) Feltzin, J.; Restaino, A. J.; Mesrobian, R. B. *J. Am. Chem. Soc.*, **1955**, *77*, 206–210.

(8) Nasini, A. G.; Trossarelli, L.; Saini, G. *Macromol. Chem. Physic*. **1961**, *44*, 550–569.

(9) Busch, B. B. Ph.D. Thesis, University of California, Irvine, 1999.

(10) Staiger, C. Ph.D. Thesis, University of California, Irvine, 2001.

(11) Stoddard, J. M. Ph.D. Thesis, University of California, Irvine, 2003.

(12) Stoddard, J. M.; Shea, K. J. *Chem. Commun.* **2004**, 830–831.

(13) Luo, J.; Zhao, R.; Shea, K. J. *Macromolecules* **2014**, *47*, 5484–5491.

(14) Entwistle, C. D.; Marder, T. B. *Angew. Chem., Int. Ed*. **2002**, *41*, 2927–2931.

(15) Hudnall, T. W.; Chiu, C.-W.; Gabba ï, F. P. *Acc. Chem. Res*. **2009**, *42*, 388–397.

(16) Wade, C. R.; Broomsgrove, A. E. J.; Aldridge, S.; Gabba ï, F. P. *Chem. Rev*. **2010**, *110*, 3958–3984.

(17) Braunschweig, H.; Kupfer, T. *Chem. Commun.*, **2011**, *47*, 10903–10914.

(18) H übner, A.; Qu, Z-W.; Englert, U.; Bolte, M.; Lerner, H-W.; Holthausen, M. C.; Wagner, M. *J. Am. Chem. Soc*. **2011**, *133*, 4596–4609.

(19) Jorgensen, W. L.; Tirado-Rives, J. *Proc. Natl. Acad. Sci. U.S.A.* **2005**, *102*, 6665–6670.

(20) Tao, J.; Perdew, J. P.; Staroverov, V. N.; Scuseria, G. E. *Phys. Rev. Lett.* **2003**, *91*, 146401.

(21) Staroverov, V. N.; Scuseria, G. E.; Tao, J.; Perdew, J. P. *J. Chem. Phys.* **2003**, *119*, 12129.

(22) Grimme, S.; Antony, J.; Ehrlich, S.; Krieg, S. *J. Chem. Phys*. **2010**, *132*, 154104.

(23) Grimme, S.; Ehrlich, S.; Goerigk, L. *J. Comp. Chem.* **2011**, *32*, 1456.

(24) Klemt, A. *J. Phys. Chem.*, **1995**, *99*, 2224–2235.

(25) Robiette, R.; Fang, G.; Harvey, J. N.; Aggarwal, V. K. *Chem. Commun.* **2006**, 741–743.

(26) Becke, A. D. *J. Chem. Phys*. **1993**, *98*, 5648–5652.

(27) Lee, C.; Yang, W.; Parr, R. G. *Phys. Rev. B* **1988**, *37*, 785–789.

(28) Vosko, S. H.; Wilk, L.; Nusair, M. *Can. J. Phys*. **1980**, *58*, 1200–1211.

(29) Stephens, P. J.; Devlin, F. J.; Chabalowski, C. F.; Frisch, M. J. *J. Phys. Chem*. **1994**, *98*, 11623–11627.

(30) Rakow, J. R.; Tüllmann, S.; Holthausen, M. C.; *J. Phys. Chem. A* **2009**, *113*, 12035–12043.

(31) Hübner, A.; Diefenbach, M.; Bolte, M.; Lerner, H-W.; Holthausen, M. C.; Wagner, M. *Angew. Chem., Int. Ed.* **2012**, *51*, 12514–12518.

(32) Purvis, G. D.; Bartlett, R. J. *J. Chem. Phys*. **1982**, *76*, 1910−1918.

(33) Watts, J. D.; Gauss, J.; Bartlett, R. J. *J. Chem. Phys*. **1993**, *98*, 8718−8733.

(34) Knizia, G.; Adler, T. B.; Werner, H. J. *J. Chem. Phys*. **2009**, *130*, 054104.

(35) Werner, H.-J.; Adler, T. B.; Manby, F. R. *J. Chem. Phys.*, **2007**, *126*, 164102.

(36) Werner, H.-J.; Manby, F. R.; Knowles, P. J. *J. Chem. Phys.*, **2003**, *118*, 8149.

(37) Karton, A.; Tarnopolsky, A.; Lamère, J.-F.; Schatz, G. C.; Martin, J. M. L. *J. Phys. Chem. A* **2008,** *112*, 12868–12886.

(38) Werner, H.-J.; Adler, T. B. *J. Chem. Phys.*, **2011**, *135*, 144117.

(39) Montgomery, J. A.; Frisch, M. J.; Ochterski, J. W.; Petersson, G. A. *J. Chem. Phys*. **1999**, *110*, 2822.

(40) Busch, B. B.; Paz, M. M.; Shea, K. J.; Staiger, C. L.; Stoddard, J. M.; Walker, J. R.; Zhou, X.-Z.; Zhu, H. *J. Am. Chem. Soc*. **2002**, *124*, 3636–3646.

(41) Dunning, T. H. *J. Chem. Phys*. **1989**, *90*, 1007−1023.

(42) Dunning, T. H.; Peterson, K. A.; Wilson, A. K. *J. Chem. Phys*. **2001**, *114*, 9244−9253.

(43) Cohen, S. C.; Fenton, D. E.; Shaw, D.; Massey, A. G. *J. Organometal. Chem.* **1967**, *8*, 1−8.

(44) Cohen, S. C.; Massey, A. G. *J. Organometal. Chem.* **1967**, *10*, 471.

(45) Nising, C. F.; Schmid, U. K.; Nieger, M.; Bräse, S. *J. Org. Chem.* **2004**, *69*, 6830–6833.

(46) Ishiyama, T.; Murata, M.; Miyaura, N. *J. Org. Chem.* **1995**, *60*, 7508–7510.

(47) Miyaura, N.; Suzuki, A. *Chem. Rev.*, **1995**, *95*, 2457–2483.

(48) Chase, P. A.; Piers, W. E.; Patrick, B. O. *J. Am. Chem. Soc.* **2000**, *122*, 12911–12912.

(49) Niedenzu, K. K. *Organometal. Chem. Rev*. **1966**, *1*, 305–329.

(50) Xu, F.; Dong, P.; Cui, K.; Bu, S.-Z.; Huang, J.; Li, G.-Y.; Jiang, T.; Ma, Z. *RSC Adv.* **2016**, *6*, 69828.

(51) Dougherty, T. K.; Lau, K. S. Y.; Hedberg, F. L. *J. Org. Chem*. **1983**, *48*, 5273.

(52) Biswas, S.; Oppel, I. M.; Bettinger, H. F. *Inorg. Chem*. **2010**, *49*, 4499–4506.

(53) Gamble, A. B.; Garner, J.; Gordon, C. P.; O'Conner, S. M. J.; Keller, P. A. *Synth. Commun*. **2007**, *37*, 2777.

(54) Corey, E. J.; Chaykovsky, M., *Org. Synth., Coll. Vol*. **1973**, *5*, 755.

5.5. Experimental

General considerations. Appendix A and B. The following compounds were prepared according to literature: 2,2'-dibromo-1,1'-biphenyl **10**,[51] 9-bromo-9-borafluorene **11**,[52] 2-bromo-3-methylaniline **13**,[53] 1,2,3,4,6,7,8,9-octafluoro-5,5-dimethyl-5*H*-dibenzo[*b*,*d*]stannole **19**,[48] $MeBBr_2$[49] and dimethylsulfoxonium methylide **2**.[54] Diethylsulfoxonium ethylide **29** was prepared according to Chapter 3. For calculation of monomer contents $–CH_2–$ and $–CH(CH_3)–$, please refer to Chapter 3.5 experimental section.

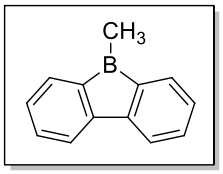

Synthesis of cat-H (1a). Compound **11** (590 mg, 2.43 mmol) was dissolved in hexane (25 mL) in a round bottom flask in the glovebox. Cp_2ZrMe_2 (308 mg, 1.225 mmol) was added to the solution. The reaction was stirred at room temperature for 24 h before the flask was assembled for Kugelrohr distillation. Volatile solvents were removed under high vacuum first before Kugelrohr distillation to afford light yellow oil (314 mg, 73%). ^{1}H NMR (600 MHz, C_6D_6) δ 7.39 (d, *J* = 6.6 Hz, 2H), 7.12 (d, *J* = 7.8 Hz, 2H), 7.07 (td, *J* = 7.2, 1.2 Hz, 2H), 6.92 (t, *J* = 7.2 Hz, 2H), 1.02 (s, 3H); ^{13}C NMR (150 MHz, C_6D_6) δ 153.9, 134.3, 133.6, 128.40, 128.35, 119.7; ^{11}B NMR (160 MHz, C_6D_6) δ 72.9.

Synthesis of cat-Me (1b).

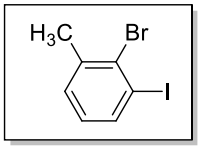

Synthesis of 2-bromo-1-iodo-3-methylbenzene (14). To a solution of *p*-TsOH·H_2O (10.91 g, 57.35 mmol) in MeCN (75 mL) was added compound **13** (3.409 g, 18.32

mmol). The resulting suspension was cooled to 0–5 ℃ and gradually added a solution of $NaNO_2$ (2.551 g, 37.0 mmol) and KI (7.63 g, 46.0 mmol) in H_2O (11 mL). The reaction mixture was stirred for 20 min before slowly warmed to room temperature and stirred overnight. Then to the reaction mixture was added H_2O (100 mL), Na_2CO_3 (saturated, until pH = 9–10) and ethyl acetate (50 mL). The organic layer was washed with $Na_2S_2O_3$ (saturated, 20 mL) before drying over $MgSO_4$ and concentrated *in vacuo*. The crude product was purified by flash chromatography (EtOAc/hexane = 1/8) to afford **14** as colorless oil (4.601 g, 85%). ^{1}H NMR (500 MHz, $CDCl_3$) δ 7.71 (d, *J* = 8.0 Hz, 1H), 7.19 (d, *J* = 7.5 Hz, 1H), 6.91 (t, *J* = 8.0 Hz, 1H), 2.50 (s, 3H); ^{13}C NMR (125 MHz, $CDCl_3$) δ 140.3, 138.2, 131.8, 130.3, 128.6, 102.6, 26.2.

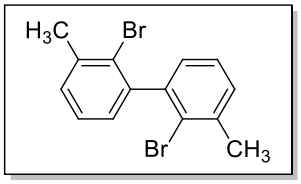

Synthesis of 2,2'-dibromo-3,3'-dimethyl-1,1'-biphenyl (15). Compound **14** (5.282 g, 17.79 mmol), $Pd(dppf)_2Cl_2{\cdot}CH_2Cl_2$ (701 mg, 0.858 mmol), bis(pinacolato)diboron (2.499 g, 9.84 mmol) and K_3PO_4 (11.391 g, 53.66 mmol) were added to a two-neck round bottom flask equipped with a condenser. Then the system was purged with N_2 by vacuum–N_2 for three times. Degassed DMSO (125 mL) was injected at room temperature and the reaction was heated at 100 ℃ overnight. After cooling down to room temperature, the reaction mixture was poured into H_2O (100 mL). The resulting mixture was extracted with Et_2O (3 × 30 mL). The organic layer was dried over $MgSO_4$ before evaporation to dryness and purified by column chromatography packed with silica gel using hexane as the eluent. The product was afforded as white solids (2.171 g, 72%). ^{1}H NMR (500 MHz, CD_2Cl_2) δ 7.25–7.30 (m, 4H), 7.04 (dd, *J* = 6.5, 2.5 Hz, 2H), 2.48 (s, 6H); ^{13}C NMR (125 MHz, CD_2Cl_2) δ 143.8, 139.0, 130.4, 128.7, 127.1, 126.2, 24.0.

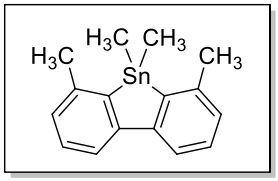

Synthesis of 4,5,5,6-tetramethyl-5*H*-dibenzo[*b,d*]stannole (16). To a N_2 flushed round bottom flask containing compound **15** (826 mg, 2.43 mmol) and THF (25 mL) was slowly added *n*-butyllithium (2.5 M in hexane, 2.16 mL, 5.4 mmol) at −78 °C. Then a solution of Me_2SnCl_2 in THF (596 mg in 15 mL, 2.71 mmol) was gradually injected to the reaction in 5 min. After 1 h of stirring at −78 °C, the reaction was slowly warmed to room temperature and stirred overnight. After removal of solvents in *vacuo*, hexane (50 mL) was added to the residue and sonicated for 5 min before filtration and washed the solids with hexane (3 × 10 mL). The filtrate was evaporated to dryness and purified by column chromatography (hexane) to afford white solid (536 mg, 67%). ^{1}H NMR (500 MHz, CD_2Cl_2) δ 7.76 (d, *J* = 6.5 Hz, 2H), 7.32 (t, *J* = 6.5 Hz, 2H), 7.16 (d, *J* = 6.5 Hz, 2H), 2.50 (s, 6H), 0.60 (s, 6H); ^{13}C NMR (125 MHz, CD_2Cl_2) δ 148.6, 144.7, 142.2, 130.0, 127.6, 120.3, 26.4, 9.6.

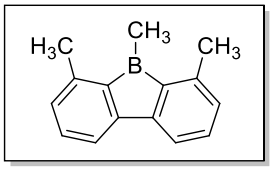

Synthesis of 4,5,6-trimethyl-5*H*-dibenzo[*b,d*]borole (1b). To a round bottom flask in the glovebox was charged $MeBBr_2$ (77.5 mg, 0.417 mmol) and hexane (2.5 mL). After addition of compound **16** (134 mg, 0.408 mmol), the solution was stirred at 40 ℃ overnight. The resulting mixture can be directly used for polymerization. ^{1}H NMR (600 MHz, C_6D_6) δ 7.07 (dd, *J* = 7.2, 2.4 Hz, 2H), 7.02 (td, *J* = 7.8, 2.4 Hz, 2H), 6.74 (d, *J* = 7.8 Hz, 2H), 2.28 (s, 3H), 1.13 (s, 3H); ^{13}C NMR (150 MHz, C_6D_6) δ 153.9, 145.7, 134.0, 130.8, 128.4, 117.3, 21.7, 6.27; ^{11}B NMR (160 MHz, C_6D_6) δ 79.1.

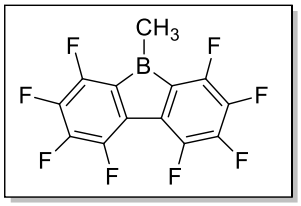

Synthesis of 1,2,3,4,6,7,8,9-octafluoro-5-methyl-5*H*-dibenzo[*b*,*d*]-borole (1c). To a small vial was charged $MeBBr_2$ (111 mg, 0.60 mmol) and benzene-d_6 (2 drops). After addition of compound **19** (91 mg, 0.205 mmol), the reaction was sealed with a teflon cap and heated at 120 ℃ for 24 h. After cooling down to room temperature, the reaction mixture was evaporated to dryness under high vacuum at room temperature to afford the product (with Me_2SnBr_2) as yellow green solid. It can be directly used for polymerization after addition of a specific volume of solvent to obtain a known concentration of the catalyst. ^{1}H NMR (600 MHz, C_6D_6) δ 1.06 (s, 3H); ^{19}F NMR (470 MHz, C_6D_6) δ −126.4 (m, 2F), −131.7 (m, 2F), −144.2 (m, 2F), −153.9 (m, 2F); ^{11}B NMR (160 MHz, C_6D_6) δ 67.3.

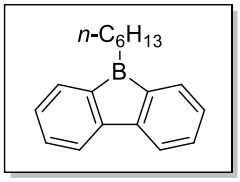

Synthesis of 9-(*n*-hexyl)-9-borafluorene (1d). To a N_2 purged round bottom flask was added compound **11** (261 mg, 1.07 mmol), 1-hexene (0.136 mL, 1.09 mmol) and toluene (2.6 mL). At room temperature the mixture was stirred and added triethylsilane (0.344 mL, 2.15 mmol) dropwise. Then the reaction was heated to 40 ℃ and stirred for 3 h before removal of all volatile compounds under high vacuum at room temperature. The resulting liquid was characterized as a pure compound and directly used for polymerization. ^{1}H NMR (500 MHz, CD_2Cl_2) δ 7.66 (d, *J* = 6.0 Hz, 2H), 7.38 (d, *J* = 6.0 Hz, 2H), 7.34 (td, *J* = 6.0, 0.5 Hz, 2H), 7.16 (t, *J* = 6.0 Hz, 2H), 1.88–1.91 (m, 4H), 1.47–1.53 (m, 2H), 1.37–1.44 (m, 4H), 0.97 (t, *J* = 6.0 Hz,

3H); ^{13}C NMR (125 MHz, CD_2Cl_2) δ 153.9, 134.4, 134.1, 128.6, 119.8, 33.5, 32.4, 25.7, 23.2, 14.5, 8.3; ^{11}B NMR (160 MHz, CD_2Cl_2) δ 73.1.

Representative procedure for polymerization of ylide monomers catalyzed by 9-borafluorene derivatives (Table 5.7, entry 4). To a two-neck round bottom flask equipped with a condenser and purged under N_2 was charged with degassed dimethylsulfoxonium methylide **2** (0.556 M, 10.0 mL, 5.56 mmol). The mixture was preheated on an oil bath at 70 ℃ for 5 min followed by a quick injection of **cat-H 1a** (0.363 M in THF, 0.425 mL, 0.154 mmol). After the reaction being stirred at 70 ℃ for 15 min, an aliquot was titrated to indicate no ylide remaining in the solution. Then a degassed solution of trimethylamine *N*-oxide dihydrate (84 mg/mL in H_2O, 1.25 mL, 0.945 mmol) was injected. The reaction was stirred at 70 ℃ for 6 h before cooling down to room temperature. After evaporation *in vacuo*, the residue was dispersed in methanol (30 mL) and filtered. The resulting solid was washed with deionized water (3 × 5 mL), methanol (3 × 5 mL) and dichloromethane (10 mL) to afford white solid (108 mg, 95%). GPC analysis: M_n = 631, M_w = 1346, PDI = 2.13.

Calculation of polymer ratios of 21 : 22 for the polymerization of methylide 2. Diagnostic peaks were used for calculation at 0.7–1.0 ppm (CH_3 at chain end) and 7.1–7.4 ppm (ArH) with integration values denoted as I_a and I_b, respectively. The molar ratio of polymer **21**:**22** can be calculated as Equation 5.1.

$$\frac{n(21)}{n(22)} = \frac{I_a / 3}{I_b / 8} \qquad \text{Eq. (5.1)}$$

Chapter 6. Development of Air-stable Borane Initiators for the C1 Polyhomologation Reaction

6.1. Introduction

The living C1 polymerization of sulfoxide ylides initiated by organoboranes is one of the few methods for controlling the molecular weight, polydispersity, and topology of simple hydrocarbon polymers.[1] This polyhomologation reaction is a living polymerization with the capability to achieve a PDI that approaches the theoretical limit of 1.01 when the polymer molecular weight is below 10 kDa. However, in the cases of molecular weights over 50 kDa, this method often results in some erosion of polydispersity (PDI 1.3–2.0).[2] In earlier studies it was learned that a contributing factor to PDI erosion can arise during the oxidation step where double-massed polymer fractions were generated as a result of the dimerization of radicals generated between tris-polymethylene borane and oxygen.[3] This amounted to 1–2% in some cases and could be minimized by the use of amine oxides as oxidizing reagents. However, in the case of high molecular weight polymer synthesis, Gel Permeation Chromatography (GPC) analysis indicated that low molecular weight fractions are responsible for the increased PDI.

We found that in the absence of known chain transfer or termination steps, the origin of the PDI erosion could be attributed to small quantities of a borinic ester impurity **3** that arises from the oxidation of the trialkylborane initiator/catalyst **1** by trace oxygen (Scheme 6.1).[2] During the course of the polymerization, borinic ester **3** can engage in the polymerization but at a slower rate by a 1,2–oxygen migration of the **3**·ylide complex compared to the 'regular' chain initiation from the unoxidized trialkylborane **1**. Once homologated, the resulting species

R_2BCH_2OR **4** is a more reactive initiator/catalyst than its borinic ester precursor **3** with the chain propagation rate that is similar to BR_3 **1**. This reactive initiator/catalyst **4** 'kicks in' during the polymerization but later than **1**, contributing to the formation of low MW polymer fractions **5**.

Scheme 6.1. Production of low molecular weight polymers from the oxidized organoborane catalyst.

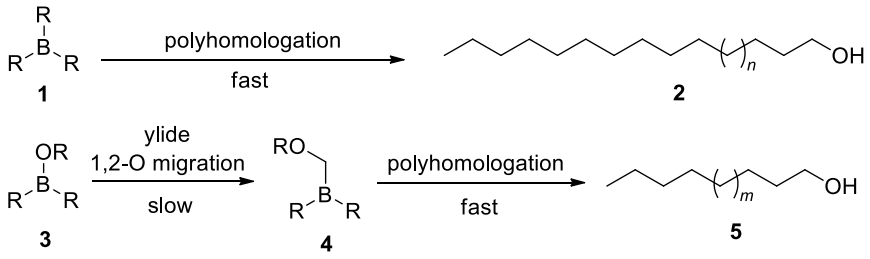

A survey of the previously reported catalysts for C1 polymerization reveals a variety of organoboranes that have been used including BH_3·THF **6**[2], triethylborane **7**[3-5], tris-(4-methoxyphenylethyl) borane **8**[4,5], 9-BBN derivatives **9**[6], 1-boraadamantane **10**[7], and tris-*m*PEG borane **11**[8] (Scheme 6.2). Most of the catalysts are designed for obtaining either novel polymer topologies or linear telechelic polymers. All these organoborane initiators are air sensitive chemicals. Challenges remain on the preparation of many organoboranes in high purities.

Scheme 6.2. Some of the reported organoborane catalysts for the polyhomologation reaction.

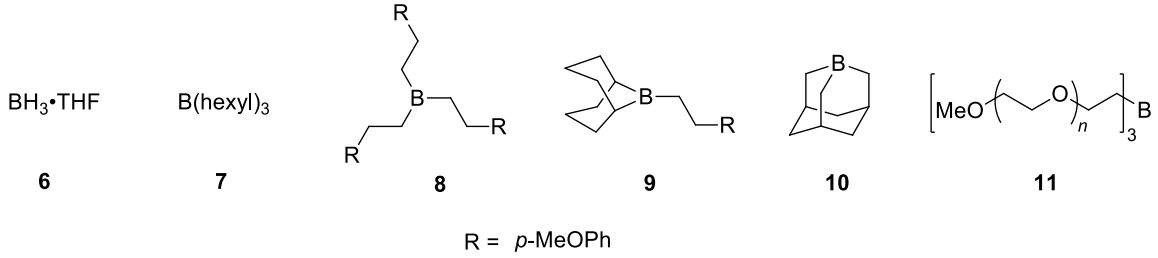

As the polymer molecular weight distribution is highly dependent on the purity of the catalysts, one needs to be very meticulous with the preparation, storage and handling of organoborane reagents to avoid any degradation of the purity. There are two main reasons to develop an air-stable borane initiator for the C1 polymerization: synthesis of high molecular

weight polymers with low polydispersity and long-term storage of the catalyst with ease of preparation and handling.

6.2. Results and Discussion

Borane (BH_3) is a pyrophoric gas and exists as the diborane (B_2H_6). For convenient handling, borane complexes with Lewis bases are used as precursors of BH_3. Well-established borane complexes such as BH_3·THF and BH_3·SMe_2 are widely used in organic synthesis. Ethers and sulfides are labile Lewis bases which are quite limited in stabilizing BH_3. In fact, BH_3·THF complex is not stable over long periods; while BH_3·SMe_2 possesses volatility and flammability problems from an environmental point of view. In contrast, boranes stabilized with amines and phosphines are generally much less oxygen-sensitive and are readily soluble in a variety of solvents.

To achieve air-stability, the interaction between BH_3 and the Lewis base must be strong enough to avoid release of the free borane in air. On the contrary, an effective initiator/catalyst requires the readily release of its active trivalent component upon heating in the polyhomologation reaction. In the amine–/phosphine–borane category, the simplest form is the ammonia–borane adduct BH_3·NH_3. Despite its high stability towards air and moisture, this reagent is so thermally stable that it requires significantly higher temperatures above 100 ℃ to dissociate and undergo the hydroboration reaction. Its slow dissociation made the adduct difficult to release all the active trivalent borane to undergo the polyhomologation reaction.[9,10] One solution is to increase the steric bulk at the nitrogen or phosphorus center which will decrease the stability of the adduct. This was exemplified by measuring a series of molar enthalpies of the ligand exchange reactions between various amines and BH_3·THF at room temperature.[11] The

order of molar enthalpies was determined as $Et_2NH{\cdot}BH_3$ > $(n\text{-Pr})_2NH{\cdot}BH_3$ > $(n\text{-Bu})_2NH{\cdot}BH_3$ and $n\text{-BuNH}_2{\cdot}BH_3$ > $(n\text{-Bu})_2NH{\cdot}BH_3$ > $(n\text{-Bu})_3N{\cdot}BH_3$. Additional steric constraints made the B–N bond weaker by poorer overlap of orbitals.

6.2.1. Preliminary studies with $BH_3{\cdot}NMe_3$

For my first attempt, I employed trimethylamine–borane adduct $BH_3{\cdot}NMe_3$ for the polyhomologation reaction (Scheme 6.3). To achieve a polymer with low PDI and controlled molecular weight, the reaction needs to be maintained homogeneous till the consumption of all ylide monomers. Toluene or decalin at elevated temperatures is required to avoid the early precipitation of the propagating polymer chain, since polymethylene has low solubility in most solvents even at high temperatures. For higher molecular weight (>50 kDa) polymethylene synthesis, decalin has to be introduced to further improve the solubility of the polymer.

Scheme 6.3. C1 polyhomologation catalyzed by $BH_3{\cdot}NMe_3$.

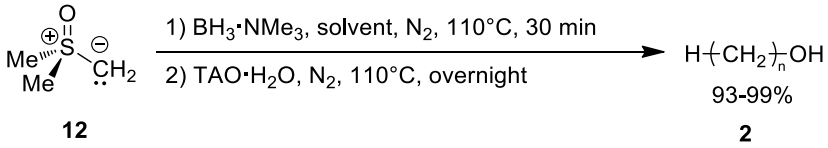

12 **2**

For better reaction control and higher reaction yield, the monomer dimethylsulfoxonium methylide **12** was prepared in THF rather than in toluene. Then a solvent exchange is mandatory as the solvent for polymerization needs to be largely composed of toluene or decalin. My initial attempt of the solvent exchange was performed *via* precipitation of the ylide at low temperatures (−20 ℃) followed by decantation of the top clear supernated solution under nitrogen refilling with toluene. However, this method proved inefficient as only 54% of recovery of ylide was achieved. I found that a controlled distillation gave near quantitative recovery by gradually

replacing THF with toluene. This method does not completely replace THF with toluene but is sufficient to have the reaction carried out at 110 ℃.

Following addition of the borane adduct initiation, polymethylene was obtained in high yield. The high molecular weight polymers were synthesized with a predicted molecular weight and low degree of polydispersity (Table 6.1, entry 7–9). In comparison, polymethylenes synthesized with the conventional BH_3·THF catalyst have a low PDI for polymers with low molecular weights (Table 6.1, entry 1); but high PDI for polymers with high molecular weights (Table 6.1, entry 2). The results clearly show that the borane catalyst complexed with a stronger Lewis base, i.e., NMe_3 rather than THF, has a reduced chance of being oxidized and can lower the polymer PDI. When applied to low molecular weight polymer synthesis, however, this amine–borane complex failed to give a controlled molecular weight (Table 6.1, entry 3–6). The obtained polymer molecular weights are much higher than the predicted values based on stoichiometric ratios of [monomer]/[catalyst].

Table 6.1. Summary of polymerization results with BH_3·THF and BH_3·NMe_3.

entry	catalyst	solvent	DP[a]	MW_{th}[a] (g/mol)	M_n[b] (g/mol)	M_w[b] (g/mol)	PDI[b]
1	BH_3·THF	Toluene	200	2.85×10^3	2.82×10^3	3.19×10^3	1.13
2	BH_3·THF	Decalin/Toluene	7,142	1.00×10^5	5.76×10^4	1.09×10^5	1.90
3	BH_3·NMe_3	Toluene	70	1.00×10^3	7.43×10^3	9.23×10^3	1.24
4	BH_3·NMe_3	Toluene	177	2.50×10^3	1.26×10^4	1.51×10^4	1.21
5	BH_3·NMe_3	Toluene	356	5.00×10^3	1.77×10^4	2.05×10^4	1.16
6	BH_3·NMe_3	Toluene	714	1.00×10^4	1.95×10^4	2.26×10^4	1.16
7	BH_3·NMe_3	Decalin/Toluene	3,570	5.00×10^4	5.70×10^4	6.64×10^4	1.16
8	BH_3·NMe_3	Decalin/Toluene	5,356	7.50×10^4	7.11×10^4	8.59×10^4	1.21
9	BH_3·NMe_3	Decalin/Toluene	7,142	1.00×10^5	9.56×10^4	1.14×10^5	1.19

a. Theoretical DP and MW were calculated from feed ratio of methylide over BH_3·NMe_3. DP = [methylide]/3[BH_3·NMe_3]. $MW_{th} = M_{CH2} \times DP + M_H + M_{OH}$.
b. Obtained from GPC analysis.

One possible explanation is that for short reaction times, dissociation of the borane complex became the rate limiting step and can compete with the polyhomologation reaction. In a

study of hydroboration reactions with amine–borane adducts, it was found that the increased stability of the complex raises the required reaction temperature to rapidly release the borane.[7] In the case of low molecular weight polymer synthesis, the polymerization is fast (<5 min) during which only part of the borane complex dissociates and participates in propagating polymer chains. The experimental molecular weight will be higher than calculated. In contrast in the case of high molecular weight polymer synthesis, the polymerization can take more than 30 min where nearly all borane complexes will be dissociated early in the reaction and contribute to the final polymer. The slow and incomplete dissociation of the borane complex can be responsible for the lack of control in the low molecular weight polymer synthesis as a result of the strong interactions between BH_3 and the Lewis base.

The air-stability which demands strong Lewis acid–base interactions conflicts with the control of molecular weight which requires fast release of the active borane initiator. To circumvent this problem, we can utilize the different conditions between storage/handling temperatures and the reaction temperature. Therefore, the catalyst complex should be stable at room temperature in air but undergo fast dissociation under the polymerization condition (110 ℃ in toluene). This can be accomplished by tuning the reactivity of borane complexes with different amine/phosphine moieties.

6.2.2. Evaluation of other air-stable amine–/phosphine–boranes

I searched for all the commercially available air-stable amine–/phosphine–boranes **14**–**19** (Scheme 6.4). By screening different initiators and reaction conditions, my aim is to achieve the control of polymer molecular weight as well as polydispersity over a wide molecular weight range.

Scheme 6.4. A list of commercially available amine–/phosphine–borane complexes evaluated for the polyhomologation reaction. BH_3·THF **13** was used as the reference.

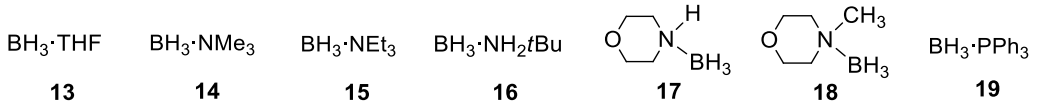

Scheme 6.5. C1 polyhomologation catalyzed by borane complexes **13** to **19**.

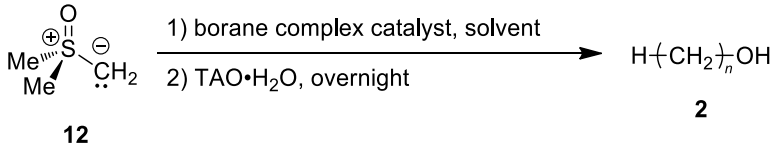

To avoid introduction of oxygen, the initiators need to be prepared separately as a solution for injection into a solution of ylide monomers under nitrogen. In my initial study, I chose toluene to dissolve the catalysts as it is also a good solvent for polymethylene at elevated temperatures. The polyhomologation reactions were carried out with the methylide and the amine–borane initiators from **16** to **18** (Scheme 6.5). For each catalyst, both solutions of ylides in THF and in toluene were carried out for comparison. The results are shown in Table 6.2. Although low PDI was achieved, all reactions gave much higher molecular weights than the values calculated on the basis of stoichiometry of the ylide monomer over the initiator. In preparing the solutions of catalysts, I found that small particles of some borane complexes were still present even after swirling the stock solution for long period of time. Clearly some of the borane complexes in Scheme 6.4 have a low solubility in toluene including *tert*-butylamine–borane **16**, morpholine–borane **17** and 4-methylmorpholine–borane **18**, due to the large differences in polarities between toluene (a nonpolar solvent) and most of the amine–borane complexes which are quite polar. The low solubility of the borane complexes would reduce the actual amount of the initiator involved in the polymerization resulting in the experimental high molecular weight.

Table 6.2. Results of the polyhomologation reaction initiated with THF solutions of borane complexes.

entry	initiator	solvent	temperature (˚C)	yield (%)	MW_{th}[a] (g/mol)	M_n[b] (g/mol)	M_w[b] (g/mol)	PDI[b]
1	**16**	THF	reflux	82	1000	6,378	6,668	1.05
2	**16**	Toluene	90	89	1000	4,452	4,720	1.06
3	**17**	THF	reflux	98	1000	7,189	7,304	1.02
4	**17**	Toluene	90	95	1000	7,331	7,381	1.01
5	**18**	THF	reflux	86	1000	1,901	2,124	1.12
6	**18**	Toluene	90	91	1000	2,470	2,813	1.14

a. Theoretical MW were calculated from feed ratio of methylide over $BH_3{\cdot}NMe_3$. DP = [methylide]/3[$BH_3{\cdot}NMe_3$]. $MW_{th} = M_{CH2} \times DP + M_H + M_{OH}$.
b. Obtained from GPC analysis.

Table 6.3. Results of the polyhomologation reaction initiated with THF solutions of borane complexes.

entry	initiator	solvent	temperature (˚C)	yield (%)	MW_{th}[a] (g/mol)	M_n[b] (g/mol)	M_w[b] (g/mol)	PDI[b]
1	**13**	THF	reflux	95	1000	2113	2417	1.14
2	**13**	Tol	90	83	1000	1207	1231	1.02
3	**14**	THF	reflux	70	1000	4691	10858	2.32
4	**14**	Tol	110	90	1000	8235	10288	1.25
5	**15**	THF	reflux	92	1000	1862	3443	1.85
6	**15**	Tol	110	91	1000	3698	4187	1.13
7	**16**	THF	reflux	90	1000	7390	7485	1.01
8	**16**	Tol	90	94	1000	5004	5142	1.03
9	**17**	THF	reflux	39	1000	7397	7489	1.01
10	**17**	Tol	90	92	1000	2703	3207	1.19
11	**18**	THF	reflux	85	1000	1250	1339	1.07
12	**18**	Tol	90	70	1000	2427	2889	1.19
13	**19**	THF	reflux	80	1000	2695	3621	1.34
14	**19**	Tol	110	100	1000	3629	4022	1.11

a. Theoretical MW were calculated from feed ratio of methylide over $BH_3{\cdot}NMe_3$. DP = [methylide]/3[$BH_3{\cdot}NMe_3$]. $MW_{th} = M_{CH2} \times DP + M_H + M_{OH}$.
b. Obtained from GPC analysis.

To eliminate influences by the solubility of the initiators, THF was used instead for preparation of the initiator solution (Table 6.3). The polyhomologation reactions were carried out with the methylide and the amine–/phosphine–borane initiators from **13** to **19** (Scheme 6.5). The reactions were monitored by titration of an aliquot to determine the consumption of all ylide monomers. To simplify comparison, all polymerizations targeted the same low molecular weight

(1000 g/mol). Following the polymerization, oxidation with trimethylamine *N*-oxide gave the desired α-hydroxypolymethylene. Oxidation with hydrogen peroxide was not employed to avoid the introduction of radicals which could result in the PDI erosion.

For the control run, polymethylene synthesized from BH_3·THF **13** in toluene yielded a low PDI and a predicted molecular weight (Table 6.3, entry 2). However, the same polymerization carried out in THF resulted in a higher PDI and molecular weight (Table 6.3, entry 1). In THF, the borane adduct is in an environment of Lewis bases. The abundant THF competed with ylide which would cause a slow rate of chain propagation. On the other hand, polymerization performed in THF has a lower temperature than those in toluene due to the low boiling point of THF. The lower reaction temperature also decreases the decomplexation rate of the borane complexes. In summary, both the Lewis basic environment and low reaction temperatures for polymerizations carried out in THF would contribute to the difficulties to instantaneously produce the active borane catalyst which eventually accounts for the higher molecular weight and PDI than expected. For borane complexes **14**–**19**, the differences between THF and toluene solvent are not always the same as the case of BH_3·THF (Table 6.3, entry 3–14). To fully rationalize these results, another factor needs to be taken into consideration with the solubility of amine–borane complexes in toluene.

Polymethylenes synthesized from catalysts **15**, **18** and **19** have molecular weights closer to the theoretical values than those from catalysts **14**, **16** and **17** (Table 6.3, entry 3–14). This is because the corresponding Lewis bases NEt_3, 4-methylmorpholine and PPh_3 are sterically bulkier than NMe_3, *t*-$BuNH_2$ and morpholine. The more sterically congested Lewis base leads to an easier decomplexation of the adduct leading to a lower molecular weight. Surprisingly, the polymerization carried out in THF with the catalyst BH_3·4-methylmorpholine **18** has almost

identical results compared to the control run (Table 6.3, entry 2 and 11). Compared to BH_3·morpholine **17**, the extra methyl group on BH_3·4-methylmorpholine **18** provided sufficient steric hindrance for a faster release of BH_3 which gave a lower molecular weight (Table 6.3, entry 9–12).

With these results, I continued to evaluate the catalyst BH_3·4-methylmorpholine **18** for the polyhomologation reaction for synthesis of polymethylene with a wide molecular weight range (Table 6.4). In this case, the complex as well as the ylide monomer was prepared in THF except for polymers with molecular weight higher than 1000 g/mol in which case decalin/toluene was used instead. All polymers were obtained in high yields with predicted molecular weights and low PDIs. For the highest molecular weight (300 kDa) in this set of tests, the polymer PDI starts to deteriorate (Table 6.4, entry 6).

Table 6.4. Evaluation of BH_3·4-methylmorpholine **18** as the catalyst for the polyhomologation reaction in a wide molecular weight range.

entry	DP[a]	MW_{th}[a] (g/mol)	M_n[b] (g/mol)	M_w[b] (g/mol)	PDI[b]
1	27	396	582	617	1.06
2	49	704	748	799	1.07
3	283	3.98×10^3	3.75×10^3	3.86×10^3	1.03
4	3,570	5.00×10^4	4.09×10^4	4.71×10^4	1.15
5	7,142	1.00×10^5	8.16×10^4	1.02×10^5	1.25
6	21,427	3.00×10^5	1.83×10^5	2.92×10^5	1.60

a. Theoretical DP and MW were calculated from feed ratio of methylide over BH_3·NMe_3. DP = [methylide]/3[BH_3·NMe_3]. $MW_{th} = M_{CH2} \times DP + M_H + M_{OH}$.
b. Obtained from GPC analysis.

It should be noted that all catalysts **14**–**19** evaluated in this study are air-stable and are relatively inexpensive from commercial sources. By screening of the catalysts and solvents, BH_3·4-methylmorpholine **18** was found to be effective as an air-stable catalyst for the polyhomologation reaction in the molecular weight rage of 400–300,000 with control of molecular weight and polydispersity. For a better control on the molecular weight in a wider

molecular weight range, other air-stable borane complexes with tertiary amines need to be designed and synthesized.

6.3. Conclusion

Air-stable initiators were developed for the polyhomologation reaction to solve the high PDI problem arising from small amounts of oxidized impurities that are present with conventional air-sensitive organoborane initiators (i.e., BH_3·THF, BH_3·SMe_2). The use of a trimethylamine−borane initiator/catalyst results in the synthesis of high molecular weight (>50 kDa) polymethylene with low PDI. However, the increased stability of BH_3·NMe_3 over BH_3·SMe_2 also raises the required temperature to rapidly release the active initiator BH_3. This amine−borane complex does not provide a level of control for low MW polymer synthesis.

Studies using different amine– and phosphine–borane complexes were carried out to identify borane initiators for control of the low molecular weight polymers. BH_3·4-methylmorpholine was found to be effective as an air-stable catalyst for the polyhomologation reaction in the molecular weight rage of 400–300,000 with control of molecular weight with low polydispersity. The bulky Lewis base 4-methylmorpholine facilitates the decomplexation of the borane complex while still maintaining sufficient air-stability. The fast initiation benefited from fast dissociation resulting in a living polymerization. For a better control of molecular weight with low PDI, additional borane complexes need to be designed and synthesized to balance between the air-stability and fast decomplexation at elevated temperatures. To further unravel the competing reactions between the decomplexation and the polymerization (complexation with ylide followed by 1,2-migration), kinetic studies as well as solubility tests on all catalysts are required.

6.4. References

(1) Luo, J.; Shea, K. J. *Acc. Chem. Res*. **2010**, *43*, 1420–1433.

(2) Luo, J.; Zhao, R.; Shea, K. J. *Macromolecules* **2014**, *47*, 5484−5491.

(3) Busch, B. B.; Paz, M. M.; Shea, K. J.; Staiger, C. L.; Stoddard, J. M.; Walker, J. R.; Zhou, X-Z.; Zhu, H. *J. Am. Chem. Soc*. **2002**, *124*, 3636–3646.

(4) Shea, K. J.; Zhu, H. D.; Walker, J.; Paz, M.; Greaves, J. *J. Am. Chem. Soc*. **1997**, *119*, 9049–9050.

(5) Shea, K. J.; Busch, B. B.; Paz, M. M. *Angew. Chem. Int. Ed*. **1998**, *37*, 1391–1393.

(6) Busch, B. B. Ph.D. Thesis, University of California, Irvine, 1999.

(7) Wagner, C. E.; Shea, K. J. *Org. Lett*. **2001**, *3*, 3063–3066.

(8) Shea, K. J.; Staiger, C. L.; Lee, S. Y. *Macromolecules* **1999,** *32*, 3157–3158.

(9) Lane, C. F. *Aldrichim. Acta* **1973**, *6*, 51.

(10) Roesky, H. W.; Atwood, D. A. *Group 13 Chemistry I: Fundamental New Developments*; Springer: New York, 2002.

(11) Flores-Segura, H.; Torres, L. *Struct. Chem*. **1997**, *8*, 227.

6.5. Experimental

General considerations. Appendix A. The solutions of amine–/phosphine–boranes were degassed before use in the polyhomologation reaction.

Solvent change for methylide 12 from THF to toluene. A known concentration of methylide **12** in THF (0.635 M, 72 mL) was injected to a Schlenk round-bottom flask that was assembled for distillation and purged under N_2 beforehand. THF was removed in batches of 15–20 mL via vacuum distillation at 40 ℃. Each time toluene was refilled to the Schlenk flask to maintain a low concentration of the ylide. Distillation was halted after ~4 cycles of THF removal with a total of 52 mL toluene added. The actual volume of ylide solution was measured to be 53 mL during the filtration process over celite under N_2. The ylide after distillation was titrated as 0.86 M with 99% of recovery.

Representative synthesis of polymethylene 2 using amine–/phosphine–borane complexes as the initiators (Table 6.1, entry 8). To a flame-dried and N_2 purged flask was added dimethylsulfoxonium methylide (0.715 M, 14.0 mL, 10.0 mmol) and dry decalin (degassed, 28 mL). The initiator $BH_3{\cdot}NMe_3$ (2.5 mg) was dissolved in toluene (9.0 mL, 3.8 μmol/mL) and degassed before use. The ylide solution was stirred in a pre-heated oil bath at 110 ℃ for 2 minutes followed by a quick injection of the initiator solution (0.164 mL, 0.624 μmol). The reaction was stirred vigorously at 110 ℃ for another 30–40 minutes (monitored by titration of an aliquot). Then trimethylamine *N*-oxide dihydrate (30 mg/mL dissolved and degassed in DMSO/H_2O = 50/50 v/v, 0.1 mL, 27 μmol) was injected and the reaction was left overnight at 110 ℃. After cooling down to room temperature, the polymer product was precipitated with 200 mL MeOH and stirred for 5 minutes. After filtration, the resulting white solid was sequentially

washed with H_2O (3×15 mL), DCM (1×15 mL) and methanol (3×15 mL). The product was dried in a vacuum oven at 70 ℃ for 24 h to give a white powder (136 mg, 97%). GPC analysis: M_n = 71,116, M_w = 85,925, PDI = 1.21.

Appendix A

Instrumentation. ^{1}H and ^{13}C spectra of all samples were acquired on a Bruker GN500 or AVANCE600 spectrometer. NMR spectra of small organic molecules were recorded at room temperature. For ^{1}H NMR analysis of polymers, all samples (5–10 mg) were preheated in toluene-d_8 or 1,1,2,2-tetrachloroethane-d_2 ($C_2D_2Cl_4$) at 90 ℃ for at least 0.5 h to achieve a homogenous solution before at 363 K. The ^{13}C NMR samples were solutions of polymer (70–100 mg) with a relaxation agent $Cr(acac)_3$ (7–10 mg) in 1,1,2,2-tetrachloroethane-d_2 ($C_2D_2Cl_4$, 0.6 mL). ^{13}C NMR experiments were recorded with inverse-gated decoupling. The interpulse relaxation time (T_1) was 6 s, and the number of scans was 5000–6000 to achieve adequate signal to noise ratio. The chemical shifts were internally referenced to the residual solvent signal.

Infrared Spectroscopy (IR). IR spectra were recorded on Jasco FT/IR-4700 ATR-PRO ONE with wavenumber ranging from 400 cm^{-1} to 4000 cm^{-1}. IR spectra were obtained with background subtraction and CO_2 and H_2O reduction.

Gas Chromatography–Mass Spectrometry (GC-MS). GC-MS was taken using two Finnigan Trace-MS instruments. The one with electron ionization (EI) was mainly used to determine the percentage of each components in the mixture; while the other one with chemical ionization (CI) was mainly used for relative pure samples to obtain accurate mass with high resolution.

Gel Permeation Chromatography (GPC). GPC analysis was performed with Agilent PL-GPC 220 at 110 ℃ using 1,2,4-trichlorobenzene as eluent at a flow rate of 1.0 mL/min. The GPC instrument was equipped with 3 sets of MesoPore 3 μm 300×7.5 mm columns calibrated with seven narrow PE standards (M_n = 326–5300) using the conventional method. The samples for chromatography were prepared as 1.0–2.0 mg/mL solutions in 1,2,4-trichlorobenzene.

Differential Scanning Calorimetry (DSC). DSC was performed on a TA instruments DSC Q2000 differential scanning calorimeter at a scan rate of 10 ℃/min with a N_2 flow rate of 50 mL/min. The random copolymers were cooled to −80 °C from room temperature and maintained for 10 min. They were then heated to 180 ℃ and kept for 10 min to erase the thermal history of the samples. Samples were further cooled to −80 °C, and kept for 10 min before heating back to 180 ℃. The gradient copolymers were measured in the same way except for heating to 140 ℃ rather than 180 ℃. DSC traces of random copolymers were obtained on 1.2 to 11.3 mg and gradient copolymers on 1.2 to 3.7 mg. Crystallinity % was reported from the second heating cycle and calculated based on a melt enthalpy of 281 J/g for completely crystalline polyethylene.[1]

Tensile Test. The bulk static tensile properties of the polyesters were measured using an Instron 3365 with a 500 N load cell with a pulling rate of 5 mm/min. Rectangular Samples were prepared by melting and pressing the resin into Teflon molds (20 mm × 10 mm × 2 mm) at 130 ℃. The samples were pulled at ambient temperature until break. The polyesters were mixed with 1 wt% of (±)-α-tocopherol to avoid oxidative degradation. Young's modulus, tensile strength and elongation at break were obtained by averaging four to five parallel testing specimens.

[1] Sperling, L. H. *Introduction to Physical Polymer Science*, 4th ed.; Wiley: Hoboken, NJ, **2005**.

Appendix B

Computational Calculations. All DFT and *ab initio* calculations were performed on Greenplanet with Gaussian 09, Turbomole 7.1, Molpro 2012 and Orca 3.0.3. A complete conformational search was first performed using Maestro on **cat-H·ylide**, **cat-Me·ylide** and **cat-F·ylide** structures of both ground and transition states. For all cases, only the global minimum was reported in the text and in the appendix. For other 9-borafluorene derivatives including ***p*-NMe$_2$**, ***p*-Me, *p*-Cl, *p*-NO$_2$, *o*-*t*Bu, *o*-CF$_3$** and ***o*,*p*-di-CF$_3$**, geometry optimizations were started by direct replacement of the hydrogen atoms with the corresponding substituent in the already optimized **cat-H·ylide** ground and transition states geometries. In these cases, the starting geometries for transition states were generated by scanning the breaking CH_2–S bond using the Orca program.

All ground (GS) and transition state (TS) geometries were first optimized in their gas phase at TPSS-D3(BJ)/def2-SVP level and then at TPSS-D3(BJ)/def2-TZVP level using the Turbomole program (Chapter 5.2.1.1). Solvent THF was also taken into consideration with a continuum solvation model as Conductor-like Screening Model (COSMO). The energy threshold, gradient threshold of Cartesian coordinates and the integration grid size was set to 10^{-7}, 10^{-4} and m4, respectively. The results were confirmed by frequency analysis with zero and one imaginary frequency for GS and TS, respectively.

Potential energy surface (PES) scan along two dihedral angles was accomplished with B3LYP-D3(BJ)/def2-TZVP using Turbomole (Chapter 5.2.1.2). Resolution of identity was used to speed up the process. The corresponding def2-TZVP was used as the Coulomb fitting

auxiliary basis set. The energy threshold of 10^{-6} and gradient threshold of Cartesian coordinates of 10^{-3} were set in PES scan.

Evaluation of DFT single-point calculations on the model reaction (Chapter 5.2.1.3) were performed with the Gaussian program (except for PW6B95 performed using Turbomole) based on optimized geometries at level of B3LYP-D3BJ/def2-TZVP. The corresponding dispersion corrections (D3 and D3BJ) were obtained with the external dftd3 program. Various DFT functionals were examined including pure GGA functionals (BP86, B97D, OLYP, BLYP, MPWLYP), pure meta-GGA functionals (TPSS, M06-L), hybrid GGA functionals (PBE0, B1B95, B3PW91, B3LYP, O3LYP), hybrid meta-GGA functionals (M06, M06-2X, TPSSh, PW6B95, BMK, MPWB1K, MPW1B95) and range-separated functionals (LC-ωPBE, CAM-B3LYP, ωB97XD). The ultrafine integration grid was used in all calculations.

Calculations with double-hybrid density functional B2GPPLYP and *ab initio* methods including Møller-Plesset perturbation (MP2) and coupled cluster (CC) were performed with the Molpro program package. In the B2GPPLYP calculations, augmented basis sets A'VnZ were used with aug-cc-pVnZ for B, C, O; cc-pVnZ for H and aug-cc-pV(n+d)Z for S. Calculations with the composite method CBS-QB3 were completed using the Gaussian program.

The explicitly correlated coupled cluster (CC) method CCSD(T)-F12 was chosen to obtain accurate energies as the references. I employed the CCSD(T)-F12b method for single-point calculations with the diagonal fixed amplitude 3C(FIX) Ansatz. cc-pVDZ-F12 (VDZ-F12) was used as the basis set with the standard auxiliary basis sets as implemented in Molpro. The germinal Slater exponent $\beta = 0.9$ was chosen for VDZ-F12. For the density-fitting (DF) of the Fock and exchange matrices, the auxiliary basis set cc-pVDZ/JKfit was used while aug-cc-pVDZ/MP2fit auxiliary sets were employed for the two-electron integrals (MP2fit). cc-pVDZ-

F12/OptRI auxiliary basis set was used as the RI basis for the many-electron integrals within the complementary auxiliary basis set (CABS) approach.

For both MP2 and B2GPPLYP calculations, complete basis set (CBS) extrapolation was also performed. The MP2-F12/(D,T) results were obtained with the reference energies at the TZ level without extrapolation while the correlation energies were extrapolated according to the method proposed by Peterson and coworkers.[2] The B2GPPLYP/(T,Q) results were obtained with the reference energies from A'QZ basis set while the correlation energies calculated based on the formula $E_{corr}(T,Q) = [E_{corr}(T)*3^3 - E_{corr}(Q)*4^3]/(3^3-4^3)$.

Summary of PES data (Chapter 5.2.1.2)

Table B.1. Summary of PES grid points from Figure 5.9a (cat-H·ylide).

Tors (S-C-B-Me)	Tors (O-S-C-B)	Energy	Tors (S-C-B-Me)	Tors (O-S-C-B)	Energy
0	-180	-1119.24195	90	15	-1119.23594
0	-165	-1119.24074	90	30	-1119.23818
0	-150	-1119.23742	90	45	-1119.24088
0	-135	-1119.23363	90	60	-1119.2427
0	-120	-1119.23199	90	75	-1119.24236
0	-105	-1119.23325	90	90	-1119.23927
0	-90	-1119.23608	90	105	-1119.23672
0	-75	-1119.23944	90	120	-1119.23554
0	-60	-1119.24134	90	135	-1119.23601
0	-45	-1119.24067	90	150	-1119.23838
0	-30	-1119.23693	90	165	-1119.24214
0	-15	-1119.23373	90	180	-1119.24603
0	0	-1119.23221	105	-180	-1119.24535
0	15	-1119.23373	105	-165	-1119.24238
0	30	-1119.23692	105	-150	-1119.2392
0	45	-1119.24067	105	-135	-1119.23475
0	60	-1119.24134	105	-120	-1119.23269
0	75	-1119.23945	105	-105	-1119.23349
0	90	-1119.2361	105	-90	-1119.23761
0	105	-1119.23325	105	-75	-1119.24222
0	120	-1119.23198	105	-60	-1119.24529
0	135	-1119.2336	105	-45	-1119.24458
0	150	-1119.2374	105	-30	-1119.23965
0	165	-1119.24069	105	-15	-1119.23438
0	180	-1119.24195	105	0	-1119.23233
15	-180	-1119.24325	105	15	-1119.23295

[2] Hill, J. G.; Peterson, K. A.; Knizia, G.; Werner, H.-J. *J. Chem. Phys.* **2009**, *131*, 194105.

15	-165	-1119.24148	105	30	-1119.23612
15	-150	-1119.23787	105	45	-1119.23959
15	-135	-1119.2348	105	60	-1119.24078
15	-120	-1119.23386	105	75	-1119.23927
15	-105	-1119.23518	105	90	-1119.2361
15	-90	-1119.23796	105	105	-1119.23369
15	-75	-1119.24118	105	120	-1119.23227
15	-60	-1119.24253	105	135	-1119.23388
15	-45	-1119.24099	105	150	-1119.23781
15	-30	-1119.2374	105	165	-1119.2429
15	-15	-1119.23448	105	180	-1119.24535
15	0	-1119.23351	120	-180	-1119.24514
15	15	-1119.2351	120	-165	-1119.24252
15	30	-1119.23853	120	-150	-1119.23796
15	45	-1119.2417	120	-135	-1119.23447
15	60	-1119.24196	120	-120	-1119.23346
15	75	-1119.23976	120	-105	-1119.23578
15	90	-1119.23603	120	-90	-1119.24037
15	105	-1119.2333	120	-75	-1119.24448
15	120	-1119.23279	120	-60	-1119.24524
15	135	-1119.23492	120	-45	-1119.24233
15	150	-1119.23875	120	-30	-1119.2369
15	165	-1119.24162	120	-15	-1119.23263
15	180	-1119.24325	120	0	-1119.23118
30	-180	-1119.24501	120	15	-1119.23267
30	-165	-1119.24244	120	30	-1119.23666
30	-150	-1119.23994	120	45	-1119.23975
30	-135	-1119.23807	120	60	-1119.2399
30	-120	-1119.2372	120	75	-1119.23815
30	-105	-1119.23804	120	90	-1119.23497
30	-90	-1119.24032	120	105	-1119.23229
30	-75	-1119.24334	120	120	-1119.23229
30	-60	-1119.24364	120	135	-1119.23519
30	-45	-1119.24186	120	150	-1119.24049
30	-30	-1119.23969	120	165	-1119.24453
30	-15	-1119.23716	120	180	-1119.24514
30	0	-1119.23652	135	-180	-1119.2469
30	15	-1119.23843	135	-165	-1119.24397
30	30	-1119.24181	135	-150	-1119.24039
30	45	-1119.24411	135	-135	-1119.23805
30	60	-1119.2435	135	-120	-1119.23782
30	75	-1119.24105	135	-105	-1119.24077
30	90	-1119.23751	135	-90	-1119.24429
30	105	-1119.2352	135	-75	-1119.24675
30	120	-1119.2355	135	-60	-1119.24601
30	135	-1119.2377	135	-45	-1119.24217
30	150	-1119.24105	135	-30	-1119.23748
30	165	-1119.24466	135	-15	-1119.23382
30	180	-1119.24501	135	0	-1119.23321
45	-180	-1119.24533	135	15	-1119.2355
45	-165	-1119.24426	135	30	-1119.23932
45	-150	-1119.24315	135	45	-1119.24158
45	-135	-1119.2416	135	60	-1119.24116
45	-120	-1119.23984	135	75	-1119.23924
45	-105	-1119.2401	135	90	-1119.23622
45	-90	-1119.24237	135	105	-1119.23462

45	-75	-1119.24402	135	120	-1119.23562
45	-60	-1119.24379	135	135	-1119.23977
45	-45	-1119.24355	135	150	-1119.24471
45	-30	-1119.24233	135	165	-1119.24748
45	-15	-1119.241	135	180	-1119.2469
45	0	-1119.2403	150	-180	-1119.24992
45	15	-1119.24183	150	-165	-1119.24789
45	30	-1119.24427	150	-150	-1119.2452
45	45	-1119.2454	150	-135	-1119.24323
45	60	-1119.24457	150	-120	-1119.24351
45	75	-1119.24248	150	-105	-1119.24543
45	90	-1119.24021	150	-90	-1119.24763
45	105	-1119.23858	150	-75	-1119.24849
45	120	-1119.23845	150	-60	-1119.24746
45	135	-1119.23997	150	-45	-1119.24417
45	150	-1119.24372	150	-30	-1119.24034
45	165	-1119.24593	150	-15	-1119.23774
45	180	-1119.24533	150	0	-1119.23735
60	-180	-1119.24519	150	15	-1119.23994
60	-165	-1119.24624	150	30	-1119.2428
60	-150	-1119.24579	150	45	-1119.24449
60	-135	-1119.24285	150	60	-1119.24387
60	-120	-1119.24009	150	75	-1119.24208
60	-105	-1119.24049	150	90	-1119.24003
60	-90	-1119.24176	150	105	-1119.23943
60	-75	-1119.24261	150	120	-1119.24127
60	-60	-1119.24389	150	135	-1119.24519
60	-45	-1119.24532	150	150	-1119.24898
60	-30	-1119.245	150	165	-1119.25081
60	-15	-1119.24369	150	180	-1119.24992
60	0	-1119.24218	165	-180	-1119.25316
60	15	-1119.24251	165	-165	-1119.2518
60	30	-1119.24388	165	-150	-1119.24985
60	45	-1119.24508	165	-135	-1119.24829
60	60	-1119.24473	165	-120	-1119.24757
60	75	-1119.24372	165	-105	-1119.24803
60	90	-1119.24206	165	-90	-1119.24918
60	105	-1119.24064	165	-75	-1119.24929
60	120	-1119.23957	165	-60	-1119.24843
60	135	-1119.24137	165	-45	-1119.24667
60	150	-1119.24389	165	-30	-1119.24394
60	165	-1119.24495	165	-15	-1119.24177
60	180	-1119.24519	165	0	-1119.24117
75	-180	-1119.24568	165	15	-1119.2431
75	-165	-1119.24755	165	30	-1119.24574
75	-150	-1119.2457	165	45	-1119.24695
75	-135	-1119.24112	165	60	-1119.24673
75	-120	-1119.2385	165	75	-1119.24589
75	-105	-1119.23813	165	90	-1119.24438
75	-90	-1119.23892	165	105	-1119.24463
75	-75	-1119.24131	165	120	-1119.24623
75	-60	-1119.24429	165	135	-1119.24911
75	-45	-1119.2467	165	150	-1119.25234
75	-30	-1119.24613	165	165	-1119.25364
75	-15	-1119.24295	165	180	-1119.25316
75	0	-1119.24	180	-180	-1119.25415

75	15	-1119.23973	180	-165	-1119.25383
75	30	-1119.2414	180	-150	-1119.25269
75	45	-1119.24288	180	-135	-1119.25045
75	60	-1119.24384	180	-120	-1119.24847
75	75	-1119.24414	180	-105	-1119.24789
75	90	-1119.24214	180	-90	-1119.24789
75	105	-1119.23956	180	-75	-1119.24837
75	120	-1119.23869	180	-60	-1119.24859
75	135	-1119.23964	180	-45	-1119.2477
75	150	-1119.24115	180	-30	-1119.24609
75	165	-1119.24286	180	-15	-1119.24396
75	180	-1119.24568	180	0	-1119.24273
90	-180	-1119.24603	180	15	-1119.24395
90	-165	-1119.24617	180	30	-1119.2461
90	-150	-1119.24376	180	45	-1119.2477
90	-135	-1119.23784	180	60	-1119.24859
90	-120	-1119.23498	180	75	-1119.24835
90	-105	-1119.23466	180	90	-1119.24789
90	-90	-1119.23723	180	105	-1119.24788
90	-75	-1119.24086	180	120	-1119.24848
90	-60	-1119.24485	180	135	-1119.25045
90	-45	-1119.24652	180	150	-1119.25266
90	-30	-1119.24382	180	165	-1119.25381
90	-15	-1119.23883	180	180	-1119.25415
90	0	-1119.23569			

Table B.2. Summary of PES grid points from Figure 5.9b (cat-Me·ylide).

Tors (S-C-B-Me)	Tors (O-S-C-B)	Energy	Tors (S-C-B-Me)	Tors (O-S-C-B)	Energy
0	-180	-1197.85405	90	15	-1197.84611
0	-165	-1197.85375	90	30	-1197.84922
0	-150	-1197.85149	90	45	-1197.85225
0	-135	-1197.84907	90	60	-1197.85244
0	-120	-1197.84744	90	75	-1197.84874
0	-105	-1197.8491	90	90	-1197.84565
0	-90	-1197.85149	90	105	-1197.84429
0	-75	-1197.85358	90	120	-1197.84371
0	-60	-1197.85436	90	135	-1197.84518
0	-45	-1197.85347	90	150	-1197.84912
0	-30	-1197.85115	90	165	-1197.85273
0	-15	-1197.84893	90	180	-1197.8551
0	0	-1197.84803	105	-180	-1197.85377
0	15	-1197.84891	105	-165	-1197.85282
0	30	-1197.85114	105	-150	-1197.8493
0	45	-1197.85346	105	-135	-1197.84556
0	60	-1197.85431	105	-120	-1197.84438
0	75	-1197.85359	105	-105	-1197.84683
0	90	-1197.85152	105	-90	-1197.85154
0	105	-1197.84912	105	-75	-1197.85536
0	120	-1197.84745	105	-60	-1197.85659
0	135	-1197.84908	105	-45	-1197.85481
0	150	-1197.8515	105	-30	-1197.85014
0	165	-1197.85359	105	-15	-1197.84541
0	180	-1197.85405	105	0	-1197.84408

14	90	-1197.85114	105	15	-1197.8456
15	-180	-1197.85361	105	30	-1197.84881
15	-165	-1197.85218	105	45	-1197.84773
15	-150	-1197.84989	105	60	-1197.84833
15	-135	-1197.84825	105	75	-1197.84712
15	-120	-1197.84806	105	90	-1197.84513
15	-105	-1197.84919	105	105	-1197.84327
15	-90	-1197.85024	105	120	-1197.84289
15	-75	-1197.85174	105	135	-1197.84595
15	-60	-1197.85237	105	150	-1197.85004
15	-45	-1197.85121	105	165	-1197.85294
15	-30	-1197.84931	105	180	-1197.85377
15	-15	-1197.84815	120	-180	-1197.85564
15	0	-1197.84861	120	-165	-1197.85398
15	15	-1197.85025	120	-150	-1197.85011
15	30	-1197.85274	120	-135	-1197.84718
15	45	-1197.85472	120	-120	-1197.84728
15	60	-1197.85495	120	-105	-1197.85008
15	75	-1197.8536	120	-90	-1197.85431
15	105	-1197.84899	120	-75	-1197.85713
15	120	-1197.84886	120	-60	-1197.8572
15	135	-1197.85016	120	-45	-1197.85452
15	150	-1197.85167	120	-30	-1197.84947
15	165	-1197.85297	120	-15	-1197.84552
15	180	-1197.85361	120	0	-1197.84466
30	-180	-1197.85262	120	15	-1197.8464
30	-165	-1197.85153	120	30	-1197.84803
30	-150	-1197.85055	120	45	-1197.84863
30	-135	-1197.8494	120	60	-1197.84928
30	-120	-1197.84858	120	75	-1197.84858
30	-105	-1197.84717	120	90	-1197.84592
30	-90	-1197.84787	120	105	-1197.84404
30	-75	-1197.85035	120	120	-1197.84525
30	-60	-1197.85108	120	135	-1197.84846
30	-45	-1197.85074	120	150	-1197.85168
30	-30	-1197.85061	120	165	-1197.85453
30	-15	-1197.85004	120	180	-1197.85564
30	0	-1197.84933	135	-180	-1197.85937
30	15	-1197.85054	135	-165	-1197.85684
30	30	-1197.85218	135	-150	-1197.85328
30	45	-1197.85434	135	-135	-1197.85144
30	60	-1197.85447	135	-120	-1197.85202
30	75	-1197.85324	135	-105	-1197.85496
30	90	-1197.85129	135	-90	-1197.85769
30	105	-1197.84997	135	-75	-1197.8596
30	120	-1197.8493	135	-60	-1197.85885
30	135	-1197.84897	135	-45	-1197.8555
30	150	-1197.84961	135	-30	-1197.85105
30	165	-1197.85163	135	-15	-1197.84763
30	180	-1197.85262	135	0	-1197.84753
45	-180	-1197.85294	135	15	-1197.84779
45	-165	-1197.85366	135	30	-1197.84969
45	-150	-1197.85282	135	45	-1197.8524
45	-135	-1197.85045	135	60	-1197.85284
45	-120	-1197.84675	135	75	-1197.85122
45	-105	-1197.8463	135	90	-1197.84872

45	-90	-1197.84861	135	105	-1197.84789
45	-75	-1197.85084	135	120	-1197.8494
45	-60	-1197.85187	135	135	-1197.8522
45	-45	-1197.85335	135	150	-1197.85571
45	-30	-1197.85363	135	165	-1197.85858
45	-15	-1197.85178	135	180	-1197.85937
45	0	-1197.84961	150	-180	-1197.8637
45	15	-1197.84986	150	-165	-1197.86106
45	30	-1197.85185	150	-150	-1197.85878
45	45	-1197.85417	150	-135	-1197.85743
45	60	-1197.85433	150	-120	-1197.85794
45	75	-1197.85392	150	-105	-1197.85965
45	90	-1197.85263	150	-90	-1197.86148
45	105	-1197.85058	150	-75	-1197.86189
45	120	-1197.84746	150	-60	-1197.86091
45	135	-1197.84677	150	-45	-1197.85801
45	150	-1197.84993	150	-30	-1197.85452
45	165	-1197.85241	150	-15	-1197.85185
45	180	-1197.85294	150	0	-1197.8509
60	-180	-1197.85463	150	15	-1197.85227
60	-165	-1197.85544	150	30	-1197.85471
60	-150	-1197.85406	150	45	-1197.85693
60	-135	-1197.84867	150	60	-1197.8568
60	-120	-1197.84636	150	75	-1197.85526
60	-105	-1197.84702	150	90	-1197.85375
60	-90	-1197.84874	150	105	-1197.85367
60	-75	-1197.85131	150	120	-1197.85513
60	-60	-1197.85445	150	135	-1197.85792
60	-45	-1197.85676	150	150	-1197.86101
60	-30	-1197.8554	150	165	-1197.86402
60	-15	-1197.85138	150	180	-1197.8637
60	0	-1197.84853	165	-180	-1197.86749
60	15	-1197.84886	165	-165	-1197.86596
60	30	-1197.85145	165	-150	-1197.86404
60	45	-1197.85398	165	-135	-1197.86277
60	60	-1197.85473	165	-120	-1197.86227
60	75	-1197.85484	165	-105	-1197.86284
60	90	-1197.85243	165	-90	-1197.86388
60	105	-1197.84773	165	-75	-1197.86365
60	120	-1197.84556	165	-60	-1197.86307
60	135	-1197.84749	165	-45	-1197.86086
60	150	-1197.85035	165	-30	-1197.85812
60	165	-1197.85241	165	-15	-1197.85567
60	180	-1197.85463	165	0	-1197.85443
75	-180	-1197.85538	165	15	-1197.85618
75	-165	-1197.85569	165	30	-1197.85906
75	-150	-1197.85178	165	45	-1197.86089
75	-135	-1197.84792	165	60	-1197.86044
75	-120	-1197.84619	165	75	-1197.85987
75	-105	-1197.84603	165	90	-1197.85883
75	-90	-1197.84841	165	105	-1197.85896
75	-75	-1197.85249	165	120	-1197.86023
75	-60	-1197.85676	165	135	-1197.86273
75	-45	-1197.85749	165	150	-1197.86608
75	-30	-1197.85419	165	165	-1197.86762
75	-15	-1197.8496	165	180	-1197.86749

75	0	-1197.84681	180	-180	-1197.86855
75	15	-1197.84737	180	-165	-1197.86792
75	30	-1197.85032	180	-150	-1197.86683
75	45	-1197.85325	180	-135	-1197.86461
75	60	-1197.85424	180	-120	-1197.86275
75	75	-1197.85336	180	-105	-1197.86275
75	90	-1197.84824	180	-90	-1197.8629
75	105	-1197.84525	180	-75	-1197.86313
75	120	-1197.84509	180	-60	-1197.86303
75	135	-1197.84666	180	-45	-1197.86207
75	150	-1197.84915	180	-30	-1197.85992
75	165	-1197.85267	180	-15	-1197.8573
75	180	-1197.85538	180	0	-1197.856
90	-180	-1197.8551	180	15	-1197.85728
90	-165	-1197.85328	180	30	-1197.86005
90	-150	-1197.8502	180	45	-1197.86208
90	-135	-1197.84659	180	60	-1197.86303
90	-120	-1197.84439	180	75	-1197.86315
90	-105	-1197.84528	180	90	-1197.8629
90	-90	-1197.84922	180	105	-1197.86275
90	-75	-1197.85432	180	120	-1197.86275
90	-60	-1197.85679	180	135	-1197.8646
90	-45	-1197.856	180	150	-1197.86686
90	-30	-1197.85209	180	165	-1197.86801
90	-15	-1197.84729	180	180	-1197.86855
90	0	-1197.84493			

Table B.3. Summary of PES grid points from Figure 5.9c (cat-F·ylide).

Tors (S-C-B-Me)	Tors (O-S-C-B)	Energy	Tors (S-C-B-Me)	Tors (O-S-C-B)	Energy
0	-180	-1913.21991	90	15	-1913.21119
0	-165	-1913.21867	90	30	-1913.2151
0	-150	-1913.21564	90	45	-1913.21931
0	-135	-1913.21193	90	60	-1913.22064
0	-120	-1913.21002	90	75	-1913.21782
0	-105	-1913.21115	90	90	-1913.21315
0	-90	-1913.21389	90	105	-1913.20998
0	-75	-1913.21694	90	120	-1913.2092
0	-60	-1913.21856	90	135	-1913.21048
0	-45	-1913.21783	90	150	-1913.21366
0	-30	-1913.21509	90	165	-1913.21786
0	-15	-1913.21235	90	180	-1913.21981
0	0	-1913.21111	105	-180	-1913.2176
0	15	-1913.21237	105	-165	-1913.21467
0	30	-1913.21509	105	-150	-1913.21184
0	45	-1913.21783	105	-135	-1913.20892
0	60	-1913.21857	105	-120	-1913.20772
0	75	-1913.21693	105	-105	-1913.20912
0	90	-1913.21388	105	-90	-1913.21255
0	105	-1913.21102	105	-75	-1913.21561
0	120	-1913.21002	105	-60	-1913.21713
0	135	-1913.21195	105	-45	-1913.21671
0	150	-1913.21566	105	-30	-1913.2135
0	165	-1913.21882	105	-15	-1913.21002

0	180	-1913.21991	105	0	-1913.20915
14	-45	-1913.21738	105	15	-1913.21109
14	45	-1913.21795	105	30	-1913.21572
14	75	-1913.21617	105	45	-1913.21848
14	165	-1913.21897	105	60	-1913.21699
15	-180	-1913.22017	105	75	-1913.21388
15	-165	-1913.21867	105	90	-1913.21008
15	-150	-1913.21522	105	105	-1913.20823
15	-135	-1913.21299	105	120	-1913.20741
15	-120	-1913.21234	105	135	-1913.20974
15	-105	-1913.21344	105	150	-1913.21386
15	-90	-1913.21511	105	165	-1913.21706
15	-75	-1913.21735	105	180	-1913.2176
15	-60	-1913.21882	120	-180	-1913.21711
15	-30	-1913.21519	120	-165	-1913.21562
15	-15	-1913.21324	120	-150	-1913.21242
15	0	-1913.21209	120	-135	-1913.20992
15	15	-1913.21315	120	-120	-1913.2092
15	30	-1913.21576	120	-105	-1913.21076
15	60	-1913.21822	120	-90	-1913.21394
15	90	-1913.21317	120	-75	-1913.21733
15	105	-1913.21076	120	-60	-1913.21855
15	120	-1913.21072	120	-45	-1913.2174
15	135	-1913.21325	120	-30	-1913.21361
15	150	-1913.2167	120	-15	-1913.21062
15	180	-1913.22017	120	0	-1913.21041
30	-180	-1913.22001	120	15	-1913.21303
30	-165	-1913.21827	120	30	-1913.21627
30	-150	-1913.21654	120	45	-1913.21706
30	-135	-1913.21606	120	60	-1913.21537
30	-120	-1913.215	120	75	-1913.21314
30	-105	-1913.2141	120	90	-1913.21017
30	-90	-1913.21537	120	105	-1913.20826
30	-75	-1913.21783	120	120	-1913.20851
30	-60	-1913.21832	120	135	-1913.21135
30	-45	-1913.21759	120	150	-1913.21543
30	-30	-1913.21655	120	165	-1913.21748
30	-15	-1913.21519	120	180	-1913.21711
30	0	-1913.21414	135	-180	-1913.22036
30	15	-1913.21458	135	-165	-1913.21831
30	30	-1913.21637	135	-150	-1913.21539
30	45	-1913.21814	135	-135	-1913.21306
30	60	-1913.21811	135	-120	-1913.21267
30	75	-1913.2162	135	-105	-1913.21495
30	90	-1913.2144	135	-90	-1913.21784
30	105	-1913.21326	135	-75	-1913.22062
30	120	-1913.2136	135	-60	-1913.22135
30	135	-1913.21478	135	-45	-1913.21939
30	150	-1913.21706	135	-30	-1913.21556
30	165	-1913.21931	135	-15	-1913.21349
30	180	-1913.22001	135	0	-1913.21372
45	-180	-1913.2196	135	15	-1913.21582
45	-165	-1913.21998	135	30	-1913.21752
45	-150	-1913.21995	135	45	-1913.2184
45	-135	-1913.21829	135	60	-1913.21721
45	-120	-1913.2147	135	75	-1913.21541

45	-105	-1913.21353	135	90	-1913.21284
45	-90	-1913.21517	135	105	-1913.2113
45	-75	-1913.2173	135	120	-1913.21192
45	-60	-1913.21862	135	135	-1913.21514
45	-45	-1913.21898	135	150	-1913.21869
45	-30	-1913.21845	135	165	-1913.21981
45	-15	-1913.21702	135	180	-1913.22036
45	0	-1913.21488	150	-180	-1913.22441
45	15	-1913.21463	150	-165	-1913.22237
45	30	-1913.21627	150	-150	-1913.21951
45	45	-1913.21845	150	-135	-1913.21764
45	60	-1913.21872	150	-120	-1913.21767
45	75	-1913.2178	150	-105	-1913.21976
45	90	-1913.21709	150	-90	-1913.22221
45	105	-1913.21638	150	-75	-1913.22399
45	120	-1913.2148	150	-60	-1913.22427
45	135	-1913.21475	150	-45	-1913.22203
45	150	-1913.2172	150	-30	-1913.21926
45	165	-1913.21925	150	-15	-1913.21735
45	180	-1913.2196	150	0	-1913.21754
60	-180	-1913.22012	150	15	-1913.21915
60	-165	-1913.2218	150	30	-1913.22072
60	-150	-1913.22081	150	45	-1913.22109
60	-135	-1913.21641	150	60	-1913.22095
60	-120	-1913.21285	150	75	-1913.21913
60	-105	-1913.21272	150	90	-1913.2169
60	-90	-1913.21434	150	105	-1913.21567
60	-75	-1913.21702	150	120	-1913.2169
60	-60	-1913.21912	150	135	-1913.22004
60	-45	-1913.22007	150	150	-1913.22276
60	-30	-1913.21939	150	165	-1913.22464
60	-15	-1913.21599	150	180	-1913.22441
60	0	-1913.21341	165	-180	-1913.22742
60	15	-1913.21359	165	-165	-1913.22598
60	30	-1913.21594	165	-150	-1913.22376
60	45	-1913.21865	165	-135	-1913.22235
60	60	-1913.21979	165	-120	-1913.22194
60	75	-1913.22059	165	-105	-1913.22273
60	90	-1913.21923	165	-90	-1913.2245
60	105	-1913.21628	165	-75	-1913.22557
60	120	-1913.21348	165	-60	-1913.22566
60	135	-1913.21411	165	-45	-1913.2245
60	150	-1913.21647	165	-30	-1913.22251
60	165	-1913.21815	165	-15	-1913.22071
60	180	-1913.22012	165	0	-1913.22052
75	-180	-1913.22106	165	15	-1913.22195
75	-165	-1913.22154	165	30	-1913.22342
75	-150	-1913.21787	165	45	-1913.22433
75	-135	-1913.21293	165	60	-1913.2241
75	-120	-1913.21061	165	75	-1913.22237
75	-105	-1913.21092	165	90	-1913.22077
75	-90	-1913.21311	165	105	-1913.22016
75	-75	-1913.21646	165	120	-1913.22149
75	-60	-1913.21888	165	135	-1913.22376
75	-45	-1913.22011	165	150	-1913.22621
75	-30	-1913.21745	165	165	-1913.22767

75	-15	-1913.21355	165	180	-1913.22742
75	0	-1913.21186	180	-180	-1913.22822
75	15	-1913.21249	180	-165	-1913.22749
75	30	-1913.21552	180	-150	-1913.22652
75	45	-1913.21889	180	-135	-1913.22479
75	60	-1913.22126	180	-120	-1913.22327
75	75	-1913.22135	180	-105	-1913.22315
75	90	-1913.21741	180	-90	-1913.22377
75	105	-1913.21338	180	-75	-1913.22501
75	120	-1913.21154	180	-60	-1913.22592
75	135	-1913.21258	180	-45	-1913.22546
75	150	-1913.215	180	-30	-1913.22426
75	165	-1913.2176	180	-15	-1913.22255
75	180	-1913.22106	180	0	-1913.22168
90	-180	-1913.21981	180	15	-1913.22255
90	-165	-1913.21763	180	30	-1913.22425
90	-150	-1913.21363	180	45	-1913.22546
90	-135	-1913.21021	180	60	-1913.22593
90	-120	-1913.20855	180	75	-1913.22501
90	-105	-1913.20916	180	90	-1913.22378
90	-90	-1913.21246	180	105	-1913.22316
90	-75	-1913.21582	180	120	-1913.22326
90	-60	-1913.21784	180	135	-1913.22479
90	-45	-1913.2177	180	150	-1913.22655
90	-30	-1913.21495	180	165	-1913.2275
90	-15	-1913.21133	180	180	-1913.22822
90	0	-1913.20991			

Summary of calibration of methyl migration reaction/activation energies with high-level *ab initio* methods (Chapter 5.2.1.3)

Table B.4. Calculated high-level single-point energies for geometries from Scheme 5.6.

method	**1a**	**2**	**3a**	**4a**	**8**	**5a**
DF-MP2-F12/ VDZ-F12	-525.9428075	-591.7239673	-1117.731134	-1117.678174	-552.5465969	-565.1790476
DF-MP2-F12/ VTZ-F12	-525.979039	-591.7452068	-1117.788474	-1117.735799	-552.5653057	-565.2181809
B2GP-PLYP-D3BJ/A'VTZ	-526.5120046	-592.1899274	-1118.758557	-1118.715551	-552.975978	-565.7910391
B2GP-PLYP-D3BJ/A'VQZ	-526.5874211	-592.2308464	-1118.873624	-1118.82967	-553.0096694	-565.8724694
CCSD(T)-F12b/ VDZ-F12	-525.9921774	-591.7484746	-1117.796471	-1117.750512	-552.5671921	-565.2369781
LCCSD(T)-F12b/VDZ-F12	-526.0170455	-591.7673789	-1117.843316	-1117.794646	-552.5835095	-565.26365
LCCSD(T)-F12b/VTZ-F12	-526.0702117	-591.7961545	-1117.925825	-1117.876343	-552.6087248	-565.321117
MP2-F12/ (D,T)	-525.9851397	-591.7488038	-1117.798332	-1117.745861	-552.5687179	-565.2247908
B2GP-PLYPD/ (T,Q)	-526.619851	-592.2477066	-1118.922298	-1118.878165	-553.0236275	-565.9074829
CBS-QB3	-526.058136	-591.761842	-1117.880891	-1117.836758	-552.577748	-565.308185

Table B.5. Single-point energies for geometries from Scheme 5.6 with various DFT functionals (DFT-D3BJ).[a]

functional	**1a**	**2**	**3a**	**4a**	**8**	**5a**
BP86	-527.1259700	-592.6323558	-1119.818905	-1119.783620	-553.3656469	-566.4541682
B97D	-526.7678672	-592.4913803	-1119.341219	-1119.303237	-553.2472625	-566.0756138
OLYP	-527.0396571	-592.5668005	-1119.668732	-1119.627776	-553.3060465	-566.3594072
BLYP	-526.9233848	-592.5047116	-1119.479374	-1119.451701	-553.2635397	-566.2294295
mPWLYP	-526.8879776	-592.4981236	-1119.431542	-1119.406315	-553.2612935	-566.1905823
TPSS	-527.2298426	-592.6381478	-1119.924038	-1119.892088	-553.3660000	-566.5654033
PBE0	-526.4779400	-592.2114893	-1118.749212	-1118.703527	-552.9947663	-565.7569228
B1B95	-526.8765192	-592.5263193	-1119.463357	-1119.418186	-553.2843668	-566.1806900
B3PW91	-526.9415008	-592.4864628	-1119.490110	-1119.446235	-553.2317232	-566.2584855
B3LYP	-527.1578978	-592.6088605	-1119.820055	-1119.783318	-553.3423459	-566.4895566
TPSSh	-527.1720003	-592.6096021	-1119.83895	-1119.802744	-553.3411329	-566.5041689
BMK	-526.7664081	-592.3340737	-1119.170762	-1119.125611	-553.1052412	-566.0656142
mPWB1K	-526.8309225	-592.5109822	-1119.401368	-1119.351656	-553.2719826	-566.1333172
mPW1B95	-526.847056	-592.5194083	-1119.423451	-1119.378715	-553.2805027	-566.1489735
LC-wPBE	-526.7119115	-592.3480996	-1119.124927	-1119.067916	-553.1067831	-566.016344
CAM-B3LYP	-526.8080208	-592.4876093	-1119.348449	-1119.304934	-553.2493355	-566.1118238
ωB97XD	-526.9079383	-592.5052658	-1119.469857	-1119.424233	-553.2563772	-566.223187
O3LYP	-526.8942697	-592.4934735	-1119.410605	-1119.378111	-553.2488402	-566.2019361
PW6B95	-527.8145937	-593.1267198	-1120.994707	-1120.95397	-553.8139693	-567.1916231
M06	-526.6809325	-592.4168055	-1119.145143	-1119.108587	-553.1888435	-565.9750056
M06-L	-527.0266468	-592.5398894	-1119.612114	-1119.575767	-553.2825498	-566.346941
M06-2X	-526.8686626	-592.4500672	-1119.374859	-1119.329717	-553.2107966	-566.1745945

a. Functionals ωB97XD, O3LYP and the Minnesota series (M06, M06-L, M06-2X) were not added the dispersion corrections.

Table B.6. Single-point energies for geometries from Scheme 5.6 with various DFT functionals (DFT-D3Zero).[a]

functional	**1a**	**2**	**3a**	**4a**	**8**	**5a**
BP86	-527.0966719	-592.6242471	-1119.780506	-1119.746038	-553.3599488	-566.4237632
B97D	-526.7154544	-592.4745873	-1119.268867	-1119.233138	-553.2357273	-566.0201192
OLYP	-526.9402034	-592.5329038	-1119.530621	-1119.493598	-553.2826692	-566.2533629
BLYP	-526.8802922	-592.4910034	-1119.420032	-1119.394077	-553.2540012	-566.1839456
mPWLYP	-526.8674997	-592.4920941	-1119.403189	-1119.378944	-553.2571071	-566.1689316
TPSS	-527.2055849	-592.6307476	-1119.890921	-1119.860032	-553.3608329	-566.5397799
PBE0	-526.4615273	-592.2067085	-1118.726886	-1118.682003	-552.991436	-565.7396363
B1B95	-526.8529229	-592.5200113	-1119.432838	-1119.388126	-553.2800285	-566.1566071
B3PW91	-526.9073986	-592.4761956	-1119.443702	-1119.40125	-553.2245924	-566.2226514
B3LYP	-527.1221228	-592.597496	-1119.770023	-1119.735169	-553.3345199	-566.4517111
TPSSh	-527.1499781	-592.6032323	-1119.808872	-1119.773647	-553.3366994	-566.4809984
BMK	-526.7469799	-592.3300681	-1119.147772	-1119.102291	-553.1024137	-566.0463465
mPWB1K	-526.8215951	-592.5092523	-1119.390041	-1119.340164	-553.2707649	-566.1240721
mPW1B95	-526.8384007	-592.5179682	-1119.41385	-1119.368815	-553.2794537	-566.140518
LC-wPBE	-526.6947434	-592.3436115	-1119.102294	-1119.045776	-553.1036605	-565.998553
CAM-B3LYP	-526.7947561	-592.4846425	-1119.331907	-1119.288514	-553.2472334	-566.0983055
ωB97XD	-526.9079383	-592.5052658	-1119.469857	-1119.424233	-553.2563772	-566.223187
O3LYP	-526.8942697	-592.4934735	-1119.410605	-1119.378111	-553.2488402	-566.2019361
PW6B95	-527.8063189	-593.1250296	-1120.984686	-1120.943894	-553.8127781	-567.1833376
M06	-526.6809325	-592.4168055	-1119.145143	-1119.108587	-553.1888435	-565.9750056
M06-L	-527.0266468	-592.5398894	-1119.612114	-1119.575767	-553.2825498	-566.346941
M06-2X	-526.8686626	-592.4500672	-1119.374859	-1119.329717	-553.2107966	-566.1745945

a. Functionals ωB97XD, O3LYP and the Minnesota series (M06, M06-L, M06-2X) were not added the dispersion corrections.

Summary of Energies and Imaginary Frequencies (Chapter 5.2.1.1)

Table B.7. Calculated GS and TS energies for three synthesized 9-borafluorene derivatives complexed with methylide based on TPSS-D3(BJ)/def2-TZVP//TPSS-D3(BJ)/def2-TZVP in **gas phase**.

cat·ylide[a]	GS/TS[b]	Freq[c] (cm^{-1})	ZPE (hartree)	E (hartree)	E + ZPE (hartree)	H (hartree)	G (hartree)
cat-H	GS	0	0.303048	-1119.877642	-1119.5745941	-1119.5549051	-1119.6182081
	Me-TS	-329.81	0.299831	-1119.846027	-1119.5461958	-1119.5254248	-1119.5923748
	Ph-TS	-253.36	0.300382	-1119.848696	-1119.5483138	-1119.5280988	-1119.5929908
cat-Me	GS	0	0.356571	-1198.558790	-1198.2022190	-1198.1788390	-1198.2493810
	Me-TS	-325.99	0.353796	-1198.527095	-1198.1732990	-1198.1491330	-1198.2220700
	Ph-TS	-267.69	0.354273	-1198.526922	-1198.1726493	-1198.1489343	-1198.2205843
cat-F	GS	0	0.238859	-1914.159319	-1913.9204599	-1913.8930399	-1913.9726629
	TS	-341.37	0.235732	-1914.124447	-1913.8887149	-1913.8603169	-1913.9426749
	TS	-271.68	0.235978	-1914.123390	-1913.8874124	-1913.8593874	-1913.9405874

a. cat·ylide is the borate complex of 9-borafluorene derivatives with dimethylsulfoxonium methylide. Please refer to Scheme 5.5 for detailed structures.
b. GS = ground state; Me-TS = transition state of methyl migration; Ph-TS = transition state of phenyl migration.
c. Freq = Imaginary frequency

Table B.8. Calculated GS and TS energies for three synthesized 9-borafluorene derivatives complexed with methylide based on TPSS-D3(BJ)/def2-TZVP//TPSS-D3(BJ)/def2-TZVP in **THF**.

cat·ylide[a]	GS/TS[b]	Freq[c] (cm^{-1})	ZPE (hartree)	E (hartree)	E + ZPE (hartree)	H (hartree)	G (hartree)
cat-H	GS	0	0.304081	-1119.8939180	-1119.5898367	-1119.5704187	-1119.6331757
	TS	-329.54	0.300628	-1119.8604698	-1119.5598418	-1119.5393598	-1119.6051068
	TS	-260.53	0.300927	-1119.8636800	-1119.5627529	-1119.5426239	-1119.6073649
cat-Me	GS	0	0.357549	-1198.5747910	-1198.2172420	-1198.1942070	-1198.2640080
	TS	-323.02	0.354781	-1198.5416404	-1198.1868594	-1198.1631544	-1198.2347514
	TS	-273.59	0.354860	-1198.5418880	-1198.1870284	-1198.1634724	-1198.2347804
cat-F	GS	0	0.239561	-1914.1777847	-1913.9382237	-1913.9111237	-1913.9897887
	TS	-335.91	0.236329	-1914.1396459	-1913.9033169	-1913.8752889	-1913.9563849
	TS	-277.39	0.236395	-1914.1375600	-1913.9011648	-1913.8733878	-1913.9538278

a. cat·ylide is the borate complex of 9-borafluorene derivatives with dimethylsulfoxonium methylide. Please refer to Scheme 5.5 for detailed structures.
b. GS = ground state; Me-TS = transition state of methyl migration; Ph-TS = transition state of phenyl migration.
c. Freq = Imaginary frequency

Table B.9. Calculated GS and TS energies for other 9-borafluorene derivatives complexed with methylide based on TPSS-D3(BJ)/def2-TZVP//TPSS-D3(BJ)/def2-TZVP in **gas phase**.

cat·ylide[a]	Mig.[b]	Freq[c] (cm^{-1})	ZPE (hartree)	E (hartree)	E + ZPE (hartree)	H (hartree)	G (hartree)
***o*-*t*Bu**	Me	-377.12	0.520415	-1434.520682	-1434.0002672	-1433.9686742	-1434.0549402
	Ph	-236.11	0.521063	-1434.523197	-1434.0021345	-1433.9709985	-1434.0561015
***o*-CF_3**	Me	-283.89	0.308983	-1794.300190	-1793.9912067	-1793.9634737	-1794.0440007
	Ph	-223.59	0.308528	-1794.295131	-1793.9866025	-1793.9587395	-1794.0394845
***p*-NO_2**	Me	-335.09	0.303937	-1529.113984	-1528.8100473	-1528.7839533	-1528.8620253
	Ph	-265.12	0.303875	-1529.114496	-1528.8106213	-1528.7847273	-1528.8621113
***p*-Cl**	Me	-334.97	0.281096	-2039.122629	-2038.8415327	-2038.8182137	-2038.8906827
	Ph	-253.57	0.281472	-2039.124750	-2038.8432779	-2038.8203939	-2038.8916039
***p*-CH_3**	Me	-332.17	0.353106	-1198.527537	-1198.1744309	-1198.1497189	-1198.2252039
	Ph	-255.86	0.353479	-1198.530542	-1198.1770631	-1198.1527761	-1198.2270351
***p*-NMe_2**	Me	-335.14	0.441792	-1387.944126	-1387.5023336	-1387.4725836	-1387.5574896
	Ph	-268.55	0.442211	-1387.948469	-1387.5062578	-1387.4768878	-1387.5602818
***o,p-di*-CF_3**	Me	-292.99	0.316624	-2468.749174	-2468.4325500	-2468.3968450	-2468.4949130
	Ph	-248.24	0.316216	-2468.743106	-2468.4268898	-2468.3911068	-2468.4891488

a. cat·ylide is the borate complex of 9-borafluorene derivatives with dimethylsulfoxonium methylide. Please refer to Scheme 5.5 for detailed structures.
b. Mig. = migration group.
c. Freq = Imaginary frequency

Summary of Cartesian Coordinates (Me/Ph-TS = methyl/phenyl migration TS)

cat-H·ylide (GS in gas)

0.76953240131984	-1.55517546429963	-4.95006823757861	c
0.98781479016177	-1.28082641439928	-2.33508884960678	c
2.68132976456198	0.57643027518969	-1.39466557549815	c
2.13904470363426	-0.00164444978677	-6.59774215269289	c
3.76510766362190	1.84713381214444	-5.63675296893931	c
4.05687220048167	2.13586463532049	-3.02897216088043	c
-0.48310553952890	-2.98941393167374	-5.73608238529352	h
1.95146865934461	-0.23191075132186	-8.63109076844294	h
4.82407832515799	3.04688621568594	-6.92433049319390	h
5.34876792711200	3.55764396749652	-2.29559359937177	h
2.68185809968614	0.57624605723300	1.39416648737315	c
0.98841425496941	-1.28098603521906	2.33473410486955	c
0.76879947442390	-1.55410158832046	4.94985882387069	c
2.13839120468230	-0.00039338120793	6.59734603747081	c
3.76374008741662	1.84893143657184	5.63633396720958	c
4.05559668474154	2.13745652143109	3.02846324330160	c
-0.48489844135151	-2.98719834801383	5.73619941088867	h
1.95118269747372	-0.23033491083560	8.63091527838042	h
5.34593593495334	3.56052386752264	2.29489154593901	h
4.82173419201626	3.04966335913179	6.92377250215840	h
-0.42426224038969	-2.67291506226209	-0.00016787685489	b
-0.26166444914060	-5.75130952288517	-0.00015413394851	c
-3.56640747208600	-2.06190083132783	-0.00153589437602	c

-4.49312860276664	-2.86772090028599	1.67284708347570	h
-4.72369838116748	1.06144640566481	0.00193029518998	s
-4.48838113111485	-2.86091330288351	-1.68181716951572	h
-3.40202066104368	2.68813381785619	2.64834684401298	c
-3.96804072220600	1.64803416083331	4.33521848461550	h
-4.25151872792457	4.56919226022665	2.62212268294262	h
-1.34494350733638	2.72936237082276	2.49169866133542	h
-7.48140909668398	1.32055988629628	0.00470686840943	o
-3.40604920559857	2.68839767199044	-2.64625000012324	c
-3.97657945355096	1.64925407737049	-4.33226148447849	h
-1.34856319665394	2.72791947336414	-2.49301018290540	h
-4.25350342014485	4.57025418554564	-2.61779990364055	h
1.71943707634020	-6.36163878644196	0.00699781016561	h
-1.16473117138082	-6.59992302817713	1.66856169475131	h
-1.15231434426130	-6.59916735544492	-1.67572798901928	h

cat-H·ylide (GS in THF)

0.75676776932969	-1.48566066457212	-4.95471790647308	c
0.98005468475669	-1.21772051686737	-2.33739342492016	c
2.74518700592949	0.57244785717799	-1.39743315375924	c
2.20456128467550	-0.00180012067700	-6.60202373609129	c
3.91162040604741	1.77471437027679	-5.63945784268828	c
4.19848172265403	2.06449546608594	-3.02983492696673	c
-0.57071480100283	-2.84882783633684	-5.74399645091656	h
2.00749136209999	-0.22333348856453	-8.63598954340804	h
5.02638067685772	2.92487649987836	-6.92611014067285	h
5.54094116566918	3.43806840826314	-2.29458477899732	h
2.74461868652055	0.57468204969150	1.39188809476977	c
0.97948868220505	-1.21431666804368	2.33408311393229	c
0.75721028681585	-1.47988492658188	4.95179633227335	c
2.20507149785822	0.00591830710370	6.59723975201486	c
3.91159944517376	1.78178517664906	5.63245049144125	c
4.19803208810601	2.06869798615248	3.02247408720296	c
-0.56987926481425	-2.84241592864555	5.74280852831691	h
2.00853904764674	-0.21357158442145	8.63147333477707	h
5.54059191747102	3.44121315842699	2.28545433237998	h
5.02624112873251	2.93369729031818	6.91763215683010	h
-0.45668240151686	-2.58908935393343	-0.00082710026995	b
-0.21094898462881	-5.67321196957390	0.00184648870830	c
-3.59774224548836	-2.06482788964807	-0.00359721403449	c
-4.50240651827160	-2.89097550623683	1.67207799497002	h
-4.83497099002868	1.02674613771638	-0.00122363201024	s
-4.49741249076377	-2.88656221949540	-1.68410619540128	h
-3.59175515714405	2.67552735161545	2.65536040238727	c
-4.17937514186992	1.63557941173849	4.33501788101441	h
-4.44324447312439	4.55388023233898	2.60464450814805	h
-1.53559861146121	2.73864268763500	2.51389439911393	h
-7.60951268266469	1.16629415944946	-0.01202945484336	o
-3.57136328599983	2.68966317313859	-2.63920889706383	c
-4.14621244595904	1.65901318393463	-4.32896808166544	h
-1.51621914657864	2.75151986436265	-2.48184451868886	h
-4.42305434913312	4.56780059357607	-2.58445183430168	h
1.78510648623641	-6.24236334296157	0.00118549719164	h
-1.09246046240928	-6.53277966118384	1.67708890242961	h
-1.09454551415730	-6.53606129487490	-1.67061746472923	h

cat-H·ylide (Me-TS in gas)

-3.93196257092043	-3.23015742203772	0.54573531643036	c
-1.49339102292230	-2.27718057877772	0.84772042774012	c
0.44108302004913	-3.14631539462244	-0.79458476141616	c
-4.45765647319885	-5.00006971544562	-1.34913304378399	c
-2.53714454970454	-5.82450548590382	-2.96423405133538	c
-0.07784520032159	-4.90403958099923	-2.69638492221329	c
-5.45468037721655	-2.60304599113562	1.78167621269372	h
-6.36130320348093	-5.73932976428363	-1.57070479357473	h
-2.95962058472720	-7.19471480589225	-4.43461483919068	h
1.40478654785914	-5.56097994791024	-3.95899598946551	h
2.88071477554245	-1.93442214722196	-0.18177054754687	c
2.61166984585622	-0.23667863135867	1.87717363499904	c
4.73758312595567	1.06853895580466	2.72776440643112	c
7.08514295985024	0.71999558840382	1.55874963456548	c
7.31708779175426	-0.94233565544563	-0.48077245735599	c
5.21852413890371	-2.27922077442508	-1.36143417389897	c
4.59059037670523	2.37833125697044	4.30981426167124	h
8.73531358706855	1.73979225676046	2.23420618060961	h
5.42018971549622	-3.57456942270933	-2.94439078884020	h
9.14410936855412	-1.20121062383189	-1.38238272955347	h
-0.29806277818502	-0.19657842400895	2.68161013870890	b
-0.76382548697425	-0.78378016526414	5.96543117390599	c
-1.70120723526252	2.20456910224583	3.43319002536968	c
-3.74701870113893	2.22647810784149	3.66625121483718	h
-2.11289741965744	5.03210586279104	-0.38244748597555	s
-0.77111145173266	3.72915730672503	4.45895434585975	h
1.13564359642493	5.27562872006786	-1.44825936325114	c
2.07855241642294	6.60091954963977	-0.18008692205922	h
1.11842541799636	6.00941970107352	-3.37845617535188	h
2.02712213134371	3.41802097435146	-1.32732573159743	h
-3.37667639420828	7.52441181925208	-0.76865778005101	o
-3.23537636138305	2.85532970980400	-2.77968944859899	c
-5.23339642340290	2.52196260864862	-2.39382915927684	h
-2.18325039598625	1.08547967624635	-2.63773021647557	h
-2.99231891880927	3.76294936097887	-4.61871364317205	h
-0.07346539725248	-2.72802473772973	5.81170229379155	h
-2.68784930959087	-0.83417371326602	6.70282632727258	h
0.47783158326177	0.29513116095441	7.20336043866997	h

cat-H·ylide (Me-TS in THF)

-3.93242437201671	-3.22399248771964	0.51140394352247	c
-1.48932999787467	-2.27957822151112	0.81949753061188	c
0.45380407132462	-3.19240568637969	-0.78990647211543	c
-4.45002037629271	-5.03134209236309	-1.35286749780360	c
-2.51733986046101	-5.90396216927075	-2.93216626833245	c
-0.05387363145682	-4.98968662066404	-2.66040521696384	c
-5.46418576835038	-2.55619403250007	1.71372353647232	h
-6.35766285914958	-5.75963601996934	-1.58159177931932	h
-2.93382780687612	-7.30179447629561	-4.37875408860331	h
1.43646091996490	-5.67875477673798	-3.89731713749570	h
2.89457877551126	-1.97923972780312	-0.18185260412489	c
2.61506203425864	-0.23734165504115	1.83966471382643	c
4.74136154345823	1.08017664834478	2.67613237299205	c
7.09789075118634	0.69492990625981	1.53238611939506	c
7.34070868696846	-1.01737952709830	-0.46750343166233	c

5.24102303593697	-2.36472598124886	-1.33605157681073	c
4.58563123024160	2.43110828960106	4.22171140365951	h
8.74612942973904	1.72803262614950	2.19386621948553	h
5.44884321882114	-3.69381750643060	-2.89057571855867	h
9.17367711810594	-1.30348719903020	-1.34965122475361	h
-0.29770883158720	-0.18554165875760	2.64683409715687	b
-0.74884350715831	-0.78898291014799	5.91853121287212	c
-1.70459754278791	2.21542653650128	3.40368704355618	c
-3.74899837629848	2.22365568583321	3.64570700705724	h
-2.13552436938048	5.05351610561362	-0.34495296872109	s
-0.77236264351346	3.73173427333206	4.43879945908052	h
1.09522587391034	5.38803308793105	-1.39915906405806	c
2.01046942807413	6.70902886594225	-0.10687672178119	h
1.07292974607996	6.13136437285609	-3.32483537160414	h
2.00705812350598	3.53910364824135	-1.29583549434183	h
-3.44680890345671	7.55216797964211	-0.67584726903327	o
-3.25324321846696	2.92875180683944	-2.77318302279432	c
-5.24870993206715	2.57914277950471	-2.38942602214862	h
-2.18477825396987	1.16735504157901	-2.64653284874725	h
-2.99988568467322	3.85428346384954	-4.60103280039411	h
-0.05113382959757	-2.73330299673621	5.78757579336634	h
-2.67730775450438	-0.83740018329662	6.64573462245173	h
0.48202367582180	0.30764354726963	7.15263653423268	h

cat-H·ylide (Ph-TS in gas)

-3.71714776996331	-4.58716252460701	-0.62863887216243	c
-2.69352979895711	-2.15339092790206	-0.63514702320355	c
-4.05265410768855	-0.13329267506362	0.50508038381286	c
-6.10190650158867	-5.01560104188199	0.42023412466248	c
-7.43427972493970	-3.02033496013623	1.52829131845180	c
-6.42504308852935	-0.58184791501612	1.57290246530099	c
-2.67575822478811	-6.14831178864392	-1.46777252265503	h
-6.92295645953957	-6.89704271345437	0.38106450993521	h
-9.28385112638755	-3.36770068630461	2.35045405235534	h
-7.50321762654315	0.95557934424645	2.40735770671656	h
-2.73877234685451	2.29091541791115	0.19927279853360	c
-0.53117530575644	1.99713871631862	-1.29391302904861	c
0.85202212905326	4.16340027767233	-1.89493792747932	c
0.11224154994551	6.54093354939417	-0.99747604697284	c
-2.03084657988223	6.77985743061468	0.52759300058980	c
-3.47456664104613	4.65547420984973	1.12332932535736	c
2.50798820689092	4.03623813543004	-3.11283145561208	h
1.19536859325900	8.21280837915917	-1.50041558273616	h
-5.16324291820457	4.85603015828755	2.27785530705573	h
-2.59184276395452	8.62884964381495	1.22239803168200	h
-0.03844512106027	-0.94221848994794	-1.92451663990620	b
0.67108196971927	-1.87253218637892	-4.73161947776429	c
1.08244426515438	-2.37754376111998	0.42736223288784	c
0.70783309587357	-1.72658298548793	2.34603288305839	h
5.43324157582456	-1.48687966650635	1.19181535256175	s
1.41298850233682	-4.41213624394872	0.35540316059338	h
6.66178910805272	-0.45152238891963	-1.82807597778249	c
5.30640570664549	0.84248079004612	-2.68564310698698	h
6.88244394717634	-2.13732043004259	-2.99357167314082	h
8.48732029219011	0.45263883425288	-1.49238292965521	h
7.42476904121943	-2.97814451714076	2.50924609002727	o

5.13181147527362	1.56606559070383	2.70790351711689	c
4.49321135074839	1.19766023468352	4.63507147826533	h
3.72892475221399	2.68156985899784	1.67867540966575	h
6.98555647605614	2.47497689569400	2.72449872654698	h
0.97985249177646	-3.92243609053271	-4.84673791849151	h
2.39476788046073	-0.96438455371330	-5.45306271811097	h
-0.83564462138451	-1.40269031767284	-6.07478385564573	h

cat-H·ylide (Ph-TS in THF)

-3.71496524611443	-4.59208615225460	-0.58804706464426	c
-2.71255058461231	-2.14787228760384	-0.60757919814637	c
-4.10521976098326	-0.12736191563405	0.49270061627683	c
-6.10976389679904	-5.03138754551640	0.43916280502683	c
-7.47485941161419	-3.03514663328901	1.51026264295680	c
-6.48770844942336	-0.58509238016758	1.53915879176169	c
-2.64768368954940	-6.15547836945981	-1.38910486983051	h
-6.91066414039113	-6.92190982909947	0.41443502720506	h
-9.32974324582535	-3.39039791545128	2.31704327426804	h
-7.58884831824560	0.95033969876005	2.34712532520383	h
-2.81193409114314	2.30824151555085	0.18006680616698	c
-0.57779958878791	2.02316798392766	-1.27553325624062	c
0.81508859285945	4.19329783318422	-1.84599103141941	c
0.04339690220446	6.56985359897569	-0.96886713457451	c
-2.13931536135498	6.80407903597514	0.50436277602198	c
-3.58424941634277	4.67245407483215	1.08060575831274	c
2.51057724266432	4.06788895680224	-3.00679406449904	h
1.13775724223453	8.24378383875151	-1.44033981578991	h
-5.29466218773067	4.86688042454392	2.20406796074553	h
-2.72362743281156	8.65235065178670	1.18288113097547	h
-0.05914755097541	-0.91038772068935	-1.90587552823989	b
0.63342160424538	-1.83073148230143	-4.72241898138869	c
1.05206943314247	-2.35298554602694	0.42764168040404	c
0.72868323006692	-1.69335120493786	2.35203000857943	h
5.48618523996343	-1.49372260122913	1.16133040145364	s
1.39931168501827	-4.38339516808369	0.34436966712531	h
6.78450404225098	-0.52304881676776	-1.83934359011658	c
5.47061645408172	0.79749612136939	-2.72295634086465	h
6.98107576362914	-2.22355452709434	-2.98761244485528	h
8.61899518379472	0.35550605141077	-1.48834995481786	h
7.42752633276281	-3.06280390279889	2.50692136810901	o
5.28687044762819	1.54998597565034	2.68811853799780	c
4.61972696496396	1.20317512606674	4.60912846307542	h
3.92357536434484	2.70232804056476	1.64762916493719	h
7.16369803255347	2.40857481889687	2.70054138284251	h
0.91525902329019	-3.88411327136462	-4.84071965646847	h
2.37520941580375	-0.93992012545494	-5.42086239245778	h
-0.86362414199601	-1.33111574916865	-6.06887314726920	h

cat-Me·ylide (GS in gas)

0.70327136597412	-1.33997626731234	-4.94318192910556	c
0.91728313423387	-0.16665962470335	-2.56958100961203	c
0.22837803954862	2.41522894418415	-2.35794225279268	c
-0.24120883801504	0.04655725054639	-6.99881467435455	c
-0.95007838419852	2.57726825104521	-6.74417181274746	c
-0.70350441228184	3.78838739246468	-4.41781932462946	c
1.47555218395918	-4.06137907210202	-5.34917471131331	c

-0.42009116870298	-0.87018398668798	-8.83186545053241	h
-1.67702851109794	3.60173285811514	-8.36937295409103	h
-1.23096727238118	5.76529813503008	-4.22195217080558	h
0.57618191228920	3.32787563627939	0.25106022963230	c
1.50145489772151	1.37275165147752	1.83460879377255	c
1.94409937997408	1.92550138241096	4.39500933463418	c
1.39985123979040	4.35437812457388	5.31421256681532	c
0.45036461652344	6.24457367332915	3.73403498581925	c
0.04590789016738	5.74758639030111	1.17883467689735	c
3.00752056603589	-0.02598319530820	6.19189710959876	c
1.73082286137858	4.77419519864905	7.30085562500142	h
-0.66988772294981	7.22358549722799	-0.05951841303408	h
0.04568032519261	8.10699240054603	4.50015807186036	h
1.74475811253511	-1.22336495524759	0.19970215208089	b
4.48980949202236	-2.63279571790034	0.32897573004298	c
-0.32244643990835	-3.44351937798511	1.24843018356872	c
-0.28685393780759	-5.14119805035916	0.05517904380901	h
-3.58379124280319	-2.81656384314871	1.45161613938934	s
0.11966437462281	-4.04051211750134	3.18615692502761	h
-4.02255780760238	-0.08030038400635	3.37816349936667	c
-3.19666412041692	-0.50871302375001	5.21787275098478	h
-6.06559951772851	0.16999579034010	3.53157718437021	h
-3.07124872987686	1.53985292162522	2.52413530541008	h
-5.14739041430307	-4.90263502429136	2.38784222170623	o
-4.67164313197257	-1.82661918085621	-1.58622323546194	c
-3.68912934851698	-0.10471171889354	-2.15929533706634	h
-6.70963605245609	-1.56686150819579	-1.38771741910447	h
-4.25300250288477	-3.36146852232107	-2.89716680683292	h
5.98273149038652	-1.34605490747165	-0.31623617227876	h
4.58553640146312	-4.32293906932512	-0.87146756474655	h
4.99667230915922	-3.23496891713233	2.24913954888817	h
1.98564343112085	-1.82498232835485	6.08439562174955	h
2.92407705860981	0.63978895845511	8.14874972469100	h
4.98442656490427	-0.44558013017318	5.74274639505108	h
0.87899284142975	-4.73476840111412	-7.21195983997472	h
0.66325170578738	-5.32445791162451	-3.92198711864696	h
3.53079736107507	-4.27435322083505	-5.21990562303699	h

cat-Me·ylide (GS in THF)

0.66545119618971	-1.30468747569305	-4.95744828040895	c
0.88129806789877	-0.13331870609540	-2.58011304386755	c
0.26778701475015	2.46922338540024	-2.38500812956762	c
-0.18607890834481	0.11305946478516	-7.03404379482745	c
-0.80949645524448	2.67020464722700	-6.79724762871685	c
-0.57540378868012	3.87354236253589	-4.46420795666420	c
1.31459138633159	-4.06163077273061	-5.34225558355488	c
-0.36759271752558	-0.80274776962810	-8.86763279111980	h
-1.46933218973984	3.71684332196090	-8.43768183843297	h
-1.04735159170227	5.86581417277481	-4.27793195555684	h
0.61374795228321	3.38230925680369	0.22479125055199	c
1.46363124545411	1.40794955876578	1.82727504972641	c
1.90436225917821	1.96588629436325	4.38965613113445	c
1.45083773250897	4.42436980869255	5.28290430672356	c
0.58522192154722	6.33797381571039	3.67913287547687	c
0.16933138674243	5.83087204831528	1.12650564137923	c
2.84784524566526	-0.01508802075739	6.22172156890833	c

1.77829337644761	4.84636484517308	7.26997944327021	h
-0.49212021915610	7.31938996271642	-0.12769572280185	h
0.24545767050272	8.22146087815324	4.42679749368386	h
1.69569473477250	-1.19531040288526	0.19509202211745	b
4.49906883653085	-2.51275606714900	0.28700466420871	c
-0.27079646231290	-3.47842016119254	1.25068509057878	c
-0.19370999347333	-5.16581630060665	0.04688734033914	h
-3.54777409149050	-2.95683223775560	1.49572295313518	s
0.21423572191929	-4.07008230595124	3.17861178484670	h
-4.05528849596009	-0.26834981876629	3.45341740190304	c
-3.23046082169316	-0.70212135787935	5.29203261087876	h
-6.10133041076862	-0.04578638607973	3.59300790741934	h
-3.13896542764791	1.37136509683963	2.60206082679797	h
-5.00197069275234	-5.12819470975939	2.43841950481942	o
-4.70638786005584	-1.99367659715624	-1.51229084569789	c
-3.75504965250105	-0.25466778798647	-2.08085704476212	h
-6.74082738269986	-1.74179615438342	-1.28164776922024	h
-4.29439659965738	-3.52412621334117	-2.83004044519468	h
5.94668642361724	-1.17662371168196	-0.36748975916079	h
4.62861326898583	-4.19457198759632	-0.92283896792030	h
5.03686157950341	-3.10536370849228	2.20241768489181	h
1.65163419635961	-1.70650364437293	6.21468688912221	h
2.89071930438620	0.72367792674009	8.15313473404362	h
4.75985249374793	-0.63820731278737	5.72952245962196	h
0.84973319903672	-4.66993871017456	-7.26362134395037	h
0.29154143556511	-5.28791134902364	-4.02249705464921	h

cat-Me·ylide (Me-TS in gas)

-1.29030895376716	1.09179148181838	-4.99651542634979	c
-1.29030895376716	1.09179148181838	-4.99651542634979	c
-1.55342998013157	0.85658339297150	-2.36542810939571	c
-3.26690776443063	-0.96082898665846	-1.39434874753107	c
-2.73509398820667	-0.47143864222420	-6.57921422714869	c
-4.41430637310718	-2.25203551163893	-5.59404891576453	c
-4.69071842171416	-2.51261300093346	-2.98781726867394	c
0.53315810922668	2.94732616274819	-6.17643397496787	c
-2.54013560021618	-0.28690005232971	-8.61814170581104	h
-5.50763288381884	-3.43443650100223	-6.86884768944129	h
-5.99687051796857	-3.90074159028648	-2.22099409862336	h
-3.26690776443063	-0.96082898665846	1.39434874753107	c
-1.55342998013157	0.85658339297150	2.36542810939571	c
-1.29030895376716	1.09179148181838	4.99651542634979	c
-2.73509398820667	-0.47143864222420	6.57921422714869	c
-4.41430637310718	-2.25203551163893	5.59404891576453	c
-4.69071842171416	-2.51261300093346	2.98781726867394	c
0.53315810922668	2.94732616274819	6.17643397496787	c
-2.54013560021618	-0.28690005232971	8.61814170581104	h
-5.99687051796857	-3.90074159028648	2.22099409862336	h
-5.50763288381884	-3.43443650100223	6.86884768944129	h
-0.22457908386432	2.21607315495258	0.00000000000000	b
-0.68979276093861	5.56623361762806	0.00000000000000	c
2.52814881199286	3.09198109464689	0.00000000000000	c
3.43786362219185	3.78715341482295	-1.70918167721347	h
5.34593698209204	-0.71707416950369	0.00000000000000	s
3.43786362219185	3.78715341482295	1.70918167721347	h
4.03306099284091	-2.54451912834614	2.58382435448835	c

4.69883622996423	-4.48962562007636	2.39239863428947	h
1.97303885571154	-2.41567780215201	2.52338897159992	h
4.75204729287906	-1.70719578879433	4.32593477781608	h
8.14820676984644	-1.03535619636227	0.00000000000000	o
4.03306099284091	-2.54451912834614	-2.58382435448835	c
4.69883622996423	-4.48962562007636	-2.39239863428947	h
4.75204729287906	-1.70719578879433	-4.32593477781608	h
1.97303885571154	-2.41567780215201	-2.52338897159992	h
-0.10252511608580	6.58091197023234	1.69152564809506	h
-2.74982085033498	5.38262172364746	0.00000000000000	h
-0.10252511608580	6.58091197023234	-1.69152564809506	h
2.50276542680740	2.41521605663470	5.80441962135062	h
0.28864575235219	3.02192190031264	8.22792526241000	h
0.26838767705464	4.85938004469536	5.43273674500429	h
2.50276542680740	2.41521605663470	-5.80441962135062	h
0.26838767705464	4.85938004469536	-5.43273674500429	h

cat-Me·ylide (Me-TS in THF)

-1.30367235855620	1.07088095958150	-4.99552898836218	c
-1.56740494770934	0.83065133827126	-2.36349114923797	c
-3.31004958360110	-0.96203811645599	-1.39428771022505	c
-2.78650479806334	-0.45574328422950	-6.58258666446387	c
-4.49371436928963	-2.21395043533031	-5.59931772246946	c
-4.76620927251819	-2.48472152889382	-2.99108389970000	c
0.56276317379106	2.88710045352688	-6.16888845064776	c
-2.59463112213172	-0.26566218555166	-8.62168000217366	h
-5.61298660024146	-3.37099270853074	-6.87601287497421	h
-6.09395628470094	-3.85781221447641	-2.23356284950362	h
-3.31004958360110	-0.96203811645599	1.39428771022505	c
-1.56740494770934	0.83065133827126	2.36349114923797	c
-1.30367235855620	1.07088095958150	4.99552898836218	c
-2.78650479806334	-0.45574328422950	6.58258666446387	c
-4.49371436928963	-2.21395043533031	5.59931772246946	c
-4.76620927251819	-2.48472152889382	2.99108389970000	c
0.56276317379106	2.88710045352688	6.16888845064776	c
-2.59463112213172	-0.26566218555166	8.62168000217366	h
-6.09395628470094	-3.85781221447641	2.23356284950362	h
-5.61298660024146	-3.37099270853074	6.87601287497421	h
-0.23000510724980	2.19067821472164	0.00000000000000	b
-0.72592913843913	5.52562621261347	0.00000000000000	c
2.52179576939023	3.07828599739280	0.00000000000000	c
3.42021637513041	3.78558211937386	-1.70982286285131	h
5.37054005876367	-0.65906230990190	0.00000000000000	s
3.42021637513041	3.78558211937386	1.70982286285131	h
4.13785553663575	-2.51232495700067	2.58728943013090	c
4.81680545881029	-4.44989417247796	2.37581775934806	h
2.07579812893847	-2.40897375823441	2.53799422011255	h
4.85868894741205	-1.66581351115684	4.32372939307527	h
8.19989935508421	-0.89356555573438	0.00000000000000	o
4.13785553663575	-2.51232495700067	-2.58728943013090	c
4.81680545881029	-4.44989417247796	-2.37581775934806	h
4.85868894741205	-1.66581351115684	-4.32372939307527	h
2.07579812893847	-2.40897375823441	-2.53799422011255	h
-0.13264908168427	6.53744496405544	1.69177339057665	h
-2.78783562465932	5.35394973269510	0.00000000000000	h
-0.13264908168427	6.53744496405544	-1.69177339057665	h

2.51582659323546	2.30166898889688	5.79423288708525	h
0.32059298669264	2.97226136540201	8.22032286889110	h
0.34792285538363	4.80089194963531	5.41389362203800	h
2.51582659323546	2.30166898889688	-5.79423288708525	h
0.34792285538363	4.80089194963531	-5.41389362203800	h

cat-Me·ylide (Ph-TS in gas)

-4.47948894175875	-0.77136982110989	3.63484125315673	c
-3.01588415781100	-0.57301236167542	1.41985820371575	c
-3.97429545508891	0.76337792569093	-0.70607456180251	c
-6.88451587271969	0.34043813729298	3.65237989172866	c
-7.80395421222027	1.66921515741556	1.56555606345232	c
-6.36360472735358	1.88042062164230	-0.62986522935777	c
-3.61676529354472	-2.23683398145622	5.92605885565150	c
-8.05624343892163	0.15937858967259	5.33167645115483	h
-9.66902078757927	2.52504641863352	1.65242601316040	h
-7.11293801943077	2.87156119520378	-2.26535734029017	h
-2.27310139890861	0.59692044505271	-2.89069996527965	c
-0.17915016801798	-0.99628483559274	-2.37782145048867	c
1.47834990710531	-1.56755330311560	-4.37602193925889	c
1.08374048829699	-0.44754718566757	-6.75002899028199	c
-0.92508185962250	1.20645407631231	-7.18427282338878	c
-2.63835338588350	1.72062580722407	-5.25487002002232	c
3.61533108945015	-3.44691948489725	-4.09284745170722	c
2.36532646448522	-0.90277716978819	-8.29328441753925	h
-4.24399595784116	2.95528883899128	-5.59976465481468	h
-1.17142980205315	2.05084564451271	-9.03985385635053	h
-0.16398325585845	-1.75375958859117	0.59244160059507	b
0.51696314229271	-4.56880783606215	1.54006312390906	c
0.63304311361610	0.61668392388867	2.25179839172932	c
0.31555175534159	2.52169668730132	1.53385717512086	h
4.96189833569486	1.54522245053206	2.43859930995494	s
0.54160473454162	0.55472007873043	4.30875501924002	h
6.54369217207913	-1.48169092040359	2.57738730373238	c
5.60963255797321	-2.79312619271204	1.29168781417082	h
6.34876131903725	-2.13785728426440	4.52316021797330	h
8.53241065241662	-1.20213839512150	2.10000015285610	h
6.31069830020640	3.32477568688565	4.15212877220547	o
5.58864842140424	2.42929582758816	-0.80165443156856	c
4.47031302833397	1.22902980572222	-2.05516445717572	h
7.61479663703325	2.28179550442877	-1.16615584987742	h
4.96624905524233	4.38977026596926	-0.96787929969496	h
2.35342011229786	-5.22284472935901	0.82725874349783	h
-0.87811474053196	-5.94302078546645	0.85762928341122	h
0.58696108070527	-4.74463006039862	3.60494763708107	h
2.88372509733456	-5.34538753978107	-3.71235443395456	h
4.88210668277238	-2.97269615633109	-2.52564857942779	h
4.75596825165645	-3.53150866928830	-5.81583660381306	h
-3.55666460168094	-4.26432279706125	5.50946225037992	h
-4.91229454566275	-1.94163875826184	7.50927840043109	h

cat-Me·ylide (Ph-TS in THF)

-4.49236646373182	-0.75159653585266	3.64071129244123	c
-3.04095859835791	-0.56605039906956	1.41433845104619	c
-4.01624495264533	0.75187081782344	-0.71729883769642	c
-6.90005912714106	0.36089075200133	3.66422381323935	c

-7.83412876936047	1.67528085405090	1.57227492052123	c
-6.40682552568209	1.87029210343803	-0.63611608204277	c
-3.61777085323457	-2.19552326188546	5.94150345619718	c
-8.06046767965731	0.19376646700745	5.35282543278150	h
-9.69833098460004	2.53273553655353	1.66479462287671	h
-7.16698510070993	2.85163711478655	-2.27286647127261	h
-2.33106851832248	0.57124509400715	-2.91488755098803	c
-0.22795330234671	-1.01147952562693	-2.40572622328366	c
1.43745271108053	-1.56865625031399	-4.40235491310517	c
1.02856772555640	-0.45656655490984	-6.77922584318329	c
-1.00113416866898	1.17559879397679	-7.21621641760416	c
-2.71538287672740	1.68503047052746	-5.28312496001603	c
3.60149799398957	-3.41464638595563	-4.10835161717893	c
2.31913957422715	-0.89353526557683	-8.32040134657563	h
-4.32912781122844	2.90981614268802	-5.62756539591258	h
-1.25756151479732	2.01423845879320	-9.07366208283223	h
-0.19308271936392	-1.77222730067781	0.56178900511095	b
0.47344158508309	-4.59322181922428	1.50012522455335	c
0.60058801410974	0.57874332186432	2.21983945204866	c
0.33679717265168	2.49199519107221	1.50423476188722	h
5.00591508745224	1.49944086529402	2.44433031394398	s
0.54438265818860	0.50760420226442	4.27639158915178	h
6.65905032780509	-1.47479697006488	2.63243109746914	c
5.80017525069690	-2.79877392378012	1.30625762624735	h
6.41552394655484	-2.14986684681865	4.56590814704572	h
8.65105217369685	-1.14653495488035	2.20512025730765	h
6.25902548377468	3.31566758260714	4.22247435584316	o
5.72688499682806	2.43583886124112	-0.75188911551198	c
4.68386661198252	1.20990624971165	-2.04321575729689	h
7.76529917000147	2.32540084849276	-1.05096227628059	h
5.05705646811950	4.37881360670119	-0.93274330070907	h
2.33555942914829	-5.21145795669907	0.82408160215573	h
-0.89395021457161	-5.97549117700515	0.77498924585441	h
0.49715184845496	-4.77540576825074	3.56496750635208	h
2.89574023114498	-5.33871980603563	-3.81118354486861	h
4.79993563443295	-2.96575493681988	-2.48338682238765	h
4.79924988838705	-3.42236870651556	-5.79373973022113	h
-3.57440943146430	-4.22821298445841	5.54602347148232	h
-4.90182426779867	-1.87590999738783	7.52903904354215	h

cat-F·ylide (GS in gas)

1.74398574773400	-4.77825920401871	-0.41660945562916	c
1.42718990172543	-2.20893077959196	-0.70935157635981	c
0.39394134469604	-1.27676165329925	-3.01268638961338	c
1.09522260694884	-6.49924040059775	-2.30280295617755	c
0.10295178751825	-5.58112697199205	-4.56054699208948	c
-0.24755382085999	-2.98878124697069	-4.91974517157923	c
0.18942623893573	1.51300856610779	-2.90260240107383	c
1.08575030479846	2.40237225611514	-0.52611674532992	c
1.03258070903516	4.96049077988039	-0.03438149593350	c
0.13734056093766	6.71196211194544	-1.78669131705652	c
-0.72053701343484	5.83850484917086	-4.11617879600080	c
-0.69619966850242	3.25845172442003	-4.67703431137997	c
2.16033599041006	0.09252575154150	1.17383424696557	b
5.21028413571283	0.30116237429954	1.63510013403277	c
0.94205304990029	-0.12303606088653	4.08678666602472	c

1.65123690563293	-1.81482258890976	5.05479902639513	h
-2.34327230277807	-0.34770732491348	4.54754928025006	s
1.44633497598016	1.53703965968913	5.22328647384184	h
-3.76261288865922	2.33681978645212	3.07375101974834	c
-3.31966665588303	2.33062953860725	1.06020005080927	h
-2.96522314362466	4.00566097047004	3.98737779339808	h
-5.78723001305031	2.19274148738758	3.44446554766396	h
-3.19637364937039	-0.58107516317981	7.16517931235123	o
-3.45770344872859	-2.94490703232542	2.70235434947214	c
-3.01276130583810	-2.62026697350976	0.71518107501379	h
-5.48698720233193	-3.07164296671301	3.05414224245573	h
-2.48578956265048	-4.62580860756121	3.39914855169607	h
6.20739012644335	0.44427685197983	-0.17545196115835	h
5.95776831725653	-1.36337539842439	2.62105209609920	h
5.71003056299632	1.97793231654807	2.74875752521055	h
-1.59045366815679	7.49838232559285	-5.83339856208332	f
0.07026422990192	9.19909729536355	-1.26438240176679	f
1.79734326195451	5.85801578495681	2.26259564078201	f
-1.56812910955196	2.59825117545278	-6.97838417679022	f
-1.22687585846750	-2.28506062703242	-7.16448791933889	f
-0.53215353007046	-7.21143476485630	-6.40432745344422	f
1.38928196479424	-9.00305289240200	-1.97528961908174	f
2.64881011864599	-5.73203494879606	1.80490866967611	f

cat-F·ylide (GS in THF)

1.78611927590652	-4.77151886618029	-0.44268418026040	c
1.44465198284865	-2.20327823103265	-0.71673727119882	c
0.39000157981963	-1.26973148771761	-3.00951892271611	c
1.12926374331256	-6.48609635149327	-2.32920567795195	c
0.10507074242846	-5.56739771328305	-4.56843762440055	c
-0.26152217332212	-2.97912445461539	-4.91238500312407	c
0.19051385696556	1.51834064475215	-2.89871818425604	c
1.11586876941955	2.40878302062552	-0.53406425687548	c
1.09455264166289	4.97034001087071	-0.05828624760139	c
0.19012892955264	6.71759315313788	-1.80730815719891	c
-0.70919189123627	5.84154703637803	-4.11629170711384	c
-0.70785821066879	3.26261809754810	-4.66447104935984	c
2.16666458622091	0.09445743417278	1.18187936221376	b
5.21988167132573	0.29365610415204	1.65244962218041	c
0.91792768506014	-0.11381662758334	4.07096238693710	c
1.61987622210979	-1.79701265041150	5.05785635147312	h
-2.37333060172354	-0.34472457892779	4.53332362097497	s
1.40689848320403	1.54771794494150	5.21101124958447	h
-3.82063099071171	2.31504507998498	3.06914376375202	c
-3.40118016793091	2.28663251743595	1.05178326999269	h
-3.04030504481366	3.99533289300467	3.97466072681938	h
-5.84290174612644	2.14635661662903	3.43745234025573	h
-3.15015383950131	-0.55118022580842	7.18538849635826	o
-3.49883808249425	-2.96765413518609	2.75388435554860	c
-3.09893283587214	-2.65303454715752	0.75667929670388	h
-5.52437341071823	-3.08756427441004	3.12376948753689	h
-2.51722236265910	-4.63708081151835	3.46204092961249	h
6.23224399131805	0.43501784145682	-0.15178231664557	h
5.95058838646124	-1.37369629217754	2.64766924593357	h
5.71279696112227	1.96682754148160	2.77579951966142	h
-1.59137789245870	7.50436020549517	-5.83509806843703	f

0.16104893836654	9.21507299155271	-1.30258729999910	f
1.92306414403930	5.88487996298719	2.20926849156298	f
-1.61691514559140	2.60182597252523	-6.96126051044504	f
-1.26700271221009	-2.27509959215151	-7.15559447300012	f
-0.53897667988601	-7.19812758339002	-6.41871017875914	f
1.45569166450792	-8.99456300537920	-2.02207513191972	f
2.74785953227236	-5.73570364070839	1.75019374416113	f

cat-F·ylide (Me-TS in gas)

-0.58599429250134	5.05037969041787	-0.71705795336787	c
0.31590988989510	2.61934715853492	-0.97186875636156	c
2.80312672205737	2.03211528987318	-0.12441839501663	c
0.87566681976193	6.97028750389869	0.34520835916336	c
3.30712466944227	6.39768563713144	1.16784717941758	c
4.27093983574058	3.94675699953413	0.94035430239314	c
3.34718957231780	-0.68310759203907	-0.55247254166811	c
1.21723644037097	-1.88316430685532	-1.67980012479626	c
1.31392704328288	-4.43114206097205	-2.21432323105824	c
3.45238103121110	-5.88117055092681	-1.68806200550020	c
5.53513449585520	-4.70699612760556	-0.59230611036860	c
5.49061650712159	-2.12553461725267	-0.02445556011596	c
-0.98388057903581	0.13484255279741	-2.06226473119653	b
-1.93712764911372	0.51730204614993	-5.29747147662411	c
-3.78621784267527	-0.46025780831395	-1.93965232680528	c
-5.20087701257166	1.02841350121969	-1.97664058573372	h
-5.00837183690761	-1.41713246668895	2.64665370171609	s
-4.50715265701341	-2.30785845823976	-2.47222966590747	h
-2.69131806001670	-3.80369479821496	3.49186466919566	c
-0.84354441796315	-3.23576643109111	2.76839233960394	h
-3.29797664680892	-5.56260536409110	2.60132793094070	h
-2.68563123447304	-3.99633743996350	5.54763687391474	h
-7.45215495191698	-2.05748784175771	3.89380477996546	o
-3.59313689732345	1.22709630733366	4.31460910615858	c
-1.70314401988664	1.56949925652303	3.55980800040446	h
-3.54603262264666	0.76570499296756	6.32660348800732	h
-4.80523965384991	2.86089872309584	3.97408291736497	h
0.02722460621156	0.66524347964986	-5.93030732815935	h
-2.92487290876403	2.28238301302243	-5.66209716612744	h
-2.80903939753759	-1.06846798438866	-6.27844693251834	h
7.59516665948389	-1.16909511519227	1.03840069040255	f
7.60885991613581	-6.07376383098037	-0.07031806649761	f
3.52597561432171	-8.36412056326520	-2.21014874689170	f
-0.70961452331780	-5.62076603829654	-3.26454872173565	f
6.63698000200498	3.58251060675997	1.80233083845927	f
4.73908698592997	8.22166213002811	2.19868608023329	f
-0.02279383853864	9.33123062193266	0.59200037577202	f
-2.96842576828229	5.64510988526530	-1.48072120666212	f

cat-F·ylide (Me-TS in THF)

-0.57358967202502	5.05113566552733	-0.73614219309178	c
0.32040894548758	2.61707340577308	-0.98945199386468	c
2.80145926973171	2.02484333519803	-0.12846410638796	c
0.88697482628486	6.96292036454888	0.33699122823528	c
3.30897928009653	6.38454753698076	1.17369802220801	c
4.26477167442736	3.93476334323902	0.94723980358458	c
3.34602434803763	-0.68794721678151	-0.55997810942353	c

1.22351594685034	-1.88415602578292	-1.70438285284454	c
1.33107385789413	-4.42902850760461	-2.25023834960573	c
3.46721339504341	-5.87568983068271	-1.71597803539046	c
5.53867853227942	-4.70638844324793	-0.60091089520393	c
5.48529783014011	-2.13116512834819	-0.02466432084798	c
-0.98218788223225	0.13440394736514	-2.09107751405886	b
-1.94672824500595	0.51858773598200	-5.30328166176599	c
-3.78090768879974	-0.46988935193506	-1.93577357657153	c
-5.20169053970648	1.01295153756656	-1.96837367261504	h
-4.97115242886731	-1.41025323287646	2.64769638127656	s
-4.50271890163211	-2.32074021862084	-2.45518990869295	h
-2.68312828979446	-3.79102151401189	3.53220506394783	c
-0.82702921510421	-3.20264435170961	2.84771990817671	h
-3.26429922360106	-5.54859829885552	2.62325697028327	h
-2.70381804571801	-3.97917238401220	5.58764849834891	h
-7.45479938606770	-2.06957265036484	3.85420339328584	o
-3.63015609218796	1.23852722033719	4.34171479998158	c
-1.73019653029282	1.58887366240818	3.61632929016081	h
-3.59622252438890	0.77175526796874	6.35208587134728	h
-4.85141106750343	2.86042745667885	3.98016839890308	h
0.00647588535880	0.61100631917098	-5.98230402548087	h
-2.90199036501998	2.30526633971368	-5.64894734628535	h
-2.88419507297052	-1.04389678987003	-6.26243244067554	h
7.59103075343096	-1.17704585179014	1.05774602615148	f
7.61688999481479	-6.07593657709343	-0.07036330531031	f
3.55114534781472	-8.36127684674429	-2.25286067161170	f
-0.67683912933481	-5.62436316936696	-3.32646441285412	f
6.63323799599580	3.56675917275070	1.82508682028923	f
4.74387815290909	8.20831273979379	2.21764062019923	f
-0.00633159536406	9.33255501069531	0.58015903017705	f
-2.94766414098012	5.66407632800093	-1.51431073397346	f

cat-F·ylide (Ph-TS in gas)

4.41546224006385	-0.91284459925723	3.08190292889682	c
2.20940125303030	-0.68706102869757	1.68035617898969	c
-0.03451198938123	0.29691474359924	2.82212164821360	c
4.49228540835723	-0.23797476302176	5.62365161428613	c
2.30412813866788	0.69727375860504	6.74724284979665	c
0.05646609762930	0.94563280731419	5.37251042568095	c
-2.18013463555004	0.21169131413882	1.05240240997490	c
-1.47548990465521	-1.07004081452507	-1.20441265454734	c
-3.25374764809132	-1.36486870939220	-3.08410193294588	c
-5.71385682590575	-0.44832790874727	-2.84574257676857	c
-6.38197131860300	0.84698315655641	-0.65567152100148	c
-4.62113358842547	1.19886868152315	1.27703786207972	c
1.48221422545686	-1.77705975372430	-1.24082423825230	b
2.46690477162085	-4.54791435206935	-1.95466649465891	c
3.09129495429223	0.64088569602921	-1.73620727479632	c
2.31328118281642	2.53278669550945	-1.50994068167923	h
3.50866781026536	1.71536043499982	-6.40724379135340	s
5.14802982179123	0.59731083655543	-1.67609135302714	h
3.32437082495025	-1.26406565612259	-8.08999067009509	c
1.66786134763724	-2.30166571291545	-7.43242153830645	h
5.05046293694874	-2.30212726829851	-7.64904109417031	h
3.21816823461634	-0.85019723176498	-10.11039446514593	h
5.54936447739897	3.27971433389824	-7.55568316680342	o

0.47504759786784	3.00991353484205	-7.35716416655302	c
-1.02976409265863	1.75725611989921	-6.70911602513059	h
0.46899789376745	3.19605654763777	-9.41383914945493	h
0.31672665686271	4.86383562120652	-6.46678017533816	h
1.88701335708184	-5.06744895471150	-3.87684274416495	h
1.66789186992452	-5.98451264400938	-0.69399886664046	h
4.52943432051791	-4.71102700719420	-1.85762329786129	h
6.55544561156596	-1.82007725080947	2.02814383062402	f
6.60626671526960	-0.50044886110853	6.99750280876560	f
2.33899334223065	1.31888779143382	9.19899438580775	f
-1.96703450312542	1.75643816697329	6.67795299173860	f
-5.40363201629486	2.53699630565382	3.29393208220691	f
-8.73499911715176	1.76871472316539	-0.41085743418423	f
-7.42325976593545	-0.77143285607155	-4.69454318385726	f
-2.64554354016045	-2.54547047369889	-5.29756295209641	f

cat-F·ylide (Ph-TS in THF)

4.40709912065817	-0.92633336471401	3.09037731051624	c
2.20665008780747	-0.69672644566986	1.68238654293496	c
-0.03284774557163	0.30485545214809	2.81735553367119	c
4.48647484455370	-0.22807018050625	5.62344584974830	c
2.30683892703213	0.73056023065742	6.73629652347237	c
0.06425504181657	0.97752216935551	5.35883673861341	c
-2.18006807061968	0.21325619139377	1.05145088543443	c
-1.48612540234928	-1.09346282693567	-1.19426513687851	c
-3.27012008848134	-1.40112665161507	-3.06696079291520	c
-5.72399724034846	-0.47218500291467	-2.83094818460349	c
-6.37965509499650	0.84852945140960	-0.65562804862562	c
-4.61519793891536	1.21168487163139	1.26759239495475	c
1.47037419876344	-1.80605708911369	-1.23579211598350	b
2.45091175385356	-4.57914529337257	-1.94511529648234	c
3.08431532818902	0.60627163063595	-1.70711169956800	c
2.31623692623906	2.50337129331715	-1.49880284293897	h
3.50315170595545	1.70879546651175	-6.41025076601054	s
5.14024951919526	0.54935796482839	-1.66477488654717	h
3.36082625982261	-1.22505356573208	-8.15266230426651	c
1.72760285001232	-2.29885163808297	-7.49306060084927	h
5.10767800396430	-2.24413983345641	-7.75178033864871	h
3.20723171552487	-0.77629671811478	-10.16196171687065	h
5.55142402576320	3.31888340279797	-7.53415449951433	o
0.48410690222602	3.02015523466539	-7.33329335042805	c
-1.00976886731176	1.75486186836841	-6.68323333901234	h
0.45568259833013	3.21329400854751	-9.38844250164173	h
0.32583573597145	4.86024836994891	-6.41590467506246	h
1.88657156351122	-5.08185676410258	-3.87673923894311	h
1.63975843999875	-6.01817805873814	-0.69318645791652	h
4.51343311647983	-4.73927254785044	-1.83911680463054	h
6.54486016401495	-1.86139469603287	2.05141970579666	f
6.60103341107023	-0.49349335471769	7.00377286386822	f
2.34352379738410	1.37582772743138	9.18603183443382	f
-1.95805677218479	1.81479340856737	6.66163003517973	f
-5.39612921341565	2.57503587859029	3.27661641543892	f
-8.73428614794474	1.78278584992540	-0.41237267646142	f
-7.44577700016153	-0.81210730399728	-4.67093589105675	f
-2.67499431114418	-2.60938371166365	-5.26772789997877	f

***o*-*t*Bu·ylide (Me-TS in gas)**

-3.49361810019650	-3.48528688090297	-0.00459407694058	c
0.45930739427953	-3.30451889203893	-0.00255962963446	c
5.17537378133044	-2.18867688051743	0.00686617684856	s
5.58875752324874	-0.02021956900434	2.62598297441667	c
-1.24338731245354	-0.96895164724370	-0.00605348303384	b
-1.09327275326417	0.91592782759571	2.44169080458789	c
-0.22120673707177	3.22575965990637	1.38071300020198	c
0.60360780343996	5.27238872350022	2.83391862182812	c
0.55808138356211	5.05981686104946	5.44181159568991	c
-0.39344587116949	2.86473735061471	6.53956548828762	c
-1.26712689360136	0.78654049344020	5.12916103493720	c
-0.22632303730753	3.22573284758763	-1.39795131409728	c
-1.09556259093199	0.91345470351535	-2.45570858533303	c
-1.27281476211684	0.78185677434741	-5.14285141997017	c
-0.40779851900039	2.86190237673608	-6.55587704767454	c
0.53742365202932	5.06116093700308	-5.46119139934840	c
0.58763704210448	5.27497132503570	-2.85357316509004	c
-2.51018908843739	-1.39251720450253	-6.65763106056480	c
-1.14169901049871	-3.93866513102649	-6.29048122211895	c
-2.50949502089055	-1.38301019676496	6.64678594278516	c
-1.14562913517647	-3.93252488286646	6.28502656333417	c
5.58709232873210	0.03542989045340	-2.56460931560307	c
7.34502324160039	-3.99506645676001	-0.01372755629772	o
-2.49955619878448	-0.90845114679310	9.52730612038942	c
-5.32050888782317	-1.57522711617140	5.88041289962407	c
-5.32140482769727	-1.58844116330102	-5.89277345586288	c
-2.49927688273202	-0.92321540937412	-9.53901438765175	c
-0.47111709169886	2.79851987795609	8.58220118374685	h
1.20955466798736	6.59901381141921	6.63520306894485	h
1.27866048796592	6.99313132719078	1.94189040174338	h
-0.48828856161868	2.79398459307256	-8.59834000367189	h
1.25792475381707	6.99861485487021	-1.96352140053081	h
1.18031352066806	6.60237200287875	-6.65664286178534	h
0.83884927779903	-4.37332616680574	1.70726826727132	h
0.84333996367974	-4.37658744878953	-1.70943038146520	h
5.40022833971915	-1.04449780927718	-4.31146265190358	h
7.48045156136232	0.84719661992460	-2.41364072121890	h
4.11202942951936	1.47605801899349	-2.45955388436537	h
5.43887035126999	-1.14702033890902	4.34676677816621	h
4.09198595221821	1.40092215913230	2.57409909984666	h
7.46829935102305	0.82289663790126	2.47499606587652	h
-3.63787984708728	-4.64970975702685	-1.68875240091815	h
-5.06089234755972	-2.13279720508717	-0.00585206411235	h
-3.63877492245376	-4.64743733957706	1.68107997530300	h
-0.58017282325816	-0.81448285750047	10.29751995841083	h
-3.50433481128893	0.82656552025145	10.03440443661682	h
-3.47021989217866	-2.48719631747506	10.44967466749443	h
-6.32090442469933	0.14219960592754	6.45738799171048	h
-5.55718112971237	-1.78219821679220	3.84790722634093	h
-6.21415865714656	-3.19315352946843	6.81888038382144	h
-1.33727230449155	-4.66751443085656	4.37560465332527	h
0.87096430464355	-3.74658612102926	6.71443857877150	h
-1.94755131826812	-5.34339710086926	7.57211662349901	h
-5.55923109152239	-1.79243422256973	-3.86010498983255	h
-6.32430762032423	0.12633214602035	-6.47328830517217	h

-6.21166312024911	-3.20943004451685	-6.82918860414698	h
-3.50824073779722	0.80813051874324	-10.05027291931757	h
-0.57949287590340	-0.82562924285662	-10.30778095099594	h
-3.46510360742426	-2.50620113150228	-10.45919895859792	h
0.87428945387162	-3.75034706575068	-6.72172283056136	h
-1.33059203631840	-4.66897446528365	-4.37904869985441	h
-1.94211454112958	-5.35420235948711	-7.57338972604992	h

_o-t_Bu·ylide (Ph-TS in gas)

-1.01943248027795	-3.06356578321970	0.17739048140139	c
2.17347644254217	-0.64906223852491	0.75434937292876	c
-0.05354180245268	-0.31952459072048	-1.27645207470713	b
0.58308741721878	-0.42256454115227	-4.26292028396068	c
-0.44818431013358	-5.70066946478856	0.01620899977436	c
-1.69548351142276	-7.32246992281004	1.70956695109223	c
-3.40379979133387	-6.47705884731193	3.52851070063785	c
-3.96827360374655	-3.92699624875889	3.70462045635691	c
-2.76866043919843	-2.24830190692283	2.06084766389362	c
1.23526651842913	-6.97550360376800	-2.00938548015618	c
3.91152843754926	-5.83701935316560	-2.19301852179214	c
-3.25105298984345	0.47847331121878	2.02438746732553	c
-2.06847461070032	1.72048354280641	-0.03835767809390	c
-2.66293247458205	4.32087938629872	-0.39225003288999	c
-4.17992942123900	5.54295468078830	1.41381589546355	c
-5.16831361644019	4.30281192364869	3.51893948007530	c
-4.74575956233451	1.73428688709829	3.80854503517225	c
-1.90220070700292	5.82829549378596	-2.76831228906293	c
-3.20076953311357	4.60052993922914	-5.07843882794793	c
-2.77405187453427	8.60703284925822	-2.71191149538738	c
0.99116619556869	5.88882176380120	-3.07786469396575	c
1.65521802779975	-9.81863992882266	-1.49159154864379	c
-0.14305209703621	-6.80188389243489	-4.58074756081087	c
5.10592615583650	2.33035711478086	1.85324511527258	s
3.19898164358766	4.77583440263164	3.27110486698192	c
6.87175122571220	4.11814306014020	-0.47611351844490	c
6.93407913496828	1.36238002107441	3.75088623256405	o
-1.34667600681231	-9.33541785601455	1.61798497032556	h
-4.29576821515779	-7.83375459861830	4.78664244589354	h
-5.32786845432995	-3.25182934959963	5.08600445759750	h
-4.63689892021954	7.52511651643126	1.17345139555088	h
-5.56921583608968	0.71996800572604	5.39268834314879	h
-6.31033848863908	5.33884703999334	4.87553173126140	h
1.66615949796610	-0.50140856156829	2.74910997156056	h
3.70242498479802	-1.99649259807233	0.48608497789452	h
8.05506391371518	5.46248614746077	0.55253435297292	h
5.57694961237126	5.06488875162594	-1.76742055023241	h
8.04105818100556	2.74886173250367	-1.48178494671390	h
1.74096990262590	5.35385394837137	1.93155037704567	h

***p*-NMe$_2$·ylide (Me-TS in gas)**

0.38932953791032	-0.21675646762938	-0.08184982697547	c
4.41861515056686	0.39446751718169	-0.03216532184868	c
1.68989161063592	2.36991964813331	-0.07668370856839	b
1.60143418047461	4.29413910035837	2.24528511846798	c
1.37432439323128	6.78238568591525	1.27634412924141	c
1.19870472696511	8.88596549053921	2.84955171287282	c

1.23631110545922	8.58119261330332	5.50149453397405	c
1.51865742416707	6.11001639677519	6.47868281164827	c
1.68937175259366	4.02737672503446	4.86574729084813	c
1.36223249048589	6.75429775944899	-1.51792816087897	c
1.57527043932999	4.24712856073990	-2.43441182987929	c
1.52369115797249	3.91161783781434	-5.04616262802319	c
1.28377501294362	5.95490179198985	-6.69910003980896	c
1.10265868268175	8.45595233596501	-5.77460394420849	c
1.11284138672438	8.82080415499173	-3.13023865283449	c
0.94132815218620	10.50287391722136	-7.42416295153385	n
0.24294590818891	12.96125558717582	-6.41393454681997	c
0.98300786007751	10.65359782481169	7.10680782546564	n
1.58566333188333	10.34798226926276	9.77227306228192	c
1.23829713296849	13.17955949991887	6.05164584364111	c
0.37616368304644	10.03244406980327	-10.07303744128628	c
-4.22053688946014	0.40367857715515	0.13514633162044	s
-4.58845356214088	3.37320390368429	-1.52530391550243	c
-4.52474508346471	1.61336593277921	3.32624585050697	c
-6.44590518413694	-1.23585761875596	-0.43237897029547	o
1.65699742270178	2.02303159642848	-5.85744293716248	h
1.24244481945963	5.60243301514413	-8.71696827116257	h
0.92324308476206	10.70591553876282	-2.34697632344198	h
1.90857796193823	2.16359502027091	5.71592295613692	h
1.61753150210905	5.81120769121811	8.50308978805762	h
1.04518343671158	10.75786018760990	2.02819560078442	h
0.23762658164291	-1.32147584039285	-1.81401751376249	h
0.31539079476213	-1.39682665620714	1.60641349725240	h
-4.40337973730921	-0.01111271057239	4.59251779180411	h
-6.37127654691082	2.52187657104239	3.49738457890944	h
-2.97326885015555	2.93164426263944	3.68001363701248	h
-4.33418106730161	2.98757247662756	-3.53402301429984	h
-3.13758006430825	4.69056198744757	-0.87894087495222	h
-6.49830878867918	4.05869045321634	-1.13965566723436	h
5.72053310677648	1.98085216394151	-0.28783842014201	h
4.69025798079855	-0.93170542172345	-1.58801082597344	h
4.78376142656062	-0.51429850566944	1.78047716948418	h
0.95758272097135	14.55535571952884	7.56332638188172	h
3.10598750393415	13.50776615983120	5.18790677175298	h
-0.20813598613991	13.51352344253064	4.60915418139146	h
3.56430239282334	9.77834271156908	10.09160244059612	h
1.25186743172695	12.14378008078249	10.73173490632716	h
0.35561798870774	8.92597162530813	10.63723775995034	h
-1.46422021534631	9.09485166229075	-10.35119064295307	h
0.35519269612311	11.83778583376417	-11.07178775358923	h
1.84073110891473	8.84796647828267	-10.93011495336082	h
0.24682707149138	14.33226516629884	-7.95573622045818	h
-1.64250661573200	12.96319884139234	-5.52455326853345	h
1.62266424080075	13.58474324780260	-5.00259008885116	h

***p*-NMe$_2$·ylide (Ph-TS in gas)**

-0.08543103217891	0.02738777493129	0.10423970376286	c
3.93073224068676	0.14624207369111	0.30122131126528	c
4.71552032868404	2.66875849675229	0.32760586290776	c
6.50888881641774	3.52462731484865	2.05038141629254	c
7.53354488106082	1.87398379462844	3.89310352515370	c
6.74081482724268	-0.68014111382631	3.89317111096718	c

4.96132600283849	-1.51378185363694	2.14893441542682	c
1.95900533271780	-1.47901710667427	-1.52701914150374	b
2.45373374640057	-4.25746908660167	-0.36630274599381	c
4.03641015901590	-4.11091553027970	1.78966922184825	c
4.61952592216172	-6.21555344766556	3.26690439396604	c
3.68902567661197	-8.62143243765320	2.59423300095070	c
2.15047383234736	-8.79879597968079	0.41874439367620	c
1.57055190996491	-6.65625191416118	-1.01474824545940	c
-4.14661940337861	-1.35220066881355	-0.36056859810546	s
-4.00768204363602	-4.10749226374224	1.65578512052283	c
9.26893590414094	2.73880988479465	5.64975609577512	n
10.54682309133019	0.94292208317520	7.29147640193442	c
4.31600688086016	-10.76730740252852	3.99668953102824	n
5.42733050039056	-10.42388889176318	6.48688410999672	c
2.07472198836073	-0.97670575812992	-4.53162557742577	c
-4.21418797794935	-2.91059744076061	-3.39925741128998	c
-6.60249424412478	-0.03429748401092	0.03491187714892	o
10.35956252006604	5.24644339009127	5.36346946880395	c
2.87476876480750	-13.07220471593511	3.58797410200269	c
3.95613444275214	3.99959265463864	-1.04473934821159	h
7.12251407806792	5.47712131473345	1.96655143699808	h
7.55959890703231	-2.01066705716189	5.22064119673720	h
0.40979136991690	-6.92263980464329	-2.69656574400141	h
1.42347816315091	-10.61941516362479	-0.17824988921788	h
5.81704332026501	-5.99715023029058	4.91687438985045	h
-0.23131719776536	-0.31336302696712	2.13263770426935	h
-0.51569897573339	1.99185876557840	-0.36447570628700	h
-2.52898437238210	-4.08294745895169	-3.57362793898371	h
-4.21307469257721	-1.43009696419047	-4.83330989225503	h
-5.94946351802622	-4.02518980623110	-3.49362810612075	h
-4.06033597699436	-3.40857499826421	3.59655756712716	h
-2.23471261767527	-5.10512196847216	1.28643838553612	h
-5.65997522412632	-5.28213180444811	1.26611250218949	h
1.63171873456227	0.98933945874622	-5.03736165760774	h
0.76978641818866	-2.17920011518754	-5.61312650586809	h
3.97101676030770	-1.38000208717398	-5.26697952055114	h
4.19010957701161	-9.36090059343866	7.78574422386020	h
5.80223912467274	-12.28167600990835	7.30273082849881	h
7.22994305067927	-9.41676076214979	6.34483669180175	h
3.61670927451674	-14.54172972977625	4.83200535988197	h
0.84011768857116	-12.83350203462890	3.97686341104623	h
3.08630287319789	-13.72701601310802	1.63630544677681	h
11.78373033515286	1.98385955055888	8.57194561816313	h
9.17601505522184	-0.10799852754892	8.43467576133047	h
11.69430877363653	-0.42950844837966	6.22725670216002	h
11.65093207715397	5.58680033025375	6.93492889941314	h
11.41224755136263	5.45357023942655	3.58055045210447	h
8.88479353208065	6.69969612509061	5.41780306120054	h

***p*-Me·ylide (Me-TS in gas)**

-3.98075310329868	-3.25534763930630	0.53262093545210	c
-1.54608676961454	-2.29577316270493	0.83347165037378	c
0.37570656954437	-3.18458612494027	-0.80971648738644	c
-4.50210187365184	-5.04373965969610	-1.34316375498339	c
-2.60088721196600	-5.91937355276166	-2.96878396282791	c
-0.14829169043025	-4.96372814675289	-2.68715170414561	c

-5.51241573861830	-2.61538500300537	1.75123541724233	h
-6.41324840049425	-5.77290608033806	-1.55788189325746	h
1.33735876474718	-5.62215436773619	-3.94976808896032	h
2.81469969557940	-1.94963959084980	-0.23951862689048	c
2.55282992988045	-0.22087000258485	1.79460862735316	c
4.69016436144742	1.09984841327017	2.58496254719591	c
7.02130769051761	0.73631534478081	1.38746482248899	c
7.27370920874847	-0.96012014050376	-0.63008673814444	c
5.13731469331370	-2.30253109886206	-1.43805383028089	c
4.57068718801900	2.44218711687481	4.14242873038539	h
8.67301523660527	1.78284011560134	2.02442735912669	h
5.31371685797486	-3.62290881686442	-3.00690404434376	h
-0.34484849061584	-0.19868825546553	2.64268649138720	b
-0.75796073711746	-0.82031228831243	5.92944500614901	c
-1.76390897330672	2.18501061529367	3.42876662010235	c
-3.80628575087808	2.17761598412394	3.69099349494249	h
-2.19257322604807	5.03852526123549	-0.32780745261700	s
-0.84021711154365	3.70700781708278	4.46478885667011	h
1.09108992456661	5.73469570499294	-1.02284281089876	c
1.69331120140522	7.16438817129280	0.33705737307525	h
1.19860972812577	6.48004074140706	-2.94570098364254	h
2.20137962822855	4.00867042322617	-0.79290489171186	h
-3.73181937605178	7.35154893261991	-0.81625240142977	o
-2.74408094261565	2.79988373824973	-2.86092357643883	c
-4.68871845676521	2.14191712045333	-2.67264879397579	h
-1.44438926810152	1.20979886415706	-2.65971756101881	h
-2.47970023080927	3.80345250959049	-4.64646624604828	h
0.01612303969441	-2.73142159325493	5.76280345753774	h
-2.67971007531855	-0.95433109007282	6.66220009874799	h
0.43723645725385	0.29841038102169	7.17867465634022	h
-3.17504420004335	-7.89364749931192	-4.94719264129847	c
-2.98134154503236	-9.80458093026409	-4.16351952773456	h
-5.11024393843308	-7.70919472926980	-5.65475657288203	h
-1.87728657271390	-7.74682970703371	-6.55127274510056	h
9.80547752166995	-1.37621761728211	-1.87895349348610	c
11.11040848463120	0.17205217058425	-1.46033326773679	h
10.68123092126894	-3.13361864916547	-1.21083161220753	h
9.61434059494623	-1.52847524548912	-3.93439429427206	h

***p*-Me·ylide (Ph-TS in gas)**

-1.47304301184691	-2.77930931562947	-0.24514043536042	c
2.21735737597912	-2.22780768545161	1.04265340751713	c
3.46864000781676	-0.11538037595771	-0.05387221715267	c
5.91485501985112	-0.37302453649207	-1.00016532005691	c
7.15956845714427	-2.71053933214670	-0.89929966309210	c
5.90546110922934	-4.78936607894610	0.16469044652852	c
3.44700301258241	-4.56186601964935	1.09647781609004	c
-0.59478140442666	-1.24161699477093	2.15458610773177	b
-0.31130396303208	1.72675612716032	1.52413932155512	c
1.94506226802307	2.19560476179684	0.15365436700309	c
2.53808302964339	4.60234697314758	-0.75424339098920	c
0.91997278168080	6.64247186385599	-0.28251265659945	c
-1.28099803133186	6.20494407852500	1.12276981167026	c
-1.88540286809653	3.78566127588494	2.01042783999644	c
-5.79035388264126	-2.24023809963632	-1.26056327615056	s
-7.58329308333852	-3.89621708173482	-2.66383783083639	o

9.83040565038399	-2.96435488293752	-1.86439949703333	c
1.57614112331524	9.26482675205822	-1.19803613645804	c
-1.40050205158603	-2.20924850846681	4.92443292433926	c
-5.62272022952955	0.80517256679991	-2.81078079377048	c
-7.26742967309161	-1.25763623700990	1.66310420204880	c
2.50635027316306	-6.21020949352734	1.88737468877026	h
6.86908199659006	-6.60293189965023	0.25255529804855	h
6.89328542546612	1.25068065512606	-1.80033446379214	h
-3.60057727099163	3.54851063599147	3.12619544977892	h
-2.52943689094532	7.78603429024095	1.53888200194904	h
4.27121768977629	4.91865094066446	-1.81849872042255	h
-1.02636999602044	-2.11661631718991	-2.14460104963966	h
-1.63289233969723	-4.83458749702138	-0.16706292870349	h
-6.06933605472307	0.15548593226874	2.56560194677647	h
-7.42156349051226	-2.93543940628071	2.85051202914760	h
-9.13572977631036	-0.50785487407565	1.20491599514684	h
-4.84545801716337	0.45894869037786	-4.69054680282805	h
-4.36802424616720	2.03321941961843	-1.71954398307489	h
-7.53330377732298	1.57491245001496	-2.95126659345156	h
-1.54498183033364	-4.27735793183696	5.04434071108769	h
-3.23354030349391	-1.44369107573735	5.53287970247539	h
-0.02133298687447	-1.60855266370506	6.35028014371609	h
10.10822370743010	-1.87110583597848	-3.59923206142962	h
11.18773894465415	-2.25571418879013	-0.46515920459938	h
10.30344523009851	-4.93908524162303	-2.25164870177789	h
2.32728902210577	9.22192167812950	-3.12645920134375	h
-0.08125795738954	10.50096539533009	-1.17554159862292	h
3.02315379182413	10.13330202194557	0.00734033423932	h

***p*-Cl·ylide (Me-TS in gas)**

2.78535921381509	-4.85921336397176	0.58703884234431	c
6.14936801597828	-2.68771957295863	0.35745646699518	c
2.84355187922352	-2.00725306392020	0.20774220686427	b
1.96111551529074	-0.67216230071127	-2.35175046544345	c
0.72656557088148	1.62087676634376	-1.71850230184709	c
-0.33717051781832	3.17603795200639	-3.56628748367782	c
-0.14782567132935	2.41624050388276	-6.08174483339503	c
1.06101893071947	0.17719016845100	-6.77512388337275	c
2.10738460839946	-1.35523957499329	-4.89185169634741	c
-1.76132491820405	-6.26511781813822	0.99287465174089	s
-3.37603079701216	-3.99986445686686	-1.00797265839462	c
0.73390445983431	2.01666945627297	1.04443361637946	c
1.98055602950738	-0.00251034755655	2.29240530920040	c
2.17870889823158	0.08038738629199	4.91942392196869	c
1.15426623491297	2.08873292158789	6.30100044557672	c
-0.08017070732158	4.03038649027437	5.01208109489162	c
-0.30906706647220	4.03527187208727	2.38735461606273	c
-1.37601722325497	6.53506372278014	6.74238376377672	cl
-1.46827274568683	4.32546113482321	-8.44007981545490	cl
-2.62197388036369	-4.90192744028814	4.02110235226853	c
-3.03027924171506	-8.76889886203261	0.73265336262821	o
3.04184657173409	-3.10003819579869	-5.45485972813546	h
1.17283499542859	-0.34357997253728	-8.75475600535087	h
-1.29234276673815	4.93013204703644	-3.09853675740530	h
3.14013581699256	-1.42368168716484	5.94406128399532	h
1.30634202754948	2.16240622618013	8.34404806831144	h

-1.27388259564041	5.58392608712920	1.45010634577864	h
3.07203204757416	-6.15510238946975	-0.98601768328863	h
3.18275069882408	-5.72654811444470	2.41174705805396	h
-1.83090633835044	-6.13564860670857	5.47323043665167	h
-4.68230667552713	-4.86511725310347	4.15452752024498	h
-1.80734511569124	-3.00872102238102	4.15344381150651	h
-2.97022820690068	-4.51503498224763	-2.96213176097739	h
-2.65187890042551	-2.10901762754505	-0.61309126686121	h
-5.39740087265671	-4.15148515251955	-0.61343430003783	h
6.66591191622686	-0.79449159183616	-0.29637350227821	h
6.96502546719326	-4.06207152549905	-0.94437948321750	h
6.83973220600068	-2.98084884537037	2.27407636310994	h

***p*-Cl·ylide (Ph-TS in gas)**

-3.72989414822525	-4.58236765245627	-0.62175117479188	c
-2.70024994051172	-2.15081371015192	-0.63440096241684	c
-4.06921587182498	-0.13436341533829	0.50051788416539	c
-6.11093052720507	-5.02523445271430	0.42130540844078	c
-7.42078128172809	-3.00991156320579	1.51425079854046	c
-6.44145517617925	-0.56239700734619	1.56891574180348	c
-2.69591036643610	-6.15120447342244	-1.45356059785416	h
-6.95184305692010	-6.89396545874838	0.39951978581811	h
-10.39324494035012	-3.56742609650250	2.83517944223685	cl
-7.54317373275925	0.95603516197030	2.39799252192342	h
-2.76301708778657	2.29340210783518	0.19084036903622	c
-0.55610330258374	2.00269784132615	-1.30008124862803	c
0.81647341182976	4.17645084115290	-1.89453167210162	c
0.07971284161643	6.55472417344949	-1.00245275958287	c
-2.06728782408918	6.75035731583654	0.51662343029551	c
-3.52429789953183	4.64504158523927	1.12408245540825	c
2.47586428560580	4.06642517930211	-3.10706017964253	h
1.13761223603677	8.24383710698617	-1.48442573166501	h
-5.20725684791611	4.86587613766824	2.27615983980682	h
-2.96973159862440	9.72369407347368	1.65569637867737	cl
-0.05167123641023	-0.93329754186616	-1.93222334475207	b
0.66181203620158	-1.86298320753563	-4.73576063360526	c
1.04506607032778	-2.36527679248363	0.42709673518323	c
0.69713173628807	-1.69745886245438	2.34450207971893	h
5.46613867989059	-1.49678271200484	1.19794426732567	s
1.38311420095040	-4.39840249373700	0.36527073153714	h
6.71237942000596	-0.47615606751894	-1.82198686222833	c
5.36914319140392	0.82336637079837	-2.69087045550921	h
6.92716190803074	-2.16691344404000	-2.98151379463175	h
8.54230299793425	0.41843360627547	-1.48456865691394	h
7.43972339693716	-3.00753926278382	2.51888458676912	o
5.20227032547222	1.56396558370230	2.71036280010568	c
4.56425926375597	1.20692087554201	4.63983716887225	h
3.80946955122845	2.69398195704874	1.68464458053726	h
7.06467066057030	2.45498196179673	2.72157222489800	h
0.96876728899149	-3.91271955171176	-4.84979472198205	h
2.39134712543294	-0.95764471650767	-5.44587291583981	h
-0.83685299572779	-1.38924636201371	-6.08612560151489	h

***p*-NO_2·ylide (Me-TS in gas)**

-0.44081926371944	0.07684681125185	-0.01000390383616	c
3.50492657190699	-0.15138911455893	0.02921699384925	c

2.07899881935010	2.33813559260975	0.04371308409942	b
1.95607391897559	4.24647247181960	-2.28908891051933	c
2.00755658813327	6.74983039280427	-1.32074429722500	c
2.00746051413894	8.83843014587611	-2.92542912702330	c
1.93905386291216	8.38393392425004	-5.51785926435315	c
1.86298067595800	5.95812934761477	-6.54347544172358	c
1.87207581080255	3.89189934631955	-4.90301166654395	c
2.06981715812736	6.73351756526395	1.46881139293041	c
2.07043092839067	4.21813750128503	2.40497541829650	c
2.13850133228027	3.82986733394821	5.01342302439379	c
2.21018912777810	5.87651622900271	6.67681564593813	c
2.21943167531910	8.31580921738935	5.68065088388707	c
2.14959414519365	8.80350125712686	3.09421407534691	c
2.31336927812810	10.48326687130689	7.44535142107477	n
2.33569977638702	12.62656468716462	6.52357960404692	o
1.94923899295056	10.57306581455263	-7.25882416651486	n
2.01485113796550	12.70460511142942	-6.31345778862623	o
2.36723001444115	10.01868449560335	9.73144333264244	o
1.89630960519062	10.13521822804460	-9.55041662245803	o
8.25477504029061	0.79170874081841	-0.26698029775945	s
8.48872659067863	3.80288975387561	1.35864111400214	c
8.55873476116552	1.97711222130236	-3.47474316873830	c
10.53308202712835	-0.74628916940590	0.35004459593308	o
2.13709395371880	1.92481736796539	5.78746319862227	h
2.26205688884572	5.63037978289181	8.70897313479682	h
2.16114268985219	10.74477156263419	2.43850957788965	h
1.81141236921924	1.99633600544846	-5.69886855280107	h
1.79875880324124	5.73753818930251	-8.57817236604958	h
2.05530471479936	10.77120610281155	-2.24670862780293	h
3.83659648064925	-1.21278889920662	1.75940821477901	h
3.68689223210786	-1.30359281221694	-1.66589253080637	h
8.53931058558988	0.33178857599632	-4.71935404152526	h
10.35900128999330	2.97569302996385	-3.63391862911518	h
6.95784851247239	3.21560334296628	-3.88389814209884	h
8.25789713814842	3.42614908342110	3.37230545333931	h
6.98928967004094	5.05470212341330	0.69476092986702	h
10.36227837874880	4.57951220988488	0.97048387379032	h
-1.82782000827135	1.44541655852819	0.68242590647561	h
-0.46664111044135	-1.54059801464763	1.26876706956945	h
-0.88412449220472	-0.49757532281323	-1.93405973317556	h

***p*-NO_2·ylide (Ph-TS in gas)**

-3.53725229190590	-4.47362690992825	-1.32569722347386	c
-1.78392861219057	-2.49905817917131	-1.23571111325561	c
-2.54751289513931	-0.05904019549392	-0.40142032795180	c
-6.04926321396033	-4.04683269609263	-0.65939507127688	c
-6.73901778426543	-1.63644620877629	0.15176807569833	c
-5.05055326507324	0.37754817769895	0.29258374231370	c
-2.95986954313297	-6.34592728776104	-1.93951191617664	h
-7.46738286333613	-5.52050037621336	-0.74627690120373	h
-5.72880888255457	2.21366386226252	0.89835527449788	h
-0.49591608633448	1.79579054341302	-0.59802653432428	c
1.66581595495482	0.71001394452766	-1.75693129336003	c
3.75353112348315	2.26444211077155	-2.21366312955683	c
3.73590880895572	4.80441440122102	-1.50258289146797	c
1.59180998736726	5.77582945290592	-0.31726943662661	c

-0.55201367198486	4.32354607352364	0.14546914124147	c
5.41549319357623	1.52230964002827	-3.17045768095246	h
5.32704355535739	6.04572949873856	-1.85212153639220	h
-2.17676694962355	5.19157596427525	1.04330685914633	h
1.27167767336113	-2.26167318191921	-2.24629788378924	b
1.91663928317805	-3.55262346549622	-4.91328549132844	c
1.47352200105676	-3.79572654840513	0.25685245540457	c
1.20540419386045	-2.92761093120933	2.10438058302139	h
5.94355916863501	-4.47806287083792	1.63873625941818	s
1.15094578491940	-5.83008750226380	0.29239507630369	h
7.80967595476149	-4.17953491887578	-1.22021136348968	c
7.13533212191290	-2.55389796452246	-2.29443175627121	h
7.53241370715279	-5.91526522561721	-2.29751766923517	h
9.78921200828042	-3.96793464268115	-0.67251996986049	h
7.07838443117148	-6.49519112169455	3.24031613168898	o
6.65334528783297	-1.42373488357252	3.02522684510411	c
5.72203385861568	-1.38667268385653	4.86589781885759	h
5.89369064203859	0.05737484211860	1.80204598589101	h
8.69898717412766	-1.25974382955662	3.25108499266688	h
1.53137370343025	-5.59054895454993	-4.93362664769542	h
3.91934615129813	-3.31356323428398	-5.40902530856642	h
0.82830881166594	-2.69889886663265	-6.45506844065925	h
-9.40858241004466	-1.18760336324482	0.88260101630427	n
-10.88699883484593	-2.98259279407319	0.71727122819809	o
-9.97898228495323	0.95107255478456	1.61350000866823	o
1.58669994387380	8.45935474412531	0.45919335230915	n
3.51435389605565	9.70979013786449	0.04830351883826	o
-0.34226419958441	9.28637322497913	1.47820446975564	o

_o_-CF_3·ylide (Me-TS in gas)

-1.65562182504369	0.47321067722915	-5.05906530256817	c
-1.85690942016855	0.33927709979284	-2.41168978502241	c
-3.85618972513491	-1.14450160731518	-1.42938416054558	c
-3.36521769023076	-0.80287569195261	-6.63027992406151	c
-5.31262888689291	-2.24243888089930	-5.59667225664546	c
-5.56435858763917	-2.42267298459060	-2.98550337213075	c
0.44453511245900	1.91233398581143	-6.33607756850091	c
-3.16978635651663	-0.66332576063416	-8.66455199584295	h
-6.62511167878025	-3.21770066145817	-6.83638685366900	h
-7.07967972438378	-3.54899341515322	-2.17732905453678	h
-3.84300399343423	-1.16047554305760	1.35185604944773	c
-1.83131717711170	0.30681481604110	2.34976797681746	c
-1.63608205034278	0.39865368503109	5.00541045298318	c
-3.35951171887130	-0.89213707679550	6.55154329208605	c
-5.31028807203141	-2.31182668565888	5.50007012500168	c
-5.55629499416269	-2.45444711475444	2.88824859559837	c
0.39919098317867	1.88029494964601	6.34879790889912	c
-3.16662419746579	-0.78501260325690	8.58725646441817	h
-7.07305243265218	-3.56250302906401	2.05813914426301	h
-6.62607164429817	-3.29934164075836	6.72644173454463	h
-0.27709640205677	1.43956859762674	-0.03605520665802	b
0.00542528503335	4.78879840508596	0.03170494118959	c
2.57973885563164	1.76050751829879	-0.13667659877738	c
3.54385086106973	2.14926034364684	-1.90635021702629	h
4.64148508107210	-2.63498967856797	-0.10125713037321	s
3.68091294357946	2.26361561876504	1.51925530401606	h

3.37526358344958	-4.11858266688101	2.72192889949098	c
3.73463190899971	-6.14777316121174	2.58952375462116	h
1.35829800415419	-3.70088802456785	2.85455743566956	h
4.37876998322519	-3.30194866170318	4.32546640811603	h
7.34310651249396	-3.39309296622714	-0.36941923849666	o
2.78892637287285	-4.39261975415109	-2.39251518312934	c
3.21747323252870	-6.39758516697631	-2.14570550240041	h
3.37261612454778	-3.74168597402026	-4.25774123745535	h
0.78604767346718	-3.99226003966650	-2.09526793432761	h
-0.27453988207272	5.38154732548347	1.97362427494912	h
-1.60510228198052	5.23334696263329	-1.17762006457431	h
1.63762075405958	5.77285793680884	-0.76593265975760	h
2.78177675411364	1.28753850992282	5.52745809932537	f
0.42161073206959	1.47464021519946	8.88180769603026	f
0.15744850183482	4.43171579670846	6.04416565437160	f
2.74419939151395	0.73013926979173	-6.06490748568862	f
0.76426199229181	4.28747435997813	-5.39937783159989	f

_o_-CF_3·ylide (Ph-TS in gas)

-5.61928635345457	0.06050092057591	-0.66753560244035	c
-3.06122941610412	0.21719489197706	-1.40349143325673	c
-2.49023302785592	1.40251201324701	-3.74497002014535	c
-7.51246332844009	1.05130041876188	-2.22280320519718	c
-6.89842205452788	2.25510765625159	-4.48789201622003	c
-4.39562651362490	2.41359966735120	-5.26897709589708	c
-6.50398354303208	-1.39317274846018	1.63572707790657	c
-9.47499910321812	0.87113427078602	-1.66669421705027	h
-8.39599260353287	3.03377221763909	-5.65506051388189	h
-3.93389649705316	3.29044666404214	-7.06717249394831	h
0.19594787455883	1.23682027674681	-4.39766966878416	c
1.55926936478068	-0.22541126894482	-2.61591675686975	c
4.12836384773091	-0.63444523780780	-3.13995488077908	c
5.27796083898170	0.38332646811742	-5.29976546345676	c
3.89123918826204	1.86329559806039	-6.97886500848571	c
1.33512130791474	2.29062455451397	-6.53572832150110	c
5.71883887116217	-2.29187867173442	-1.46564543946778	c
7.25924193217393	0.00933644225654	-5.66529626426345	h
0.24164282442368	3.42083015066127	-7.85720512218824	h
4.80522264377567	2.65340470024645	-8.63716585983744	h
-0.24041025743832	-0.94036804159096	-0.23126079340120	b
-0.30057901548237	-3.70550548710847	1.01358009904791	c
-0.69099770734712	1.49940370694364	1.37277861418190	c
-0.33917134805841	3.36692569772090	0.57676387324033	h
2.30075880034351	2.63302473546835	4.86290721824818	s
-1.99434168415742	1.55714734811033	2.95856768125650	h
2.98073978789880	-0.26813290969039	6.54842144232294	c
3.95500986812621	-1.57449517586030	5.28707171372743	h
1.15523583880215	-1.04570452342967	7.11158499563831	h
4.11628787677652	0.19996067097064	8.20860229662827	h
1.20898771190439	4.48602256550888	6.68033489053257	o
5.50328417437707	3.62270811241746	4.12672140813680	c
6.39770880038406	2.20880939961421	2.92389037348193	h
6.51900862612641	3.87416801027873	5.90755260667296	h
5.33397279329296	5.42374561049007	3.13524054203537	h
1.56335096593697	-4.22405779887772	1.75098465774630	h
-0.81076099579239	-5.15493831960741	-0.37442998248172	h

-1.63564866606437	-3.85646061551941	2.58443101045594	h
5.10958863399946	-4.77825613421870	-1.65179364958535	f
5.48137954504019	-1.68424589636337	1.05238781114006	f
8.23312199072463	-2.11979781802504	-1.97677361897427	f
-6.40208636586886	-3.93033745226969	1.22844079528371	f
-8.94438987877179	-0.85357889686419	2.23665591774604	f
-5.14093534735484	-0.93879151702354	3.77234189040538	f

***o,p*-di-CF_3·ylide (Me-TS in gas)**

0.65275283837144	-5.27006807285836	-0.13887051138626	c
4.42500843352097	-4.19160713171896	0.01108811991949	c
1.49189361425153	-2.53002972189158	-0.02898040622042	b
1.13263745243197	-0.62300596536045	-2.38916145084034	c
0.61270474475041	1.80339188199184	-1.38848918246901	c
0.14685423268837	3.89970673296555	-2.91659904335051	c
0.18933568595430	3.60293070077048	-5.53059302955313	c
0.69114091068222	1.24396321856167	-6.59220015505483	c
1.15361658990655	-0.84393253579370	-5.03779145162006	c
-4.27354410276871	-5.40234186284836	-0.06443646487434	s
-5.17882837529783	-2.96450762536720	-2.30718580814586	c
0.59625397956942	1.77708434069756	1.39130099563555	c
1.11436247357194	-0.66551676542383	2.37017205185276	c
1.12647755118328	-0.89909151786928	5.02388009071875	c
0.65112566763516	1.18254742893443	6.58511579284893	c
0.14716181389263	3.54762379993472	5.54204330007354	c
0.11312463038819	3.85962465873376	2.93197091886300	c
-0.46795036457541	5.73697486464891	7.25191510825225	c
0.13911410475515	7.99260998440563	6.18993289834077	f
1.66208147949237	-3.37002845905548	6.35656053522244	c
4.08951202969415	-4.17198966554817	6.02756807004406	f
1.58193306468097	-3.34562992120154	-6.33990029673608	c
1.93907482139576	-3.10834798438258	-8.86200173018025	f
-0.22057802625261	5.84998766265693	-7.22771557153880	c
-1.69589529540791	7.63722632065565	-6.12157078316606	f
-5.15326020832632	-3.71346787727632	2.79402793482098	c
-6.01902532966907	-7.59190560281242	-0.37553442586298	o
2.00205249391559	7.00197967338705	-7.83594734511219	f
-1.34288436588783	5.20175700178865	-9.44263536693823	f
-0.44169666757558	-4.94245070369569	-6.04847598496147	f
3.62431019249402	-4.61344762641683	-5.42669873569986	f
0.14799507158690	-5.29344124953722	5.52674069130192	f
1.29457100861667	-3.23009901362623	8.88652909033562	f
-2.98812474690974	5.83311310558765	7.79528666052036	f
0.76133586075265	5.59335311440389	9.49803848513629	f
0.70876415698584	1.03123911951640	-8.62802259841412	h
-0.25954802508703	5.74010982252403	-2.10805987308764	h
0.67838074489152	0.96259985830462	8.61927652090299	h
-0.27512083467759	5.70683963498245	2.13009285596255	h
0.57915090514150	-6.29549286640722	-1.91398558635861	h
0.65618348996323	-6.48529658060786	1.51221168027888	h

***o,p*-di-CF_3·ylide (Ph-TS in gas)**

-5.09305340926633	-0.71066644093754	1.50456264010101	c
-2.52202612730857	-0.57082355253895	0.81139515839110	c
-1.92926673190845	0.00763971515442	-1.74098911670883	c
-6.97611499538911	-0.25921379554410	-0.28566008376603	c

-6.33530125861283	0.38065731265616	-2.76574805623373	c
-3.82047806213427	0.48410967175133	-3.51722824326800	c
-5.99251331628880	-1.60798302554460	4.07765075175713	c
-8.94770412664423	-0.40106184612319	0.24623007132577	h
-3.35423760926994	0.91636740526699	-5.46622374451734	h
0.78095164265044	-0.15664300146549	-2.28068810286479	c
2.15993488759295	-1.05080764505019	-0.16878155251776	c
4.76950800713342	-1.38448317805689	-0.51050938050007	c
5.94039949571354	-0.84800833882657	-2.81805483365349	c
4.52202885234505	0.07406194728349	-4.83953590772497	c
1.92639271414486	0.41994475049860	-4.58537359579972	c
6.39857725453664	-2.42478245214873	1.57949367841538	c
7.95629925904278	-1.13289796124649	-3.03790695658433	h
0.83601186259536	1.13087238482977	-6.17038102183336	h
0.33837610752834	-1.29164188617931	2.28315871264346	b
0.34429575541063	-3.69630617156209	4.12189412668047	c
-0.34712814091560	1.40762300539365	3.21092014678167	c
-0.03757047079476	3.06246739388305	2.02489857332809	h
2.46573260664668	3.59108036540919	6.52783167677558	s
-1.67659322042893	1.76450904795035	4.73205726031746	h
3.17655035905465	1.20594621400383	8.88304576840046	c
4.33365979611569	-0.27149370109383	8.02982246864871	h
1.36192305852528	0.43336803977940	9.48698718550850	h
4.13715292246976	2.12343995403840	10.46427545963354	h
1.10668831767612	5.70987900130055	7.79227976123118	o
5.66227523623104	4.63725942787715	5.83298544834234	c
6.73937458643652	3.06808389416269	5.04145468530011	h

Appendix C

NOE Analysis for Structural Determination of Cyclopropanation Products of (*E*)-Chalcone Using Diethylsulfoxonium Ethylide.

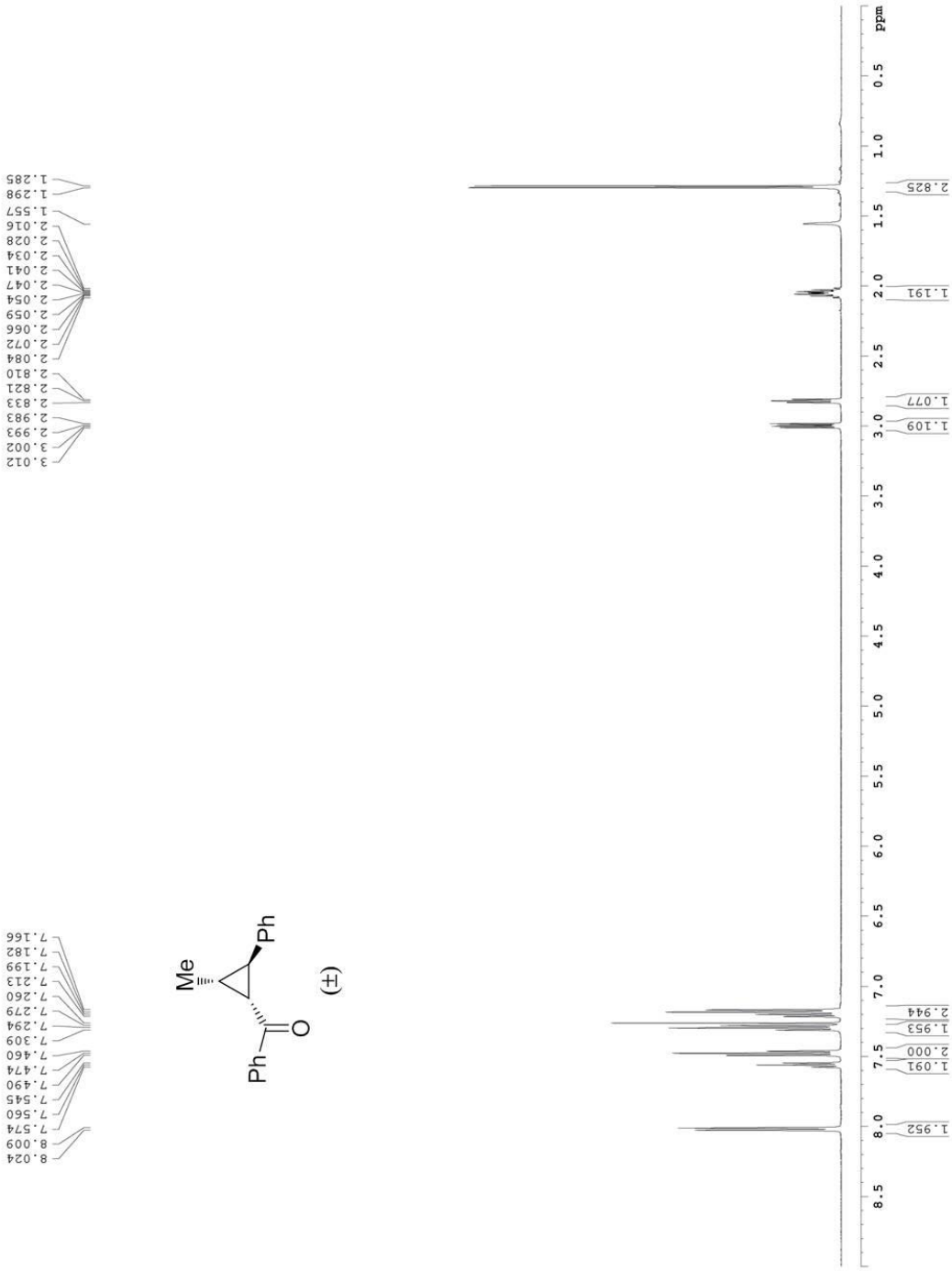

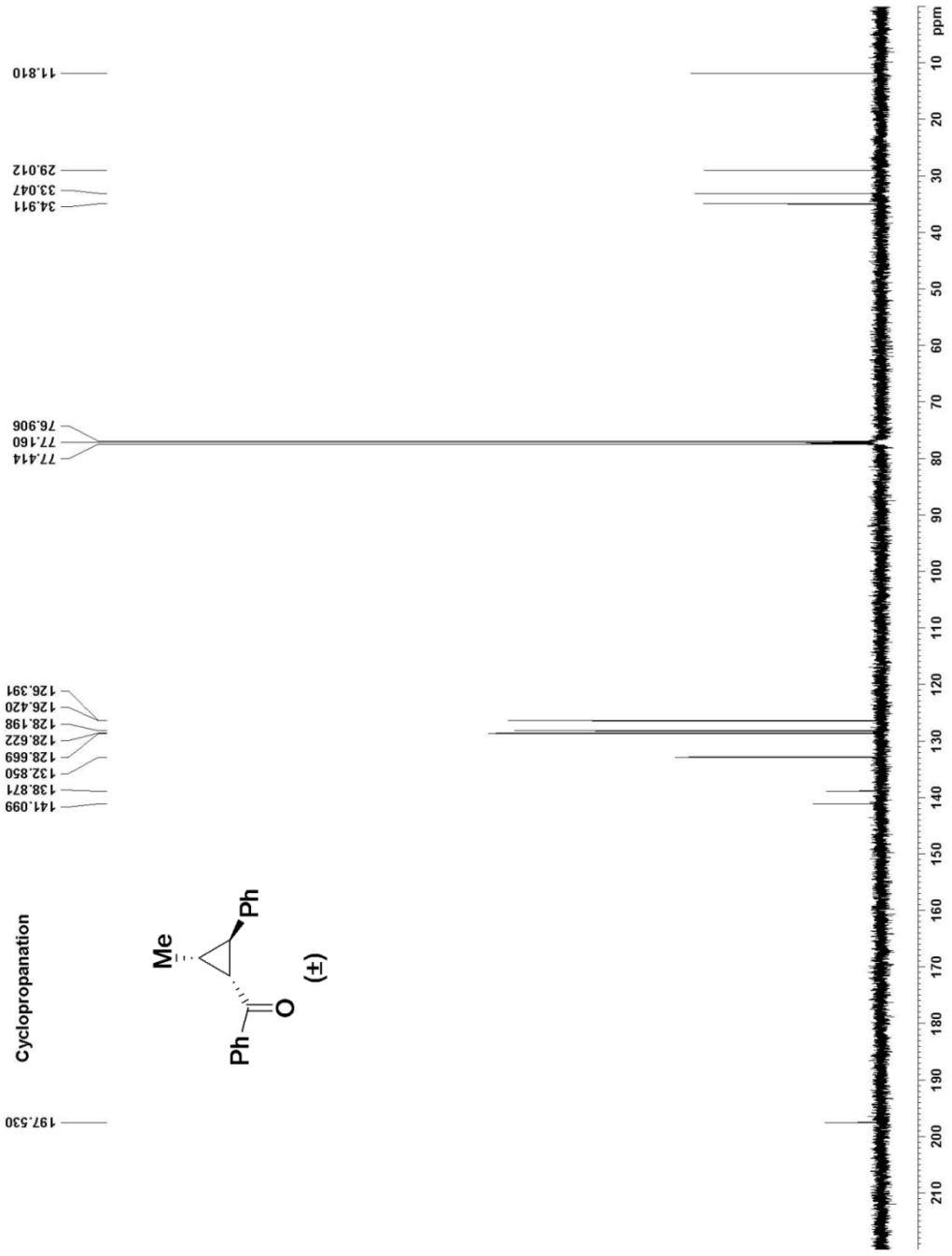
Cyclopropanation
Me
Ph
Ph
O
(±)
197.530
141.099
138.871
132.850
128.669
128.622
128.198
126.420
126.391
77.414
77.160
76.906
34.911
33.047
29.012
11.810
ppm

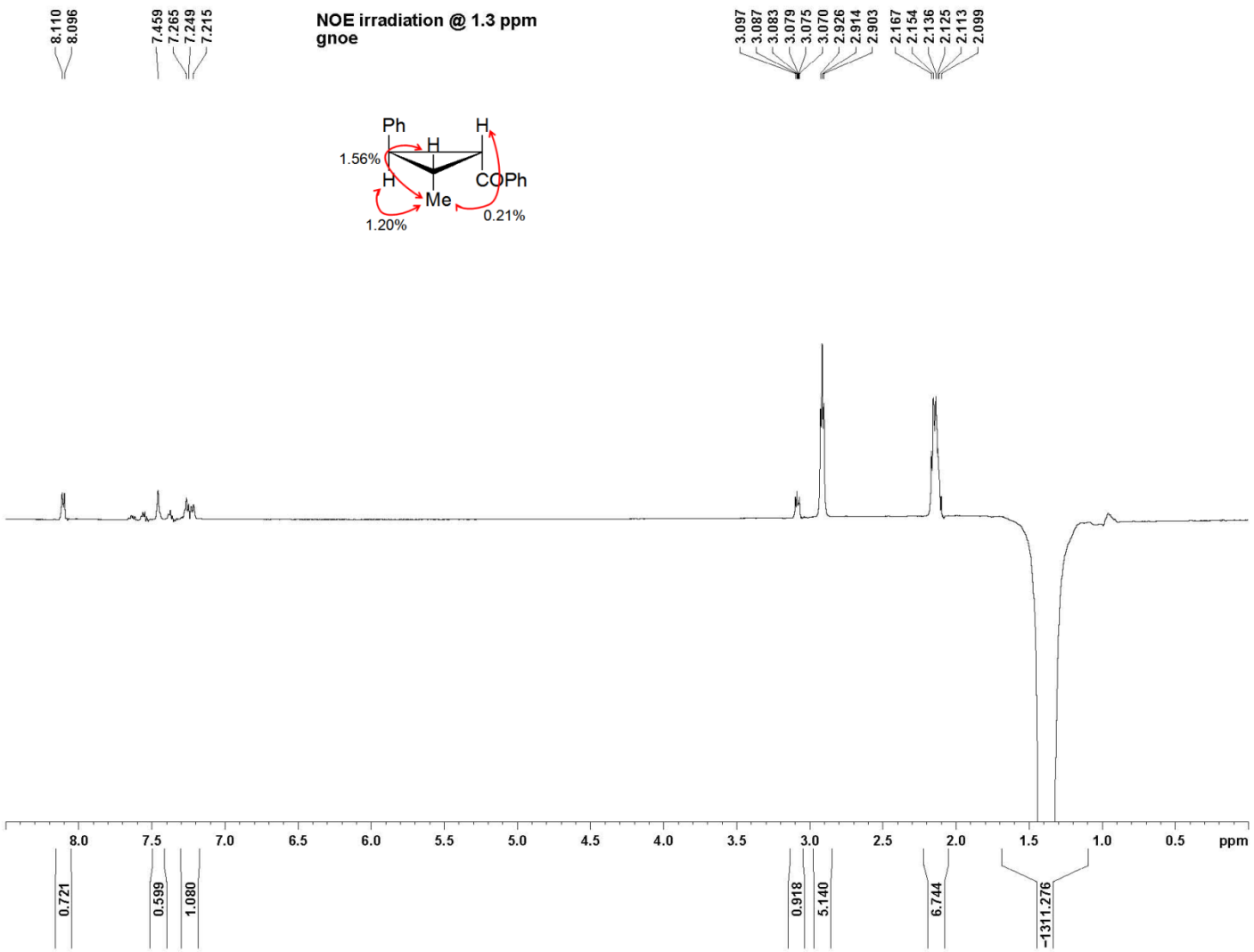
8.110
8.096
7.459
7.265
7.249
7.215
NOE irradiation @ 1.3 ppm
gnoe
3.097
3.087
3.083
3.079
3.075
3.070
2.926
2.914
2.903
2.167
2.154
2.136
2.125
2.113
2.099
Ph
H
H
1.56%
H
COPh
Me
1.20%
0.21%
8.0
7.5
7.0
6.5
6.0
5.5
5.0
4.5
4.0
3.5
3.0
2.5
2.0
1.5
1.0
0.5
ppm
0.721
0.599
1.080
0.918
5.140
6.744
-1311.276

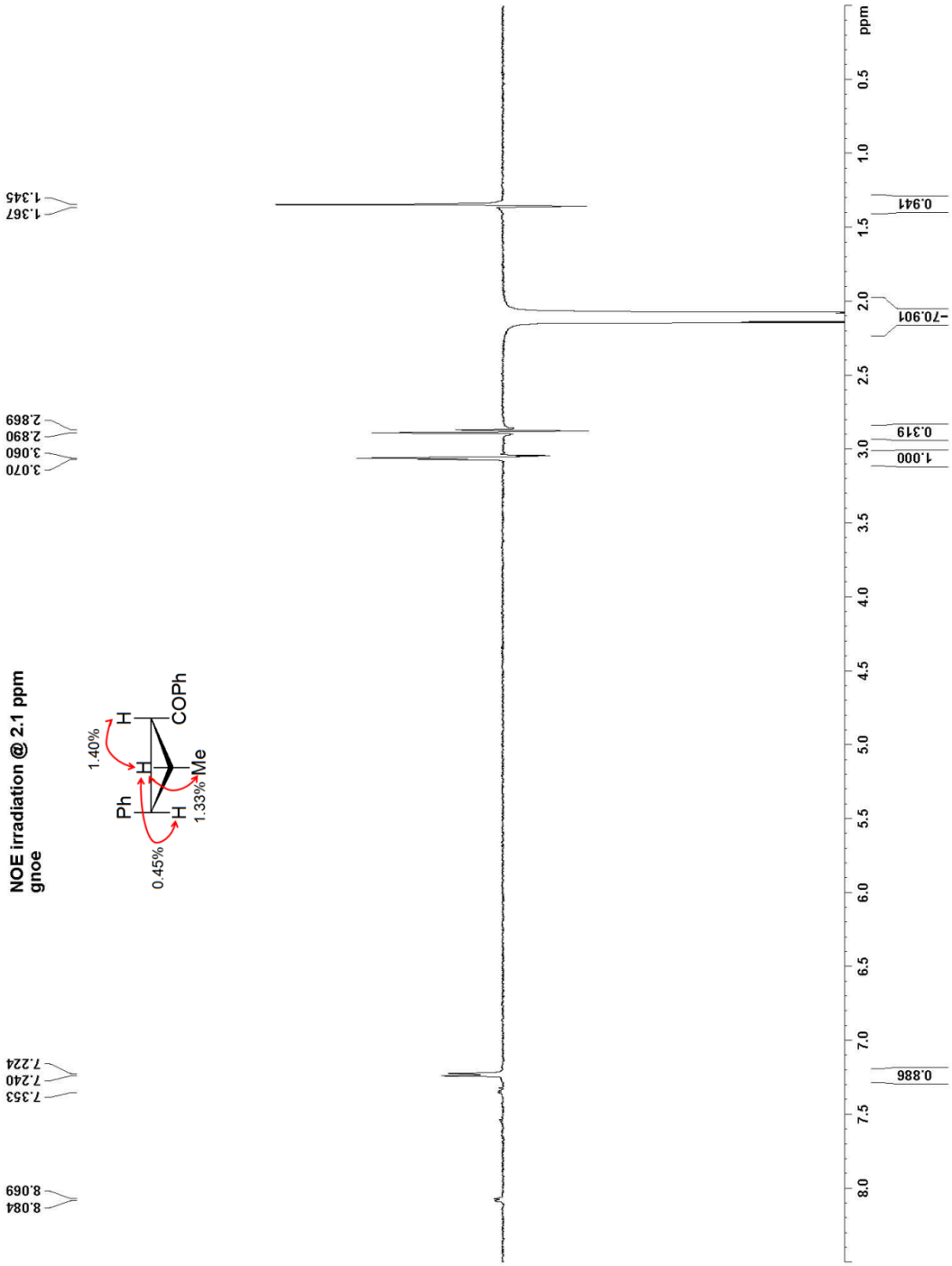
NOE irradiation @ 2.1 ppm
gnoe
1.40%
0.45%
1.33%
H
COPh
Ph
Me
8.084
8.069
7.353
7.240
7.224
3.070
3.060
2.890
2.869
1.367
1.345
0.886
70.901
1.000
0.319
0.941
ppm

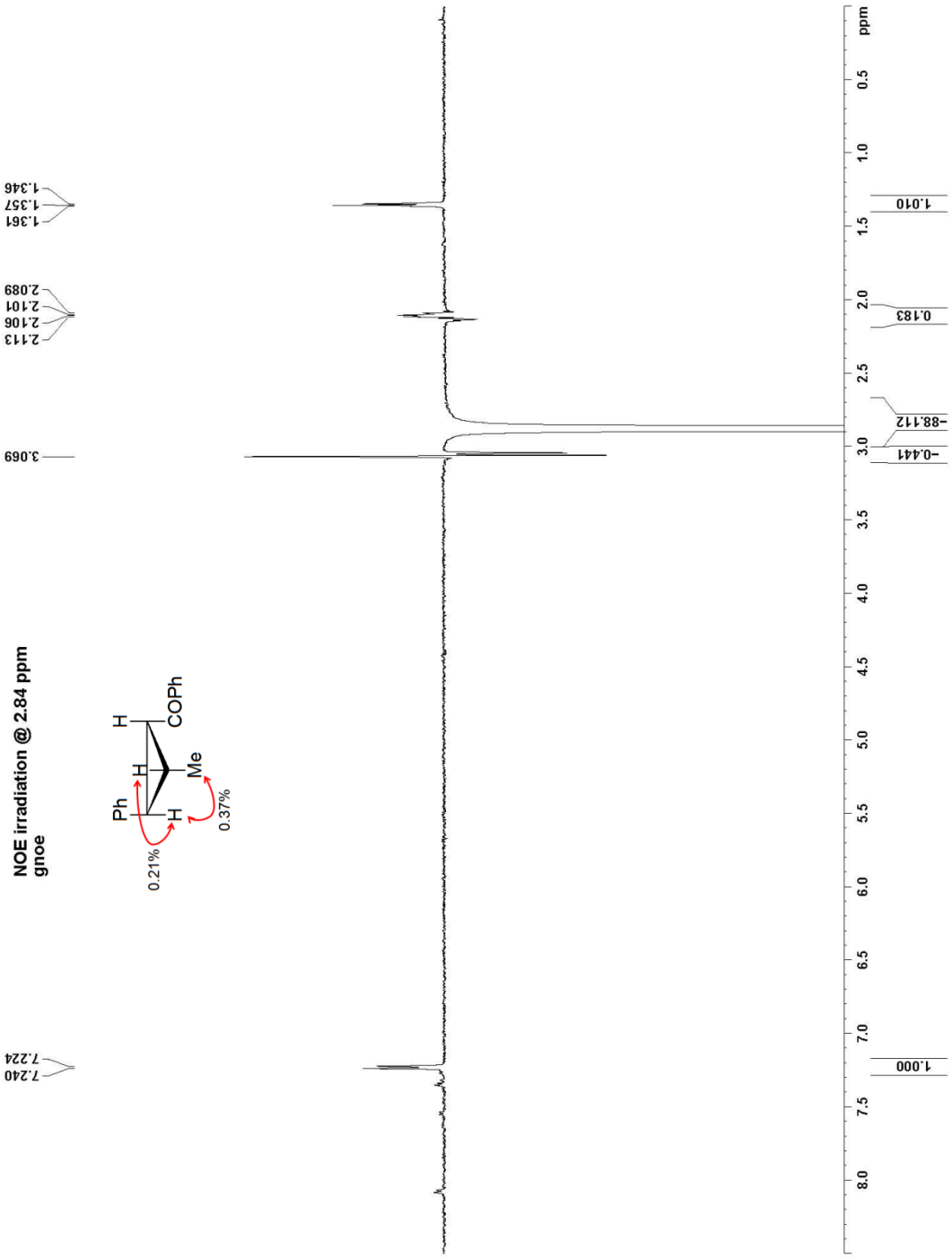
NOE irradiation @ 2.84 ppm
gnoe
H
COPh
Ph
H
Me
H
0.21%
0.37%
1.346
1.357
1.361
2.089
2.101
2.106
2.113
3.069
7.224
7.240
1.010
0.183
88.112
0.441
1.000
ppm

Cyclopropanation diastereomer mixtures
1H spectrum

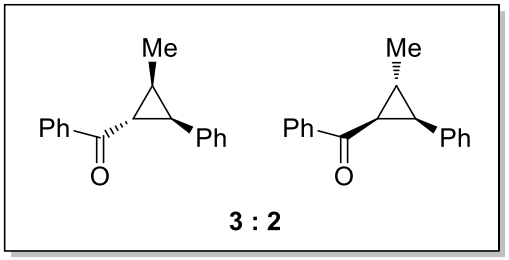

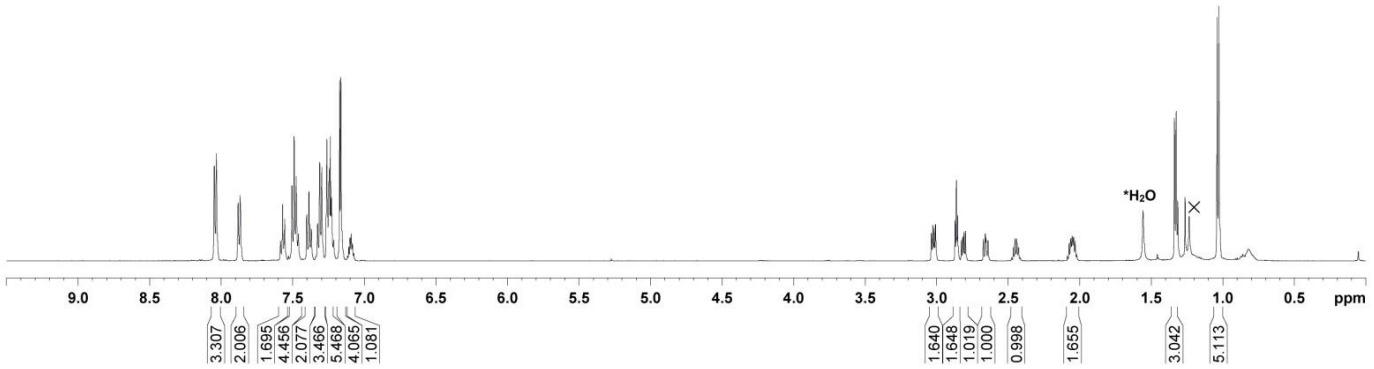

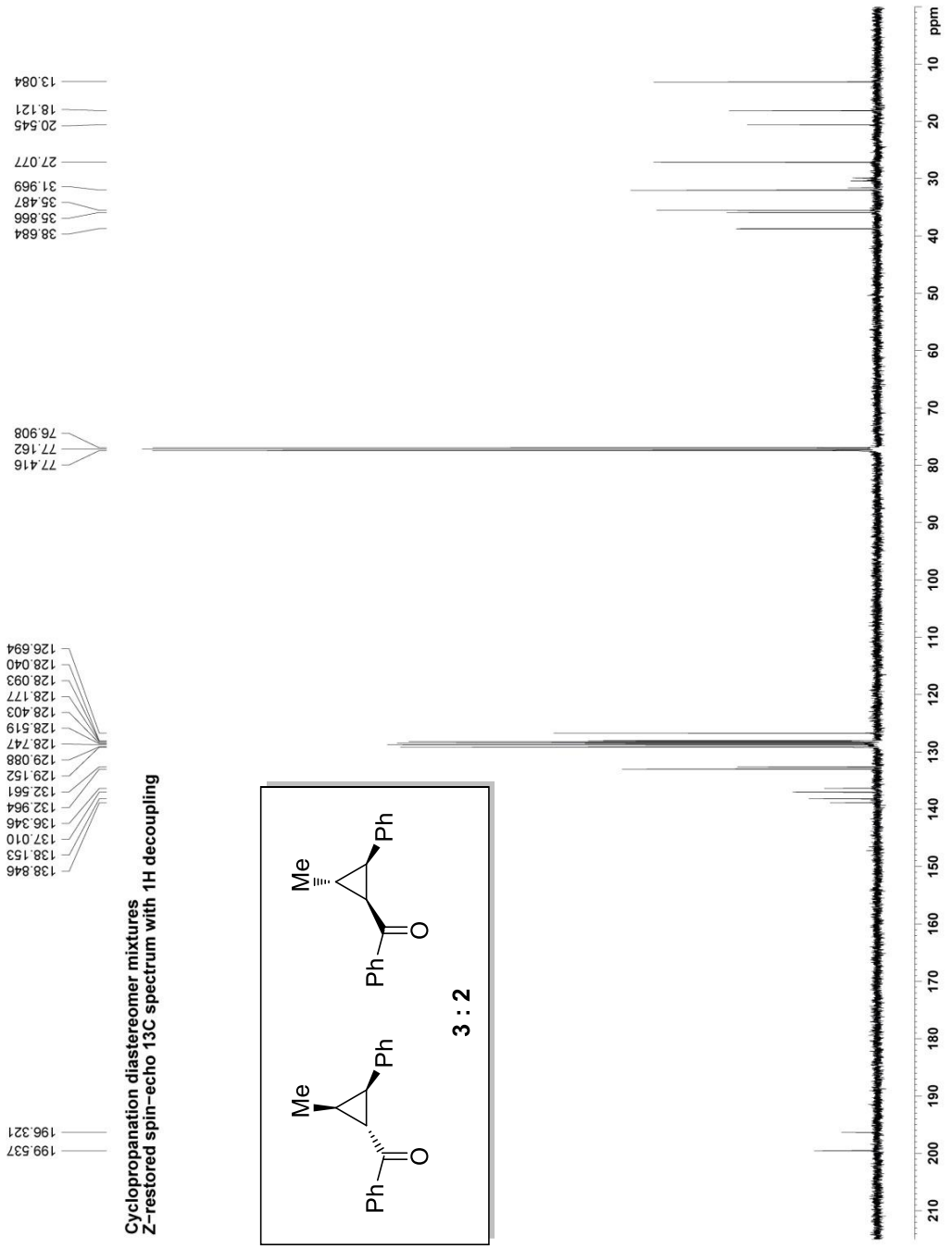
Cyclopropanation diastereomer mixtures
Z-restored spin-echo 13C spectrum with 1H decoupling
Me
Ph
Ph
O
3 : 2
Me
Ph
Ph
O
13.084
18.121
20.545
27.077
31.969
35.487
35.866
38.684
76.908
77.162
77.416
126.694
128.040
128.093
128.177
128.403
128.519
128.747
129.088
129.152
132.561
132.964
136.346
137.010
138.153
138.846
196.321
199.537
ppm

Appendix D

IR analysis results.

1. AB macromonomer HO-PM-COO^{t}Bu

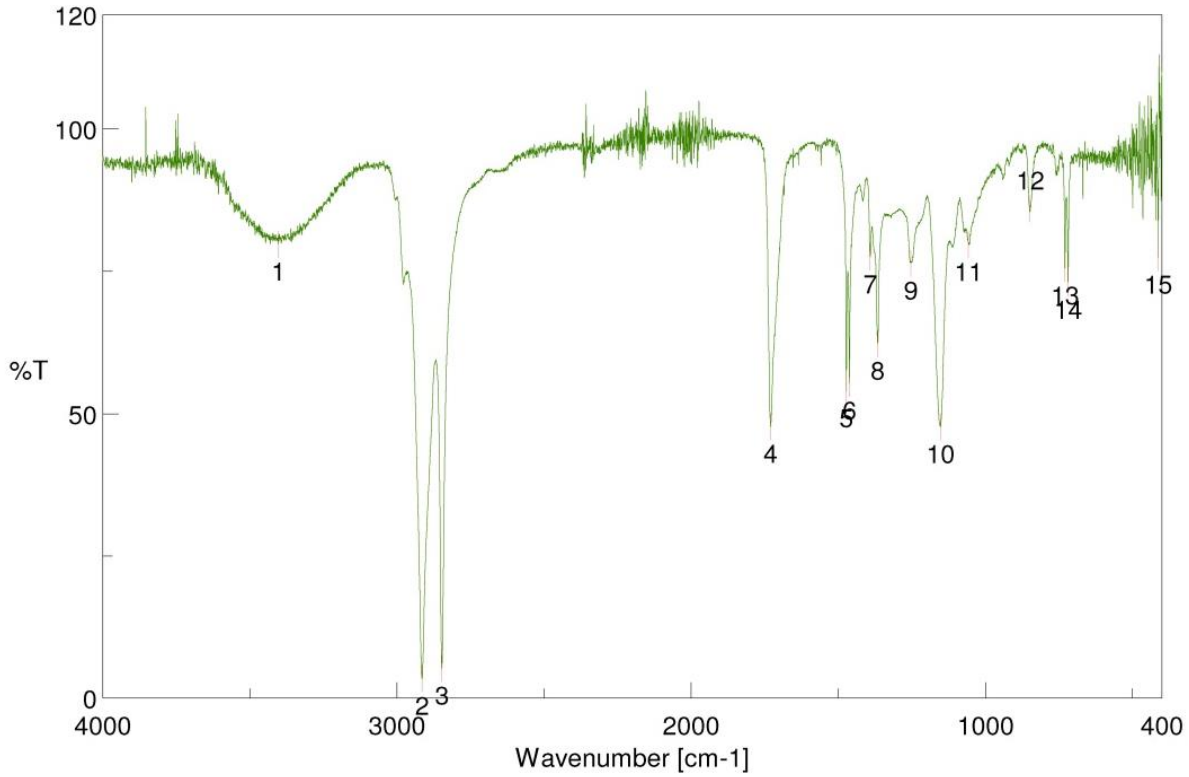

Peak No.	Position (cm^{-1})	Peak No.	Position (cm^{-1})
1	3403.3	9	1253.0
2	2914.9	10	1152.5
3	2847.6	11	1057.3
4	1729.8	12	847.6
5	1472.6	13	729.7
6	1462.3	14	719.1
7	1391.6	15	412.7
8	1366.1		

2. AA macromonomer HO-PM-OH

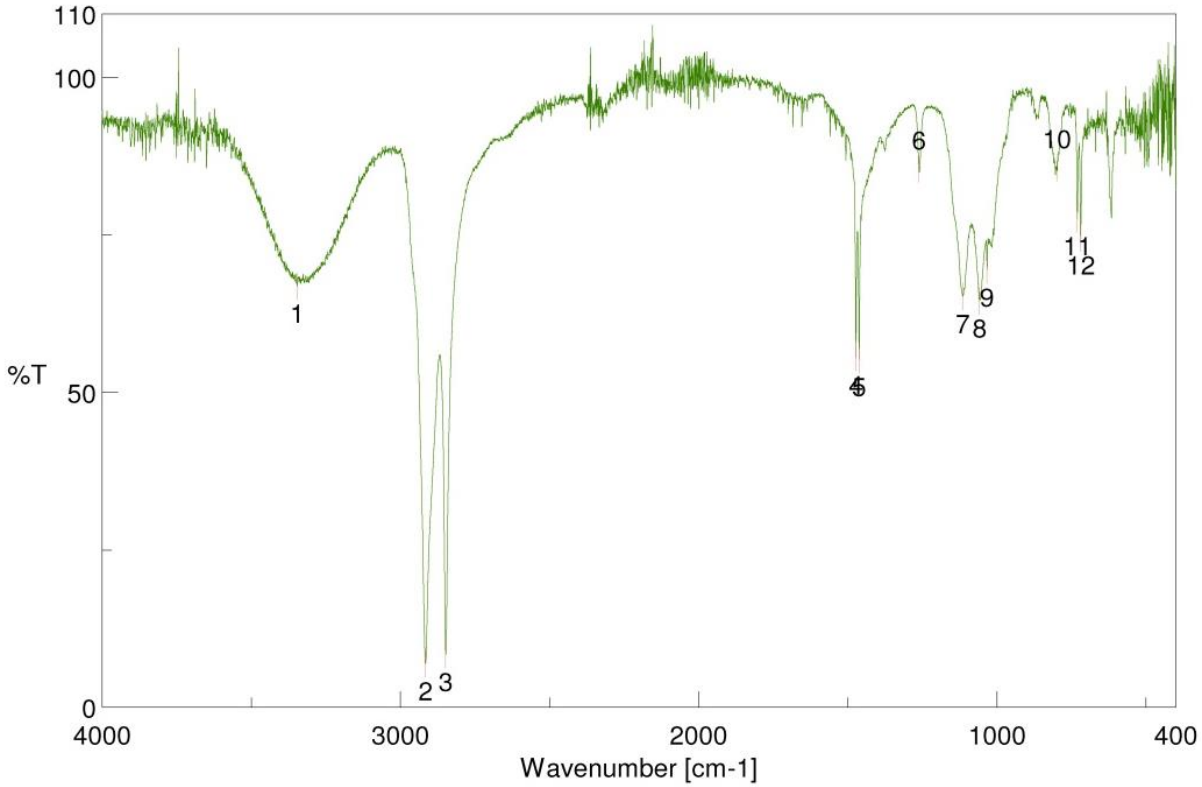

Peak No.	Position (cm^{-1})	Peak No.	Position (cm^{-1})
1	3346.1	7	1114.6
2	2915.6	8	1057.5
3	2847.9	9	1033.2
4	1472.6	10	799.4
5	1462.0	11	730.4
6	1261.5	12	718.8

3. BB macromonomer HOOC-PM-COOH

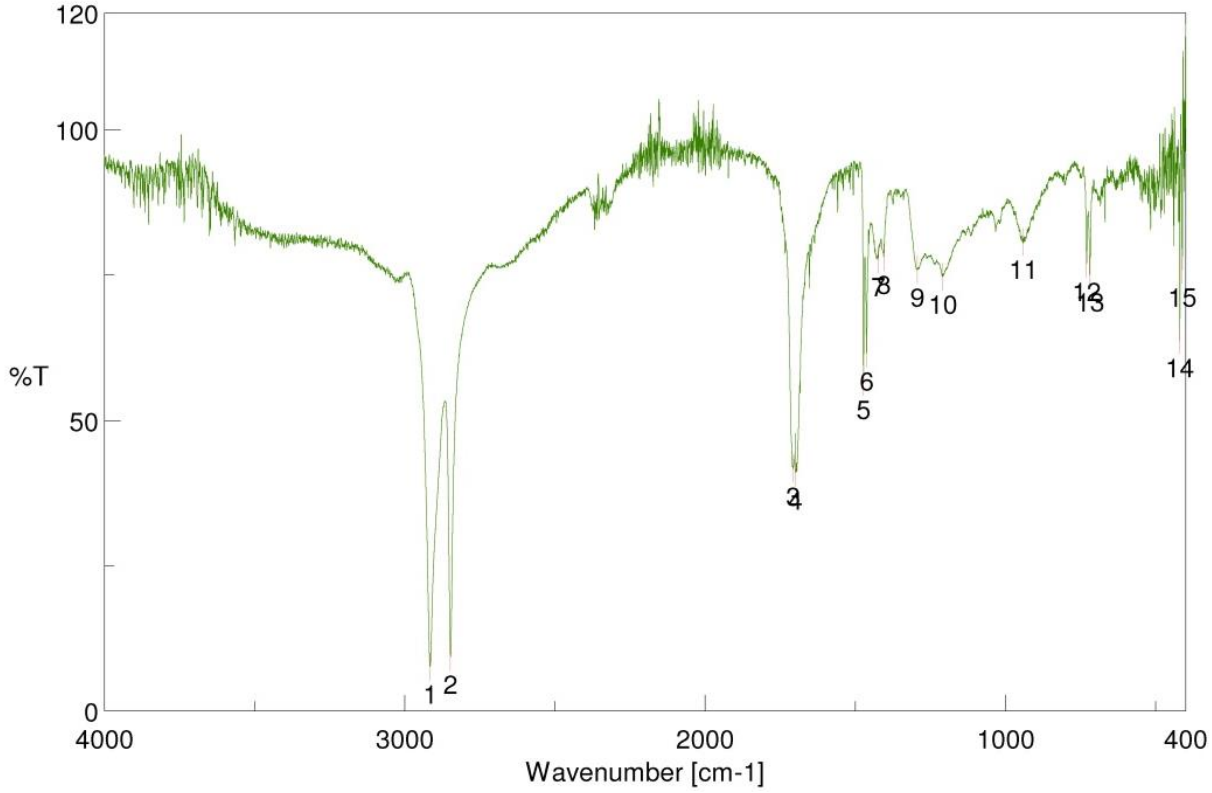

Peak No.	Position (cm^{-1})	Peak No.	Position (cm^{-1})
1	2915.8	9	1292.8
2	2848.1	10	1208.4
3	1706.4	11	940.1
4	1699.9	12	730.2
5	1472.6	13	719.3
6	1462.5	14	419.9
7	1423.9	15	411.5
8	1405.1		

4. Long-chain aliphatic polyester

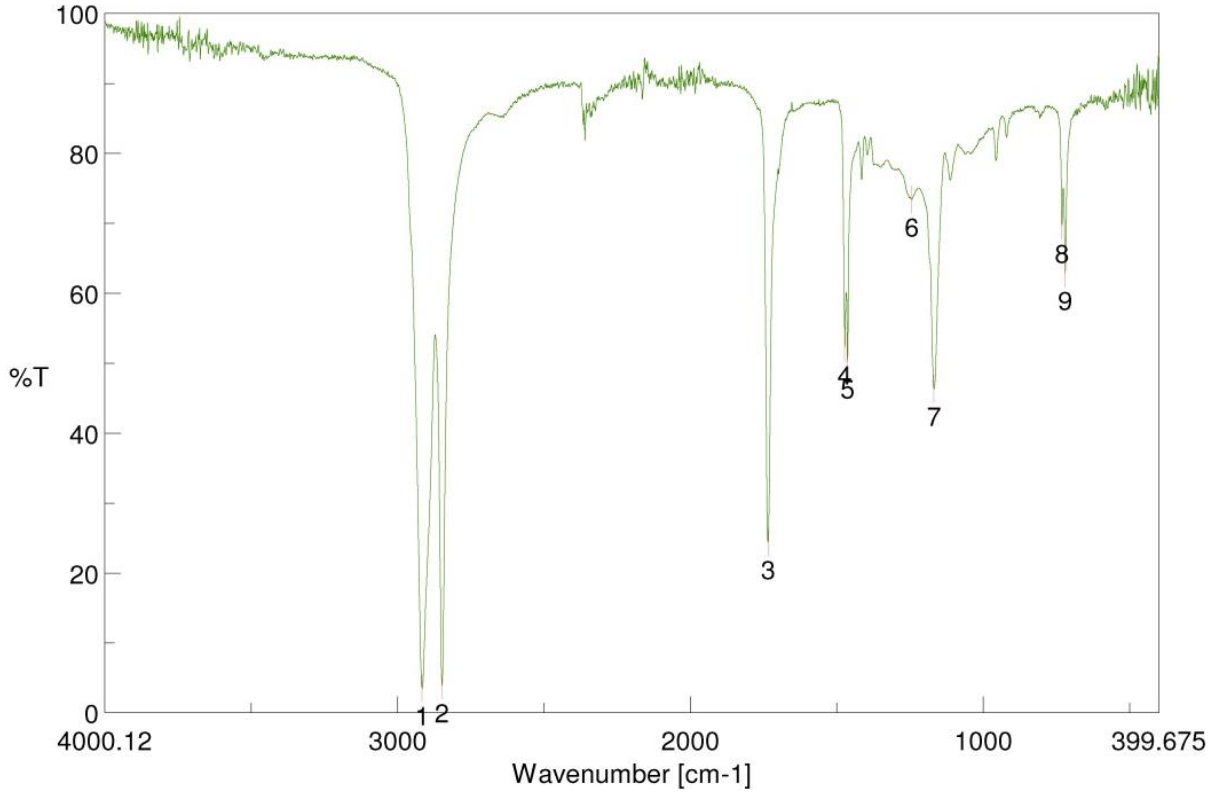

Peak No.	Position (cm^{-1})	Peak No.	Position (cm^{-1})
1	2915.8	6	1243.4
2	2848.4	7	1167.7
3	1734.7	8	730.9
4	1472.4	9	719.3
5	1463.2		

Appendix E

Gas Chromatography–Mass Spectrometry (GC-MS). GC-MS was taken using two Finnigan Trace-MS instruments. The one with electron ionization (EI) was used for product mixtures to determine the percentage of each components in the mixture; while the other one with chemical ionization (CI) was used for relative pure samples to obtain accurate mass with high resolution. In this appendix, GC-MS spectra from Chapter 4 are listed below.

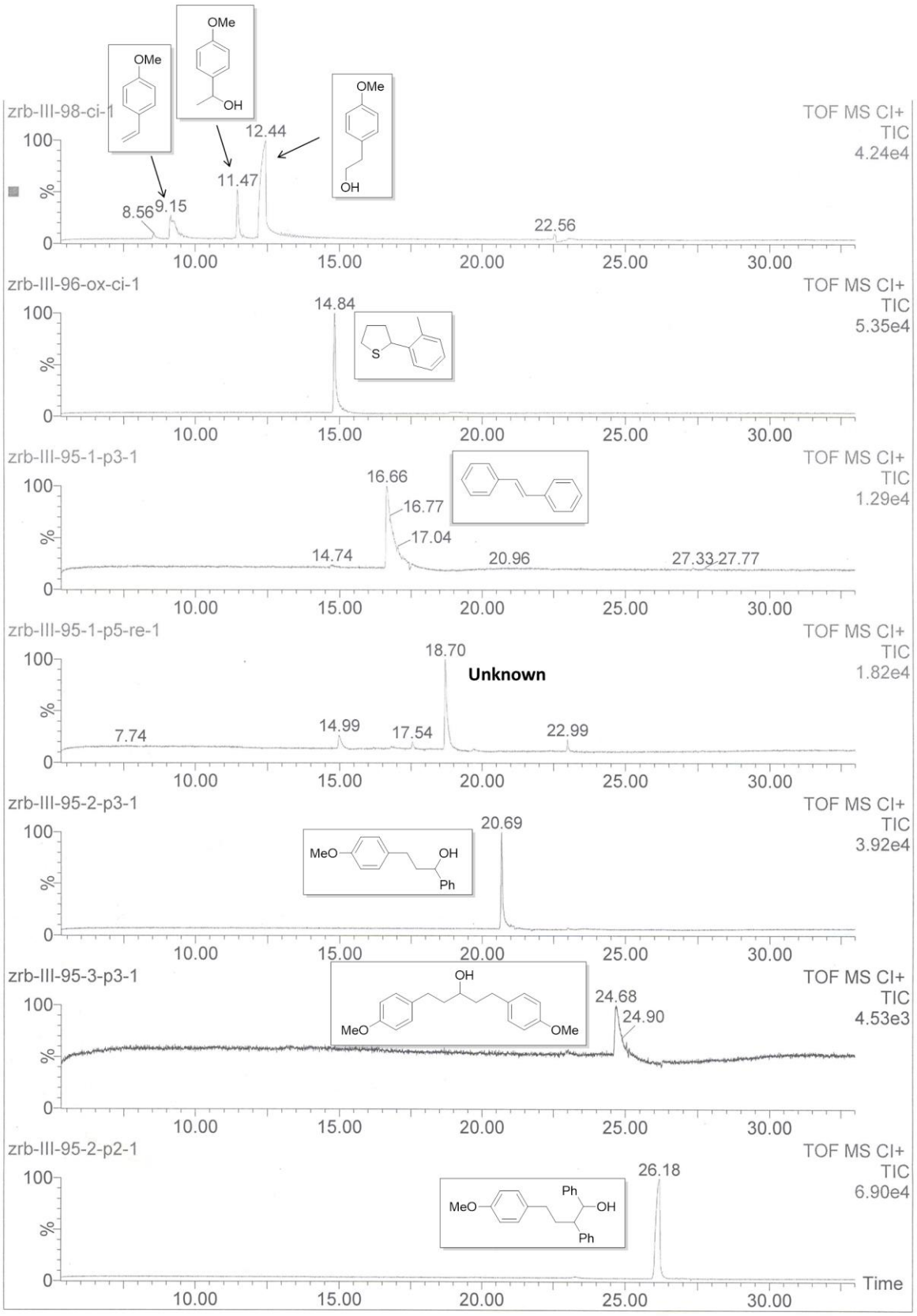
zrb-III-98-ci-1
TOF MS CI+
TIC
4.24e4
OMe
OMe
OH
OMe
OH
12.44
11.47
8.56
9.15
22.56
zrb-III-96-ox-ci-1
TOF MS CI+
TIC
5.35e4
14.84
S
zrb-III-95-1-p3-1
TOF MS CI+
TIC
1.29e4
16.66
16.77
17.04
14.74
20.96
27.33
27.77
zrb-III-95-1-p5-re-1
TOF MS CI+
TIC
1.82e4
18.70
Unknown
7.74
14.99
17.54
22.99
zrb-III-95-2-p3-1
TOF MS CI+
TIC
3.92e4
20.69
MeO
OH
Ph
zrb-III-95-3-p3-1
TOF MS CI+
TIC
4.53e3
OH
MeO
OMe
24.68
24.90
zrb-III-95-2-p2-1
TOF MS CI+
TIC
6.90e4
26.18
MeO
Ph
OH
Ph
100
%
0
10.00
15.00
20.00
25.00
30.00
Time

GC-MS (CI) analysis of reactions in Scheme 4.4 at 0 °C

Integration values in CI mode was inaccurate and was not used.

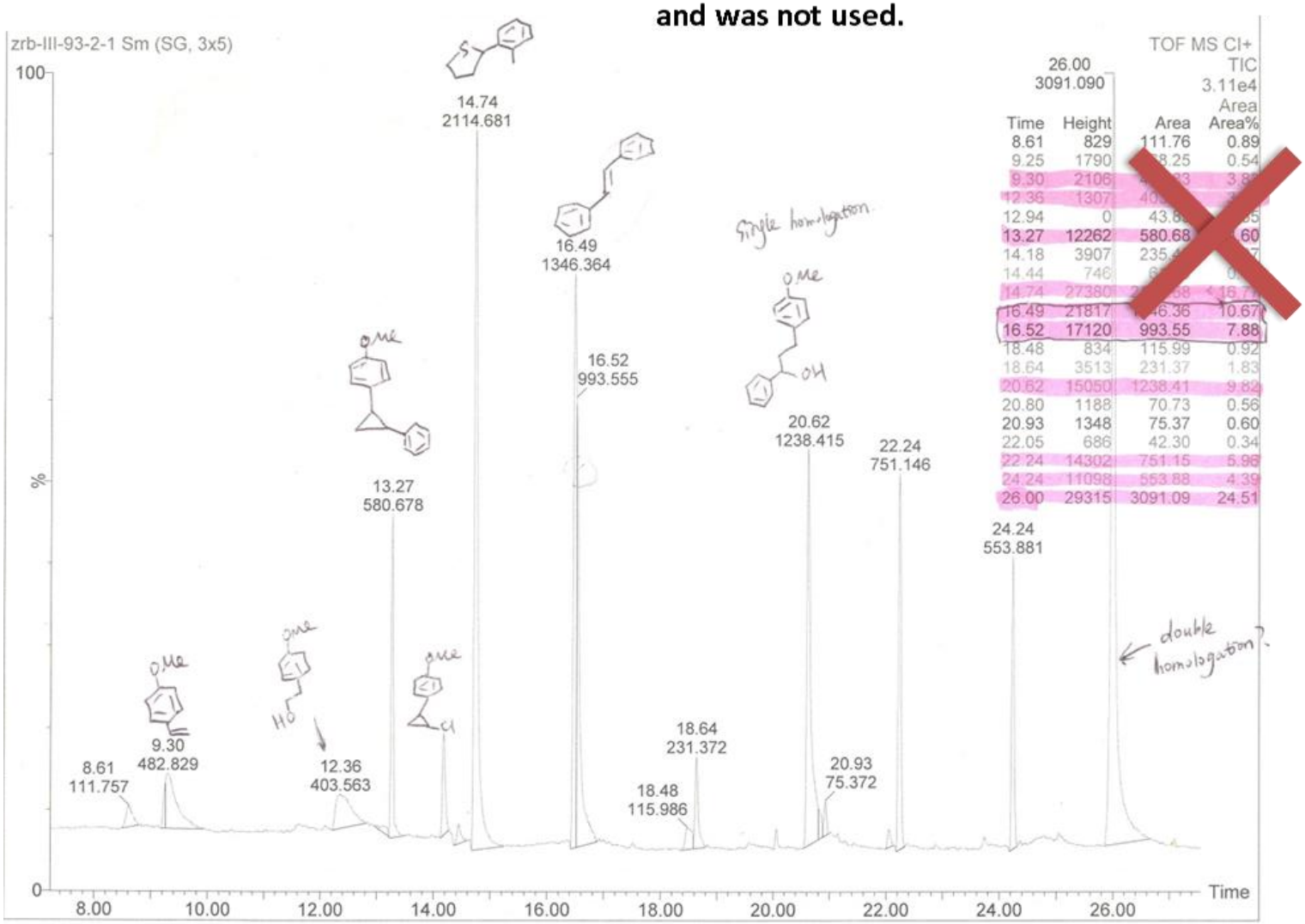

GC-MS (EI) analysis of reactions in Scheme 4.4 at 0 °C

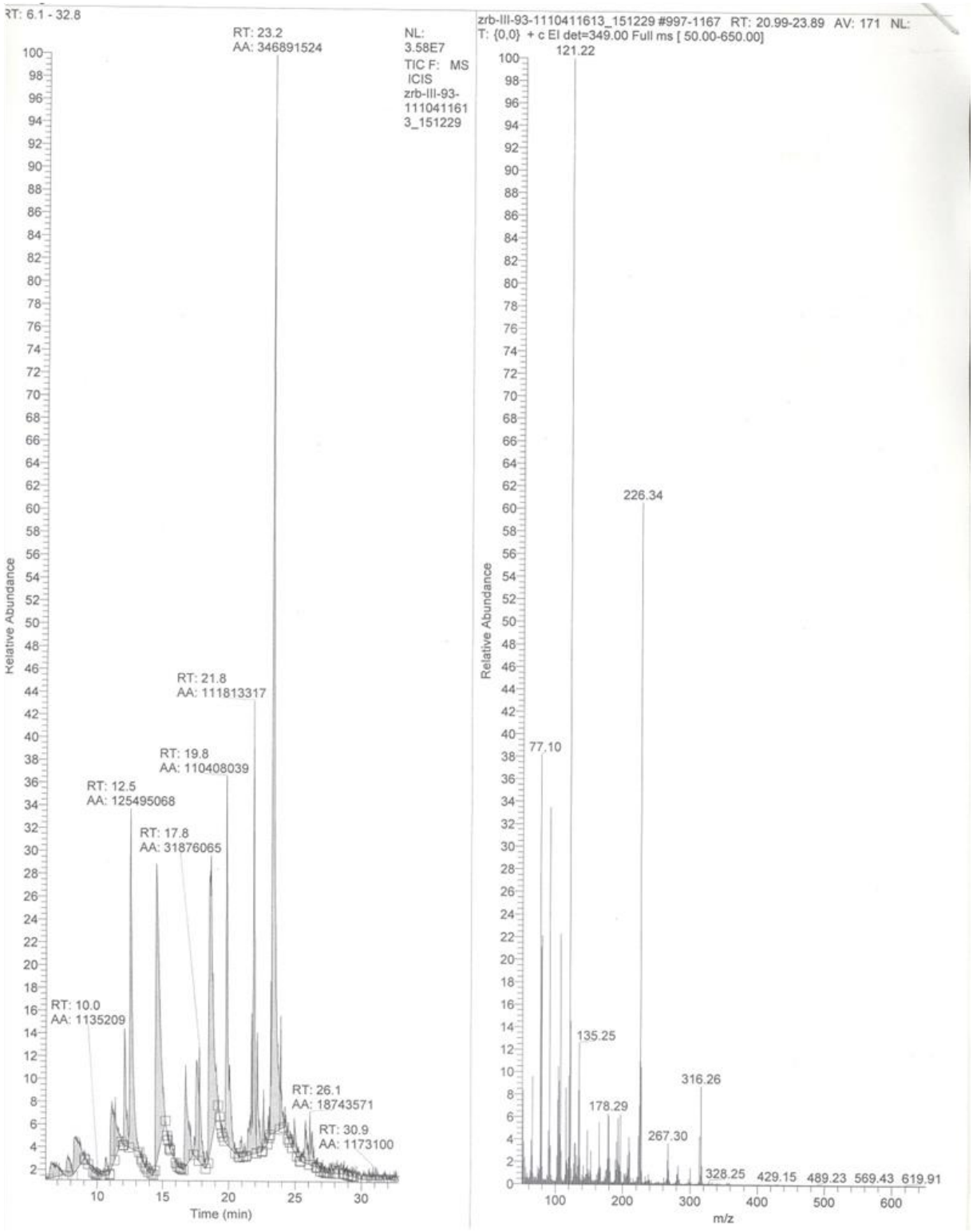

GC-MS (CI) analysis of reactions in Scheme 4.4 at –20 °C

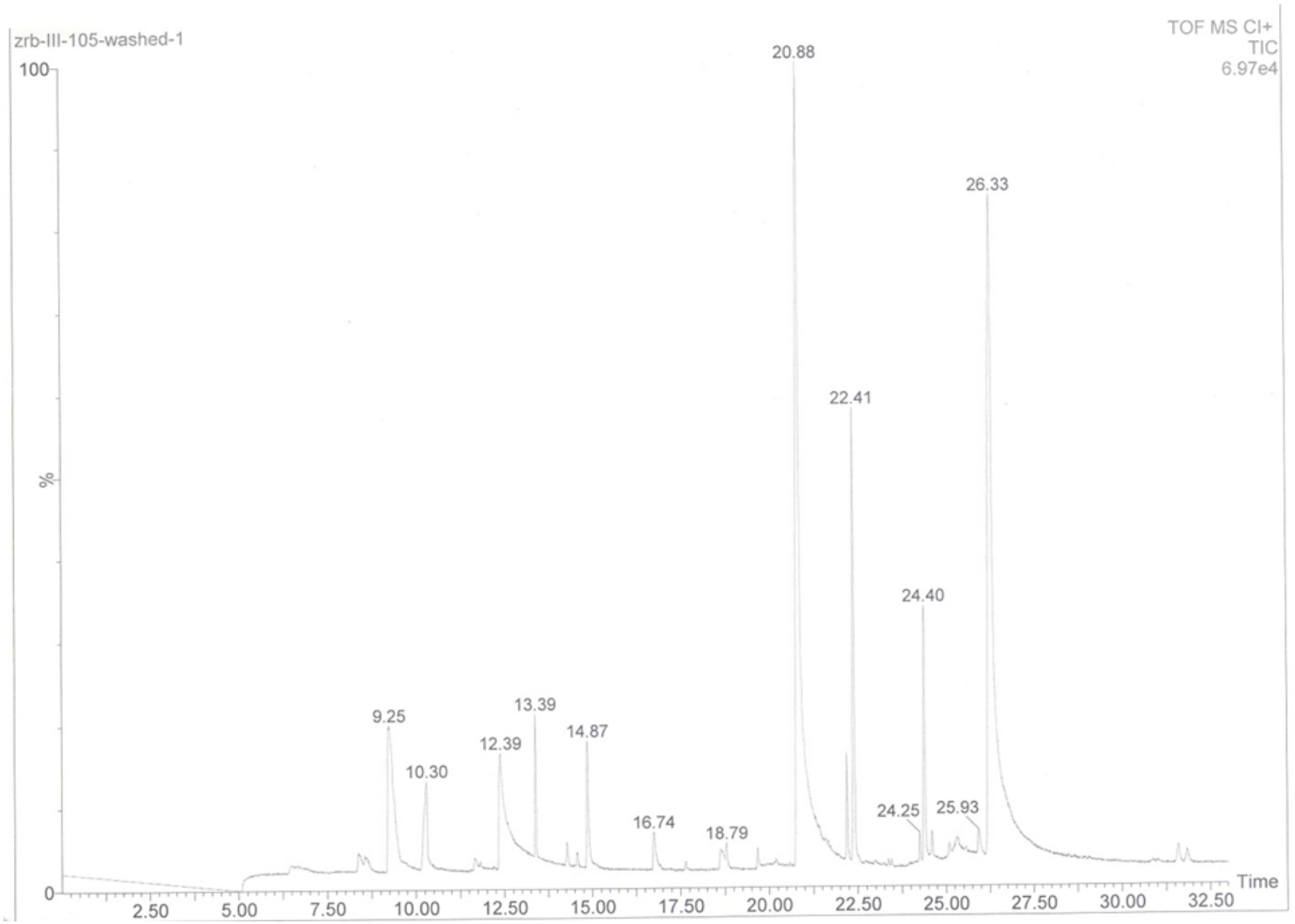

GC-MS (EI) analysis of reactions in Scheme 4.4 at −20 °C

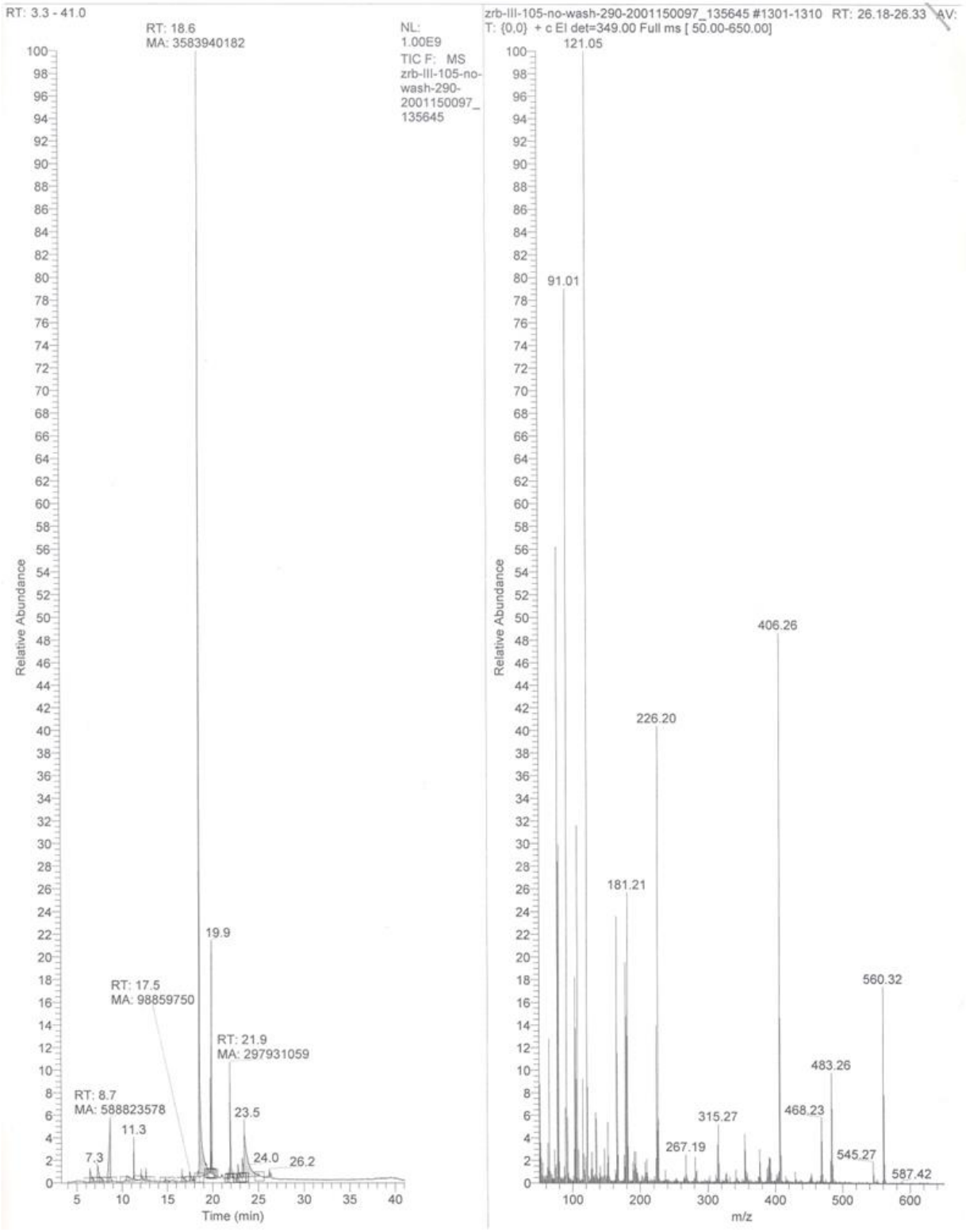

Appendix F

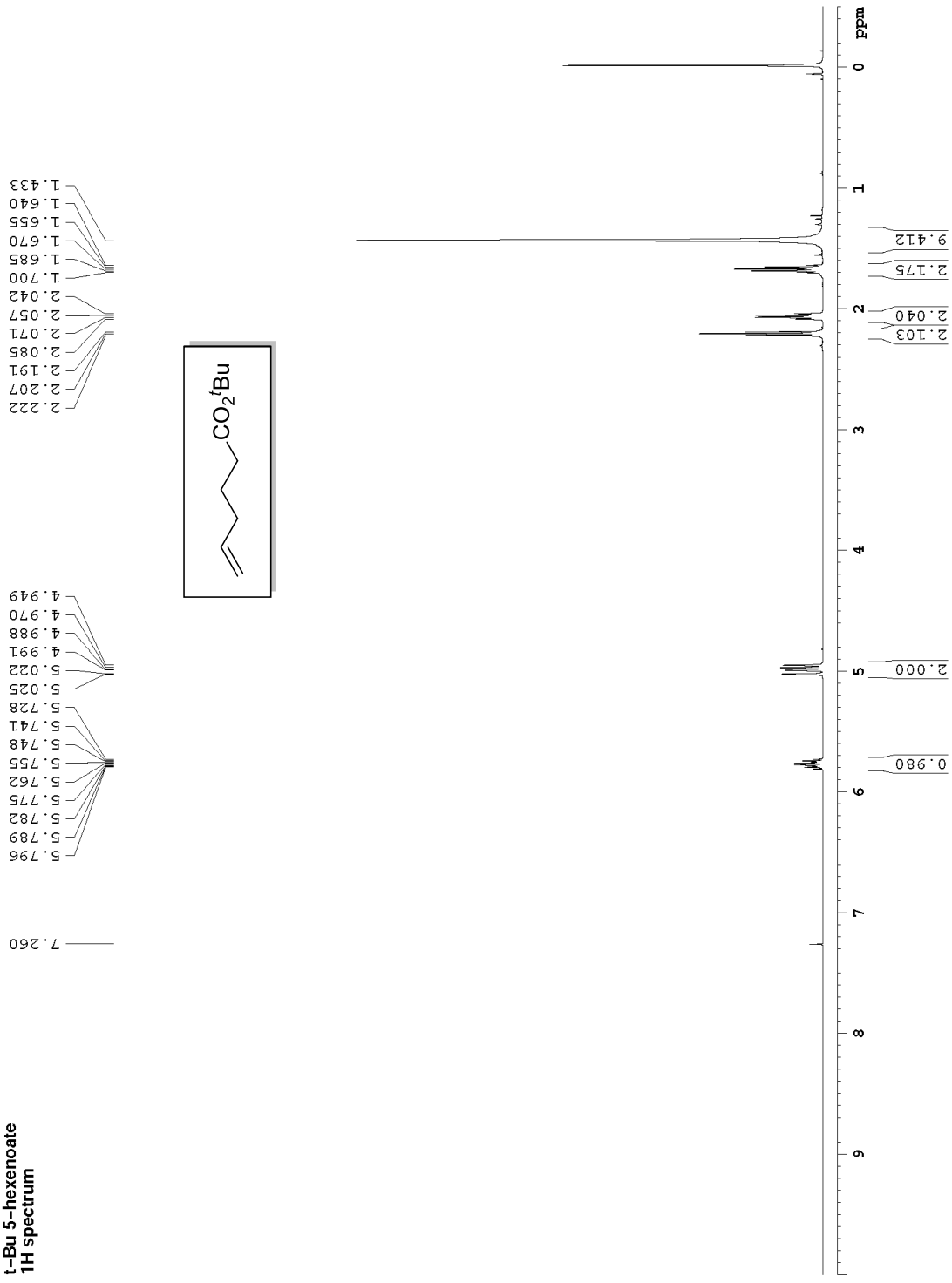
t-Bu 5-hexenoate
1H spectrum
$CO_2{}^tBu$
ppm
0
1
2
3
4
5
6
7
8
9
9.412
2.175
2.040
2.103
2.000
0.980
1.433
1.640
1.655
1.670
1.685
1.700
2.042
2.057
2.071
2.085
2.191
2.207
2.222
4.949
4.970
4.988
4.991
5.022
5.025
5.728
5.741
5.748
5.755
5.762
5.775
5.782
5.789
5.796
7.260

t-Bu 5-hexenoate
Z-restored spin-echo 13C spectrum with 1H decoupling

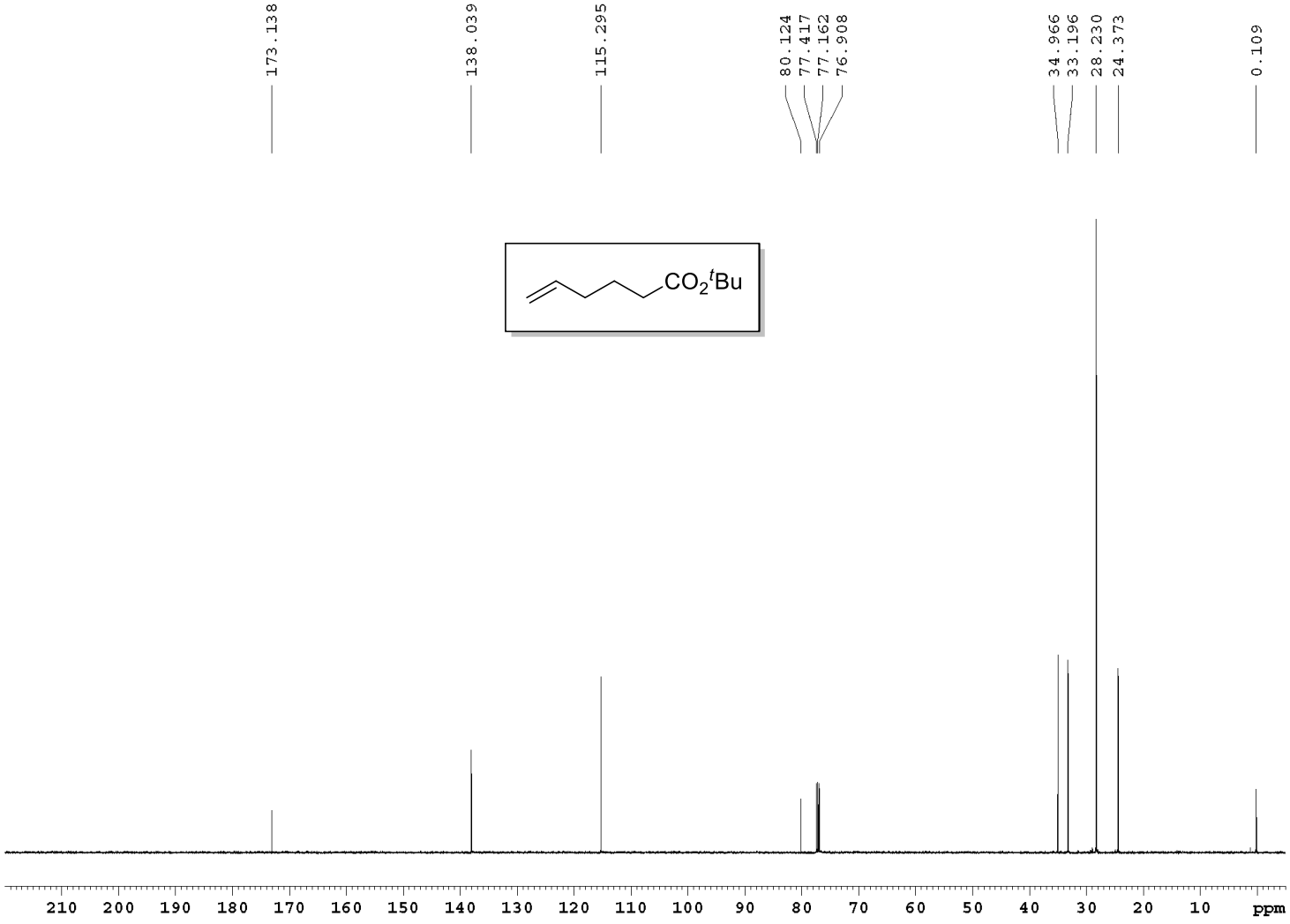

boron initiator w/ dioxane
1H spectrum

5.500
5.320
5.143

3.605
2.157
2.142
2.127
2.120
2.054
2.029
1.560
1.545
1.529
1.514
1.499
1.461
1.387
1.368
1.352
1.299
1.285
1.269
1.254
1.238
1.225
1.181
1.165
1.150
0.875
0.864

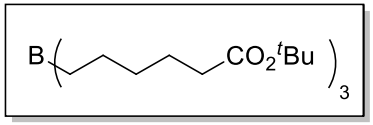

a. 1,4-dioxane internal standard
b. remaining dimethylsulfide introduced by BH_3-SMe_2
c. CH_3 from regioisomer of hydroboration

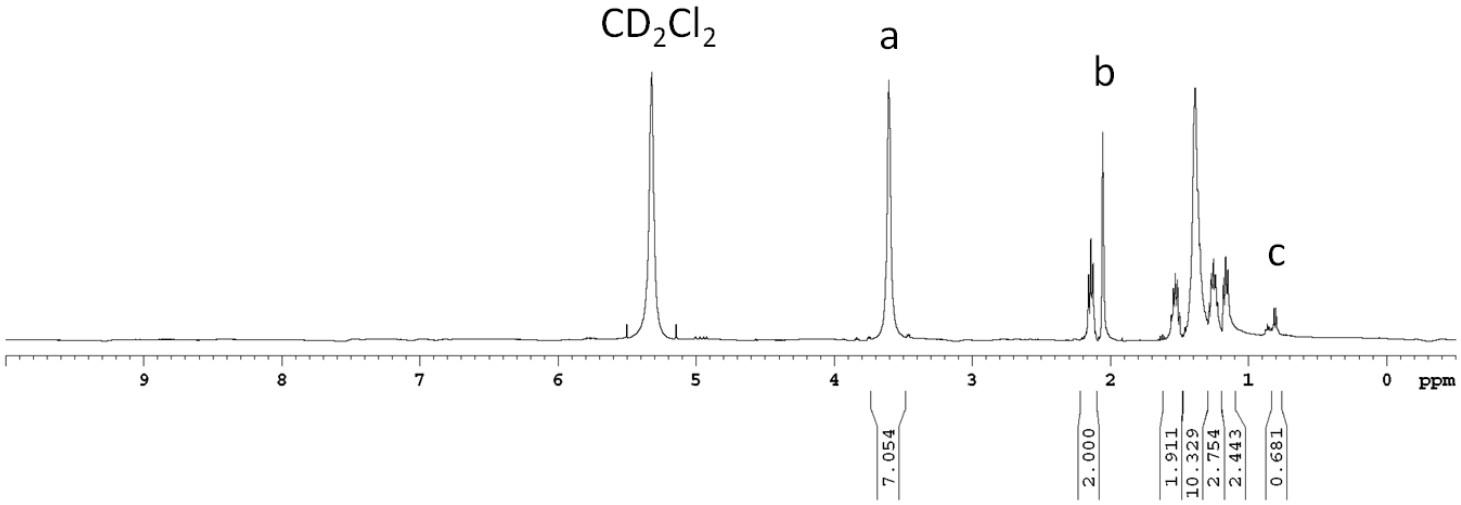

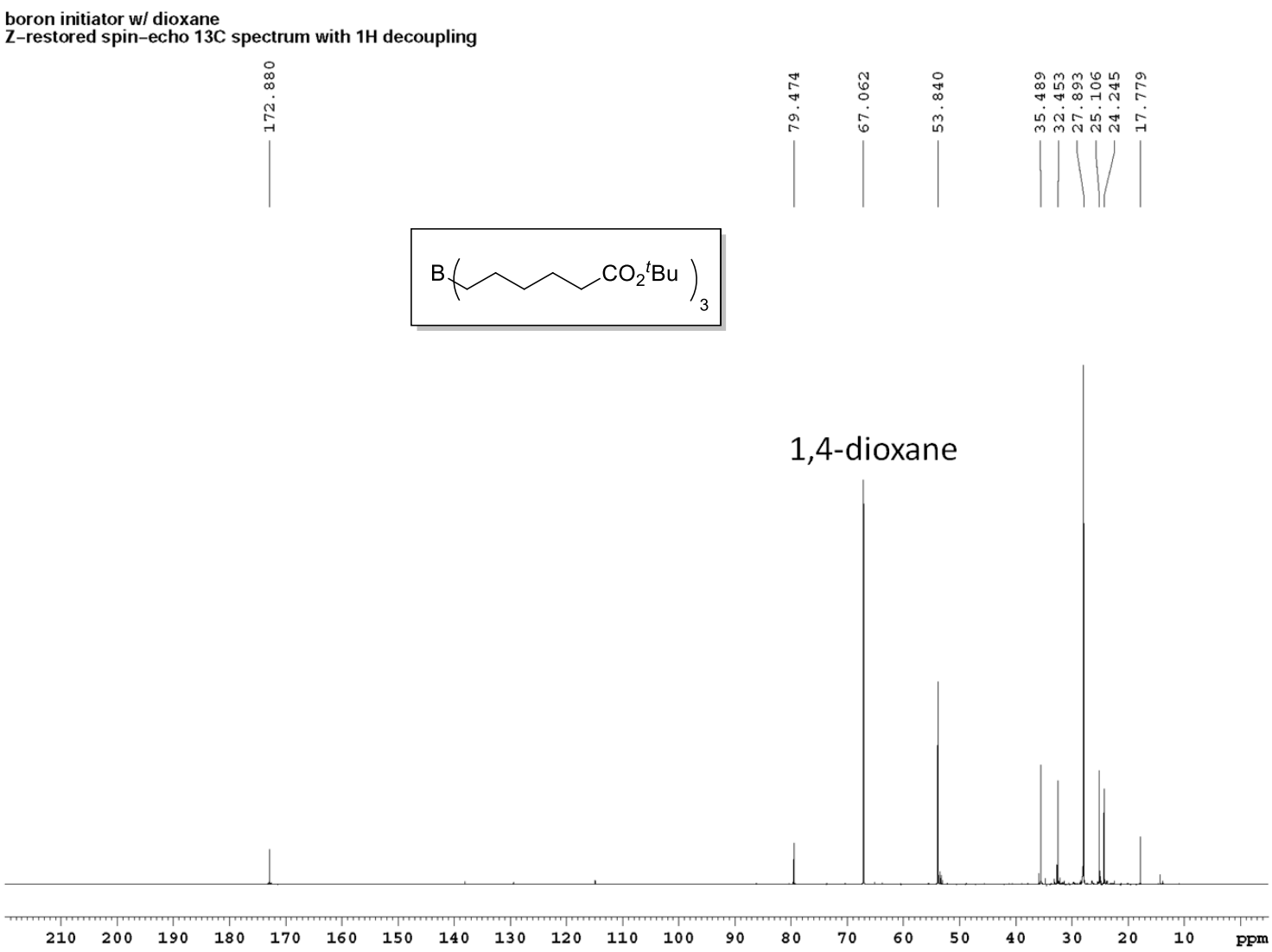
boron initiator w/ dioxane
Z-restored spin-echo 13C spectrum with 1H decoupling
172.880
79.474
67.062
53.840
35.489
32.453
27.893
25.106
24.245
17.779
B
CO2tBu
3
1,4-dioxane
210 200 190 180 170 160 150 140 130 120 110 100 90 80 70 60 50 40 30 20 10 ppm

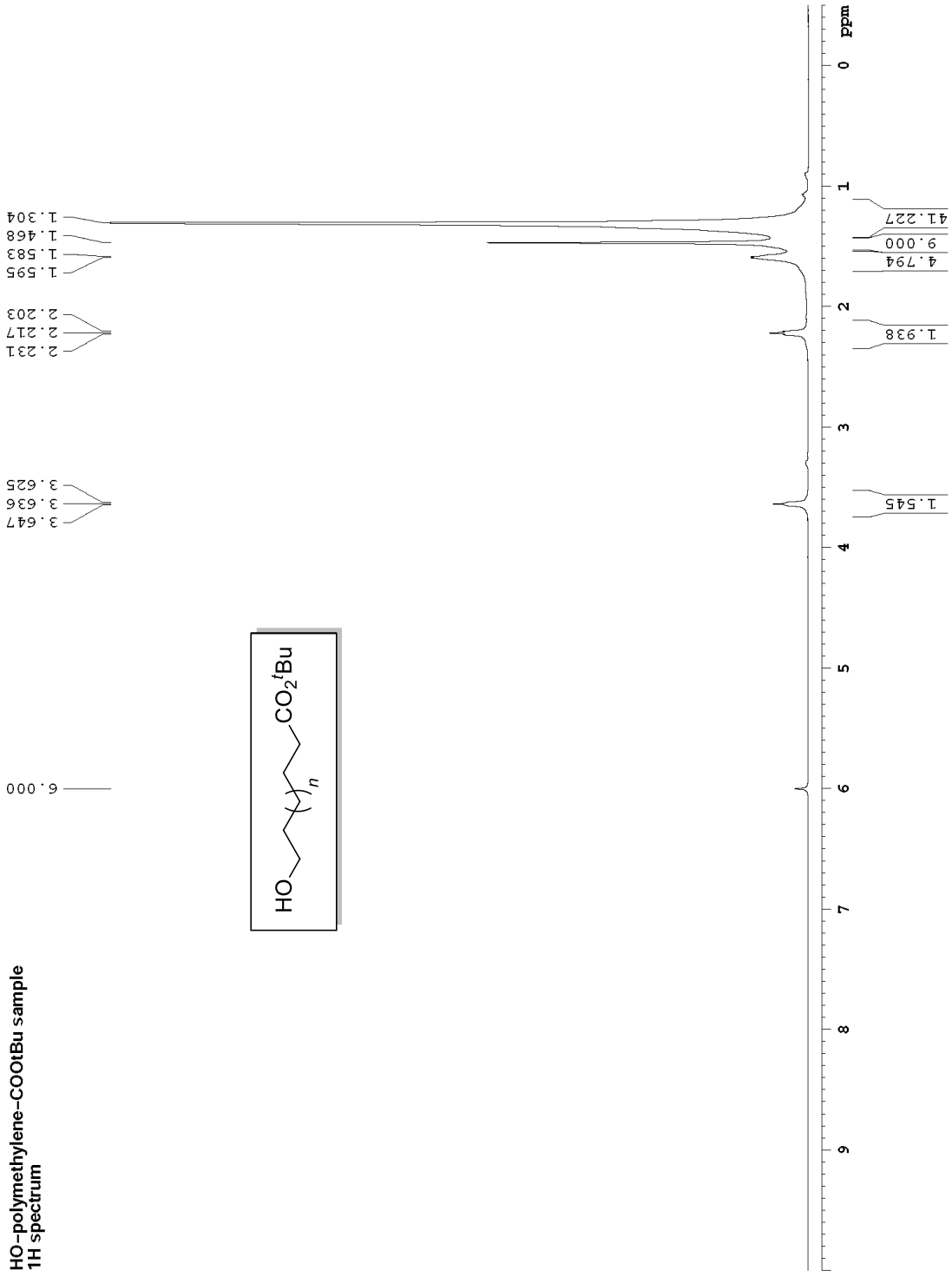
HO–polymethylene–COOtBu sample
1H spectrum
HO
CO2tBu
n
ppm
0
1
2
3
4
5
6
7
8
9
1.304
1.468
1.583
1.595
2.203
2.217
2.231
3.625
3.636
3.647
6.000
41.227
9.000
4.794
1.938
1.545

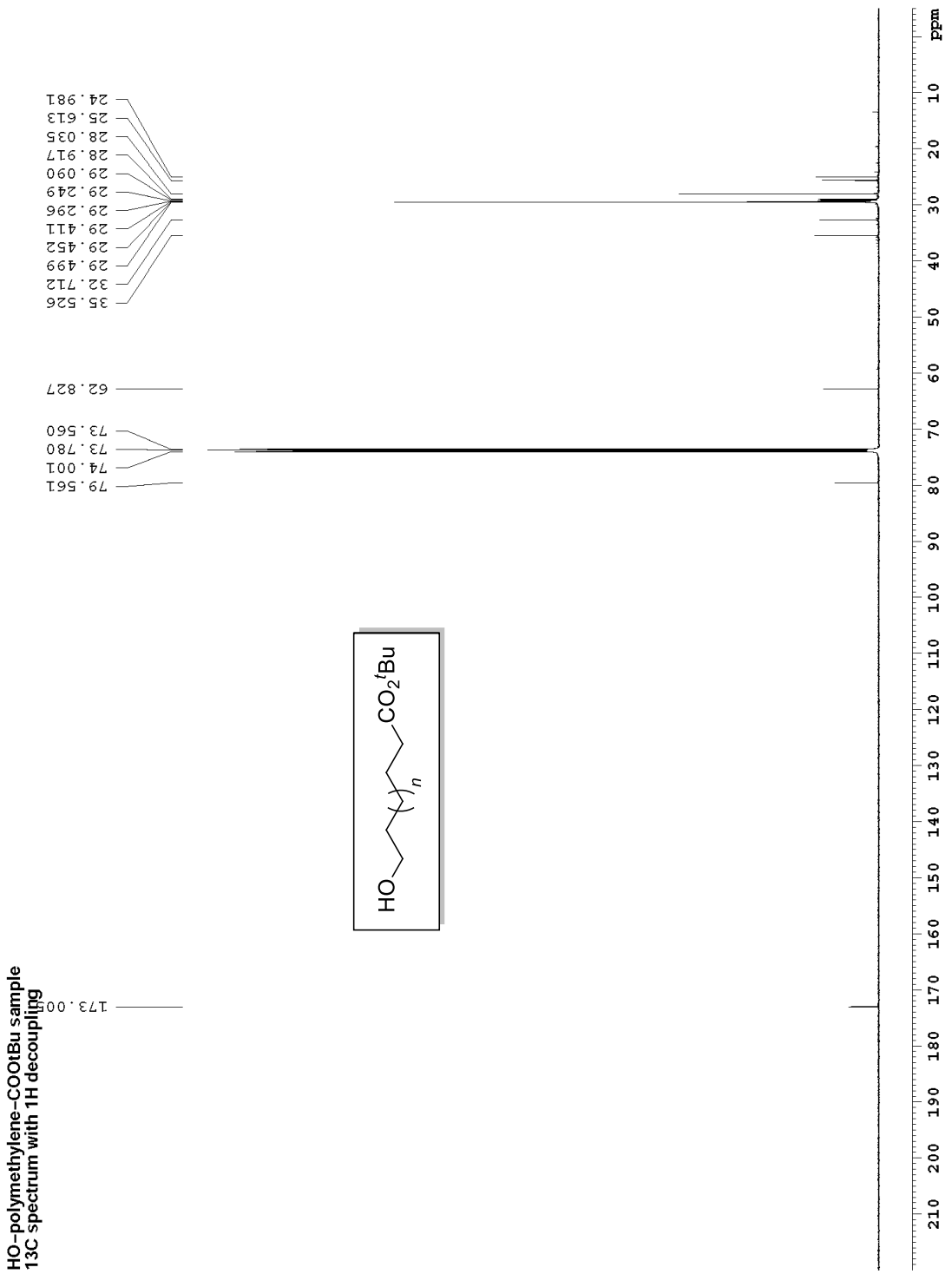
HO–polymethylene–COOtBu sample
13C spectrum with 1H decoupling
173.005
79.561
74.001
73.780
73.560
62.827
35.526
32.712
29.499
29.452
29.411
29.296
29.249
29.090
28.917
28.035
25.613
24.981
HO
$CO_2{}^tBu$
n
ppm

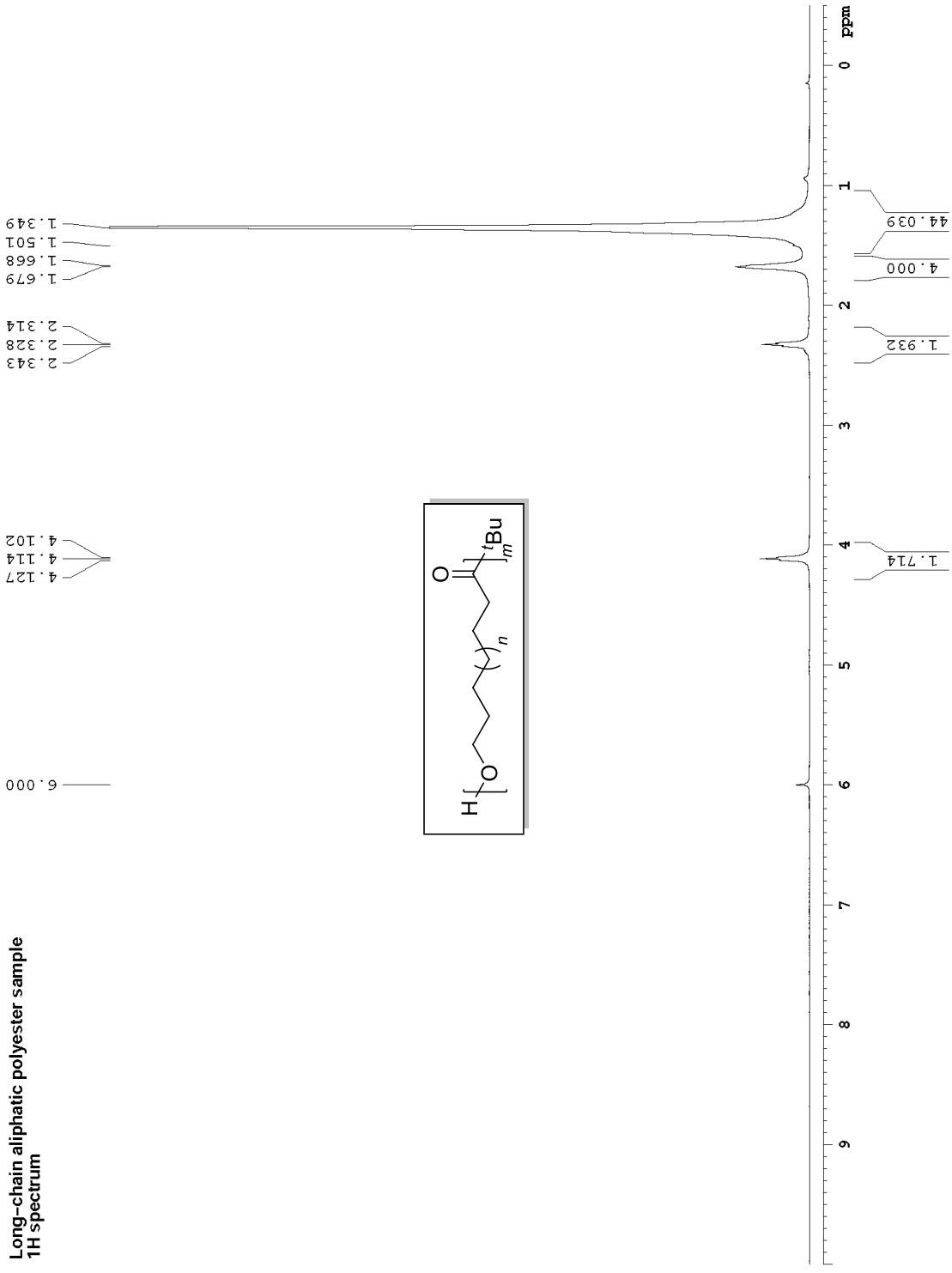
Long-chain aliphatic polyester sample
1H spectrum
ppm
0
1
2
3
4
5
6
7
8
9
1.349
1.501
1.668
1.679
2.314
2.328
2.343
4.102
4.114
4.127
6.000
1.714
44.039
4.000
1.932
H
O
O
n
O
m
tBu

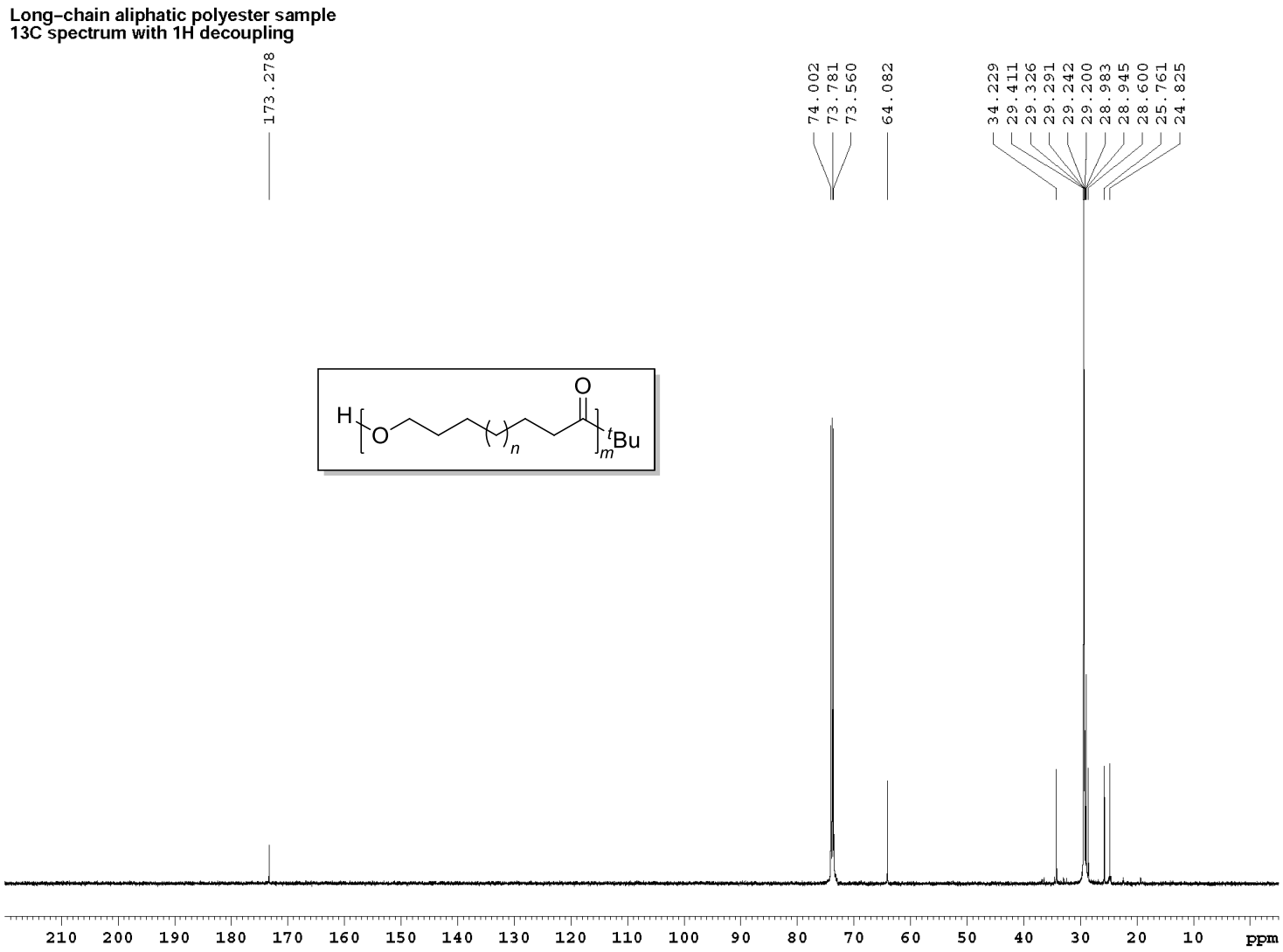
Long-chain aliphatic polyester sample
13C spectrum with 1H decoupling
173.278
74.002
73.781
73.560
64.082
34.229
29.411
29.326
29.291
29.242
29.200
28.983
28.945
28.600
25.761
24.825
H
O
n
O
m
tBu
210 200 190 180 170 160 150 140 130 120 110 100 90 80 70 60 50 40 30 20 10 ppm

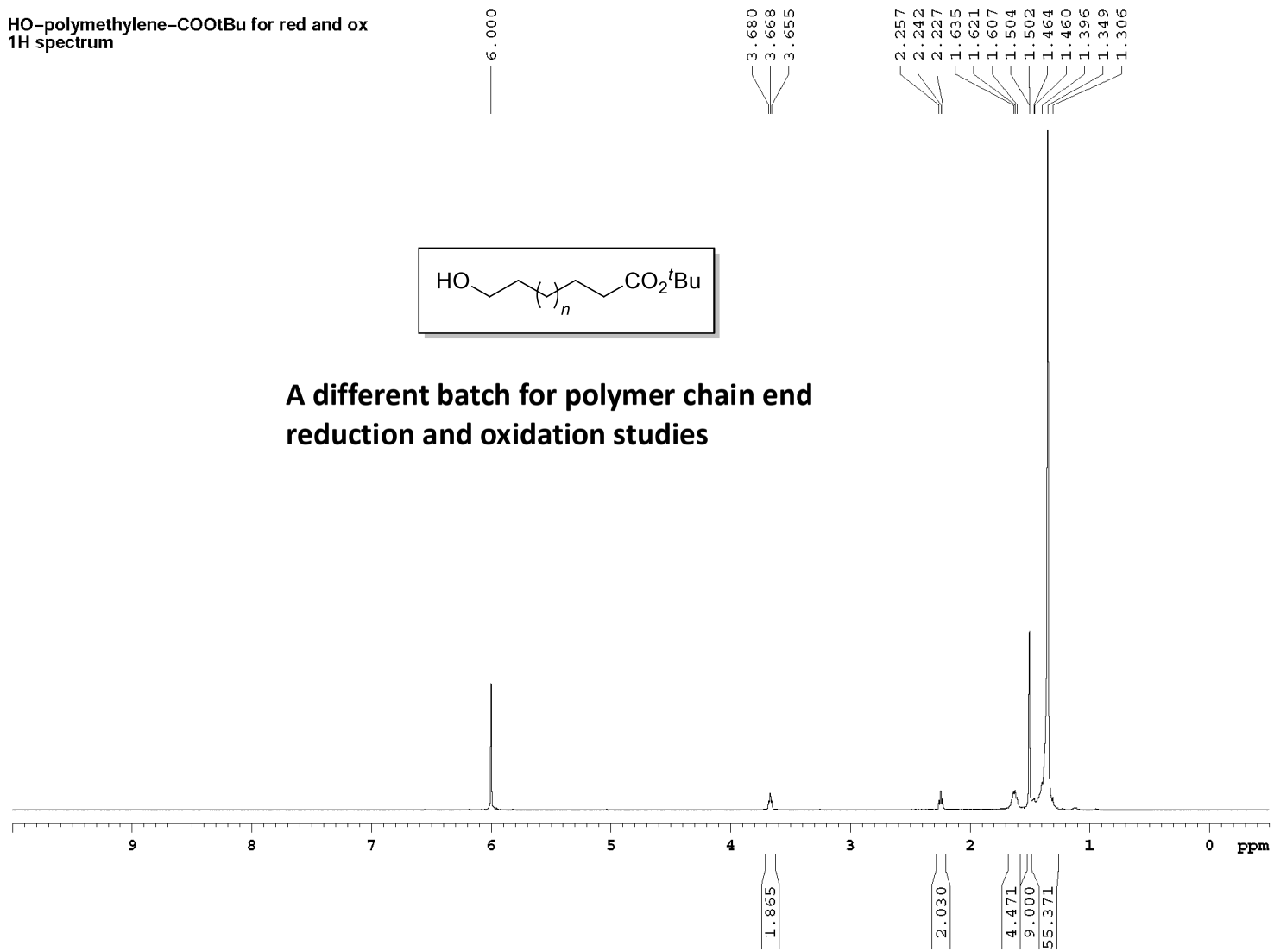
HO-polymethylene-COOtBu for red and ox
1H spectrum
6.000
3.680
3.668
3.655
2.257
2.242
2.227
1.635
1.621
1.607
1.504
1.502
1.464
1.460
1.396
1.349
1.306
HO
CO2tBu
n
A different batch for polymer chain end reduction and oxidation studies
9
8
7
6
5
4
3
2
1
0
ppm
1.865
2.030
4.471
9.000
55.371

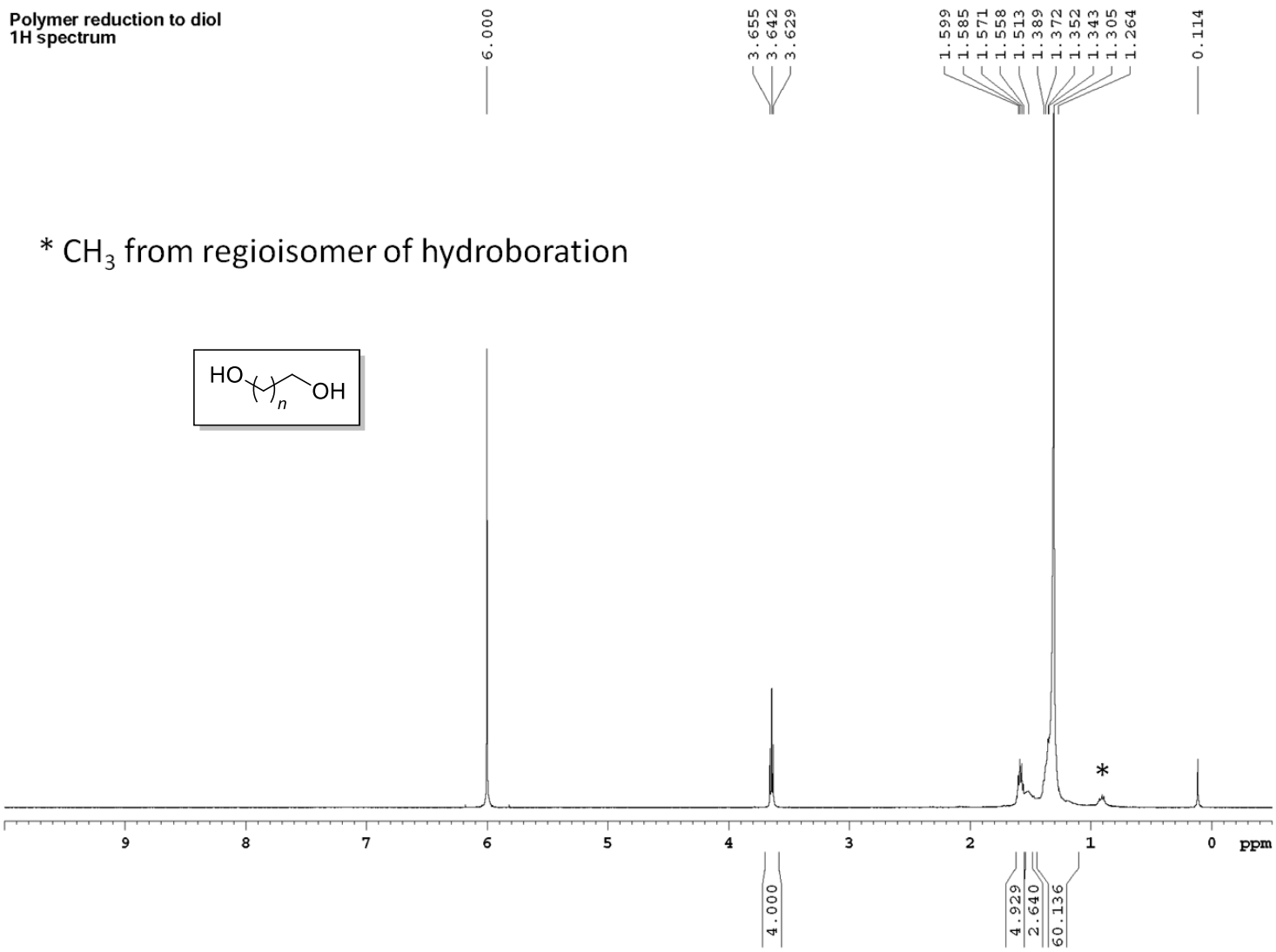
Polymer reduction to diol
1H spectrum
6.000
3.655
3.642
3.629
1.599
1.585
1.571
1.558
1.513
1.389
1.372
1.352
1.343
1.305
1.264
0.114
* CH3 from regioisomer of hydroboration
HO
n
OH
*
9
8
7
6
5
4
3
2
1
0
ppm
4.000
4.929
2.640
60.136

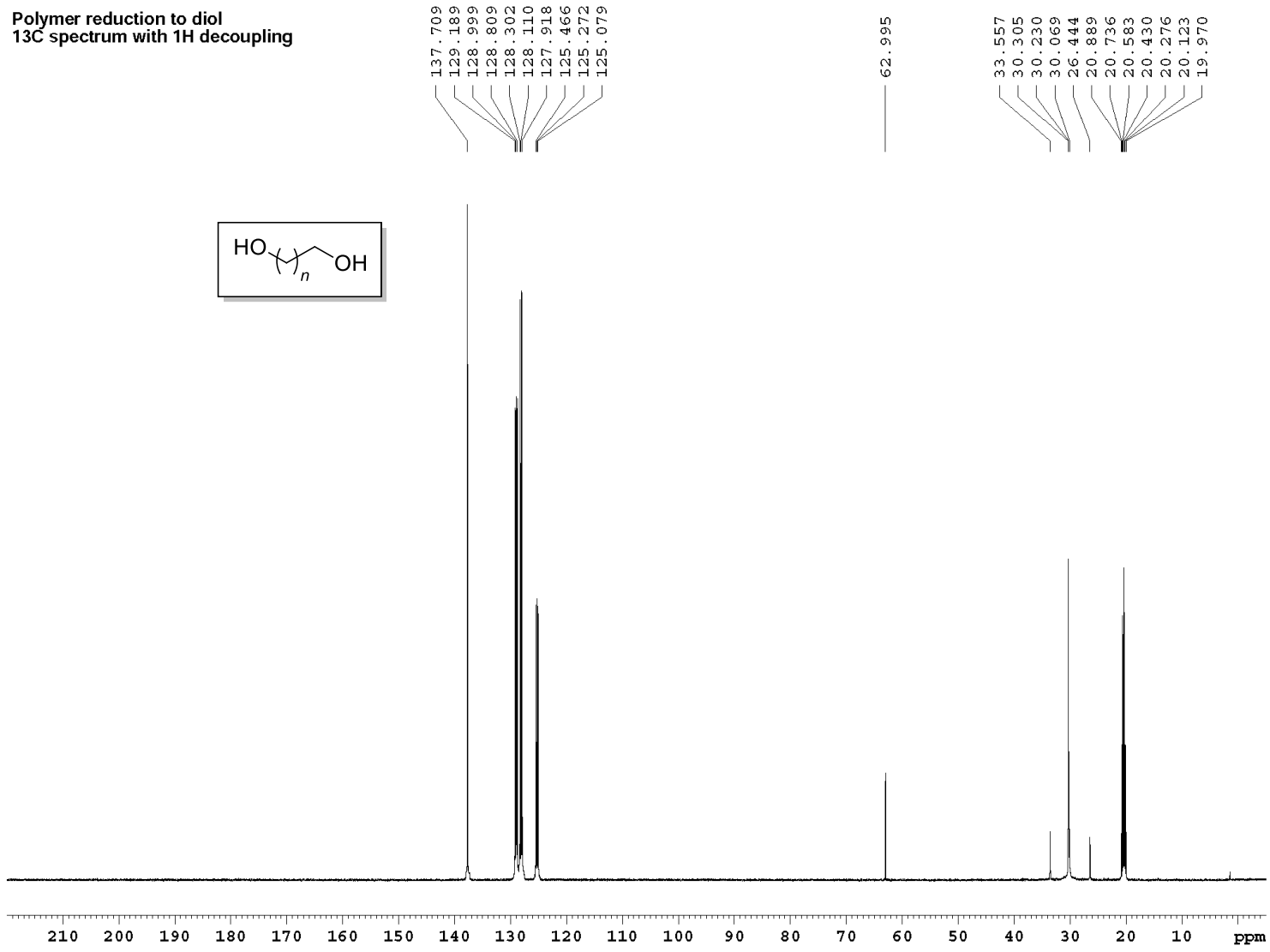
Polymer reduction to diol
13C spectrum with 1H decoupling
137.709
129.189
128.999
128.809
128.302
128.110
127.918
125.466
125.272
125.079
62.995
33.557
30.305
30.230
30.069
26.444
20.889
20.736
20.583
20.430
20.276
20.123
19.970
HO
n
OH
210 200 190 180 170 160 150 140 130 120 110 100 90 80 70 60 50 40 30 20 10 ppm

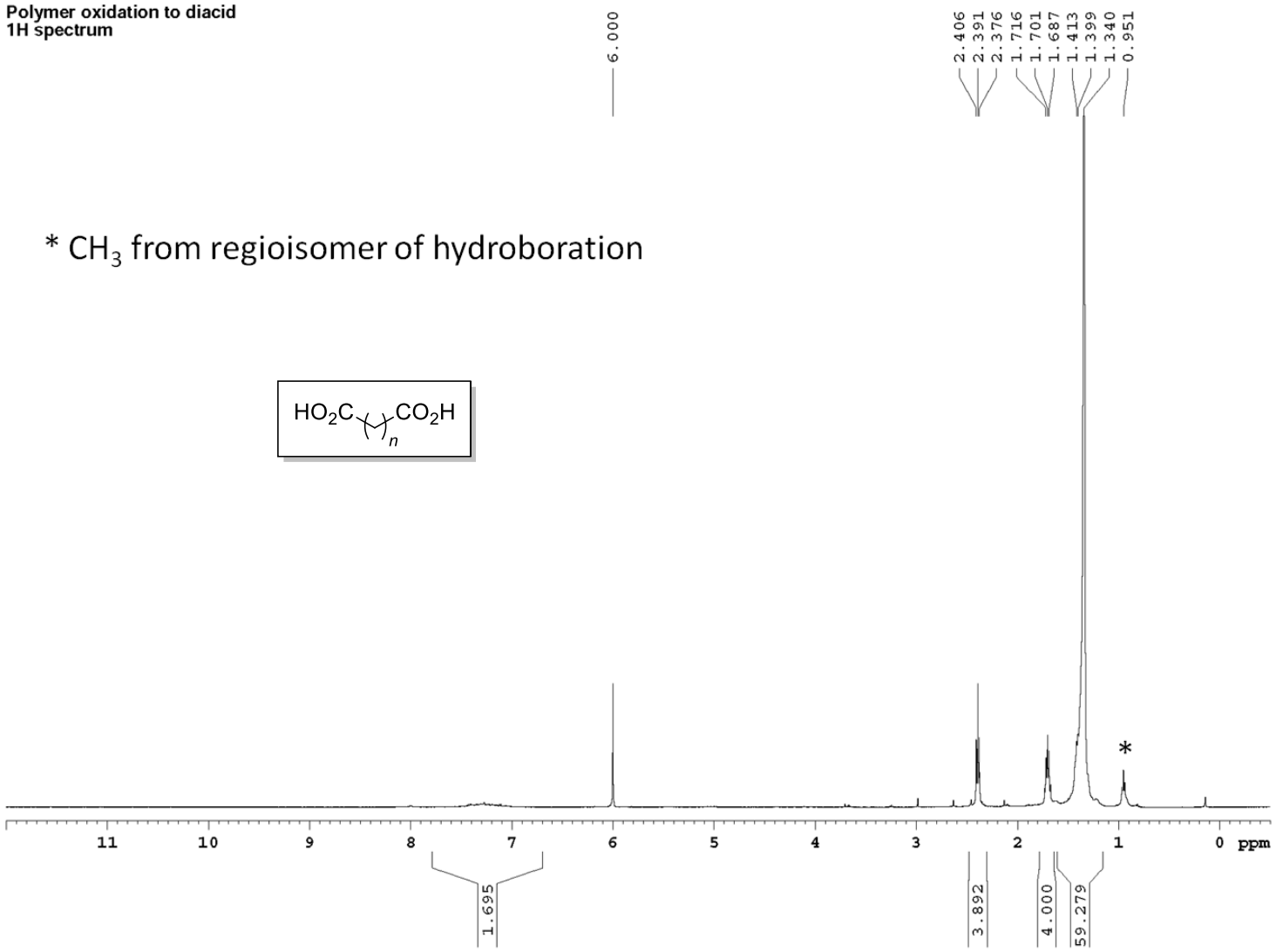
Polymer oxidation to diacid
1H spectrum
6.000
2.406
2.391
2.376
1.716
1.701
1.687
1.413
1.399
1.340
0.951
* CH3 from regioisomer of hydroboration
HO2C
CO2H
n
*
11
10
9
8
7
6
5
4
3
2
1
0
ppm
1.695
3.892
4.000
59.279

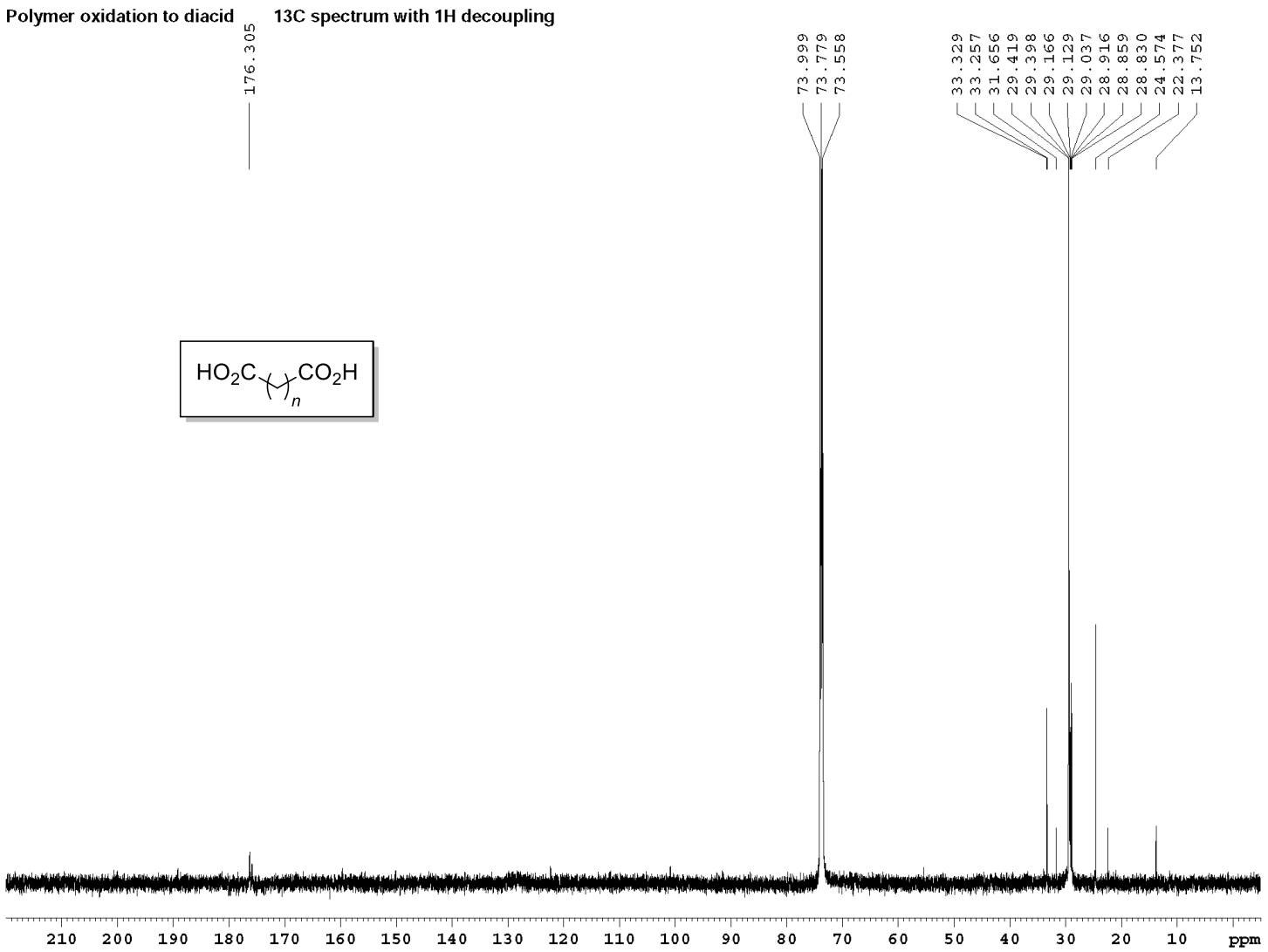
Polymer oxidation to diacid
13C spectrum with 1H decoupling
176.305
73.999
73.779
73.558
33.329
33.257
31.656
29.419
29.398
29.166
29.129
29.037
28.916
28.859
28.830
24.574
22.377
13.752
HO2C
CO2H
n
210 200 190 180 170 160 150 140 130 120 110 100 90 80 70 60 50 40 30 20 10
ppm

Triethylsulfonium chloride
1H spectrum

Current Data Parameters
USER ruzhao
NAME zrb-I-63
EXPNO 1
PROCNO 1

F2 - Acquisition Parameters
Date_ 20120618
Time 12.52
INSTRUM gn500
PROBHD 5 mm broadband
PULPROG zg30
TD 81728
SOLVENT D2O
NS 8
DS 2
SWH 8012.820 Hz
FIDRES 0.098043 Hz
AQ 5.0998774 sec
RG 90.5
DW 62.400 usec
DE 6.00 usec
TE 298.0 K
D1 0.10000000 sec
MCREST 0.00000000 sec
MCWRK 0.01500000 sec

======== CHANNEL f1 ========
NUC1 1H
P1 12.20 usec
PL1 -5.00 dB
SFO1 499.4034958 MHz

F2 - Processing parameters
SI 65536
SF 499.4000091 MHz
WDW EM
SSB 0
LB 0.30 Hz
GB 0
PC 1.00

Triethylsulfonium chloride
13C spectrum with 1H decoupling

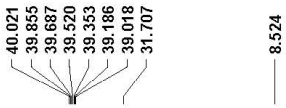

Current Data Parameters
USER ruzhao
NAME zrb−I−126
EXPNO 2
PROCNO 1

F2 − Acquisition Parameters
Date_ 20120925
Time 19.07
INSTRUM gn500
PROBHD 5 mm broadband
PULPROG zgdc30
TD 65536
SOLVENT DMSO
NS 192
DS 4
SWH 30303.031 Hz
FIDRES 0.462388 Hz
AQ 1.0813940 sec
RG 4597.6
DW 16.500 usec
DE 4.50 usec
TE 298.0 K
D1 0.25000000 sec
d11 0.03000000 sec
MCREST 0.00000000 sec
MCWRK 0.01500000 sec

======== CHANNEL f1 ========
NUC1 13C
P1 7.70 usec
PL1 0.00 dB
SFO1 125.5880432 MHz

======== CHANNEL f2 ========
CPDPRG2 waltz16
NUC2 1H
PCPD2 80.00 usec
PL2 −3.00 dB
PL12 13.20 dB
SFO2 499.4024970 MHz

F2 − Processing parameters
SI 65536
SF 125.5742951 MHz
WDW EM
SSB 0
LB 1.00 Hz
GB 0
PC 2.00

1D NMR plot parameters
CX 22.80 cm
CY 12.43 cm
F1P 229.520 ppm
F1 28821.77 Hz
F2P −10.507 ppm
F2 −1319.36 Hz
PPMCM 10.52747 ppm/cm
HZCM 1321.97949 Hz/cm

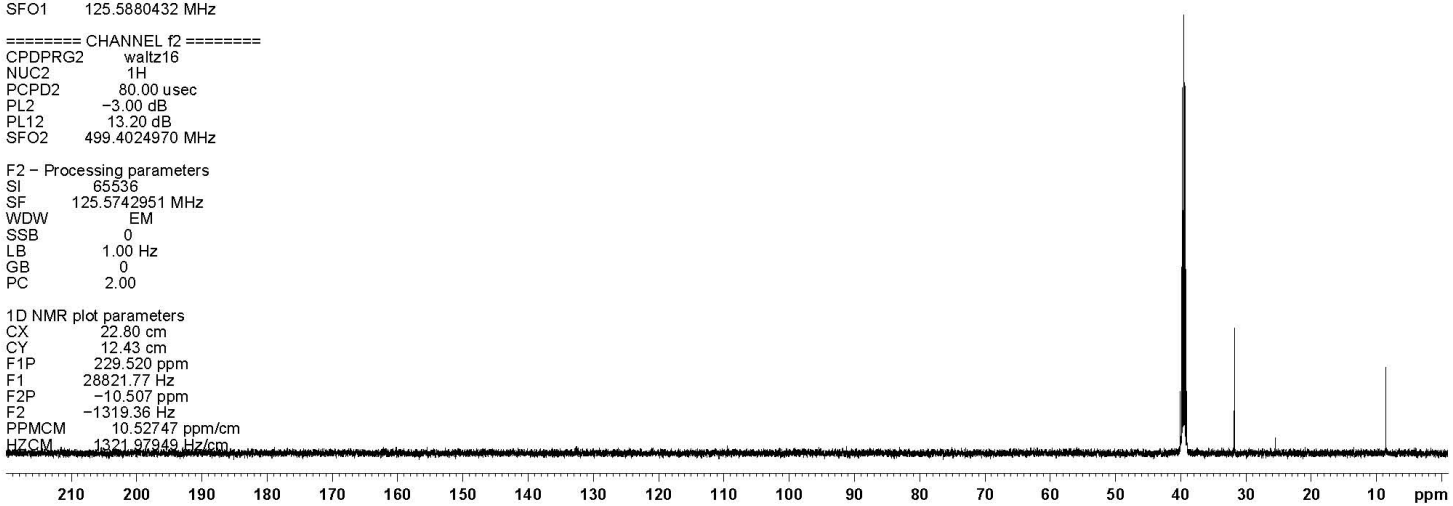

Triethylsulfoxonium Chloride
1H spectrum

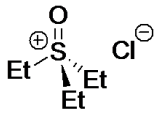

Current Data Parameters
USER ruzhao
NAME zrb−I−120
EXPNO 5
PROCNO 1

F2 − Acquisition Parameters
Date_ 20120921
Time 20.14
INSTRUM gn500
PROBHD 5 mm broadband
PULPROG zg30
TD 81728
SOLVENT D2O
NS 8
DS 2
SWH 8012.820 Hz
FIDRES 0.098043 Hz
AQ 5.0998774 sec
RG 143.7
DW 62.400 usec
DE 6.00 usec
TE 298.0 K
D1 0.10000000 sec
MCREST 0.00000000 sec
MCWRK 0.01500000 sec

======== CHANNEL f1 ========
NUC1 1H
P1 12.20 usec
PL1 −5.00 dB
SFO1 499.4034958 MHz

F2 − Processing parameters
SI 65536
SF 499.4000095 MHz
WDW EM
SSB 0
LB 0.30 Hz
GB 0
PC 4.00

1D NMR plot parameters
CX 22.80 cm
CY 15.00 cm
F1P 9.900 ppm
F1 4944.06 Hz
F2P −0.100 ppm
F2 −49.94 Hz
PPMCM 0.43860 ppm/cm
HZCM 219.03511 Hz/cm

Triethylsulfoxonium chloride
13C spectrum with 1H decoupling

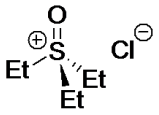

Current Data Parameters
USER ruzhao
NAME zrb-I-126
EXPNO 4
PROCNO 1

F2 - Acquisition Parameters
Date_ 20120925
Time 19.17
INSTRUM gn500
PROBHD 5 mm broadband
PULPROG zgdc30
TD 65536
SOLVENT DMSO
NS 192
DS 4
SWH 30303.031 Hz
FIDRES 0.462388 Hz
AQ 1.0813940 sec
RG 46341
DW 16.500 usec
DE 4.50 usec
TE 298.0 K
D1 0.25000000 sec
d11 0.03000000 sec
MCREST 0.00000000 sec
MCWRK 0.01500000 sec

======== CHANNEL f1 ========
NUC1 13C
P1 7.70 usec
PL1 0.00 dB
SFO1 125.5880432 MHz

======== CHANNEL f2 ========
CPDPRG2 waltz16
NUC2 1H
PCPD2 80.00 usec
PL2 -3.00 dB
PL12 13.20 dB
SFO2 499.4024970 MHz

F2 - Processing parameters
SI 65536
SF 125.5742946 MHz
WDW EM
SSB 0
LB 1.00 Hz
GB 0
PC 2.00

1D NMR plot parameters
CX 22.80 cm
CY 13.81 cm
F1P 229.520 ppm
F1 28821.77 Hz
F2P -10.507 ppm
F2 -1319.70 Hz
PPMCM 10.32747 ppm/cm
HZCM 1321.97949 Hz/cm

Tri(n-hexyl)borane
1H spectrum

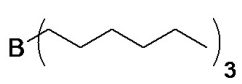

Current Data Parameters
USER ruzhao
NAME zrb-I-135
EXPNO 1
PROCNO 1

F2 - Acquisition Parameters
Date_ 20121101
Time 20.07
INSTRUM gn500
PROBHD 5 mm broadband
PULPROG zg30
TD 81728
SOLVENT CD2Cl2
NS 8
DS 2
SWH 8012.820 Hz
FIDRES 0.098043 Hz
AQ 5.0998774 sec
RG 181
DW 62.400 usec
DE 6.00 usec
TE 298.0 K
D1 0.10000000 sec
MCREST 0.00000000 sec
MCWRK 0.01500000 sec

======== CHANNEL f1 ========
NUC1 1H
P1 12.20 usec
PL1 -5.00 dB
SFO1 499.4034958 MHz

F2 - Processing parameters
SI 65536
SF 499.4000235 MHz
WDW EM
SSB 0
LB 0.30 Hz
GB 0
PC 2.00

Tri(n−hexyl)borane
13C spectrum with 1H decoupling

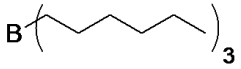

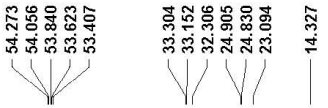

Current Data Parameters
USER ruzhao
NAME zrb−I−135
EXPNO 2
PROCNO 1

F2 − Acquisition Parameters
Date_ 20121101
Time 20.11
INSTRUM gn500
PROBHD 5 mm broadband
PULPROG zgdc30
TD 65536
SOLVENT CD2Cl2
NS 256
DS 4
SWH 30303.031 Hz
FIDRES 0.462388 Hz
AQ 1.0813940 sec
RG 13004
DW 16.500 usec
DE 4.50 usec
TE 298.0 K
D1 0.25000000 sec
d11 0.03000000 sec
MCREST 0.00000000 sec
MCWRK 0.01500000 sec

======== CHANNEL f1 ========
NUC1 13C
P1 7.70 usec
PL1 0.00 dB
SFO1 125.5880432 MHz

======== CHANNEL f2 ========
CPDPRG2 waltz16
NUC2 1H
PCPD2 80.00 usec
PL2 −3.00 dB
PL12 13.20 dB
SFO2 499.4024970 MHz

F2 − Processing parameters
SI 65536
SF 125.5741749 MHz
WDW EM
SSB 0
LB 1.00 Hz
GB 0
PC 2.00

1D NMR plot parameters
CX 22.80 cm
CY 14.64 cm
F1P 229.520 ppm
F1 28821.74 Hz
F2P −10.507 ppm
F2 −1319.36 Hz
PPMCM 10.52747 ppm/cm
HZCM −1321.97815 Hz/cm

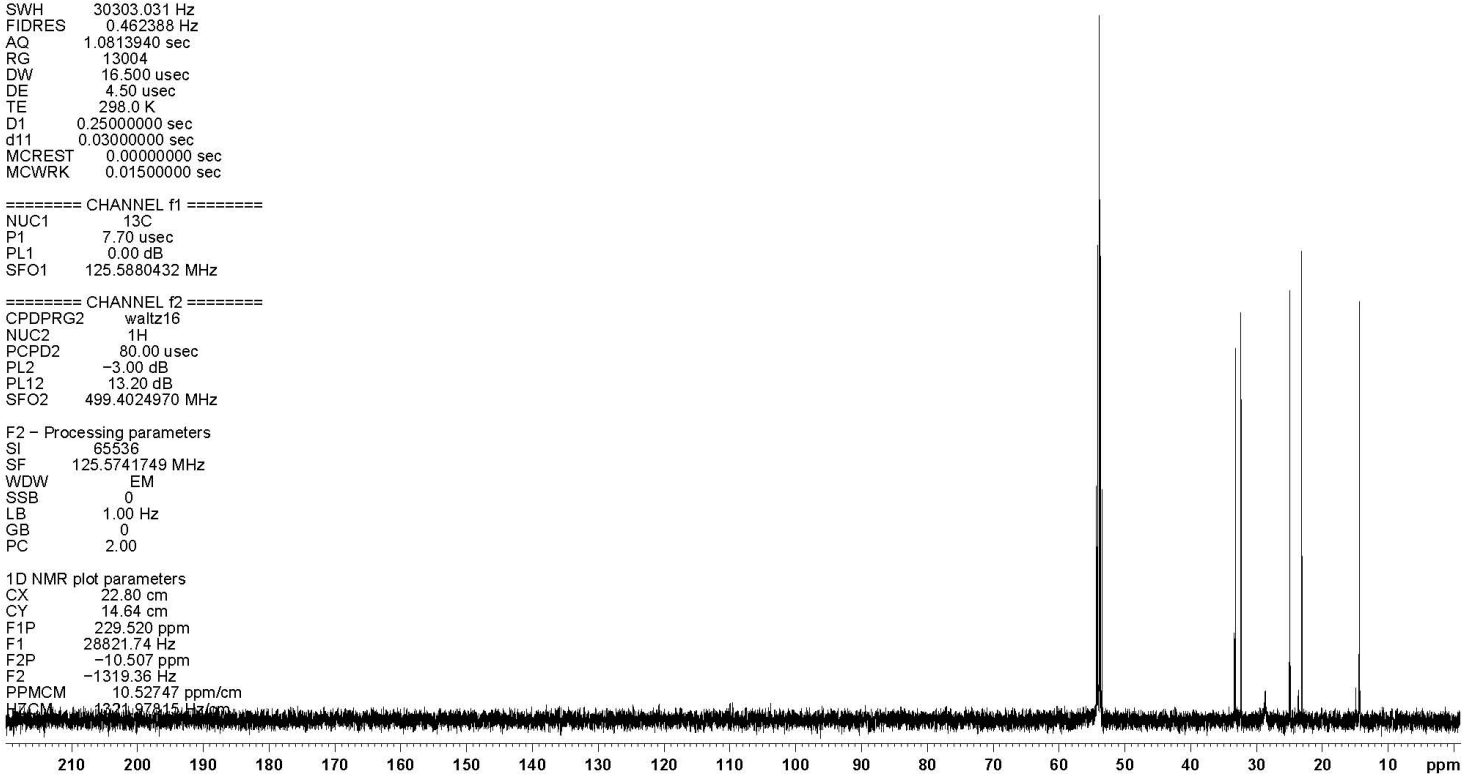

Tri(n−hexyl)borane
11B NMR

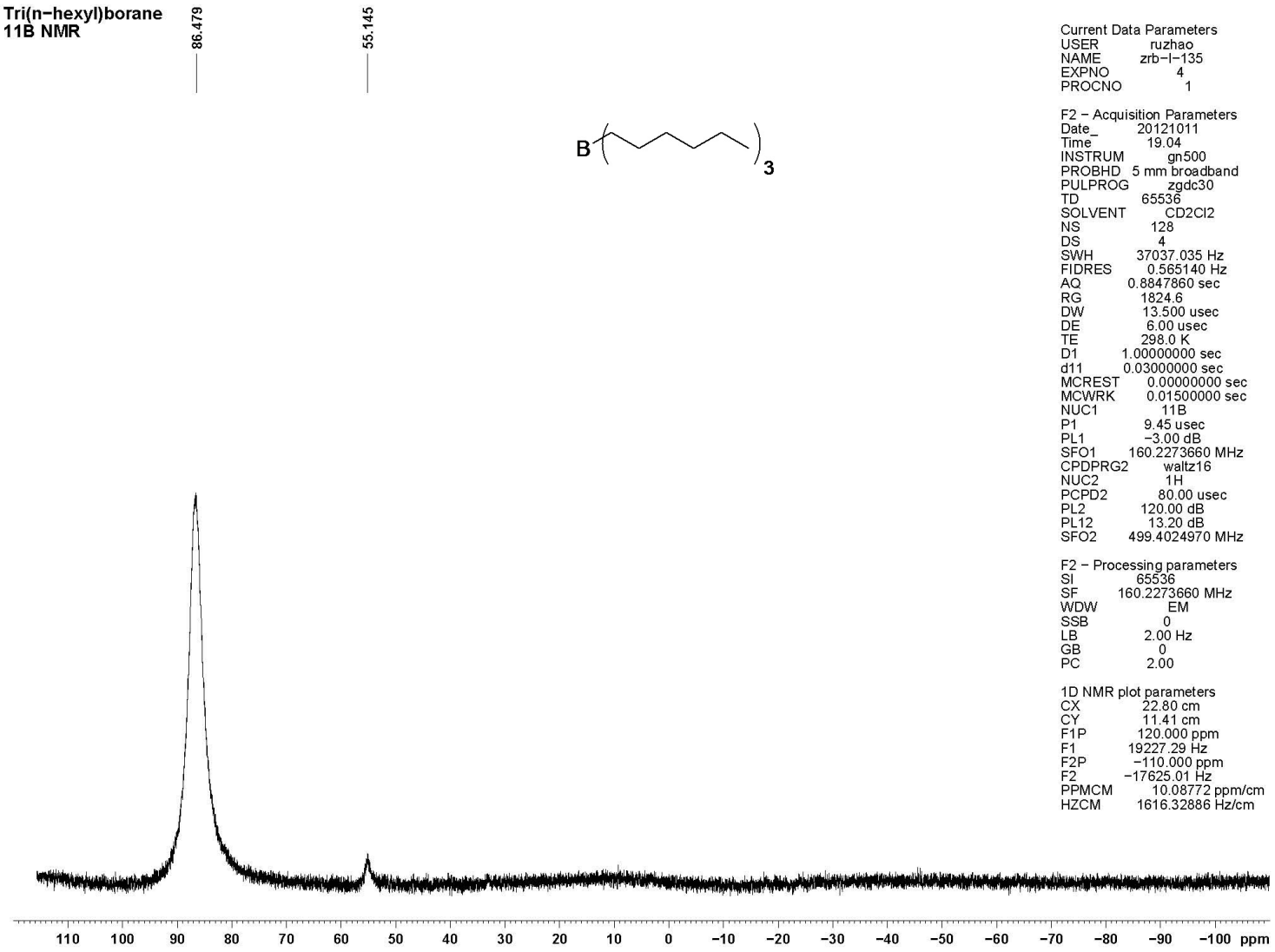

Current Data Parameters
USER ruzhao
NAME zrb−I−135
EXPNO 4
PROCNO 1

F2 − Acquisition Parameters
Date_ 20121011
Time 19.04
INSTRUM gn500
PROBHD 5 mm broadband
PULPROG zgdc30
TD 65536
SOLVENT CD2Cl2
NS 128
DS 4
SWH 37037.035 Hz
FIDRES 0.565140 Hz
AQ 0.8847860 sec
RG 1824.6
DW 13.500 usec
DE 6.00 usec
TE 298.0 K
D1 1.00000000 sec
d11 0.03000000 sec
MCREST 0.00000000 sec
MCWRK 0.01500000 sec
NUC1 11B
P1 9.45 usec
PL1 −3.00 dB
SFO1 160.2273660 MHz
CPDPRG2 waltz16
NUC2 1H
PCPD2 80.00 usec
PL2 120.00 dB
PL12 13.20 dB
SFO2 499.4024970 MHz

F2 − Processing parameters
SI 65536
SF 160.2273660 MHz
WDW EM
SSB 0
LB 2.00 Hz
GB 0
PC 2.00

1D NMR plot parameters
CX 22.80 cm
CY 11.41 cm
F1P 120.000 ppm
F1 19227.29 Hz
F2P −110.000 ppm
F2 −17625.01 Hz
PPMCM 10.08772 ppm/cm
HZCM 1616.32886 Hz/cm

Copolymer of Me/Et 9.0/1.0
1H spectrum

Current Data Parameters
USER ruzhao
NAME zrb-I-136
EXPNO 1
PROCNO 1

F2 - Acquisition Parameters
Date_ 20121015
Time 19.11
INSTRUM gn500
PROBHD 5 mm broadband
PULPROG zg30
TD 81728
SOLVENT Toluene
NS 8
DS 2
SWH 8012.820 Hz
FIDRES 0.098043 Hz
AQ 5.0998774 sec
RG 1824.6
DW 62.400 usec
DE 6.00 usec
TE 363.0 K
D1 0.10000000 sec
MCREST 0.00000000 sec
MCWRK 0.01500000 sec

======== CHANNEL f1 ========
NUC1 1H
P1 12.20 usec
PL1 -5.00 dB
SFO1 499.4034958 MHz

F2 - Processing parameters
SI 65536
SF 499.4000000 MHz
WDW EM
SSB 0
LB 0.30 Hz
GB 0
PC 1.00

1D NMR plot parameters
CX 22.80 cm
CY 15.00 cm
F1P 10.000 ppm
F1 4994.00 Hz
F2P -1.022 ppm
F2 -510.61 Hz
PPMCM 0.48344 ppm/cm
HZCM 241.43022 Hz/cm

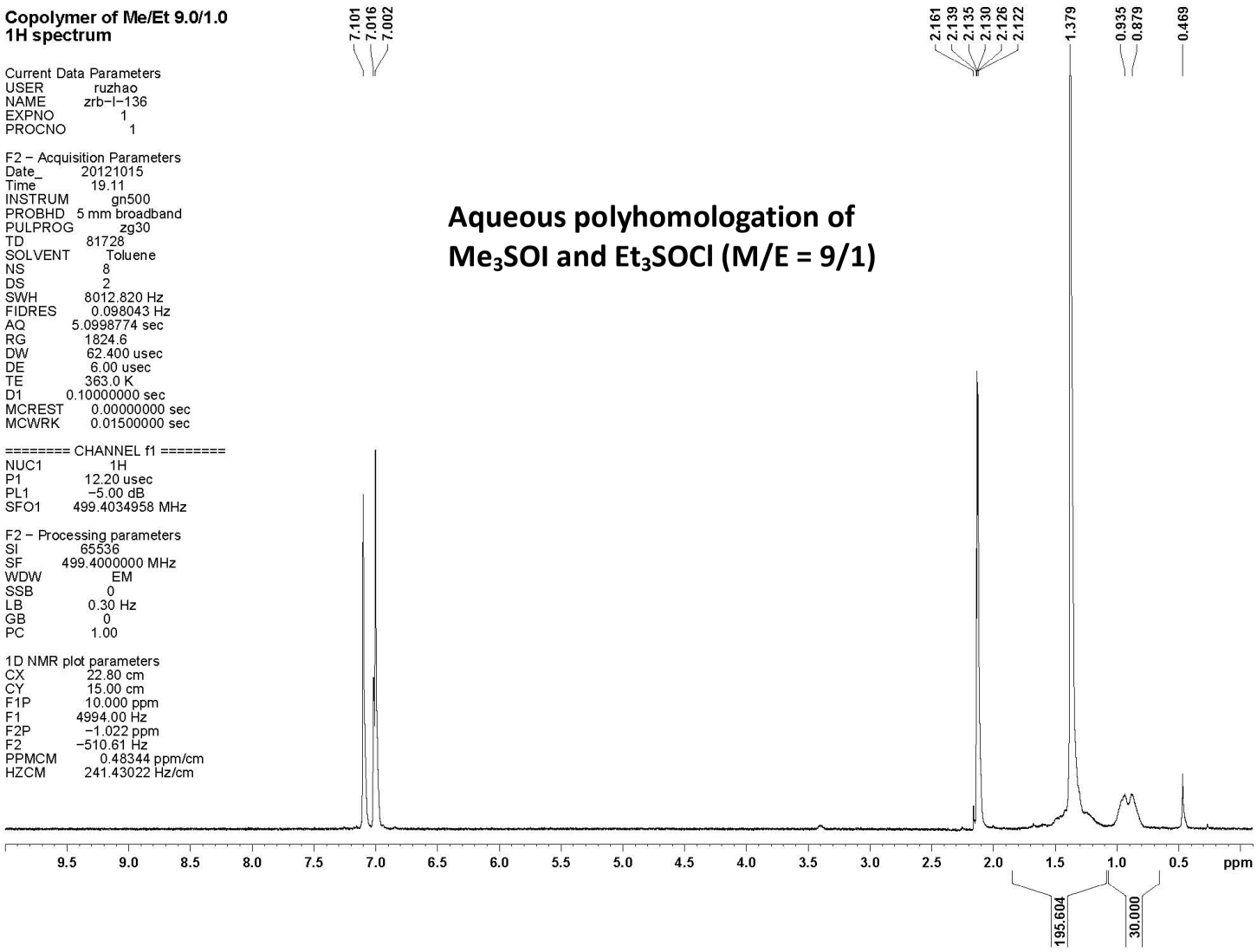

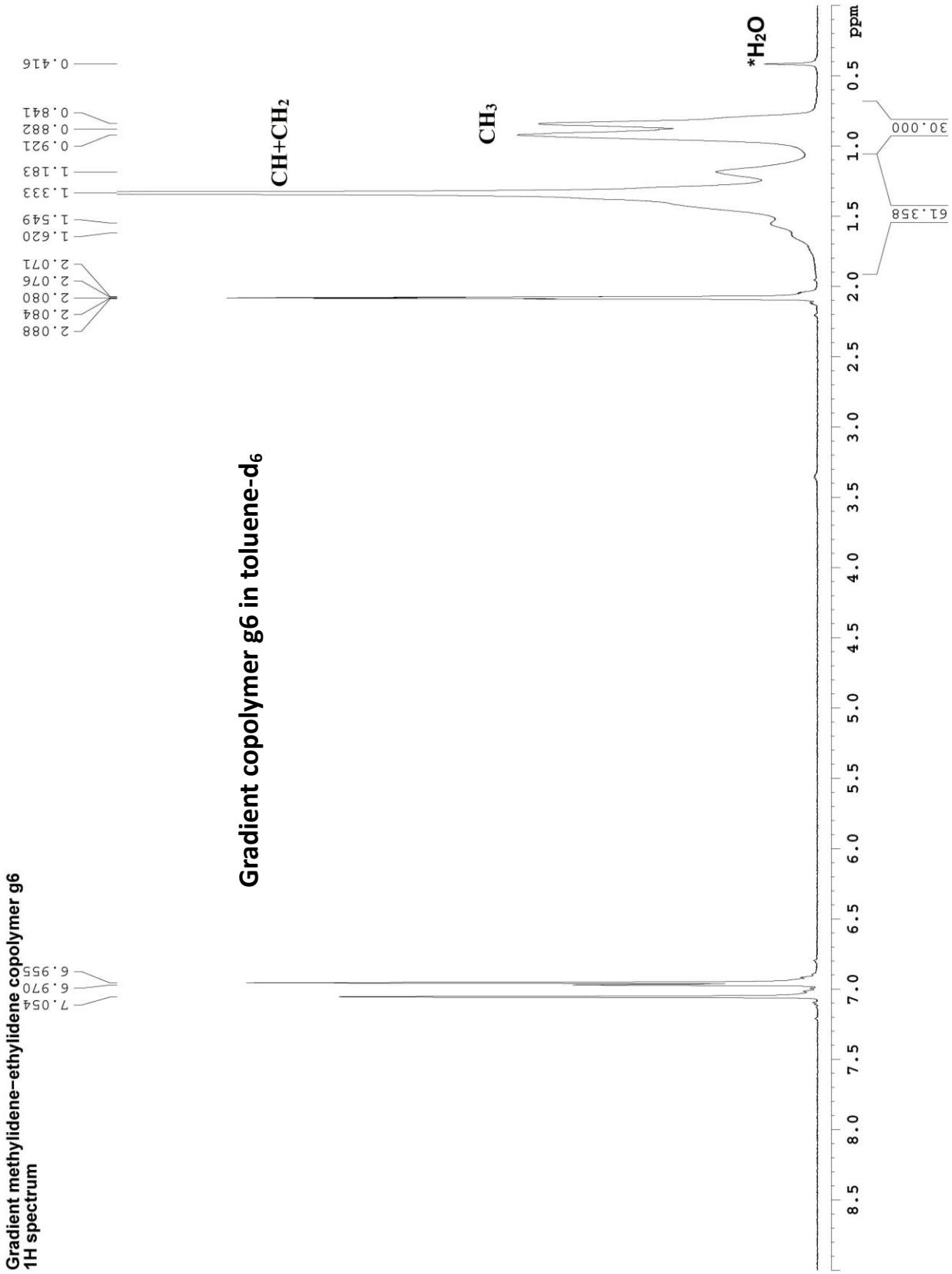
Gradient methylidene–ethylidene copolymer g6
1H spectrum
Gradient copolymer g6 in toluene-d6
CH+CH2
CH3
*H2O
ppm
30.000
61.358
0.416
0.841
0.882
0.921
1.183
1.333
1.549
1.620
2.071
2.076
2.080
2.084
2.088
6.955
6.970
7.054

^{13}C NMR of Gradient copolymer g6

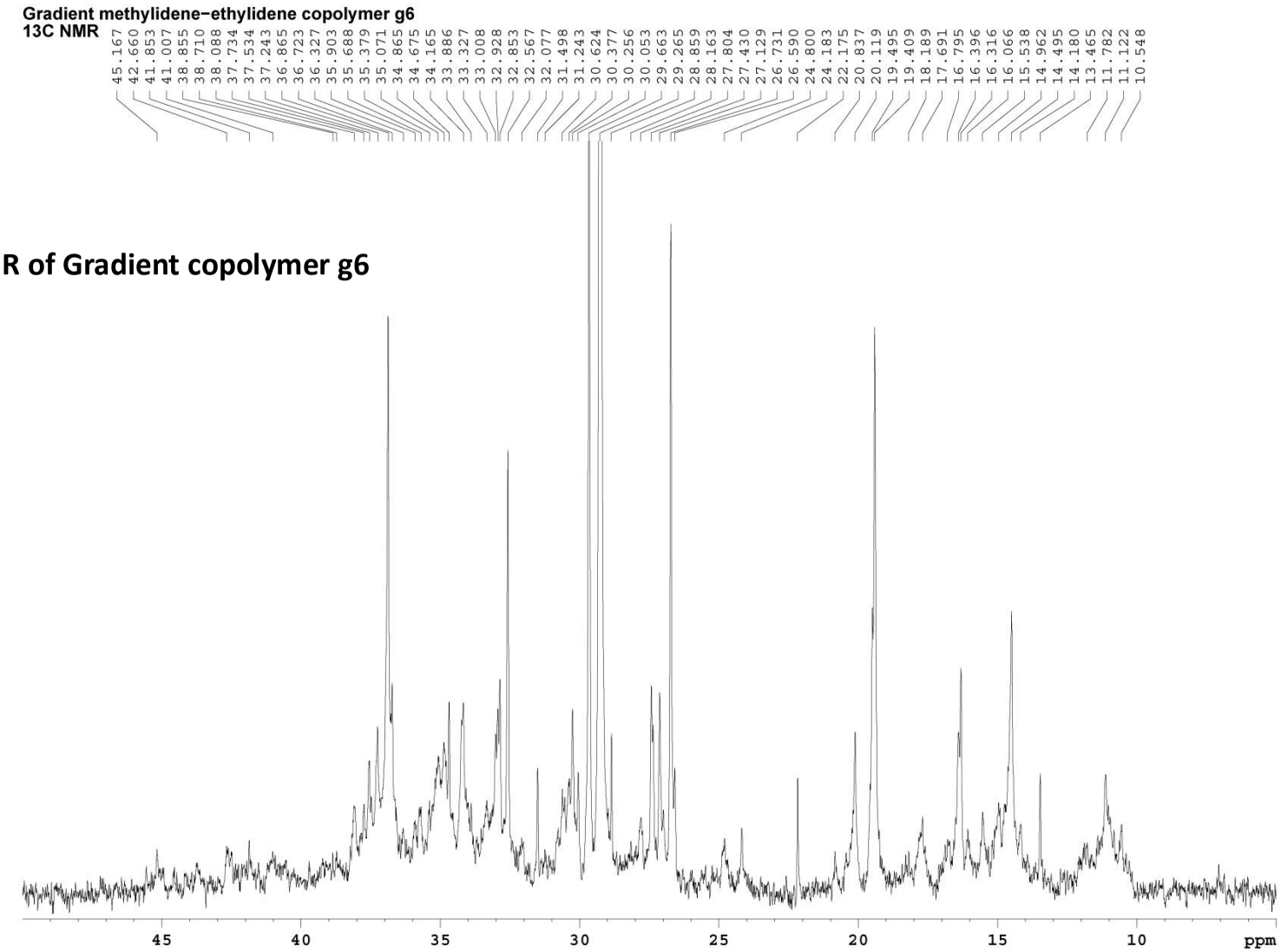

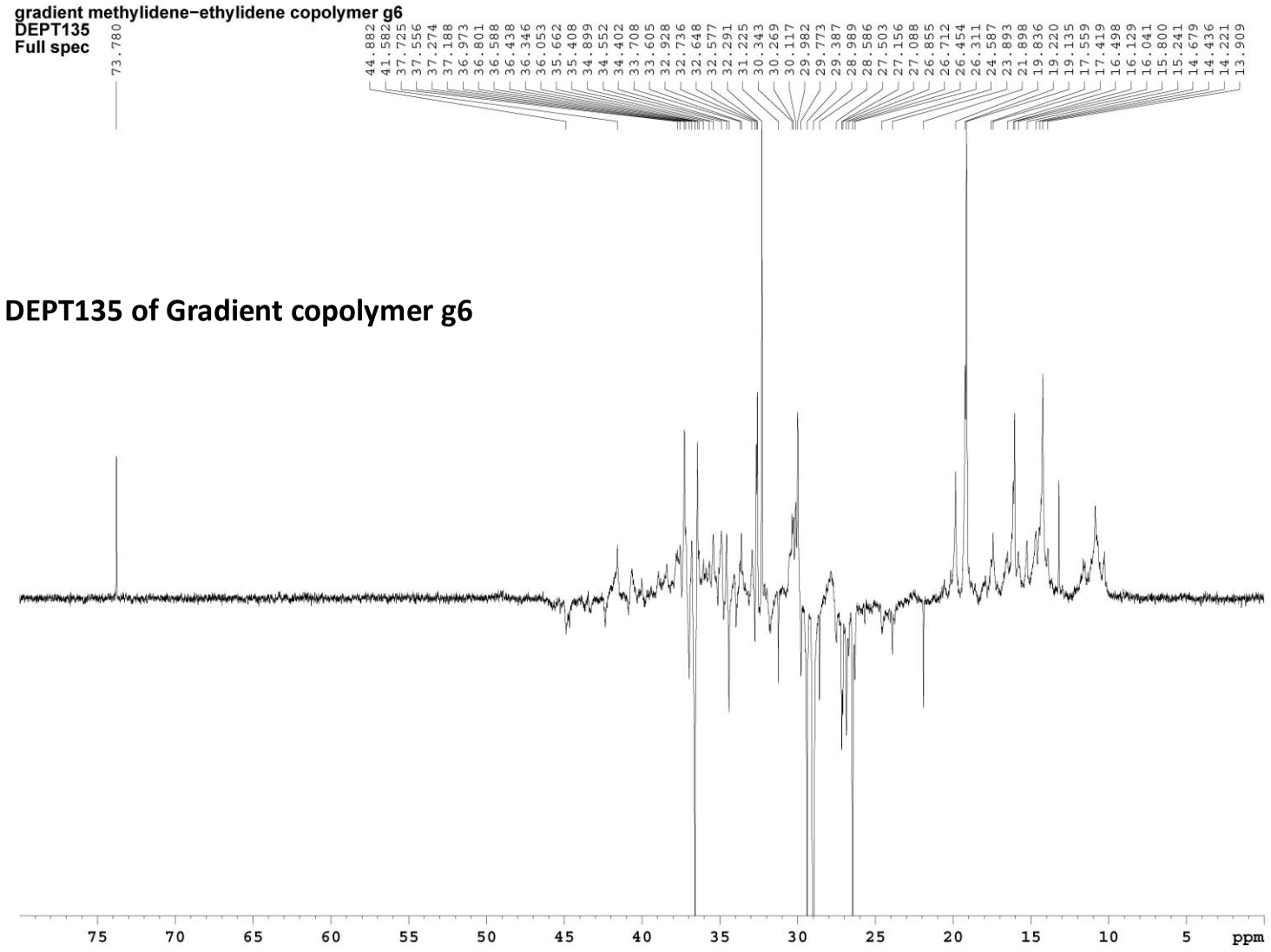

DEPT135 of Gradient copolymer g6

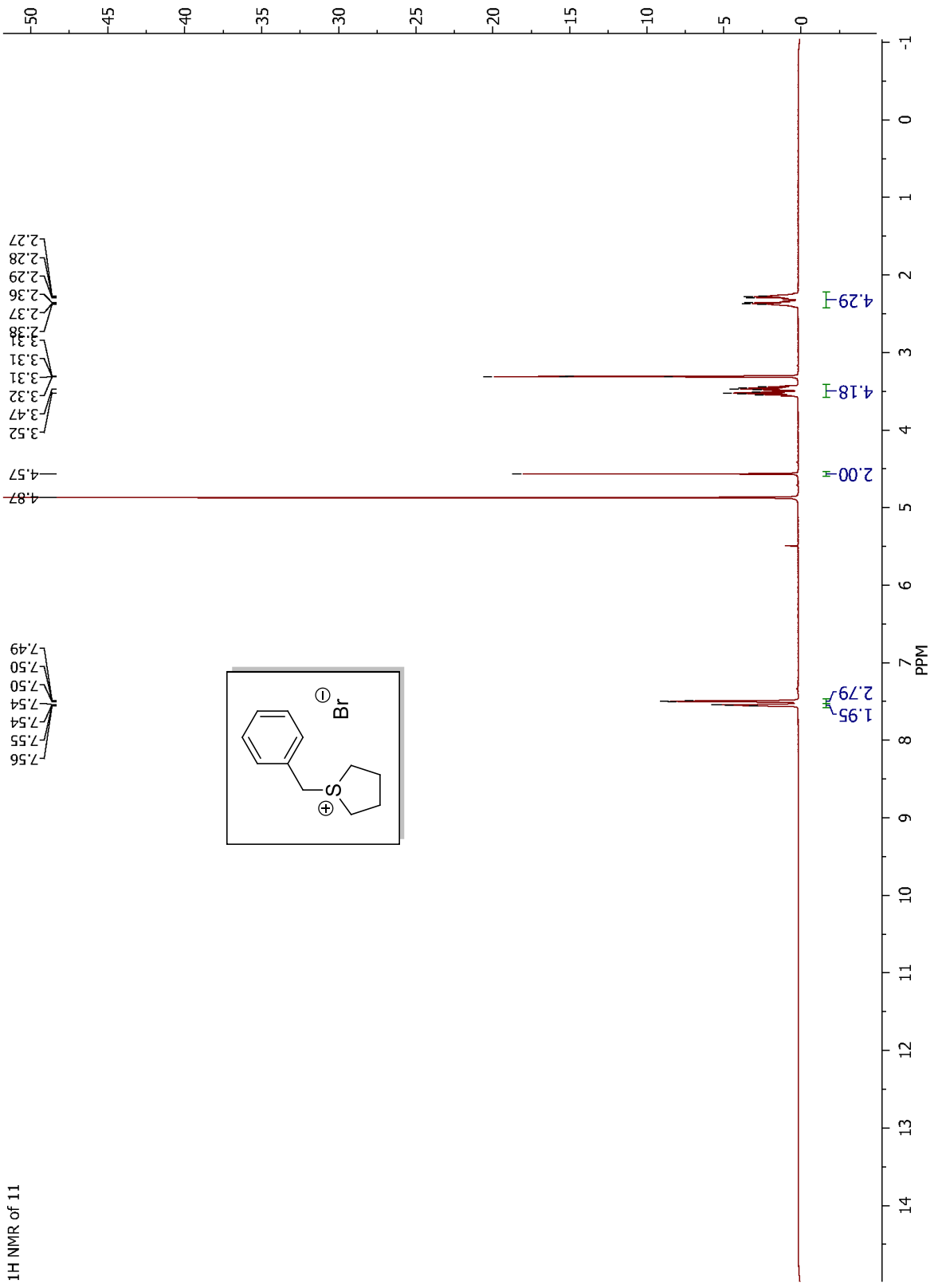
1H NMR of 11
PPM
4.29
4.18
2.00
1.95
2.79
Br
S

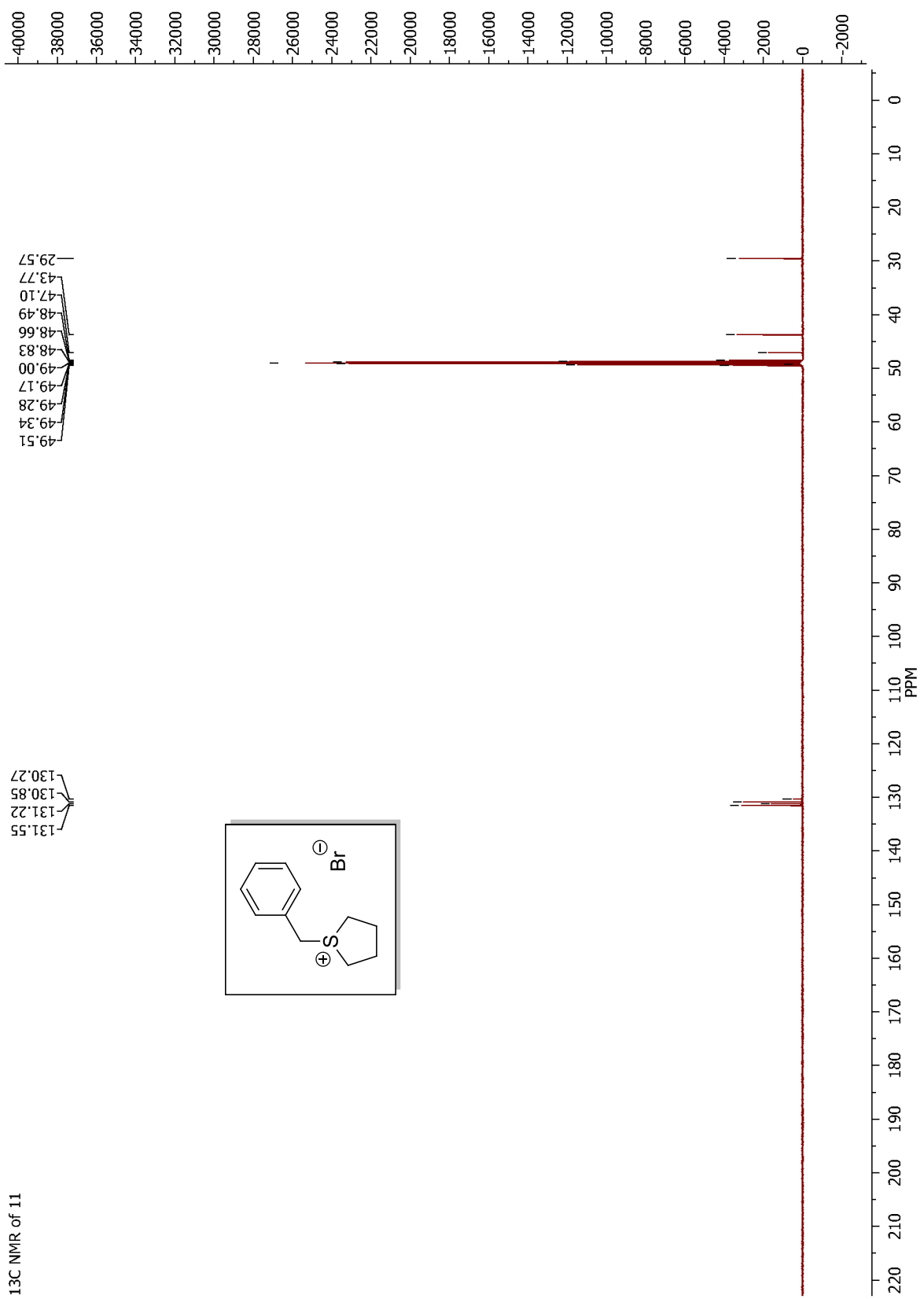
13C NMR of 11
131.55
131.22
130.85
130.27
49.51
49.34
49.28
49.17
49.00
48.83
48.66
48.49
47.10
43.77
29.57
Br
S
PPM

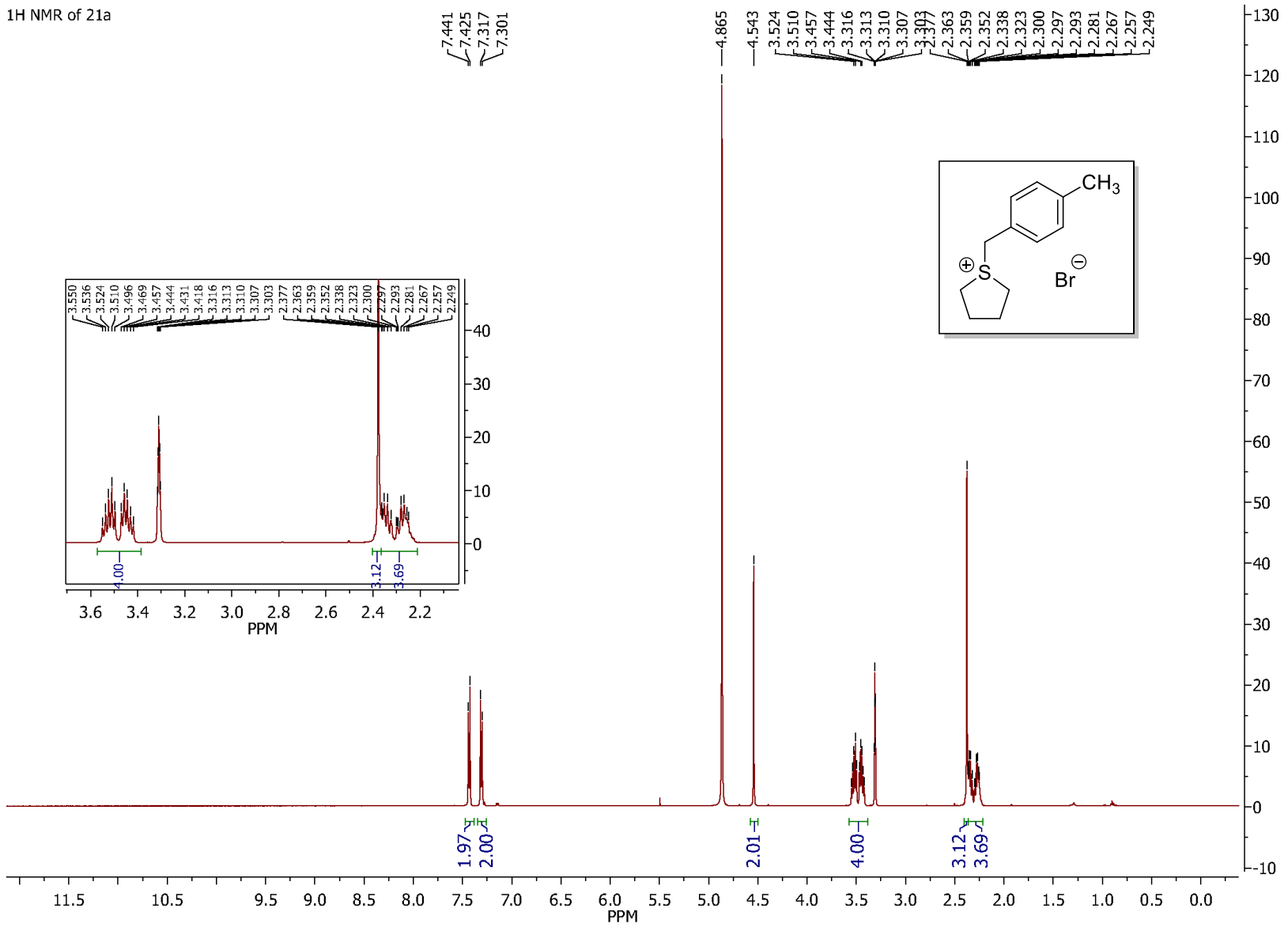
1H NMR of 21a
7.441
7.425
7.317
7.301
4.865
4.543
3.524
3.510
3.457
3.444
3.316
3.313
3.310
3.307
2.377
2.363
2.359
2.352
2.338
2.323
2.300
2.297
2.293
2.281
2.267
2.257
2.249
CH3
S
Br
1.97
2.00
2.01
4.00
3.12
3.69
PPM

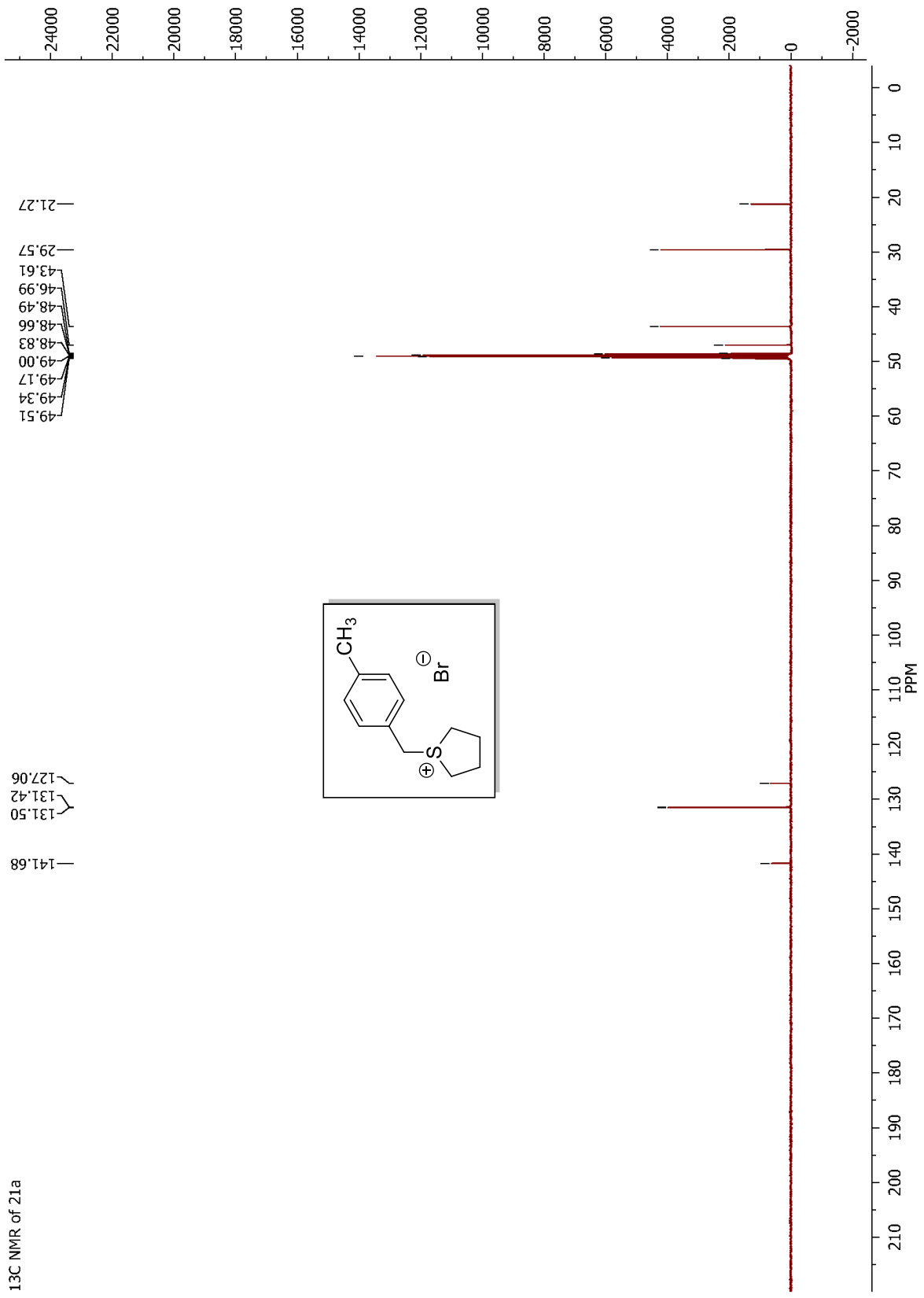
13C NMR of 21a
PPM
21.27
29.57
43.61
46.99
48.49
48.66
48.83
49.00
49.17
49.34
49.51
127.06
131.42
131.50
141.68
CH3
Br

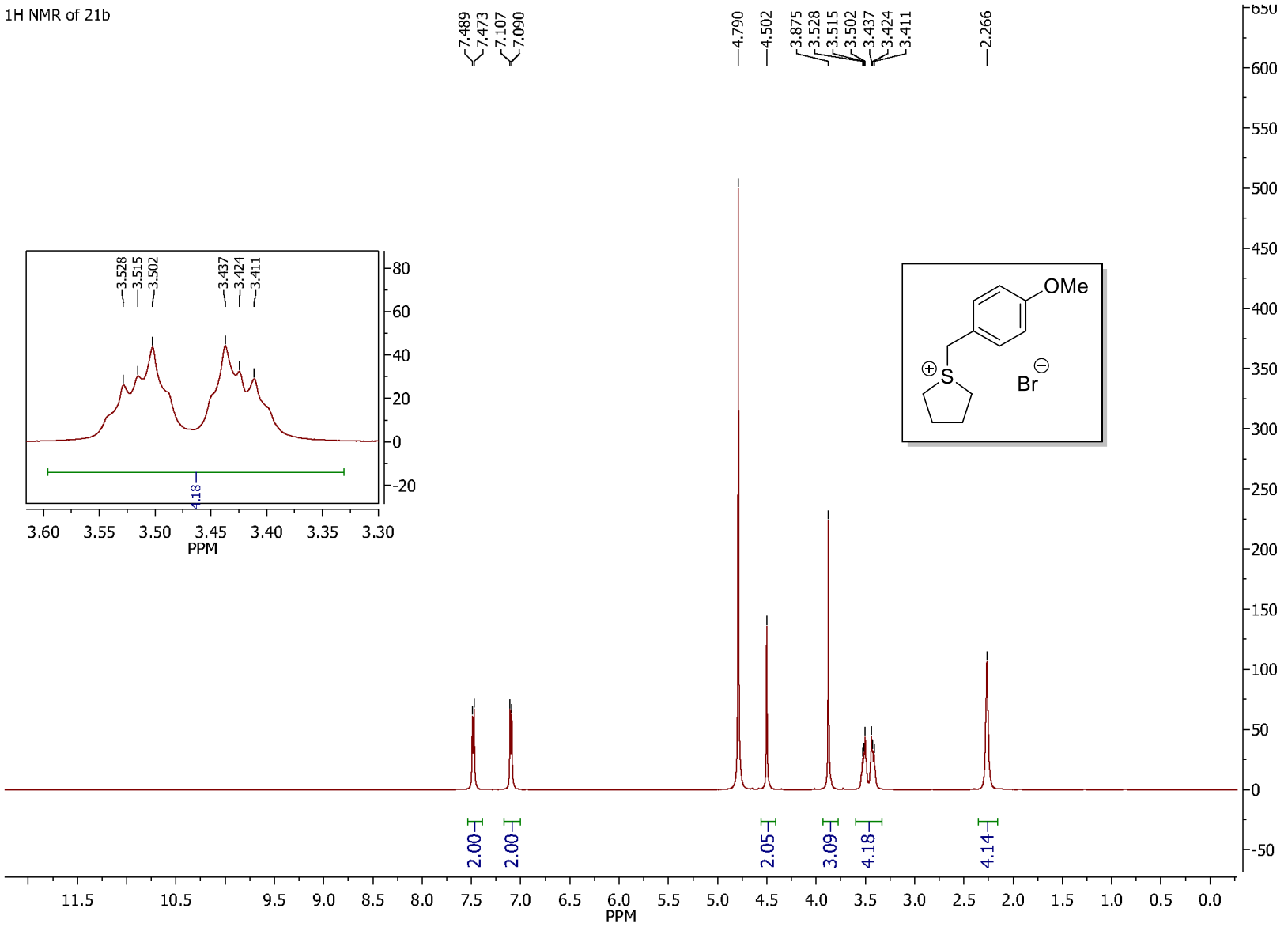
1H NMR of 21b
7.489
7.473
7.107
7.090
4.790
4.502
3.875
3.528
3.515
3.502
3.437
3.424
3.411
2.266
OMe
Br
PPM
2.00
2.00
2.05
3.09
4.18
4.14
4.18

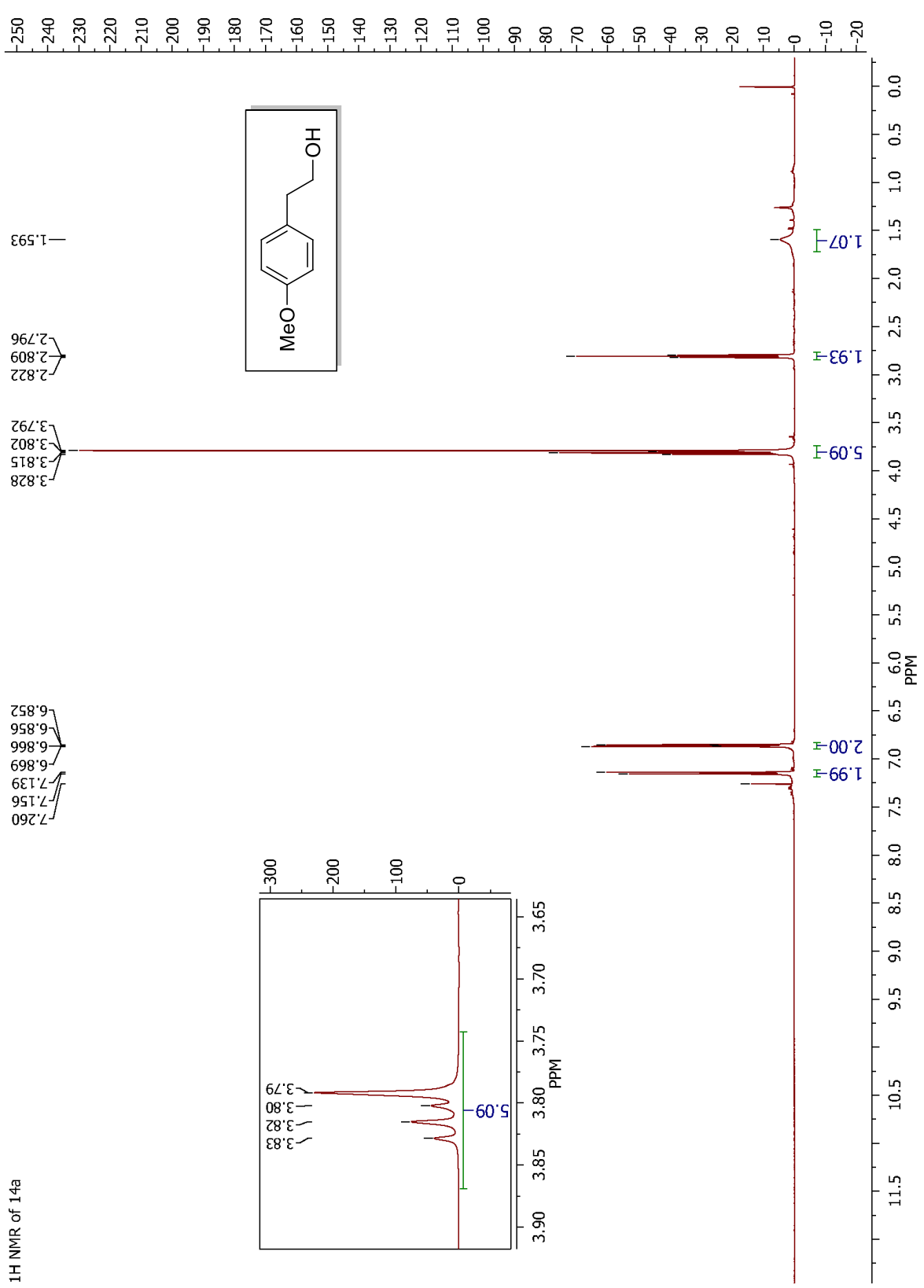
1H NMR of 14a
PPM
1.99
2.00
1.07
1.93
5.09
5.09
MeO
OH
7.260
7.156
7.139
6.869
6.866
6.856
6.852
3.828
3.815
3.802
3.792
2.822
2.809
2.796
1.593
3.83
3.82
3.80
3.79

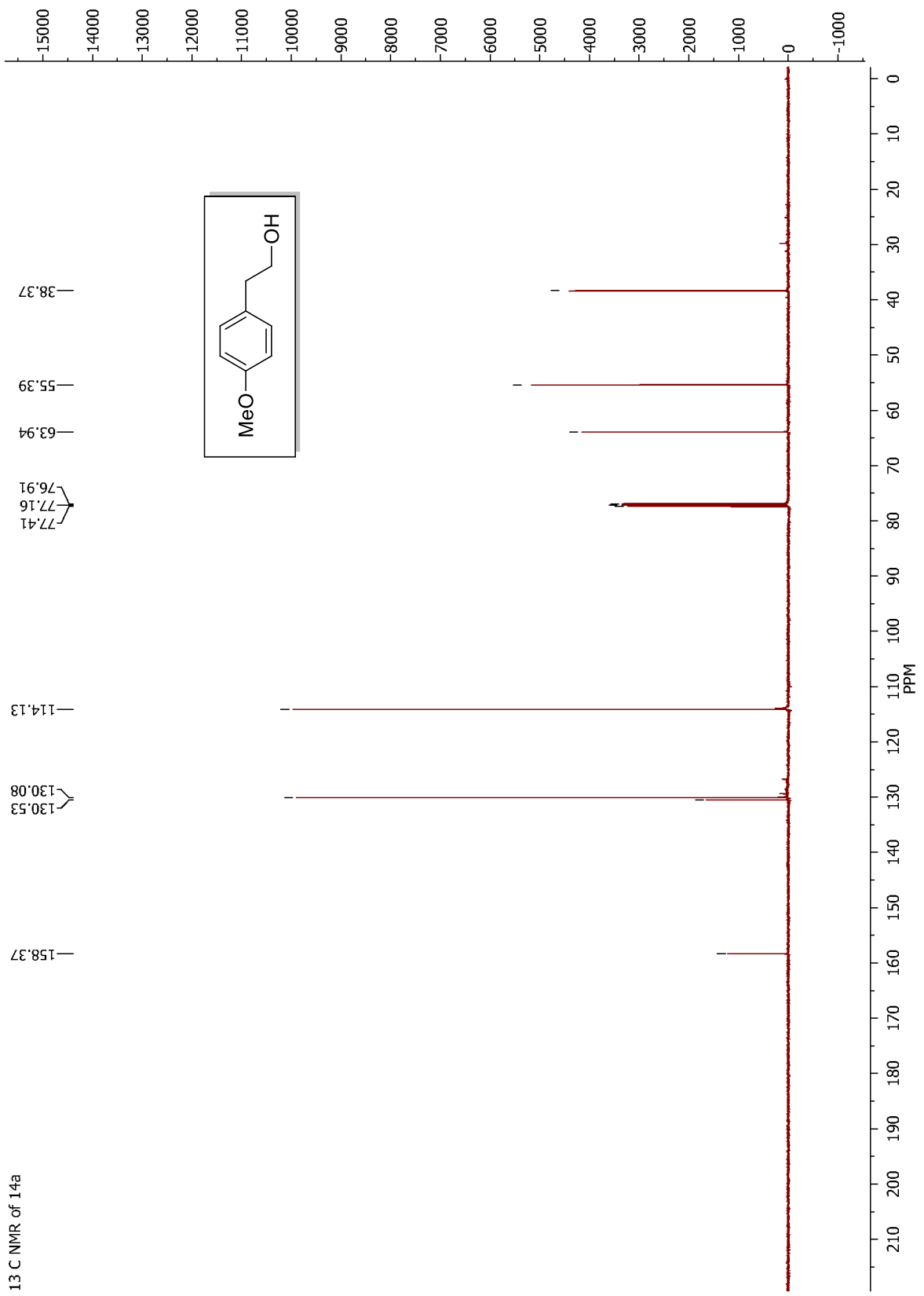
13 C NMR of 14a
158.37
130.53
130.08
114.13
77.41
77.16
76.91
63.94
55.39
38.37
MeO
OH
PPM

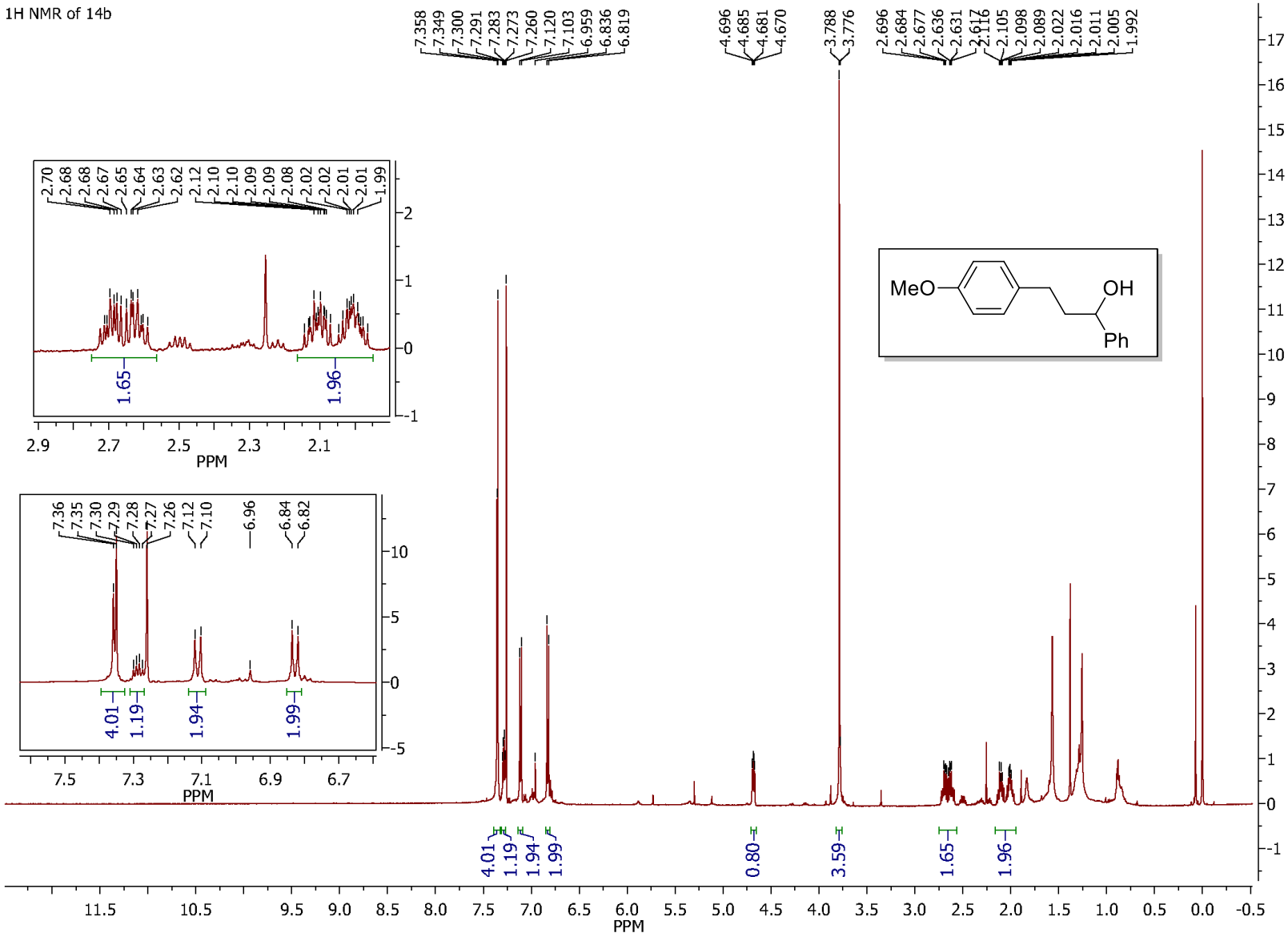
1H NMR of 14b
MeO
OH
Ph
PPM

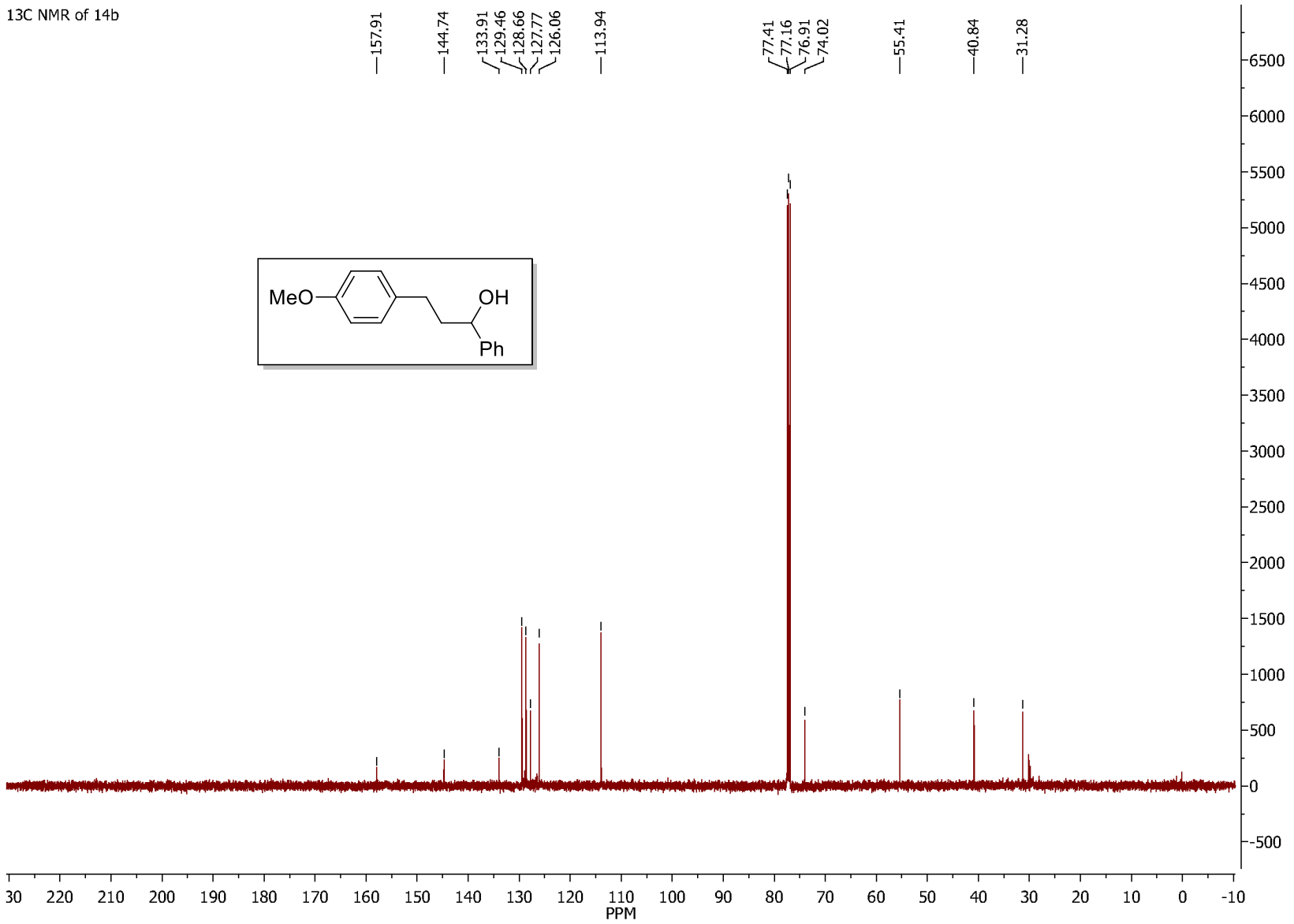
13C NMR of 14b
157.91
144.74
133.91
129.46
128.66
127.77
126.06
113.94
77.41
77.16
76.91
74.02
55.41
40.84
31.28
MeO
OH
Ph
PPM

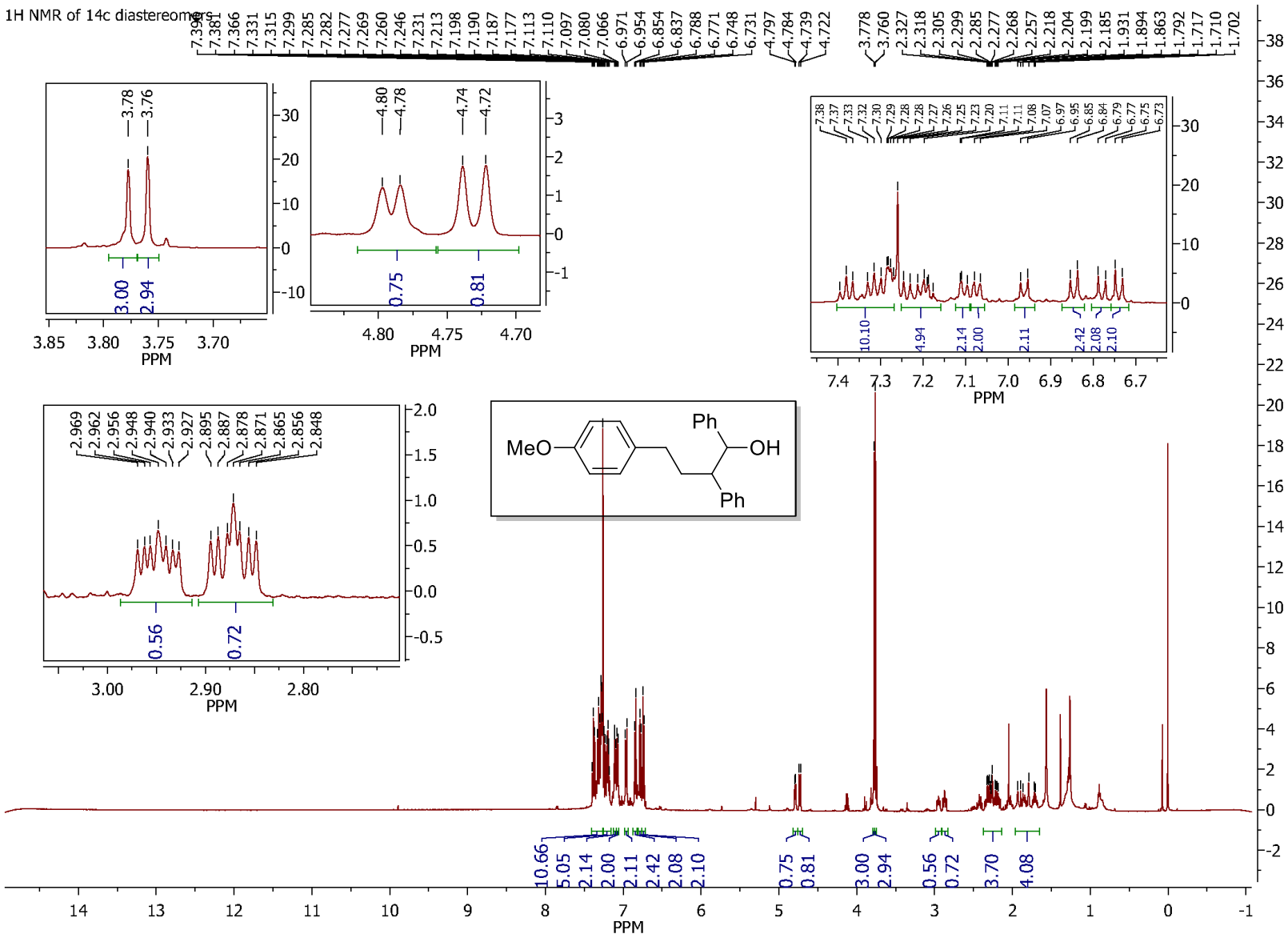
1H NMR of 14c diastereomers
MeO
Ph
OH
Ph
PPM

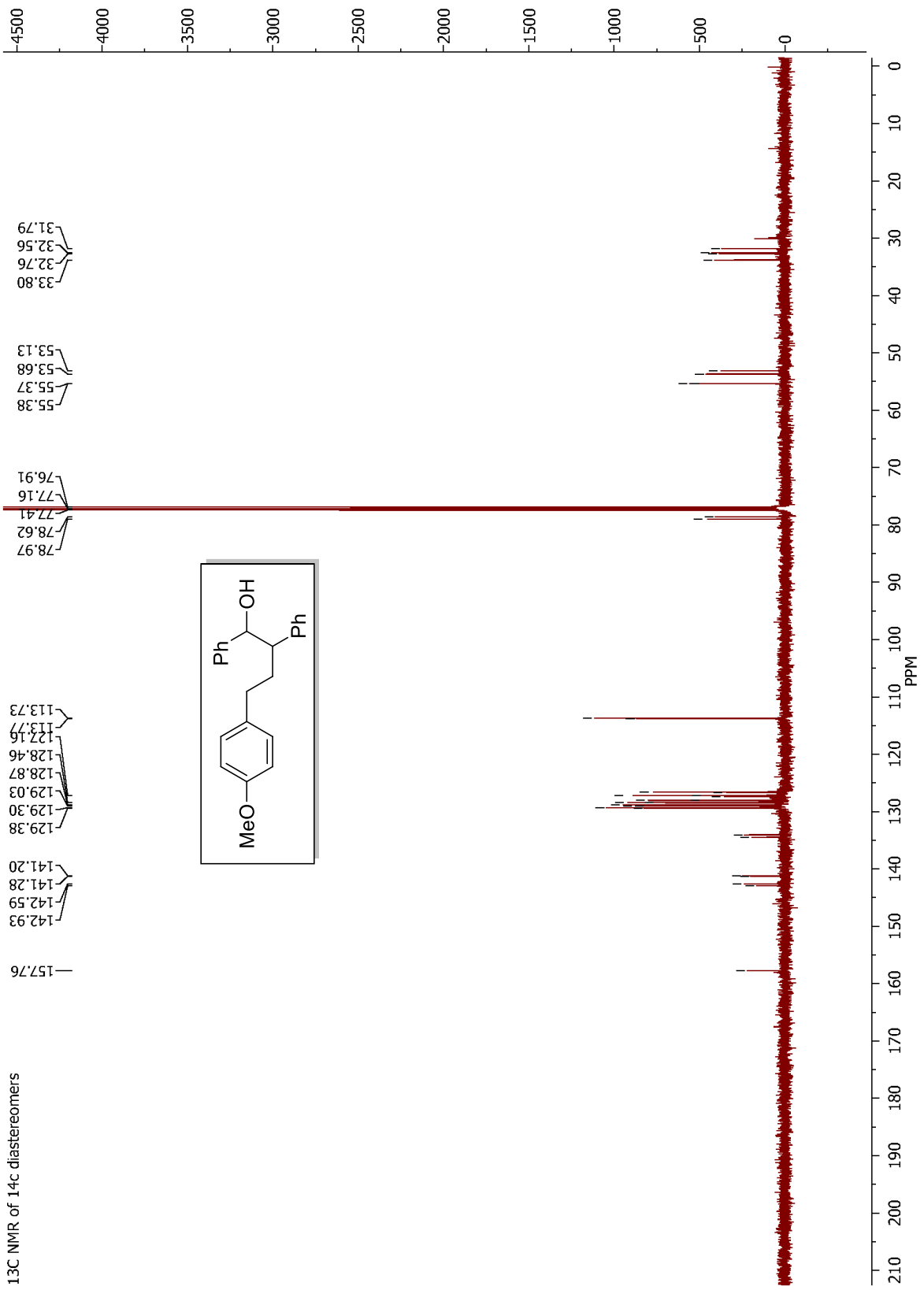
13C NMR of 14c diastereomers
157.76
142.93
142.59
141.28
141.20
129.38
129.30
129.03
128.87
128.46
127.16
113.77
113.73
78.97
78.62
77.41
77.16
76.91
55.38
55.37
53.68
53.13
33.80
32.76
32.56
31.79
OH
Ph
Ph
MeO
PPM

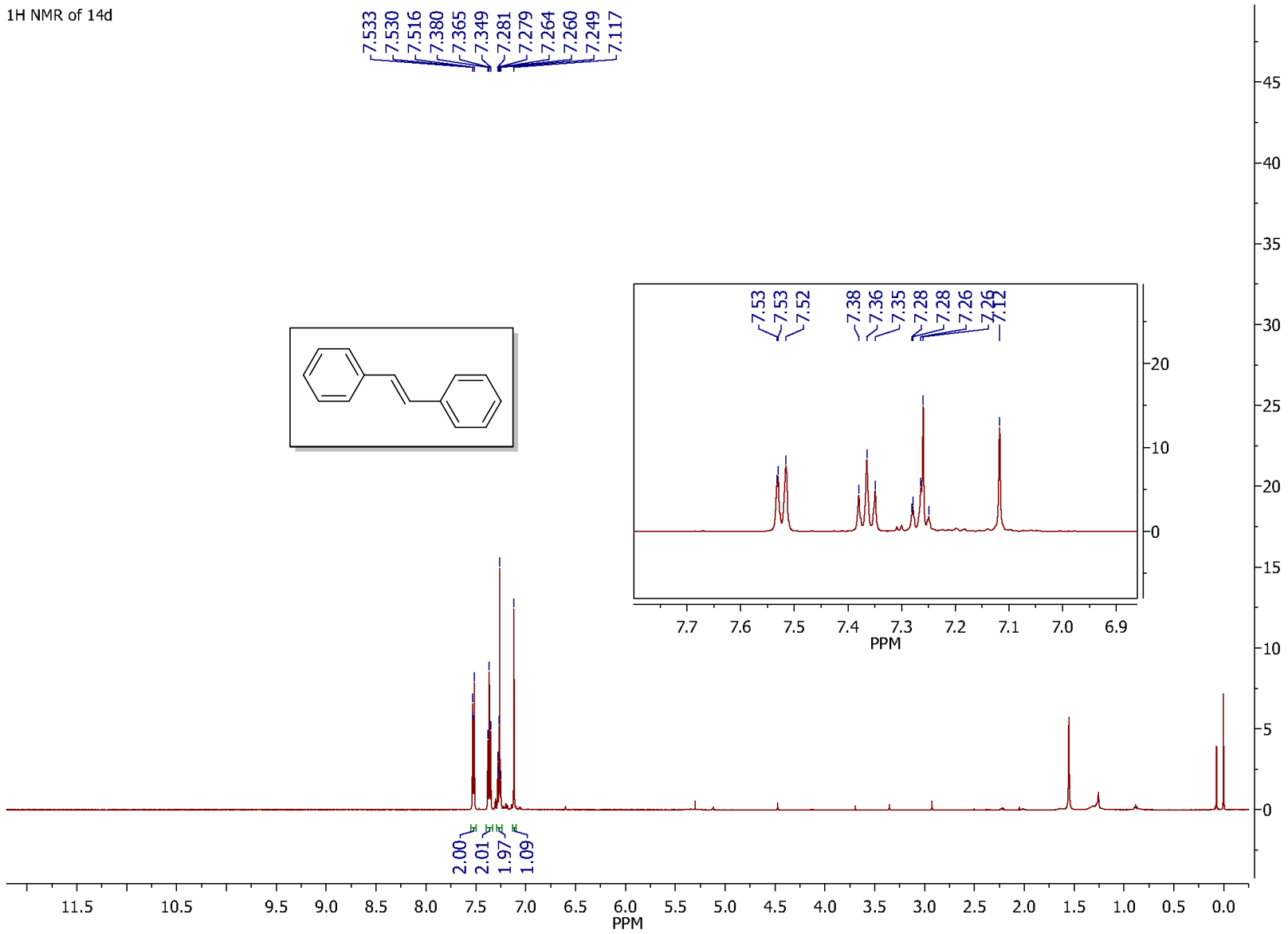
1H NMR of 14d
7.533
7.530
7.516
7.380
7.365
7.349
7.281
7.279
7.264
7.260
7.249
7.117
7.53
7.53
7.52
7.38
7.36
7.35
7.28
7.28
7.26
7.26
7.12
PPM
2.00
2.01
1.97
1.09
PPM

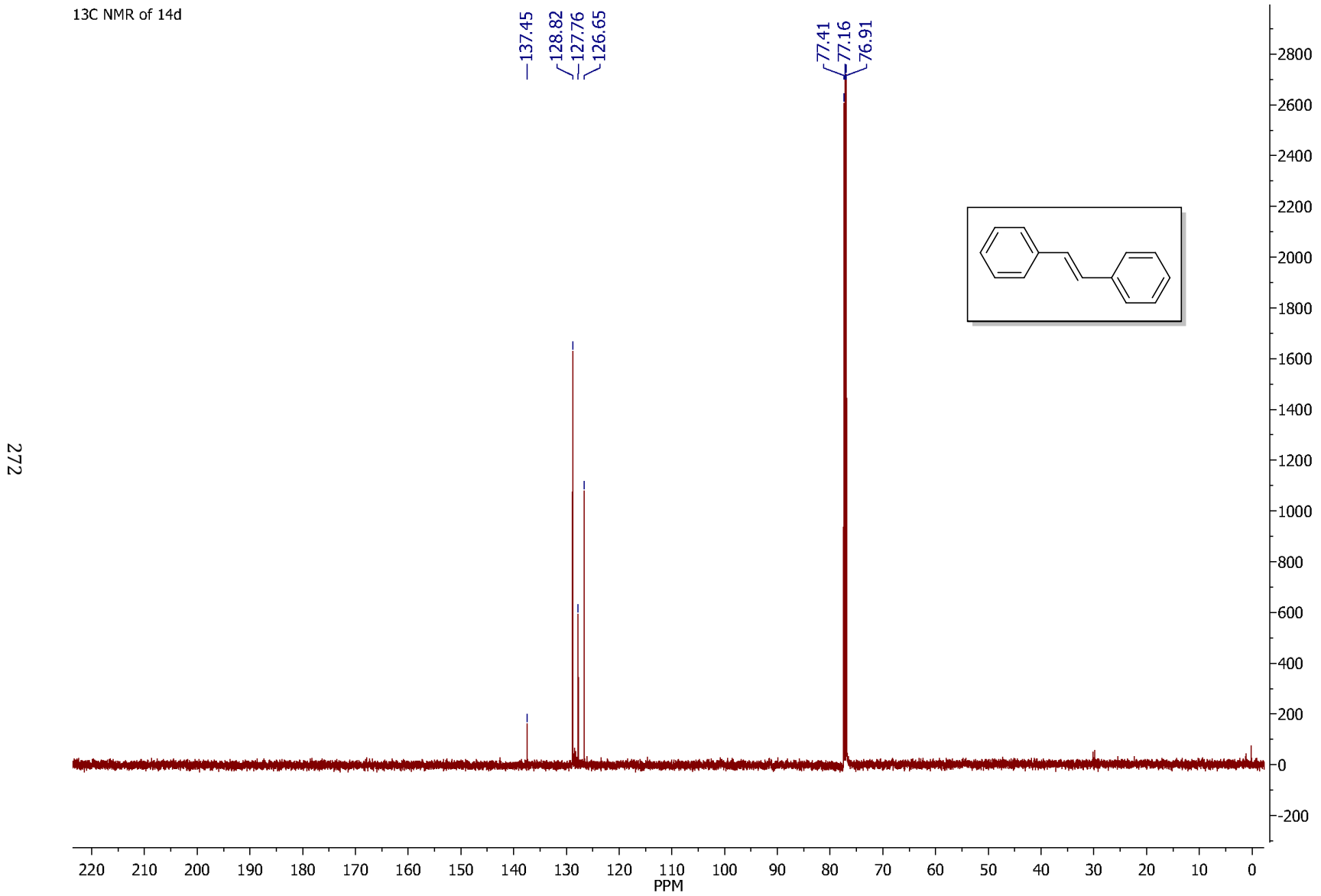
13C NMR of 14d
137.45
128.82
127.76
126.65
77.41
77.16
76.91
2800
2600
2400
2200
2000
1800
1600
1400
1200
1000
800
600
400
200
0
-200
220
210
200
190
180
170
160
150
140
130
120
110
100
90
80
70
60
50
40
30
20
10
0
PPM

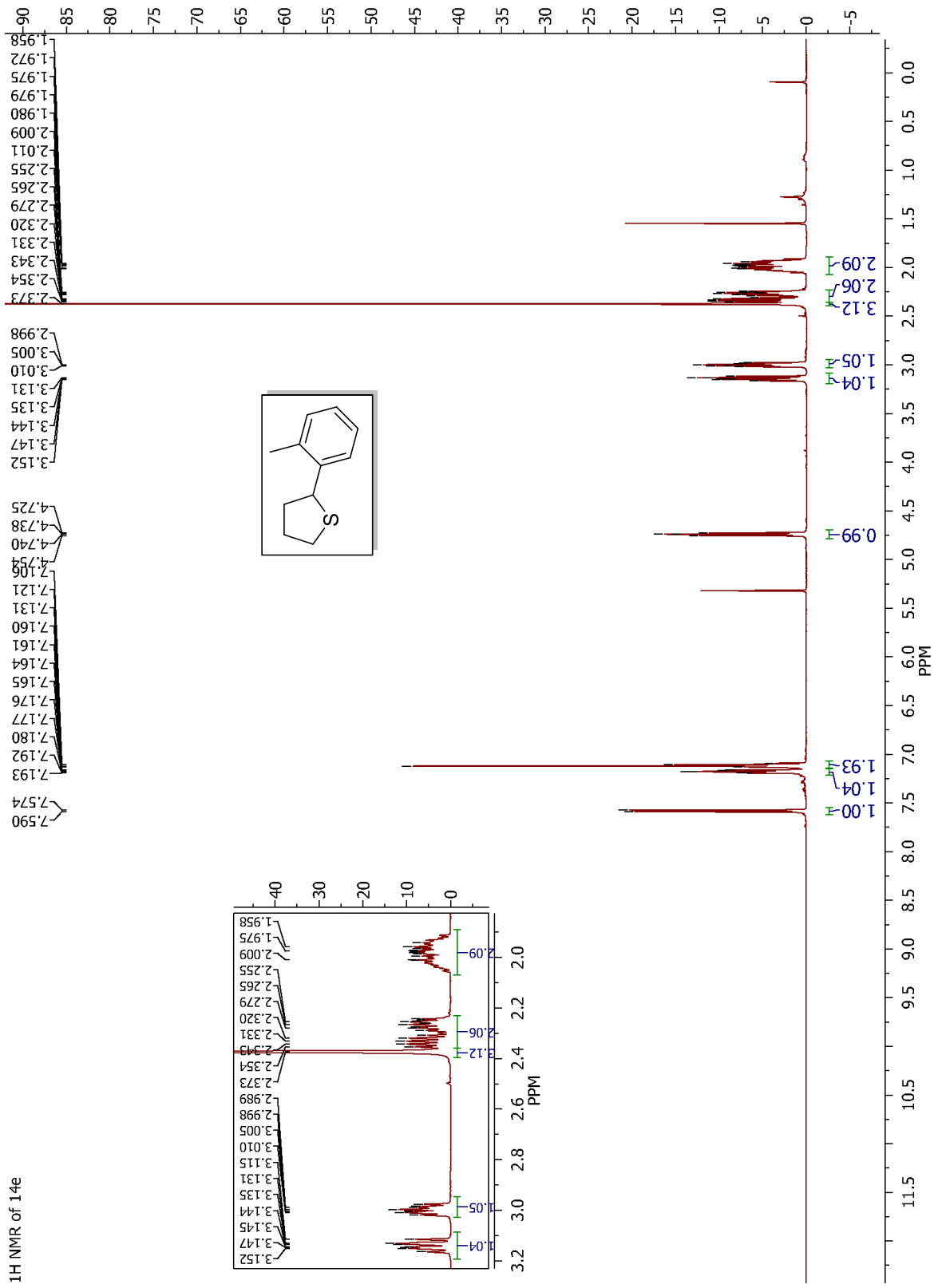
1H NMR of 14e
PPM

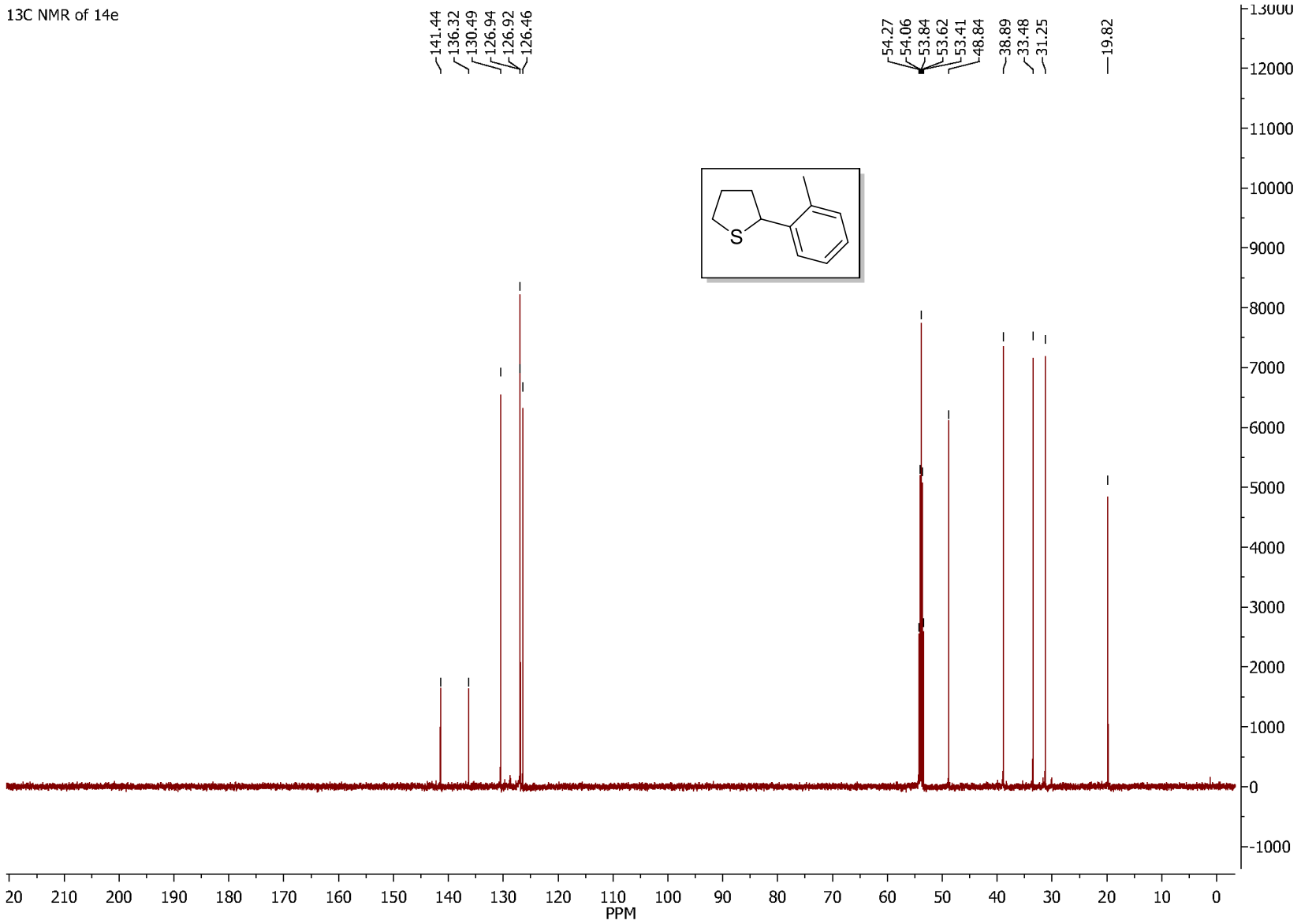
13C NMR of 14e
141.44
136.32
130.49
126.94
126.92
126.46
54.27
54.06
53.84
53.62
53.41
48.84
38.89
33.48
31.25
19.82
S
PPM

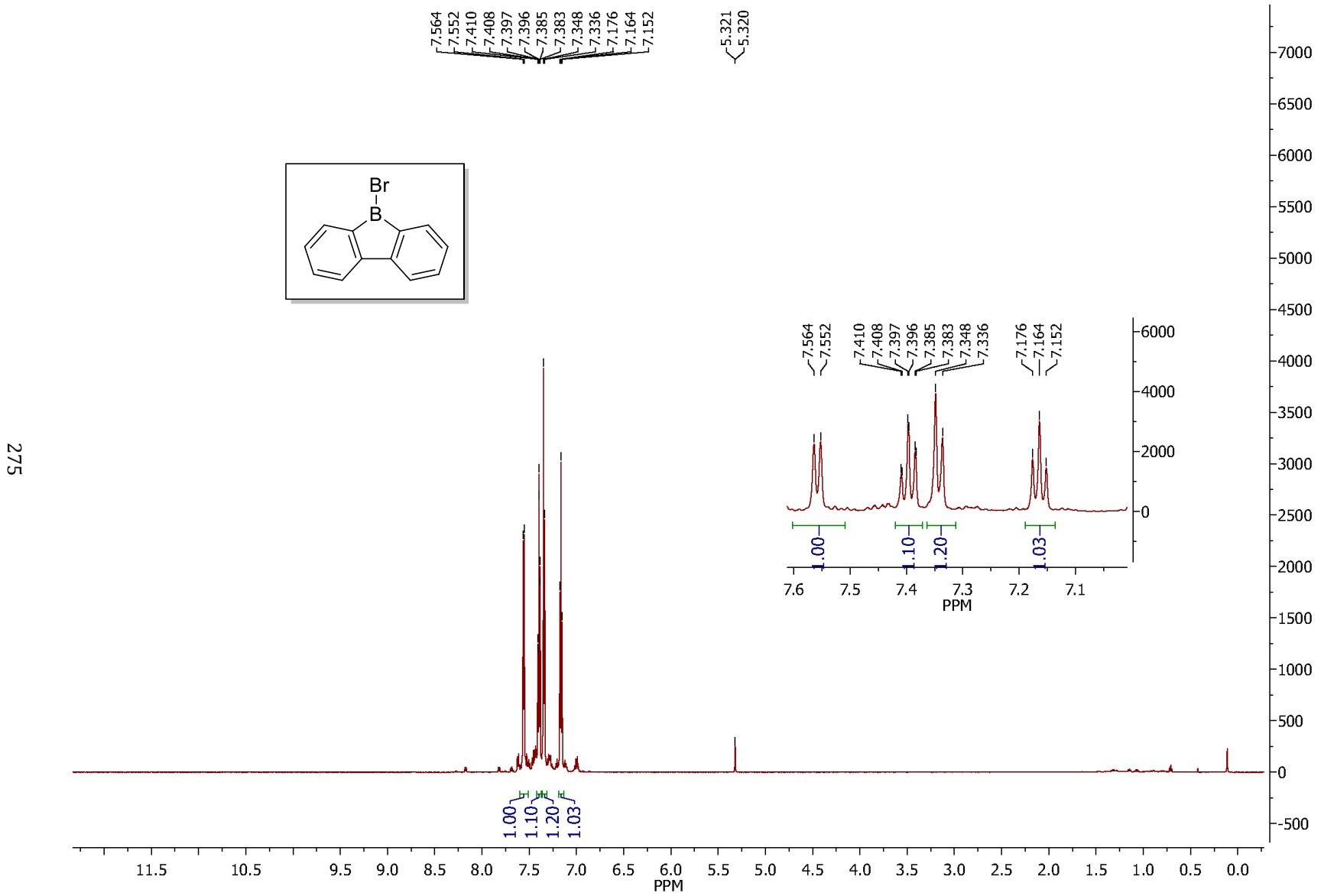
7.564
7.552
7.410
7.408
7.397
7.396
7.385
7.383
7.348
7.336
7.176
7.164
7.152
5.321
5.320
Br
B
1.00
1.10
1.20
1.03
PPM

153.256
135.956
133.692
129.170
120.170
54.199
54.020
53.840
53.659
53.478
Br
B
PPM

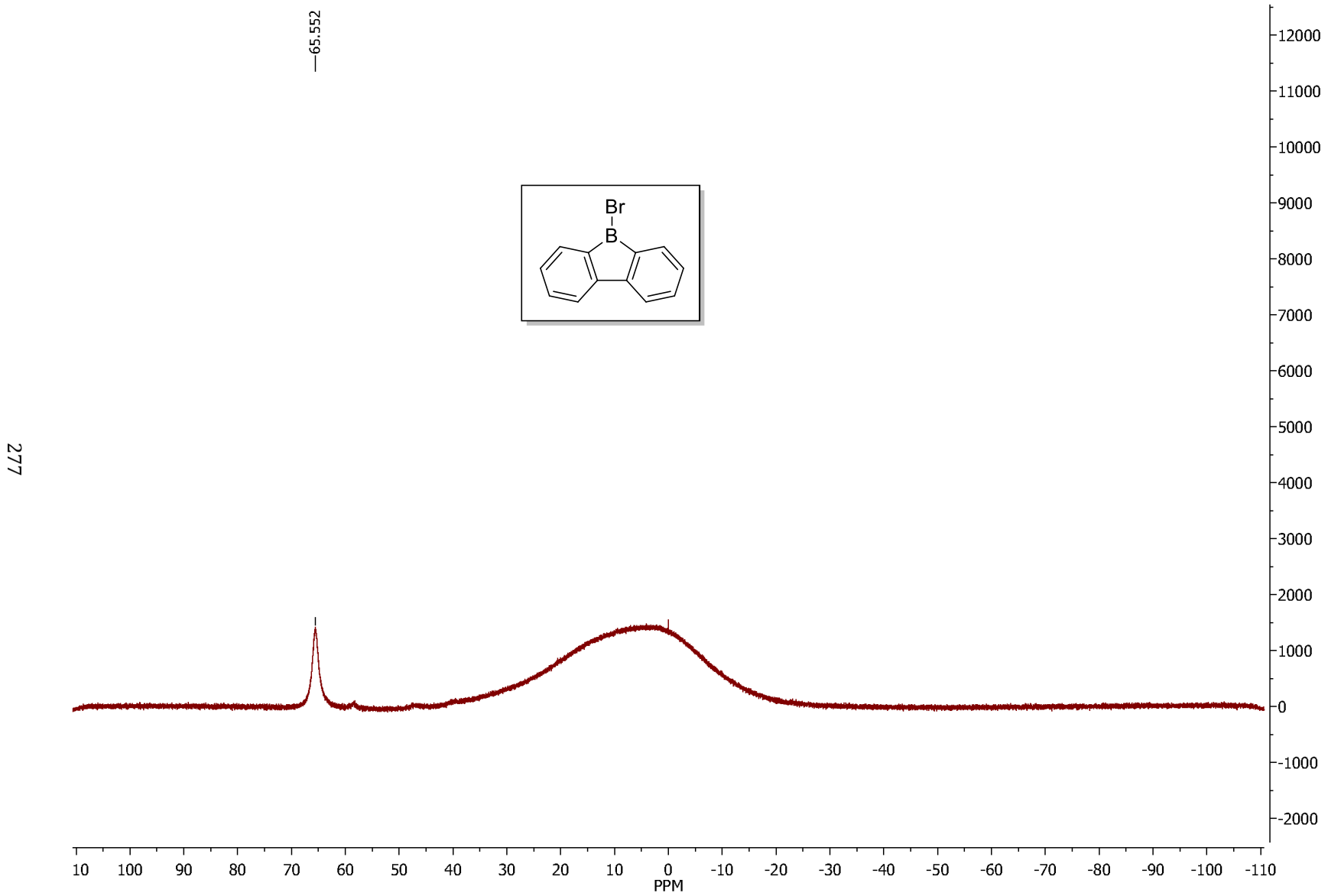
65.552
Br
B
12000
11000
10000
9000
8000
7000
6000
5000
4000
3000
2000
1000
0
-1000
-2000
10 100 90 80 70 60 50 40 30 20 10 0 -10 -20 -30 -40 -50 -60 -70 -80 -90 -100 -110
PPM

277

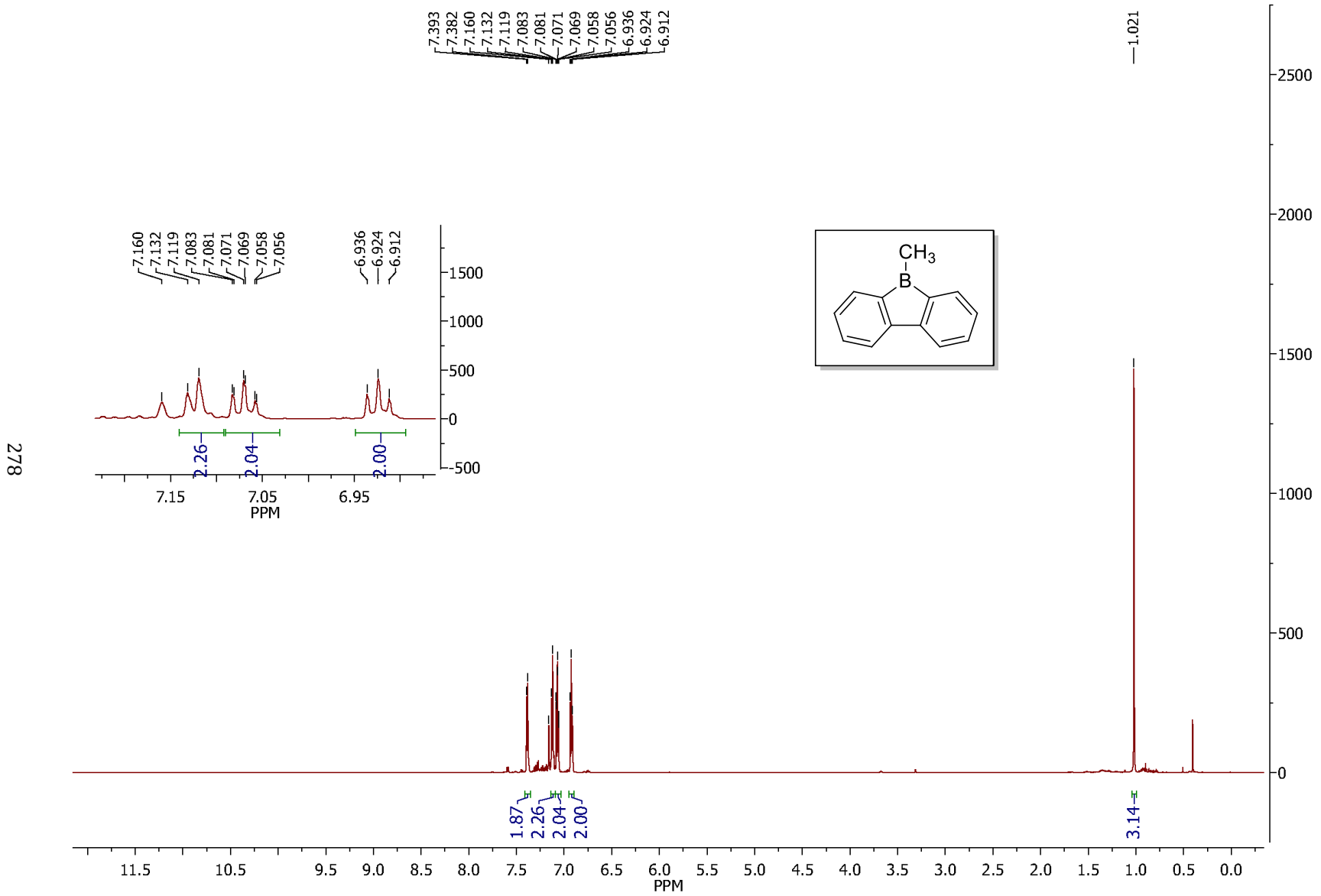
7.393
7.382
7.160
7.132
7.119
7.083
7.081
7.071
7.069
7.058
7.056
6.936
6.924
6.912
1.021
CH3
B
1.87
2.26
2.04
2.00
3.14
PPM

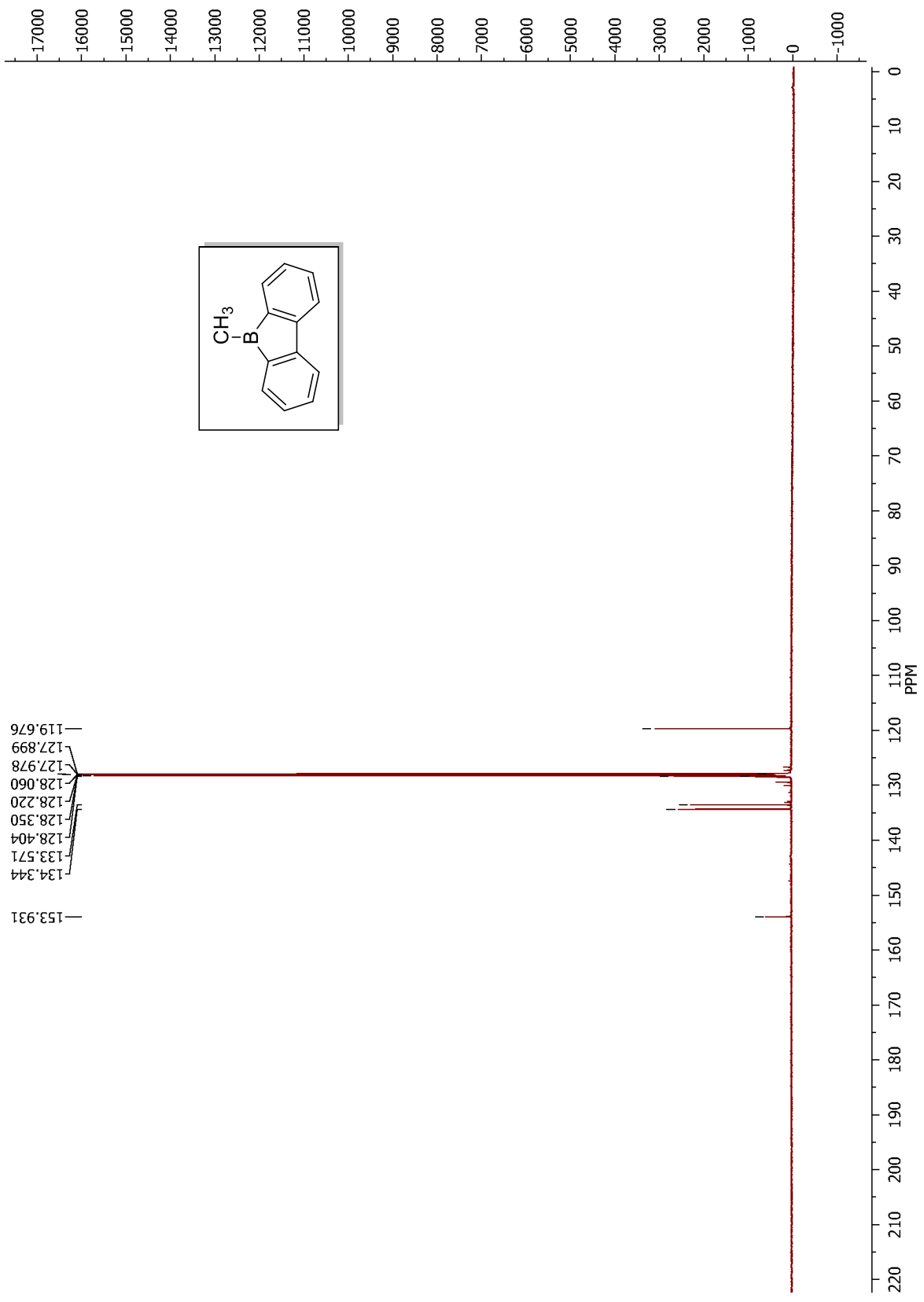
153.931
134.344
133.571
128.404
128.350
128.220
128.060
127.978
127.899
119.676
CH3
B
PPM

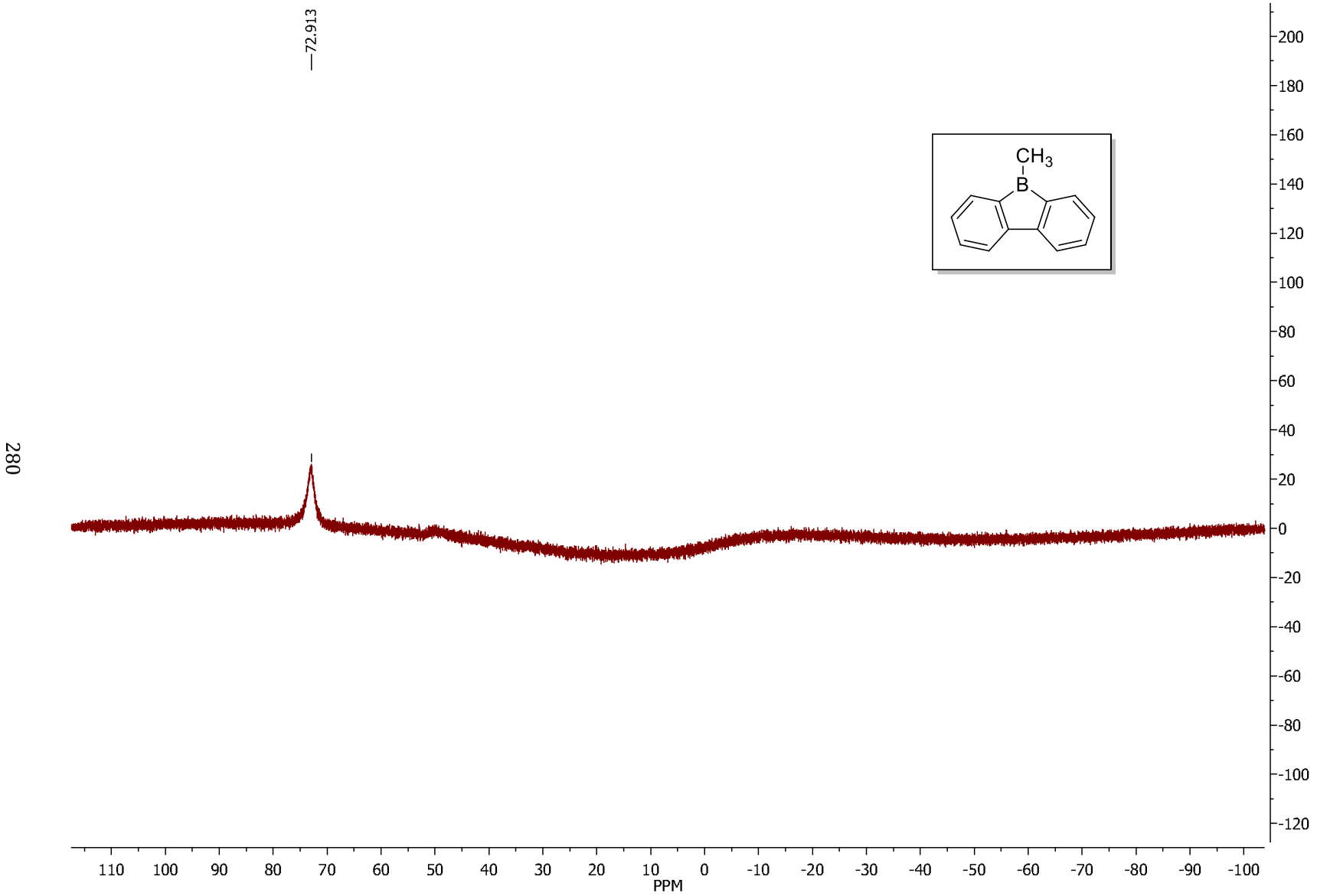
72.913
CH3
B
200
180
160
140
120
100
80
60
40
20
0
-20
-40
-60
-80
-100
-120
110
100
90
80
70
60
50
40
30
20
10
0
-10
-20
-30
-40
-50
-60
-70
-80
-90
-100
PPM

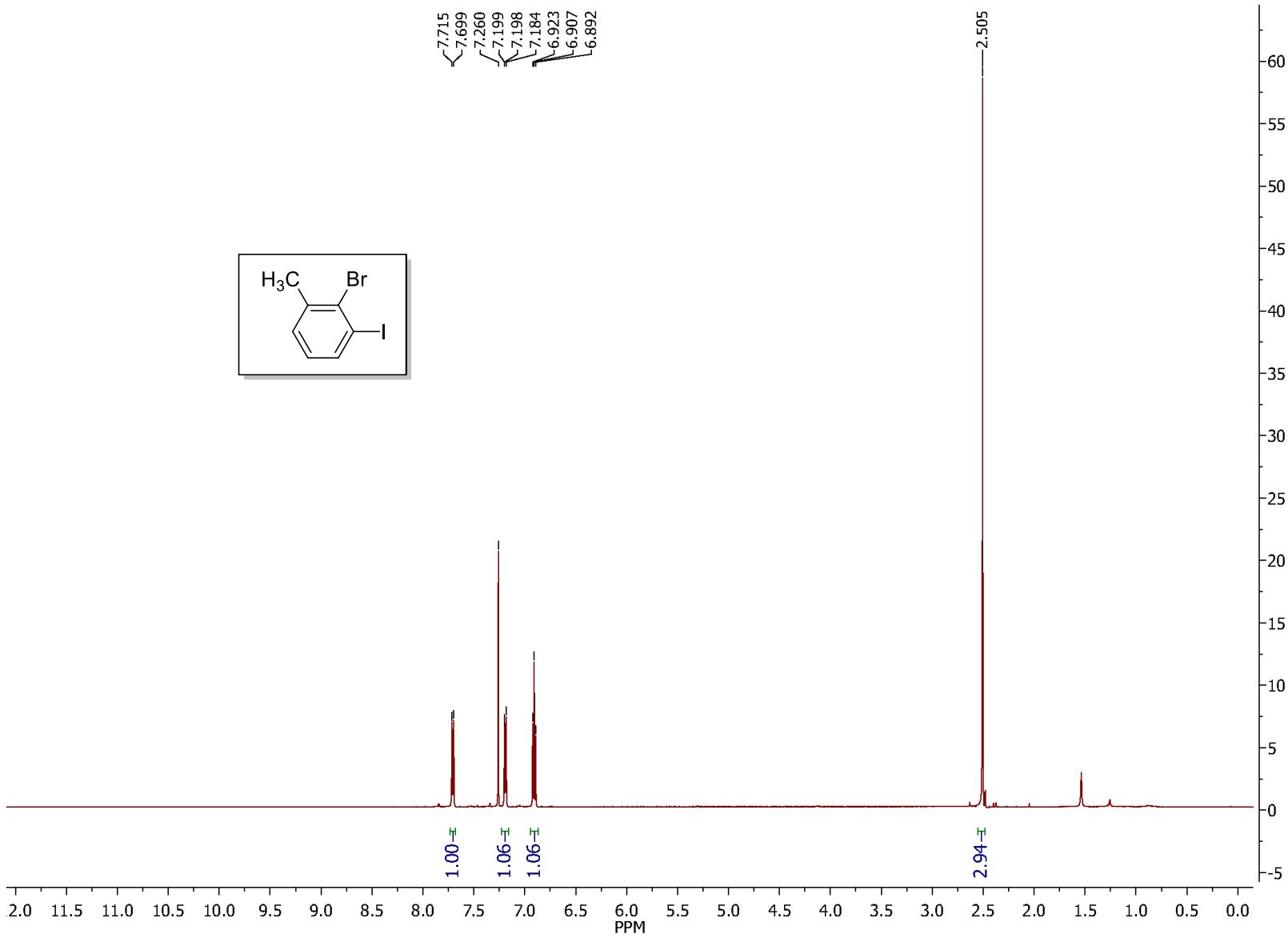
7.715
7.699
7.260
7.199
7.198
7.184
6.923
6.907
6.892
2.505
H3C
Br
I
1.00
1.06
1.06
2.94
PPM

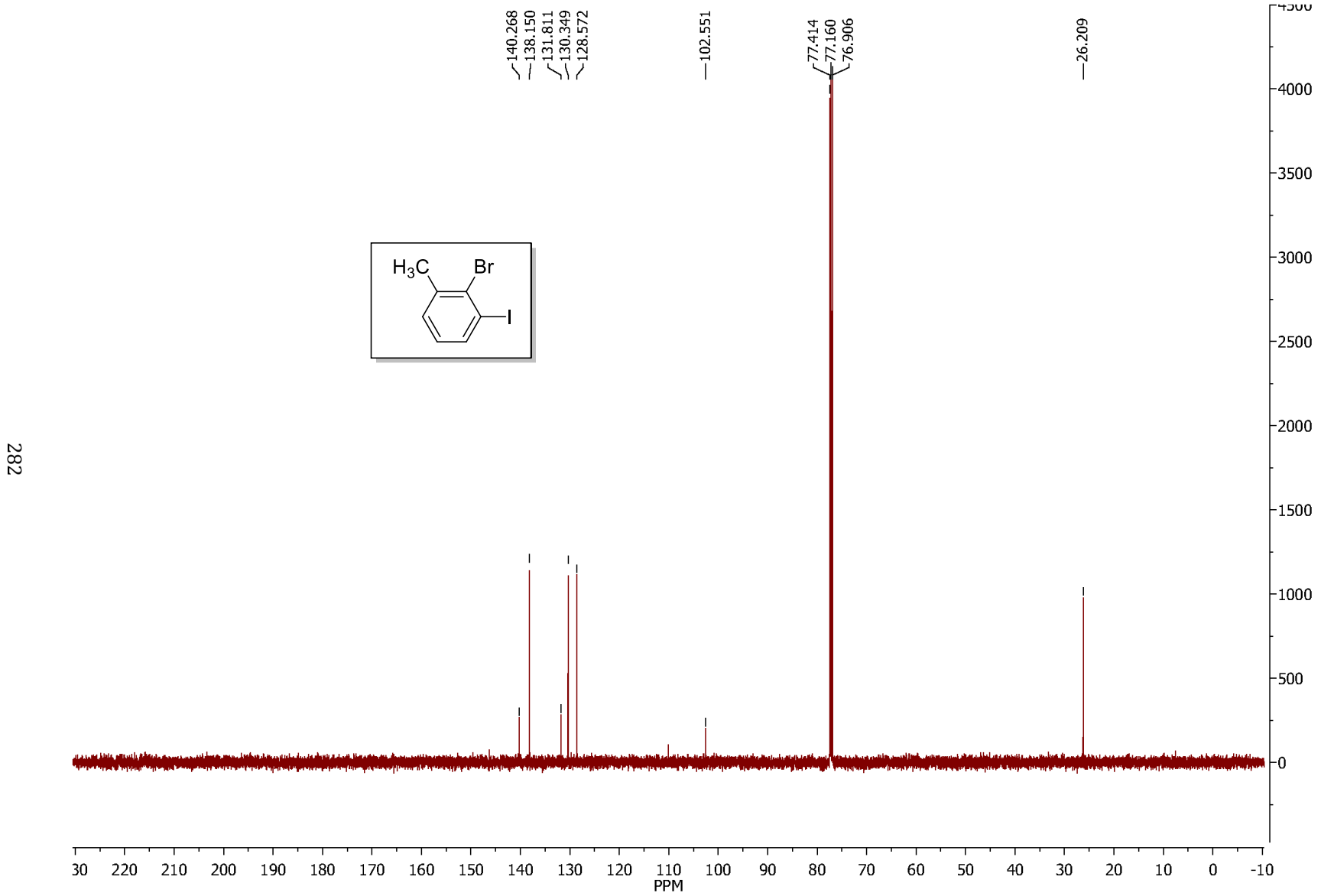
140.268
138.150
131.811
130.349
128.572
102.551
77.414
77.160
76.906
26.209
H3C
Br
I
PPM

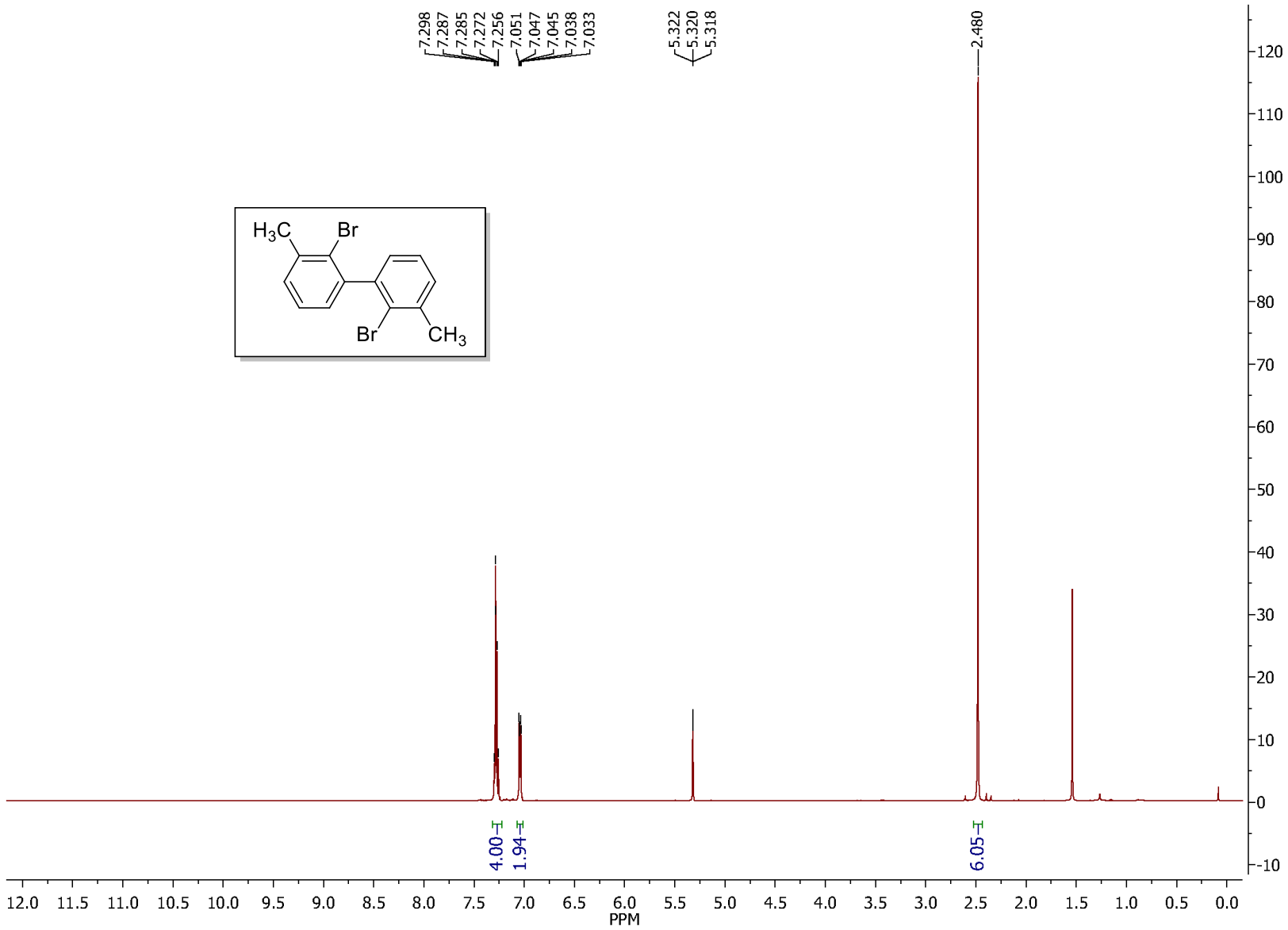
7.298
7.287
7.285
7.272
7.256
7.051
7.047
7.045
7.038
7.033
5.322
5.320
5.318
2.480
H3C
Br
Br
CH3
4.00
1.94
6.05
PPM

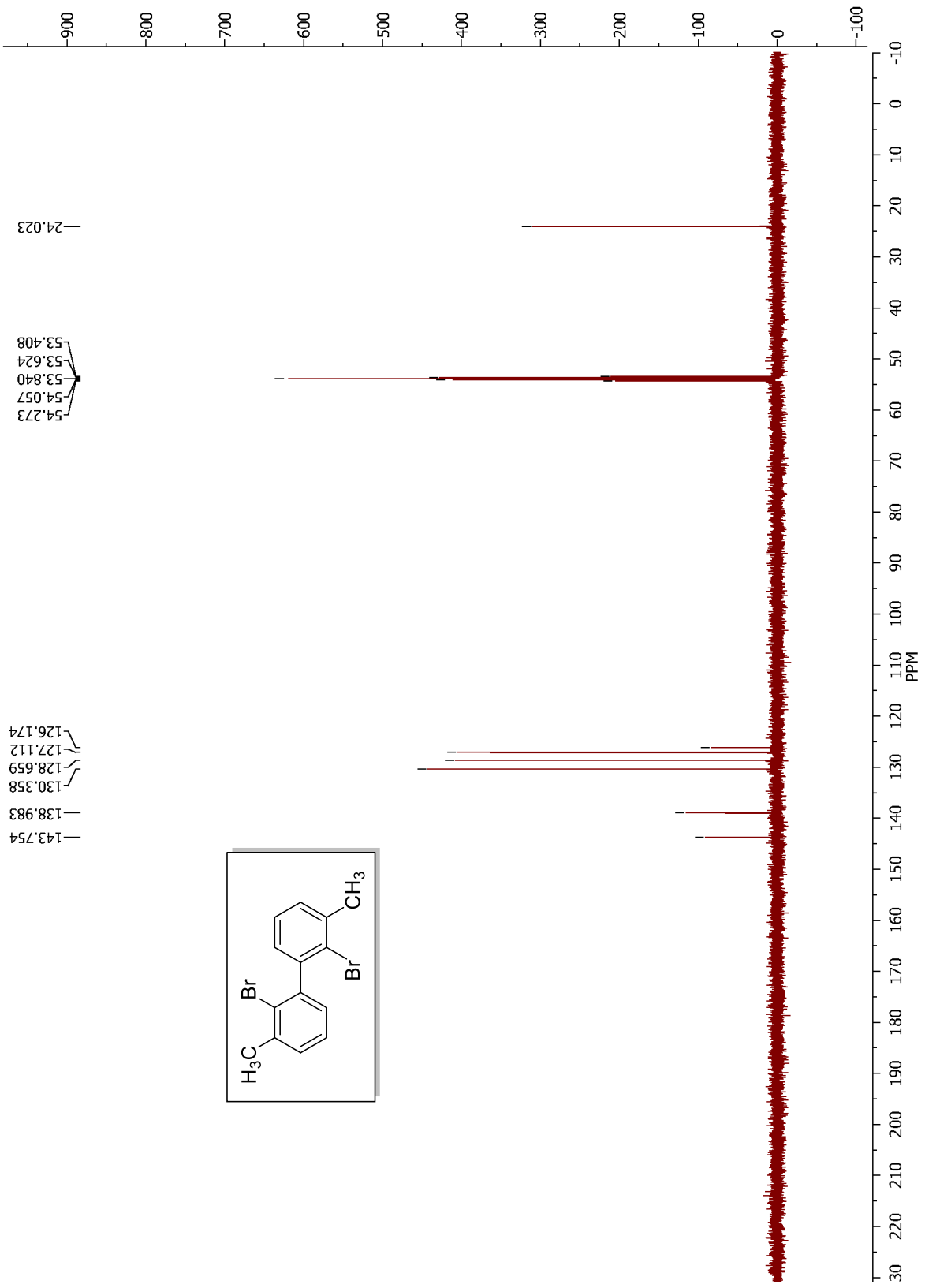
143.754
138.983
130.358
128.659
127.112
126.174
54.273
54.057
53.840
53.624
53.408
24.023
PPM
Br
Br
CH_3
H_3C

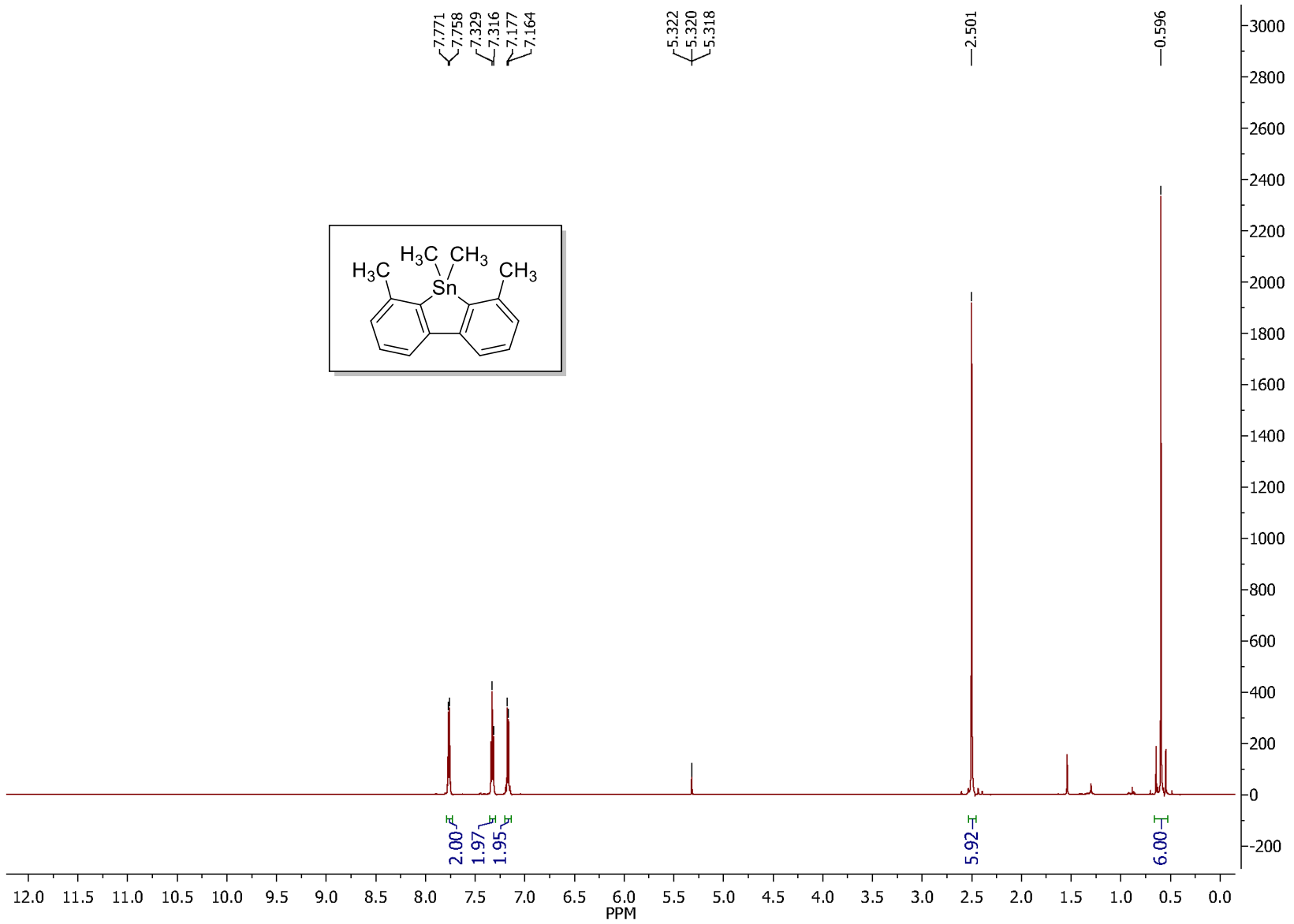
7.771
7.758
7.329
7.316
7.177
7.164
5.322
5.320
5.318
2.501
0.596
H3C
H3C
CH3
CH3
Sn
2.00
1.97
1.95
5.92
6.00
PPM

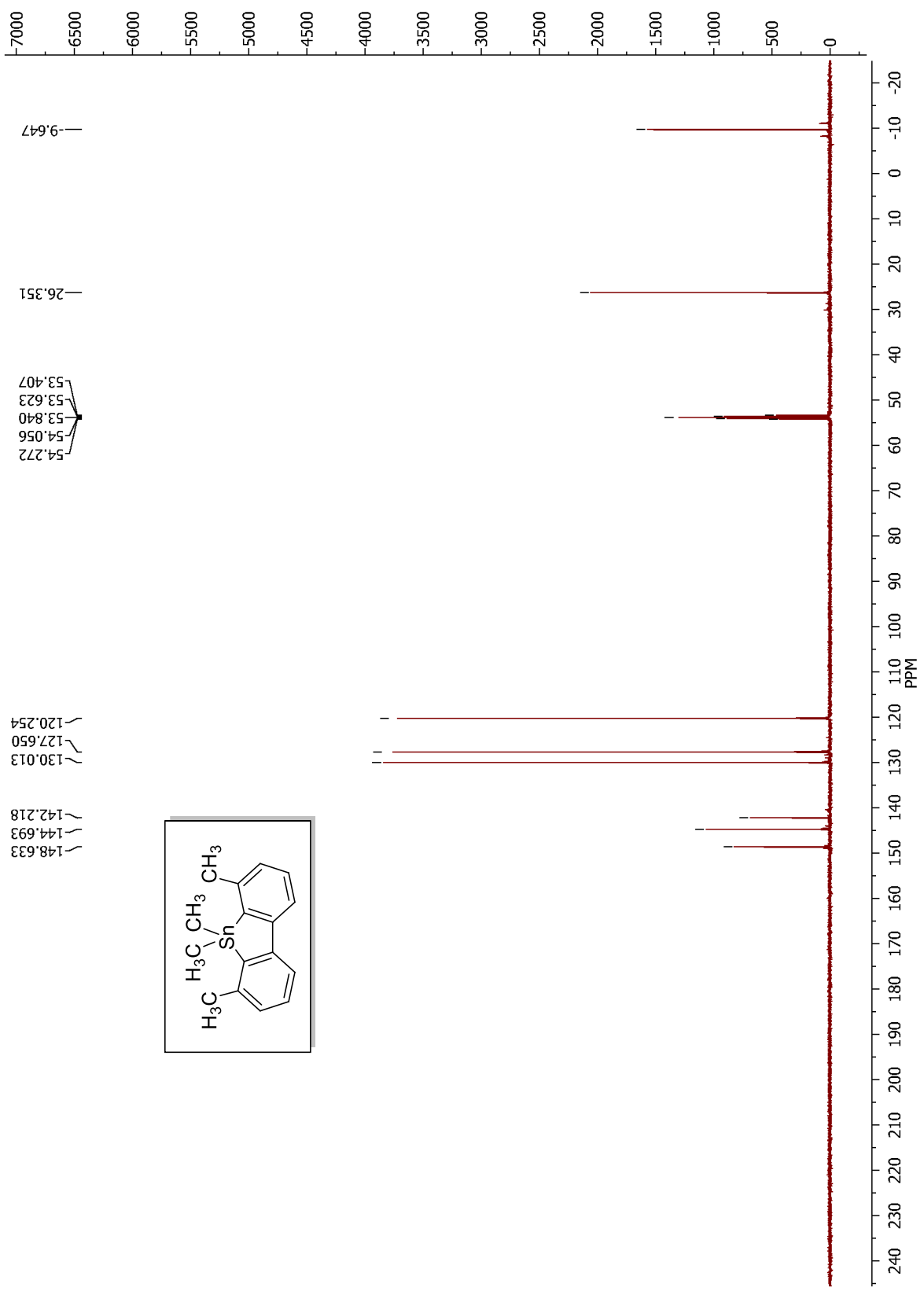
-9.647
26.351
54.272
54.056
53.840
53.623
53.407
120.254
127.650
130.013
142.218
144.693
148.633
PPM

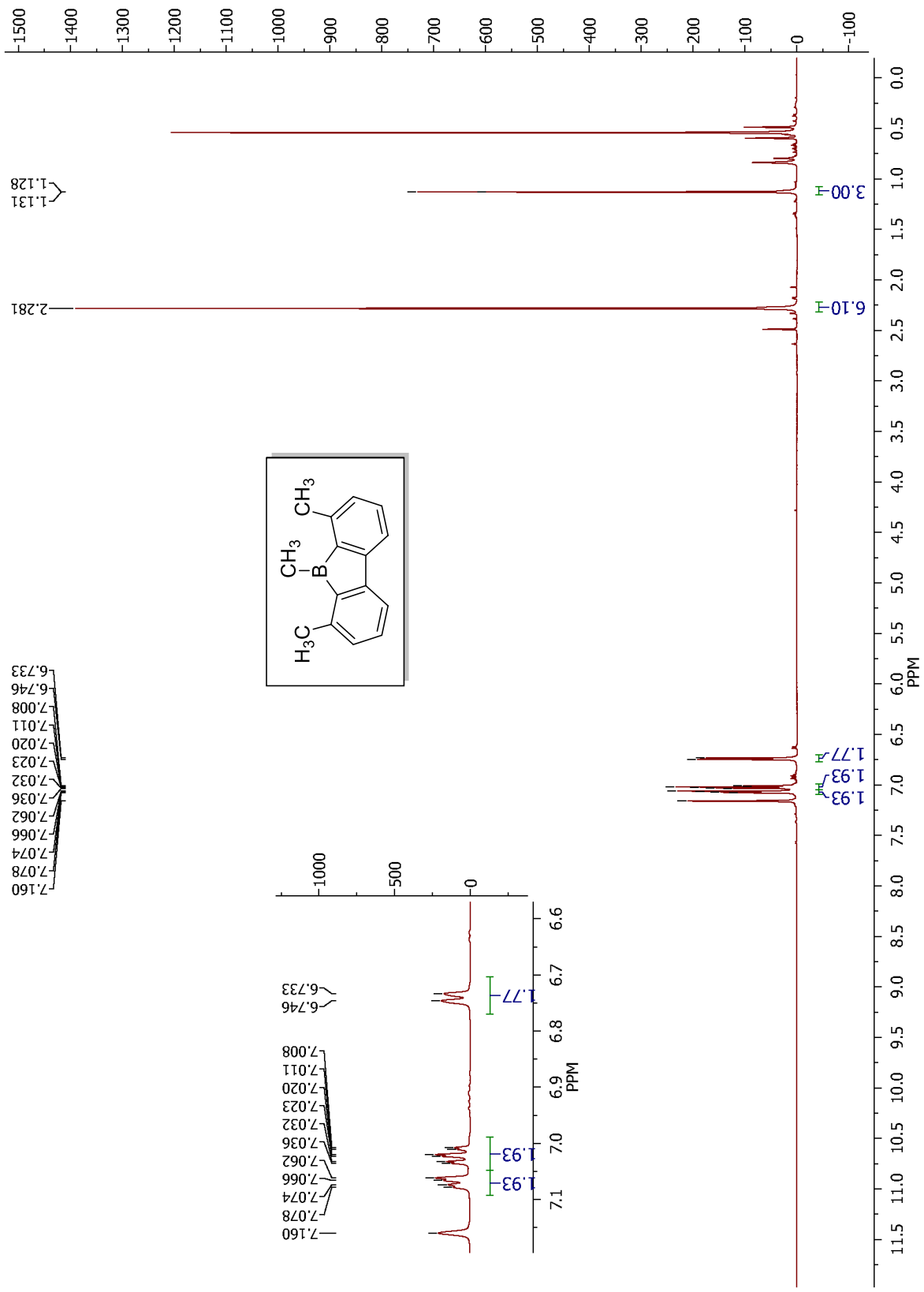
PPM
3.00
6.10
1.77
1.93
1.93
2.281
1.131
1.128
CH3
CH3
B
H3C
7.160
7.078
7.074
7.066
7.062
7.036
7.032
7.023
7.020
7.011
7.008
6.746
6.733

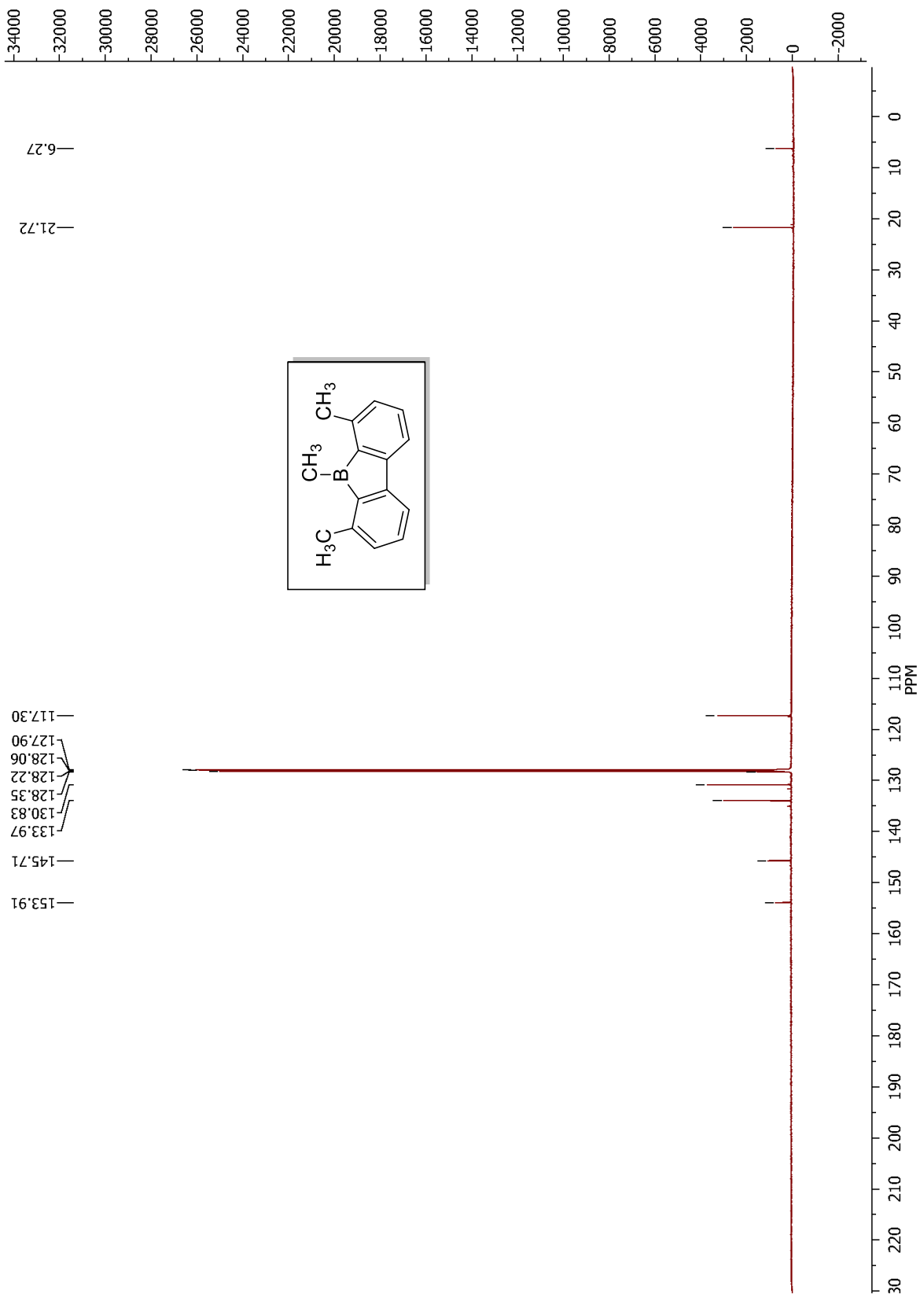
6.27
21.72
117.30
127.90
128.06
128.22
128.35
130.83
133.97
145.71
153.91
CH3
CH3
B
H3C
PPM

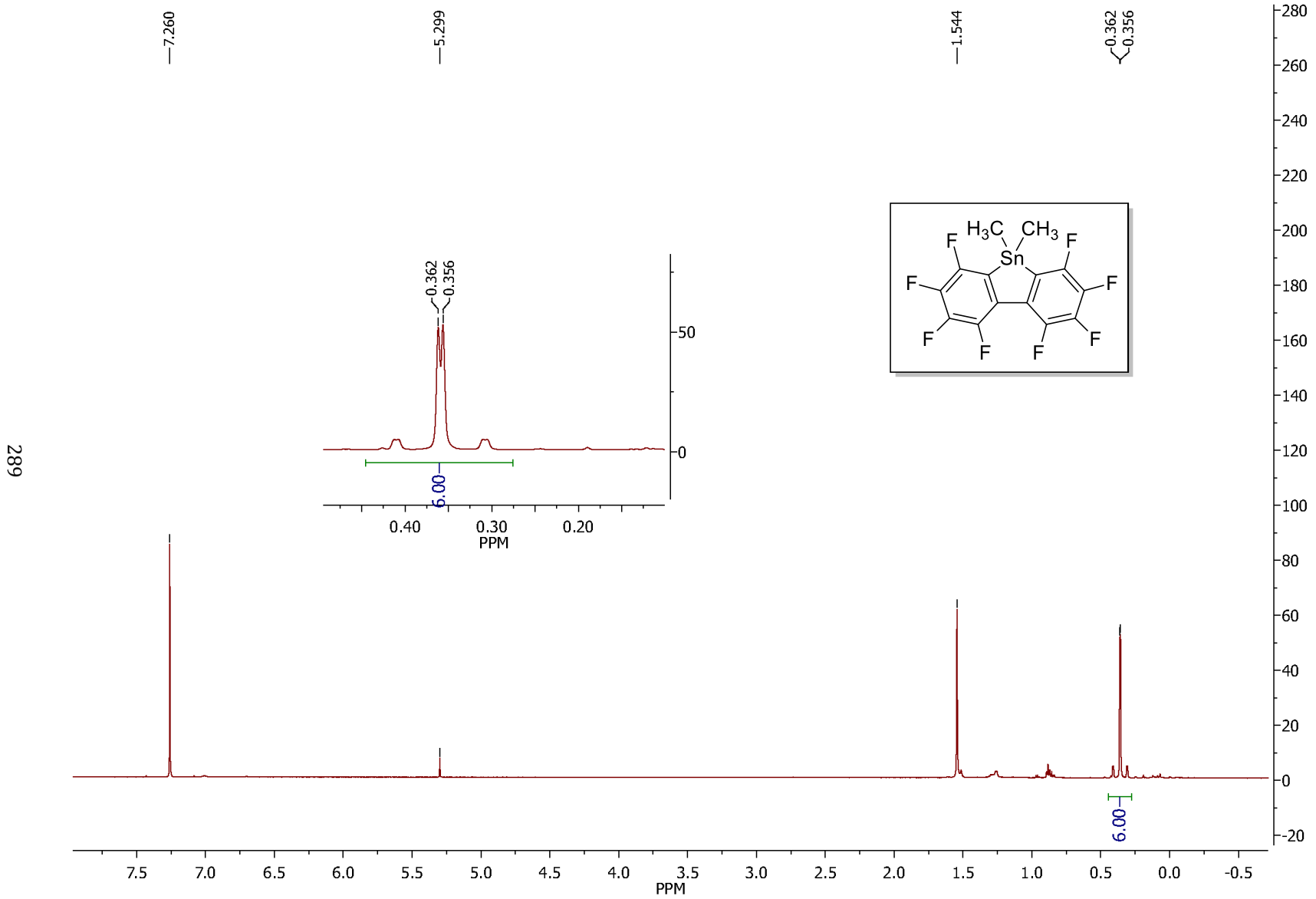
7.260
5.299
1.544
0.362
0.356
6.00
PPM
0.362
0.356
6.00
0.40
0.30
0.20
PPM
H3C
CH3
Sn
F
7.5
7.0
6.5
6.0
5.5
5.0
4.5
4.0
3.5
3.0
2.5
2.0
1.5
1.0
0.5
0.0
-0.5
PPM
280
260
240
220
200
180
160
140
120
100
80
60
40
20
0
-20
50
0

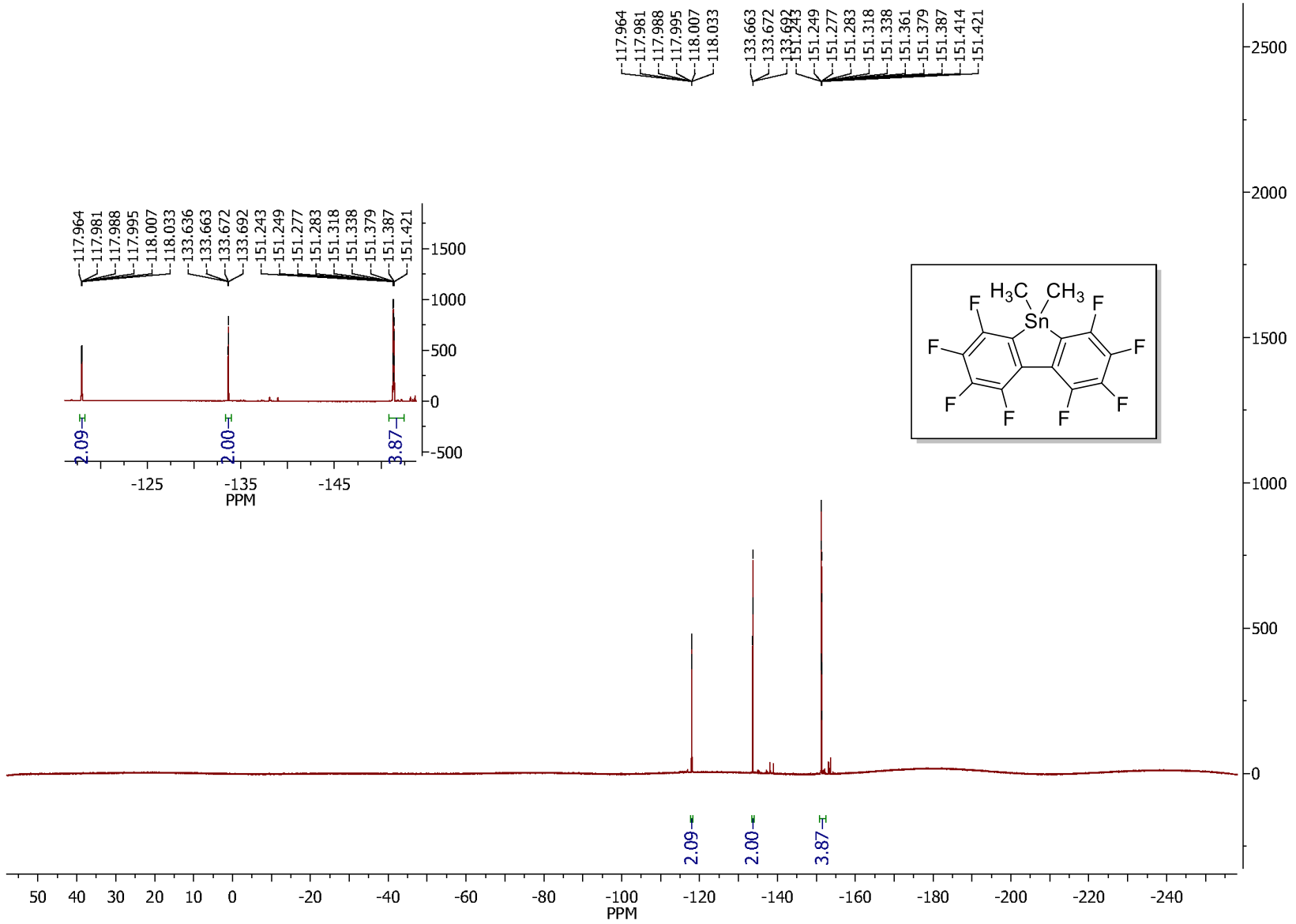
-117.964
-117.981
-117.988
-117.995
-118.007
-118.033
-133.663
-133.672
-151.243
-151.249
-151.277
-151.283
-151.318
-151.338
-151.361
-151.379
-151.387
-151.414
-151.421
2.09
2.00
3.87
PPM
H3C
CH3
Sn
F

22000
21000
20000
19000
18000
17000
16000
15000
14000
13000
12000
11000
10000
9000
8000
7000
6000
5000
4000
3000
2000
1000
0
-1000
-2000
-3000
-4000
50 40 30 20 10 0 -20 -40 -60 -80 -100 -120 -140 -160 -180 -200 -220 -240
PPM
2.00
1.95
1.87
1.97
CH3
B
F
-153.911
-153.877
-153.871
-153.837
-144.231
-144.215
-131.714
-131.708
-131.702
-131.696
-126.391
-126.379
-126.364
-126.350
-126.338
20000
15000
10000
5000
0
-130
-140
-150
PPM

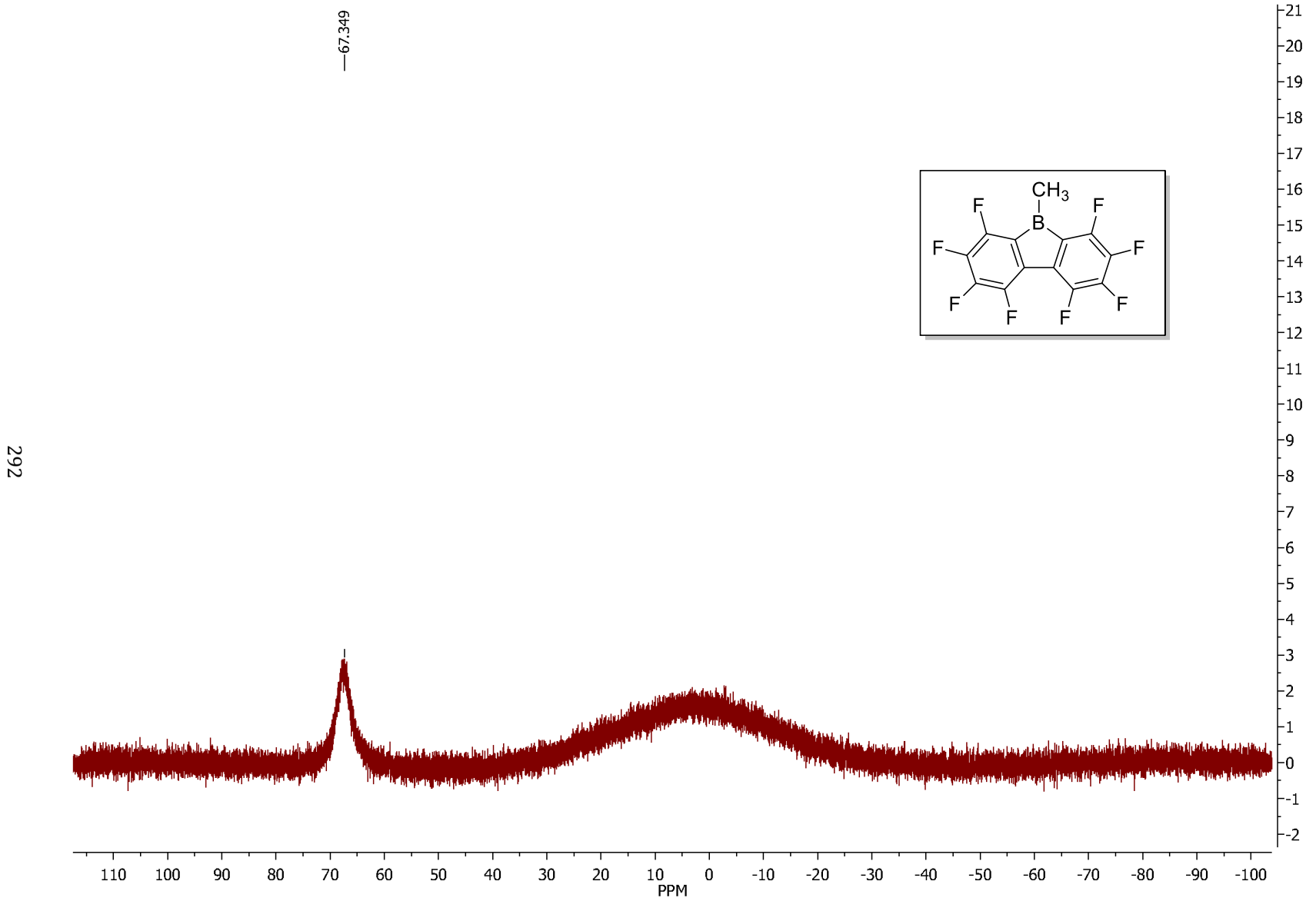
67.349
CH3
B
F
F
F
F
F
F
F
F
PPM
110 100 90 80 70 60 50 40 30 20 10 0 -10 -20 -30 -40 -50 -60 -70 -80 -90 -100
21 20 19 18 17 16 15 14 13 12 11 10 9 8 7 6 5 4 3 2 1 0 -1 -2

292

n-C6H13
B
PPM
2.00
2.40
2.32
1.99
3.96
2.15
4.50
3.66
7.662
7.650
7.390
7.378
7.354
7.353
7.342
7.340
7.329
7.328
7.169
7.157
7.145
1.897
1.891
1.412
1.406
0.981
0.969
0.957

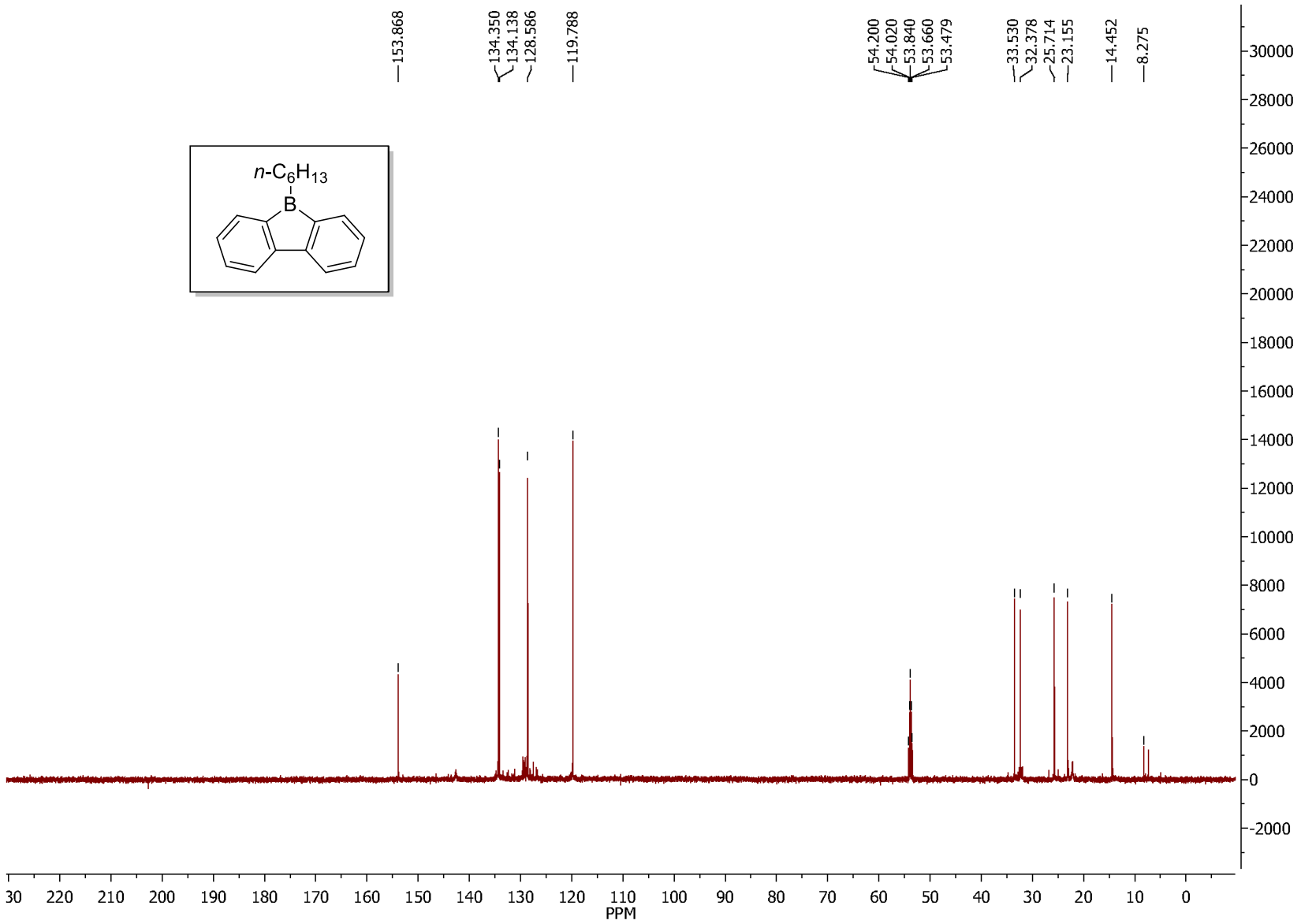
153.868
134.350
134.138
128.586
119.788
54.200
54.020
53.840
53.660
53.479
33.530
32.378
25.714
23.155
14.452
8.275
n-C6H13
B
PPM

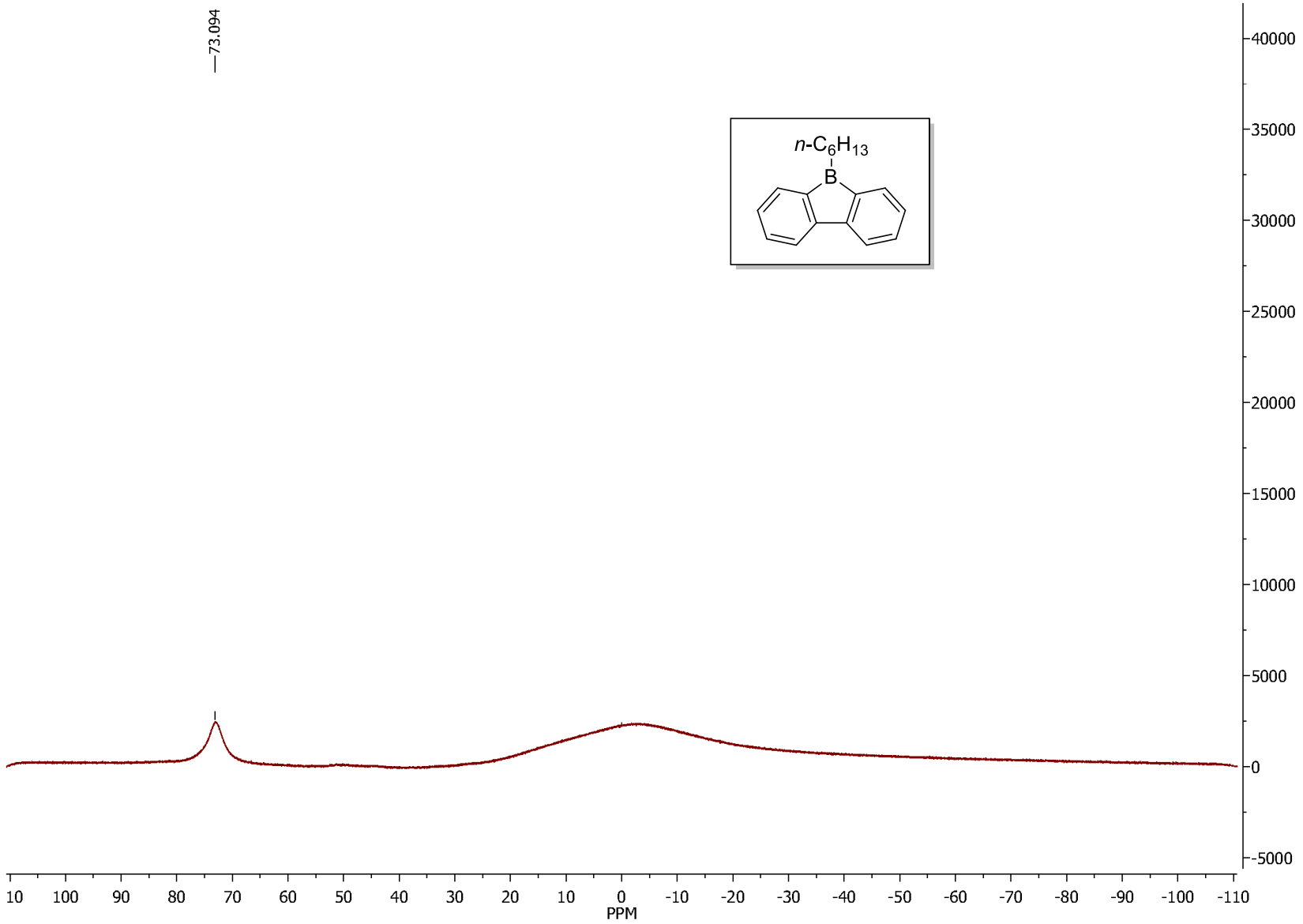
73.094
n-C6H13
B
40000
35000
30000
25000
20000
15000
10000
5000
0
-5000
10
100
90
80
70
60
50
40
30
20
10
0
-10
-20
-30
-40
-50
-60
-70
-80
-90
-100
-110
PPM

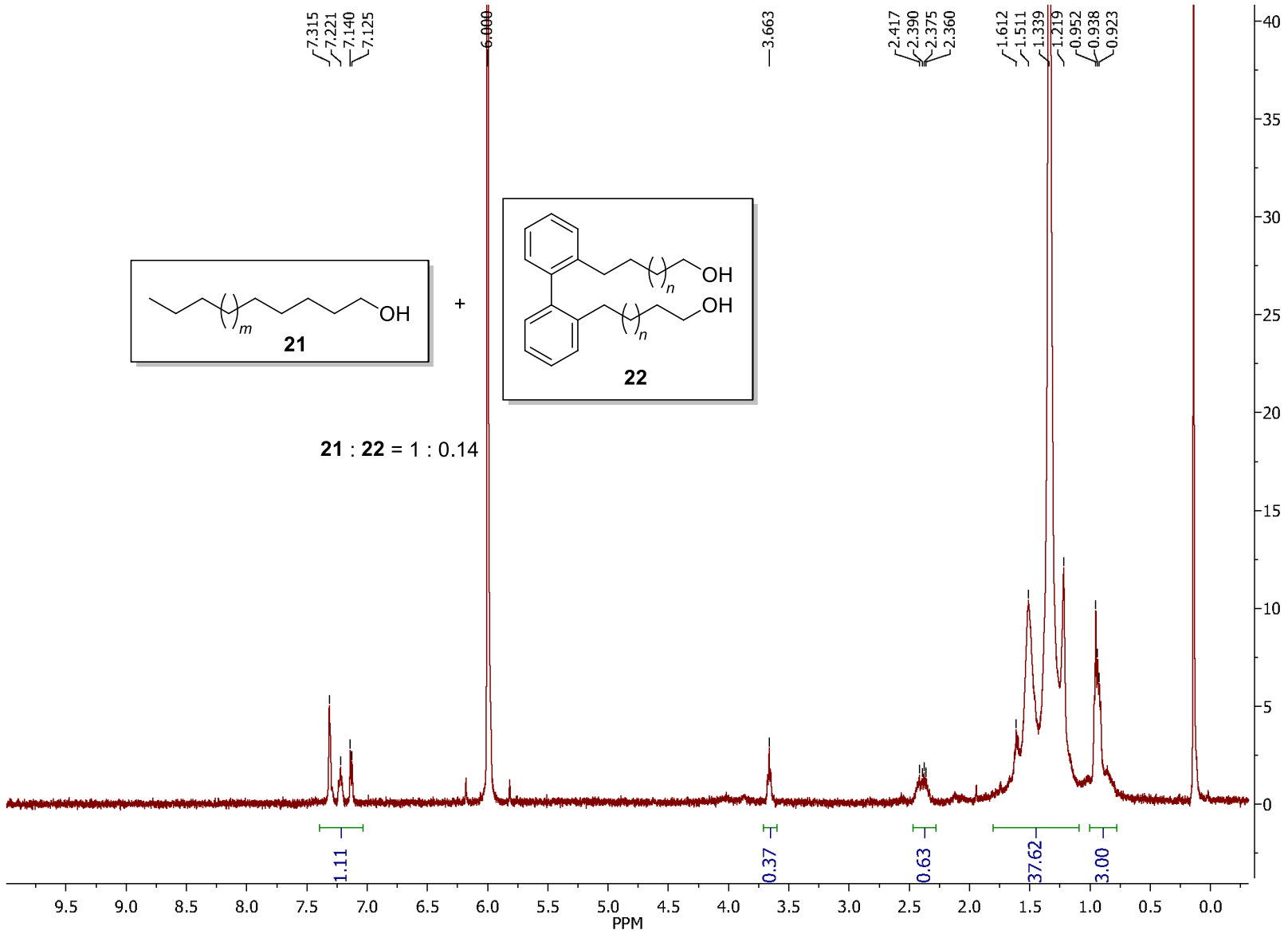
7.315
7.221
7.140
7.125
6.000
3.663
2.417
2.390
2.375
2.360
1.612
1.511
1.339
1.219
0.952
0.938
0.923
OH
m
21
+
OH
OH
n
n
22
21 : 22 = 1 : 0.14
1.11
0.37
0.63
37.62
3.00
PPM